

---

---

# Shipping Container Response to Severe Highway and Railway Accident Conditions

Main Report

---

---

Prepared by L. E. Fischer, C. K. Chou, M. A. Gerhard, C. Y. Kimura,  
R. W. Martin, R. W. Mensing, M. E. Mount, M. C. Witte

**Lawrence Livermore National Laboratory**

Prepared for  
**U.S. Nuclear Regulatory  
Commission**

## NOTICE

This report was prepared as an account of work sponsored by an agency of the United States Government. Neither the United States Government nor any agency thereof, or any of their employees, makes any warranty, expressed or implied, or assumes any legal liability of responsibility for any third party's use, or the results of such use, of any information, apparatus, product or process disclosed in this report, or represents that its use by such third party would not infringe privately owned rights.

## NOTICE

### Availability of Reference Materials Cited in NRC Publications

Most documents cited in NRC publications will be available from one of the following sources:

1. The NRC Public Document Room, 1717 H Street, N.W.  
Washington, DC 20555
2. The Superintendent of Documents, U.S. Government Printing Office, Post Office Box 37082,  
Washington, DC 20013-7082
3. The National Technical Information Service, Springfield, VA 22161

Although the listing that follows represents the majority of documents cited in NRC publications, it is not intended to be exhaustive.

Referenced documents available for inspection and copying for a fee from the NRC Public Document Room include NRC correspondence and internal NRC memoranda; NRC Office of Inspection and Enforcement bulletins, circulars, information notices, inspection and investigation notices; Licensee Event Reports; vendor reports and correspondence; Commission papers; and applicant and licensee documents and correspondence.

The following documents in the NUREG series are available for purchase from the GPO Sales Program: formal NRC staff and contractor reports, NRC-sponsored conference proceedings, and NRC booklets and brochures. Also available are Regulatory Guides, NRC regulations in the *Code of Federal Regulations*, and *Nuclear Regulatory Commission Issuances*.

Documents available from the National Technical Information Service include NUREG series reports and technical reports prepared by other federal agencies and reports prepared by the Atomic Energy Commission, forerunner agency to the Nuclear Regulatory Commission.

Documents available from public and special technical libraries include all open literature items, such as books, journal and periodical articles, and transactions. *Federal Register* notices, federal and state legislation, and congressional reports can usually be obtained from these libraries.

Documents such as theses, dissertations, foreign reports and translations, and non-NRC conference proceedings are available for purchase from the organization sponsoring the publication cited.

Single copies of NRC draft reports are available free, to the extent of supply, upon written request to the Division of Technical Information and Document Control, U.S. Nuclear Regulatory Commission, Washington, DC 20555.

Copies of industry codes and standards used in a substantive manner in the NRC regulatory process are maintained at the NRC Library, 7920 Norfolk Avenue, Bethesda, Maryland, and are available there for reference use by the public. Codes and standards are usually copyrighted and may be purchased from the originating organization or, if they are American National Standards, from the American National Standards Institute, 1430 Broadway, New York, NY 10018.

NUREG/CR-4829  
UCID-20733  
Vol. 1  
RT

---

---

# Shipping Container Response to Severe Highway and Railway Accident Conditions

Main Report

---

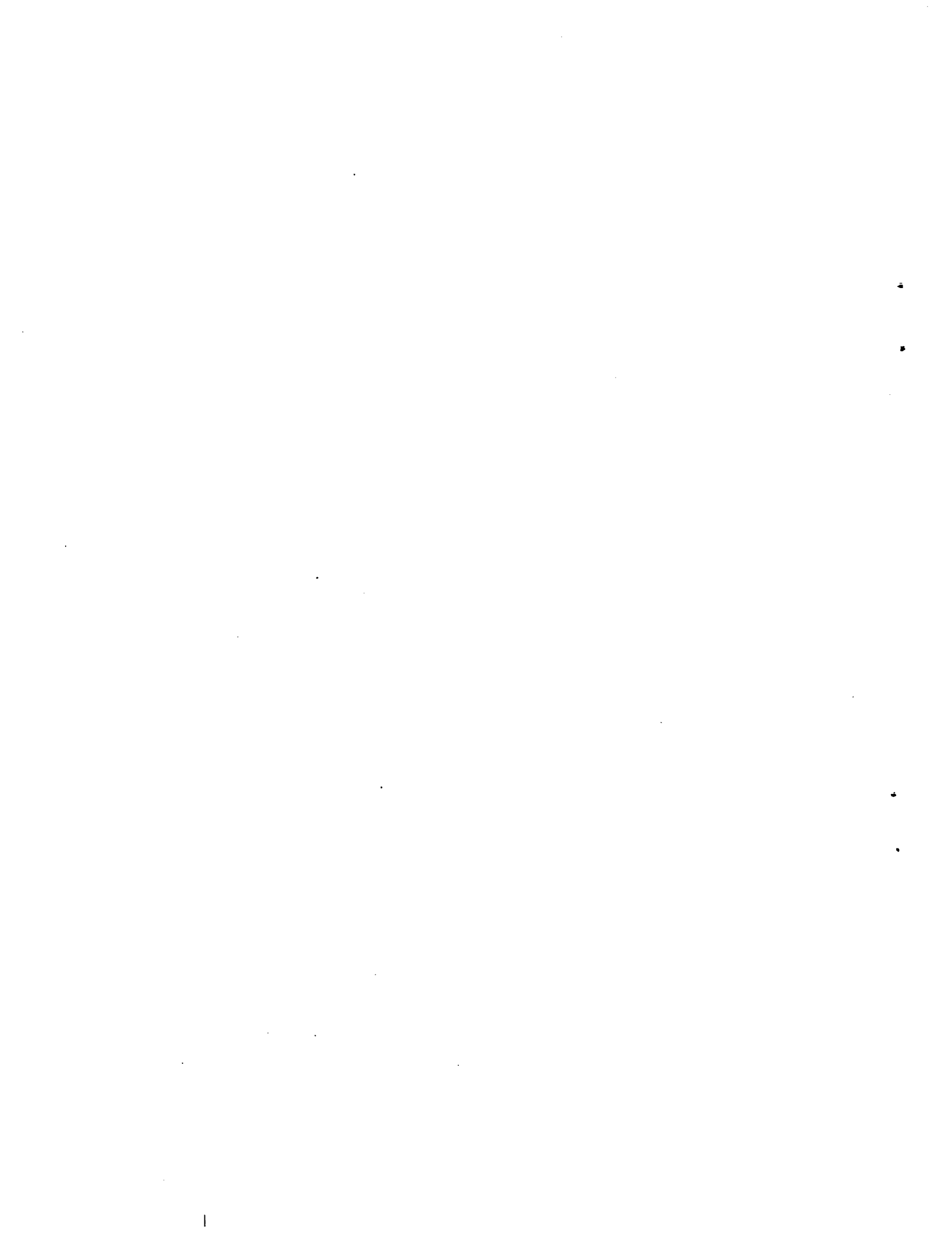
---

Manuscript Completed: April 1986  
Date Published: February 1987

Prepared by  
L. E. Fischer, C. K. Chou, M. A. Gerhard, C. Y. Kimura,  
R. W. Martin, R. W. Mensing, M. E. Mount, M. C. Witte

Lawrence Livermore National Laboratory  
7000 East Avenue  
Livermore, CA 94550

Prepared for  
Division of Reactor System Safety  
Office of Nuclear Regulatory Research  
U.S. Nuclear Regulatory Commission  
Washington, DC 20555  
NRC FIN A0397



## ABSTRACT

This report describes a study performed by the Lawrence Livermore National Laboratory to evaluate the level of safety provided under severe accident conditions during the shipment of spent fuel from nuclear power reactors. The evaluation is performed using data from real accident histories and using representative truck and rail cask models that likely meet 10 CFR 71 regulations. The responses of the representative casks are calculated for structural and thermal loads generated by severe highway and railway accident conditions. The cask responses are compared with those responses calculated for the 10 CFR 71 hypothetical accident conditions. By comparing the responses it is determined that most highway and railway accident conditions fall within the 10 CFR 71 hypothetical accident conditions. For those accidents that have higher responses, the probabilities and potential radiation exposures of the accidents are compared with those identified by the assessments made in the "Final Environmental Statement on the Transportation of Radioactive Material by Air and other Modes," NUREG-0170. Based on this comparison, it is concluded that the radiological risks from spent fuel under severe highway and railway accident conditions as derived in this study are less than risks previously estimated in the NUREG-0170 document.



## TABLE OF CONTENTS

	Page
1. INTRODUCTION .....	1-1
1.1 Background .....	1-1
1.2 Regulations and Past Assessments .....	1-4
1.2.1 Title 10, Code of Federal Regulations, Part 71.....	1-4
1.2.2 Transportation of Radioactive Material - Environmental Statement (NUREG-0170).....	1-7
1.3 Objective and Approach .....	1-9
2. ACCIDENT RATES, ACCIDENT SCENARIOS, AND LOADING PARAMETER DISTRIBUTIONS .....	2-1
2.1 Introduction .....	2-1
2.2 Highway Accident Rates .....	2-3
2.3 Railway Accident Rates .....	2-3
2.4 Accident Loading Data Requirements .....	2-4
2.5 Highway Accident Loading Parameters .....	2-10
2.5.1 Mechanical Loading Parameters .....	2-10
2.5.1.1 Accident Scenarios and Object Hardness .....	2-10
2.5.1.1.1 Collision Accident Hardness Data .....	2-11
2.5.1.1.2 Non-Collision Accident Hardness Data .....	2-14
2.5.1.2 Impact Velocity .....	2-17
2.5.1.2.1 Cask Velocity .....	2-17
2.5.1.2.2 Impact Angle.....	2-21
2.5.1.3 Cask Orientation .....	2-23
2.5.2 Thermal Loading Parameters .....	2-24
2.5.2.1 Accident Scenarios and Fire Frequency .....	2-24
2.5.2.2 Fire Duration .....	2-26
2.5.2.3 Flame Temperature .....	2-26
2.5.2.4 Fire Location .....	2-27
2.6 Railway Accident Loading Parameters .....	2-27
2.6.1 Mechanical Loading Parameters .....	2-27

## TABLE OF CONTENTS (continued)

	Page
2.6.1.1 Accident Scenarios and Object Hardness .....	2-28
2.6.1.2 Impact Velocity .....	2-30
2.6.1.2.1 Cask Velocity .....	2-31
2.6.1.2.2 Impact Angle .....	2-34
2.6.1.3 Cask Orientation .....	2-34
2.6.2 Thermal Loading Parameters .....	2-34
2.6.2.1 Accident Scenarios and Fire Frequency .....	2-35
2.6.2.2 Fire Duration .....	2-35
2.6.2.3 Flame Temperature .....	2-35
2.6.2.4 Fire Location .....	2-37
3. SELECTION OF REPRESENTATIVE SPENT FUEL CASKS FOR EVALUATION .....	3-1
3.1 Introduction .....	3-1
3.2 Cask Functions and Design Features .....	3-2
3.3 Cask Design Features Important to Safety .....	3-5
3.3.1 Containment .....	3-5
3.3.2 Radiation Shielding .....	3-8
3.3.3 Subcriticality Assurance .....	3-8
3.4 Selection of Cask Shielding Material .....	3-11
3.5 Definition of Representative Cask Designs .....	3-14
3.5.1 Shielding Features .....	3-14
3.5.2 Containment Features .....	3-15
3.5.3 Subcriticality Assurance Features .....	3-17
3.5.4 Damage-Mitigating Features .....	3-17
3.5.5 Representative Cask Design Description .....	3-18
3.6 Margins of Safety.....	3-19
4. REPRESENTATIVE CASK RESPONSE STATES, LEVELS, AND REGIONS .....	4-1
4.1 Introduction .....	4-1
4.2 Response States and Levels for Mechanical Loads .....	4-2

## TABLE OF CONTENTS (continued)

	Page
4.2.1 Structural Response Level, $S_1$ .....	4-4
4.2.2 Structural Response Level, $S_2$ .....	4-4
4.2.3 Structural Response Level, $S_3$ .....	4-6
4.2.4 Application of Response States and Levels .....	4-6
4.3 Response States and Levels for Thermal Loads .....	4-7
4.3.1 Thermal Response Level, $T_1$ .....	4-9
4.3.2 Thermal Response Level, $T_2$ .....	4-11
4.3.3 Thermal Response Level, $T_3$ .....	4-11
4.3.4 Thermal Response Level, $T_4$ .....	4-12
4.3.5 Application of Response States and Levels .....	4-12
4.4 Cask Response Regions .....	4-14
5. PROBABILITY ANALYSIS .....	5-1
5.1 Introduction .....	5-1
5.2 Probabilistic Inputs .....	5-4
5.2.1 Mechanical Loading Parameter Distributions .....	5-5
5.2.1.1 Object Hardness Distributions .....	5-5
5.2.1.2 Impact Velocity Distributions .....	5-5
5.2.1.2.1 Cask Velocity .....	5-5
5.2.1.2.2 Impact Angle .....	5-9
5.2.1.3 Cask Orientation Distributions .....	5-11
5.2.2 Thermal Loading Parameter Distributions .....	5-13
5.2.2.1 Fire Duration Distributions .....	5-13
5.2.2.2 Flame Temperature Distributions .....	5-15
5.2.2.3 Fire Location Distributions .....	5-18
5.3 Probability Calculation .....	5-20
6. FIRST-STAGE SCREENING ANALYSIS .....	6-1
6.1 Introduction .....	6-1
6.2 Structural Response Analysis .....	6-7

## TABLE OF CONTENTS (continued)

	Page
6.2.1 Cask Response Analysis for Highway Accidents .....	6-15
6.2.1.1 Response to Minor Accidents.....	6-15
6.2.1.2 Response to Other Accidents .....	6-16
6.2.1.2.1 Response for Impacts with Unyielding Surfaces .....	6-18
6.2.1.2.2 Response for Real Objects .....	6-18
6.2.2 Cask Response Analysis for Railway Accidents .....	6-21
6.2.2.1 Response to Minor Accidents.....	6-23
6.2.2.2 Response to Other Accidents .....	6-25
6.2.2.2.1 Response for Impacts with Unyielding Surfaces .....	6-25
6.2.2.2.2 Response for Real Objects .....	6-27
6.2.3 Discussion of Structural Analysis Results.....	6-31
6.3 Thermal Response Analysis .....	6-32
6.3.1 Cask Response Analysis for Highway Fire Accidents.....	6-36
6.3.2 Cask Response Analysis for Railway Fire Accidents.....	6-39
6.3.3 Discussion of Thermal Analysis Results.....	6-43
6.4 Accident Screening Analysis.....	6-45
7. SECOND-STAGE SCREENING ANALYSIS .....	7-1
7.1 Introduction .....	7-1
7.2 Structural Response Analysis .....	7-3
7.2.1 Cask Response Analysis for Highway Accidents .....	7-4
7.2.1.1 Endwise Impacts .....	7-5
7.2.1.2 Sidewise Impacts .....	7-8
7.2.1.3 Impact Response Summary .....	7-8
7.2.2 Cask Response Analysis for Railway Accidents .....	7-12
7.2.2.1 Endwise Impacts .....	7-12
7.2.2.2 Sidewise Impacts .....	7-14
7.2.2.3 Impact Response Summary .....	7-14

## TABLE OF CONTENTS (continued)

	Page
7.2.3 Discussion of Structural Analysis Results .....	7-14
7.3 Thermal Response Analysis .....	7-18
7.3.1 Cask Response Analysis for Highway Fire Accidents .....	7-19
7.3.2 Cask Response Analysis for Railway Fire Accidents .....	7-21
7.3.3 Discussion of Thermal Analysis Results .....	7-22
7.4 Accident Screening Analysis .....	7-24
8. POTENTIAL RADIOLOGICAL SIGNIFICANCE OF TRANSPORTATION ACCIDENTS .....	8-1
8.1 Introduction .....	8-1
8.2 Description of Spent Fuel .....	8-1
8.3 Measures of Radiological Significance .....	8-3
8.4 Estimates of Radiological Hazards .....	8-7
8.4.1 Potential Radioactive Material Releases to the Environment ...	8-7
8.4.2 Potential Radiation Increases from Shielding Reduction.....	8-12
8.5 Radiological Effect Estimates for Response Regions .....	8-18
9. RESULTS AND CONCLUSIONS .....	9-1
9.1 Introduction .....	9-1
9.2 Results .....	9-2
9.2.1 First-Stage Screening .....	9-2
9.2.2 Second-Stage Screening .....	9-4
9.2.3 Comparison with Previous Risk Assessments: NUREG-0170 .....	9-6
9.2.4 Estimated Responses for Sample Severe Accidents .....	9-15
9.2.4.1 Caldecott Tunnel Fire .....	9-15
9.2.4.2 I-80 Bridge Accident .....	9-16
9.2.4.3 Livingston Train Fire .....	9-17
9.2.4.4 Derailment into the Alabama River .....	9-18
9.3 Uncertainties .....	9-19
9.3.1 Uncertainty in Cask Response .....	9-20
9.3.1.1 Selection of Representative Cask Designs .....	9-20
9.3.1.2 Definition of Accident Loads .....	9-21

## TABLE OF CONTENTS (continued)

	Page
9.3.1.3 Computer Code Applications and Modeling .....	9-21
9.3.2 Uncertainty in Estimating an Accident's Potential	
Radiological Hazard .....	9-23
9.3.2.1 Radioactive Releases from Fuel Rods .....	9-23
9.3.2.2 Radioactive Releases from Casks .....	9-24
9.3.2.3 Reduction in Radiation Shielding .....	9-24
9.3.2.4 Reduction in Subcriticality Control .....	9-24
9.3.3 Uncertainty in Probability Models .....	9-25
9.3.3.1 Accident Statistics .....	9-25
9.3.3.2 Surveys of Structures and Features .....	9-26
9.3.3.3 Past Analysis and Models .....	9-26
9.3.3.4 Engineering Judgment .....	9-27
9.3.4 Overall Statement of Uncertainty .....	9-27
9.4 Conclusions .....	9-27
REFERENCES .....	R-1
APPENDIX A: Severe Accident Data .....	A-1
APPENDIX B: Truck Accident Data .....	B-1
APPENDIX C: Railroad Accident Data .....	C-1
APPENDIX D: Highway Survey Data and Bridge Column Properties .....	D-1
APPENDIX E: Structural Analysis .....	E-1
APPENDIX F: Thermal Analysis .....	F-1
APPENDIX G: Probability Estimation Techniques .....	G-1
APPENDIX H: Benchmarking for Computer Codes used in Impact Analysis .....	H-1

## LIST OF FIGURES

1-1	Schematic of a typical spent fuel cask .....	1-6
1-2	Two-stage screening process used in evaluating the regulations .....	1-11
1-3	Schematic representation of the report .....	1-13
2-1	Three impact loading parameters considered in the response analysis for impacts on surfaces .....	2-7
2-2	Three impact loading parameters considered in the response analysis for impacts with objects such as train sills .....	2-8
2-3	Truck collision accident scenarios and their percent probabilities .....	2-12
2-4	Truck non-collision accident scenarios and their percent probabilities .....	2-13
2-5	Train accident scenarios .....	2-29
3-1	Spent fuel cask features important to safety .....	3-4
3-2	Typical closure designs for spent fuel casks .....	3-7
3-3	Typical cask penetration subsystems .....	3-9
3-4	Preliminary truck cask designs with three types of gamma shielding, used for quasi-static loading response studies only .....	3-12
3-5	Preliminary rail cask designs with three types of gamma shielding, used for quasi-static loading response studies only .....	3-13
3-6	Representative truck cask design used for dynamic structural and thermal response studies .....	3-20
3-7	Representative rail cask design used for dynamic structural and thermal response studies .....	3-21
3-8	Force-deflection characteristics of the limiter design as a function of cask orientation at impact .....	3-22

## LIST OF FIGURES (continued)

	Page
4-1 Schematic representation of cask response state for mechanical load .....	4-5
4-2 Schematic representation of cask structural response for various surface hardness and impact velocities .....	4-8
4-3 Schematic representation of cask response state for thermal loads .....	4-10
4-4 Schematic representation of cask response for various fire locations and fire durations .....	4-13
4-5 Matrix of cask response regions for combined mechanical and thermal loads .....	4-15
5-1 Effect of cask orientation on the strain-impact velocity relationship for a truck cask impacting an unyielding object .....	5-2
5-2 Effect of flame temperature and fire location on lead-temperature-time relationship for a truck cask .....	5-3
5-3 Distribution of vehicle velocities adjusted for braking .....	5-7
5-4 Flow Chart of TASP computer code .....	5-32
6-1 Identification of first-stage screening .....	6-2
6-2 Methods of analysis used in cask response determinations .....	6-5
6-3 Three impact loading parameters considered in the response analysis for impacts on surfaces .....	6-8
6-4 Three impact loading parameters considered in the response analysis for impacts with objects such as train sills .....	6-10
6-5 Equivalent damage technique .....	6-13
6-6 Strain versus impact velocity and cask orientation for the representative truck cask impacting an unyielding surface .....	6-19
6-7 Impact force for a rigid truck cask dropped endwise onto real surfaces .....	6-20

## LIST OF FIGURES (continued)

	Page
6-8 Rail car coupler override of spent fuel cask car .....	6-24
6-9 Strain versus impact velocity and cask orientation for the representative rail cask impacting an unyielding surface .....	6-28
6-10 Impact force versus impact velocity for a rigid rail cask dropped endwise onto real surfaces .....	6-29
6-11 Comparison of an engulfing hypothetical fire and a real fire .....	6-34
6-12 Representative truck cask temperature response to a hypothetical 1475 <sup>0</sup> F (equivalent to a real 1700 <sup>0</sup> F) fire versus fire duration .....	6-37
6-13 Heat flux versus fire duration for the representative truck cask exposed to the regulatory 1475 <sup>0</sup> fire .....	6-38
6-14 Average heat flux factor versus temperature for the representative truck cask .....	6-40
6-15 Heat load factor for real fire versus location of representative truck cask .....	6-41
6-16 Representative rail cask temperature response to a hypothetical 1475 <sup>0</sup> F (equivalent to a real 1700 <sup>0</sup> F) fire versus fire duration .....	6-42
6-17 Heat load factor for real fire versus location of representative rail cask .....	6-44
7-1 Second-stage screening analysis relationship with response regions .....	7-2
7-2 Example showing strain response of the representative truck cask for 45 mph endwise impact on an unyielding surface (2- D model with impact limiters) without any truck cab crushing included .....	7-6
7-3 Response of the representative truck cask to endwise impacts on an unyielding surface (2-D model with impact limiters and cab crush) .....	7-7

## LIST OF FIGURES (continued)

	Page
7-4 Example showing strain response of the representative truck cask for 60 mph sidewise impact on soil (2-D model without limiters) with strain exceeding the 2% ( $S_2$ ) limit .....	7-9
7-5 Response of the representative truck cask to sidewise impacts on various surfaces .....	7-10
7-6 Response of the representative rail cask to endwise impacts on an unyielding surface (2-D model with impact limiters and railcar crush) .....	7-13
7-7 Response of the representative rail cask to sidewise impacts on various surfaces .....	7-15
7-8 Representative truck cask temperature response to a hypothetical 1475°F (equivalent to a real 1700°F) fire versus fire duration .....	7-20
7-9 Representative rail cask temperature response to a hypothetical 1475°F (equivalent to a real 1700°F) fire versus fire duration .....	7-23
7-10 Fraction of truck accidents that could result in responses within each response region, assuming an accident occurs .....	7-25
7-11 Fraction of rail accidents that could result in responses within each response region, assuming an accident occurs .....	7-26
8-1 PWR fuel bundle .....	8-4
8-2 Three mechanisms required to establish a radioactive material release path .....	8-8
8-3 Percentage of fuel rods breached as a function of force for endwise impacts .....	8-9
8-4 Percentage of fuel rods breached per fuel assembly in each cask response region .....	8-11
8-5 Lead voiding due to lead slump resulting from endwise impact of cask .....	8-15

## LIST OF FIGURES (continued)

	Page
8-6 Lead voiding due to high thermal loads and lead melting .....	8-17
8-7 Radiological hazards estimated for response regions for a representative truck cask .....	8-19
8-8 Radiological hazards estimated for response regions for a representative rail cask .....	8-20
9-1 Two-stage screening process in the 20 response regions .....	9-5
9-2 Probability-hazard estimates in curies for the 20 truck cask response regions .....	9-8
9-3 Probability-hazard estimates in curies for the 20 rail cask response regions .....	9-9



## LIST OF TABLES

	Page
1.1 Correlation of NUREG-0170 Accident Fractional Occurrence and Radiological Hazards as a Function of Accident Severity .....	1-8
2.1 Accident Loads and Loading Parameters .....	2-5
2.2 Fractional Occurrence of Surface Types below Bridges on Interstate 80 from Davis, California to Nevada Border .....	2-15
2.3 Distribution of Velocities for Trucks/Semitrailers Involved in Fatal and Injury Accidents in California, 1958-1967 .....	2-19
2.4 Distribution of Bridge Heights along Interstate 5 through Orange and Los Angeles Counties, California .....	2-20
2.5 Train Velocity Distribution for Rail-Highway Grade-Crossing Accident/Incidents Involving Motor Vehicles, 1975-1982 .....	2-22
2.6 Frequency of Fire for Truck Accident Types .....	2-25
2.7 Railroad Accident Velocity Distribution, Collisions, Main Line, 1979-1982 .....	2-32
2.8 Railroad Accident Velocity Distribution, Derailments, Main Line, 1979-1982 .....	2-33
2.9 Train-Fire Accident Types .....	2-36
5.1 Cumulative Cask Velocity Distributions for Highway Analysis .....	5-8
5.2 Cumulative Cask Velocity Distributions for Railway Analysis .....	5-10
5.3 Cumulative Impact Angle Distributions .....	5-12
5.4 Cumulative Cask Orientation Angle Distributions .....	5-14
5.5 Cumulative Fire Duration Distributions for Truck Cask Analysis .....	5-16
5.6 Cumulative Fire Duration Distributions for Rail Cask Analysis .....	5-17
5.7 Cumulative Flame Temperature Distribution .....	5-19
5.8 Cumulative Fire Location Distributions .....	5-21
5.9 Probability Inputs for Highway Analysis .....	5-25
5.10 Heat Flux Factors for Flame Temperatures (Engulfing Fire) .....	5-28
5.11 Probability Inputs for Railway Analysis .....	5-31

## LIST OF TABLES (continued)

	Page
6.1 Material Parameters Selected for Real Surfaces .....	6-14
6.2 Evaluation of Quasi-Static Force for Minor Highway Accidents .....	6-17
6.3 Impact Velocities Required to Reach the 0.2% Strain ( $S_1$ ) Level for Objects Impacted in Highway Accidents .....	6-22
6.4 Evaluation Summary of Minor Railway Accidents .....	6-26
6.5 Impact Velocities Required to Reach the 0.2% Strain ( $S_1$ ) Level for Objects Impacted in Railway Accidents .....	6-30
7.1 Impact Velocities Required to Attain 2% ( $S_2$ ) and 30% ( $S_3$ ) Strain Levels for Objects Impacted in Highway Accidents .....	7-11
7.2 Impact Velocities Required to Attain 2% ( $S_2$ ) and 30% ( $S_3$ ) Strain Levels for Objects Impacted in Railway Accidents .....	7-16
8.1 PWR Fuel Assembly Decay Heat and Radioactivity .....	8-2
8.2 10 CFR 71 Release Limits for Radioisotopes.....	8-6
8.3 Material Release Fractions from Breached Fuel Rods Occurring over 1 Week Following Rod Burst .....	8-13
8.4 Gamma Dose Summary for Lead Slump in a Rail Cask for Impacts on Closure Region .....	8-16
9.1 Comparative Measure of Risk/Accident for Spent Fuel Shipment by Truck .....	9-12
9.2 Comparison of Release Risk/Accident for Spent Fuel Shipment by Rail .....	9-13

## PREFACE

This report describes a study conducted to estimate the responses of spent fuel casks to severe highway and railway accident conditions and to assess the level of safety provided to the public during the shipment of spent fuel. The study was performed by the Lawrence Livermore National Laboratory for the U.S. Nuclear Regulatory Commission (NRC), Office of Nuclear Regulatory Research.

This report is divided into two volumes: Volume I, the main report, describes the study, the technical approach, the study results, and conclusions; and Volume II, the Appendixes, provide supporting accident data and engineering calculations. This report has been reviewed by the Denver Research Institute at the University of Denver under a separate contract to the NRC as the peer review. A companion summary report entitled "Transporting Spent Fuel-Protection Provided Against Severe Highway and Railway Accidents" (NUREG/BR-0111) has been prepared by the NRC for wide distribution to federal agencies, local governments, and interested citizens.

Commercial spent fuel shipments are regulated by both the Department of Transportation (DOT) and the NRC. The NRC evaluates and certifies the design, manufacture, operation, and maintenance of spent fuel casks, whereas the DOT regulates the vehicles and drivers which transport the spent fuel.

Current NRC regulations require spent fuel casks to meet certain performance standards. The performance standards include normal and hypothetical accident conditions which a cask must be capable of withstanding without exceeding established acceptance criteria that

- (1) limit the release of radioactive material from the cask,
- (2) limit the radiation levels external to the cask, and
- (3) assure that the spent fuel remains subcritical.

This study evaluates the possible mechanical and thermal loads generated by actual and potential truck and railroad transportation accidents. The magnitudes of the loads from accidents are compared with the loads implied from the hypothetical accident conditions. The frequency of the accidents that can produce defined levels of mechanical and thermal loads are developed from the accident data base. Using this information, it is determined that

for certain broad classes of accidents, spent fuel casks provide essentially complete protection against radiological hazards. For extremely severe accidents--those which could impose loads on the cask greater than those implied by the hypothetical accident conditions--the likelihood and magnitude of any radiological hazards are conservatively estimated. The radiological risk is then estimated and compared with risk estimates previously used by the NRC in judging the adequacy of its regulations.

The results of this study depend primarily on the quality of the cask response models, the radiation release models, and the probability models and distributions used in the analysis. Models for cask responses, radioactive releases, and distributions for the accident parameters are new developments based on current computer codes, limited test data on radioactive releases, and limited historical accident data. The results are derived using representative spent fuel casks which use design principles and materials that have been used in casks currently licensed by the NRC. The representative casks are assumed to have been designed, manufactured, operated, and maintained in accordance with national codes and standards (or equivalent) which have adequate margins of safety embedded in them. The results of this study are limited to spent fuel casks designed and fabricated under current technologies and operated under current regulations. New designs using alternative design principles and materials, or changes to regulations such as the imposition of a 75 mph national speed limit, could affect the results and conclusions of this study.

This study does not consider the effects which human factors can have on the cask design, manufacture, operation, and maintenance. If further study is conducted, human factors should be considered because they can contribute to the overall risk in each phase of transporting spent fuel.

L. E. Fischer

## ACKNOWLEDGEMENTS

The authors wish to acknowledge the technical contributions made to this report by R. C. Chun, L. L. George, T. E. McKone, and M. W. Schwartz of Lawrence Livermore National Laboratory. The authors wish to thank G. E. Cummings of Lawrence Livermore National Laboratory for his report review and comments. The authors also wish to thank J. R. Cook, W. R. Lahs, and W. H. Lake of the U.S. Nuclear Regulatory Commission for their support and comments during the research and preparation of this report. Many thanks to N. J. Barnes and E. A. Sturmer for report preparation and D. Bowden for report editing.

In addition, the authors would particularly like to thank the following organizations for providing information and counsel which were used in preparing this report:

Anatech International Corporation  
Association of American Railroads  
Bureau of Motor Carrier Safety  
California Department of Transportation  
Central Electricity Generating Board, England  
Denver Research Institute  
Department of California Highway Patrol  
Electric Power Research Institute  
Engineering Computer Corporation  
Federal Highway Administration  
Federal Railroad Administration  
Health and Safety Executive, England  
Los Alamos National Laboratory  
National Fire Protection Association  
Oak Ridge National Laboratory  
Ridihalgh, Eggers and Associates, Inc.  
Sandia National Laboratories  
Southern Pacific Transportation Company



## 1.0 INTRODUCTION

This report addresses the level of safety provided during the shipment of spent fuel from nuclear power reactors. The number of shipments will increase in the near future because of the need to transfer this fuel from the nuclear power reactors to a waste repository. During the shipments the shipping containers (casks) carrying the spent fuel could be exposed to severe highway and railway accident conditions. At the request of the U.S. Nuclear Regulatory Commission (NRC) the Lawrence Livermore National Laboratory (LLNL) has performed studies to evaluate and document the response of spent fuel casks exposed to severe highway and railway accident conditions.

### 1.1 Background

Nuclear fuel, contained in fuel rods, is used in nuclear power reactors to generate useful heat for electric power generation. The fuel rods used in most nuclear power reactors in the United States are made up of approximately one-half-inch-diameter ceramic pellets of uranium oxide encased within a cylindrical cladding. The fuel rods are approximately 15 feet in length. The cladding is made from metallic materials such as zirconium. After being capped, the cladding provides a contained environment for the uranium oxide fuel pellets. Depending on the type of nuclear power reactor, square arrays of the fuel rods numbering from about 50 to 300 are structurally assembled to form a single fuel bundle.

When nuclear fuel burns or fissions, it not only generates useful heat, but also creates radioactive fission products. Spent fuel is nuclear fuel that has been burned to its specified limits and has served its useful purpose. Spent fuel is highly radioactive when initially removed from a nuclear power reactor. Before being transported to a waste repository, spent fuel is usually stored five or more years in the spent fuel pool at the reactor site to allow the fuel to cool or decay to lower radiation levels.

Because of its radioactive nature, spent fuel is shipped in specially designed shipping containers called casks. These casks are massive, cylindrically shaped objects weighing from 25 to more than 100 tons. The

designs of several currently used casks consist of steel shells enclosing a dense metallic material (lead or depleted uranium) that is used to provide radiation shielding. In the United States, these casks must be certified by the U.S. NRC as being in compliance with the regulations contained in Title 10 of the Code of Federal Regulations, Part 71 (10 CFR 71).<sup>1</sup> These regulations, which are almost identical in substance to internationally accepted standards, have been in effect for nearly 20 years. The regulations are intended to assure that the public will be protected both during normal transportation or in the event that a spent fuel shipment is involved in a transportation accident.

Basically, the regulations state that each spent fuel cask must meet certain containment, radiation control, and criticality control requirements when it is subjected to specified normal transport conditions and also hypothetical accident conditions. The hypothetical accident conditions are of most interest to this discussion. They are specified in terms of regulation defined test conditions that include a free drop (30 feet onto a flat unyielding surface), a puncture (40-inch drop onto a vertical 6-inch-diameter mild steel bar), thermal exposure (30 minutes to a defined 1475<sup>o</sup>F environment), and immersion under specified depths of water. The test conditions must be sequentially imposed on all casks in a manner that would cause maximum damage. The resulting cask response must then be determined by test or analysis.

The regulations do not define the allowable structural or thermal damage a cask may sustain, but instead use radiological criteria, i.e., radioactivity release (leakage) and radiation levels external to the cask as a measure of the acceptability of the design. The cask response must be such that the cask can (1) meet containment requirements (any radioactive material release must be restricted within extremely small limits), (2) keep radiation levels external to the cask within stated limits, and (3) ensure that a criticality event cannot occur. In more practical terms, these compliance criteria require the cask structural integrity to be effectively unimpaired.

Historically, the few shipments of spent fuel that have been involved in transportation accidents have never created any significant radiological hazard. However, the number of these events has been limited. To quantify the radiological risk to the public from all shipments of radioactive material, including spent fuel, the NRC published, NUREG-0170, in 1977 entitled, "Final Environmental Statement on the Transportation of Radioactive Material by Air and Other Modes."<sup>2</sup> The study was primarily performed using conservative engineering judgments. The analysis performed in that document presumed that, in certain classes of accidents, transportation accident loads could exceed those implied by the hypothetical accident conditions specified in the regulations. The analysis further presumed that for these classes of accident, releases of radioactive material could occur. Even under these presumptions, the analysis indicated that the potential radiological hazards from real transportation accident loadings on a spent fuel cask were most often very small (i.e., limited to minor property contamination which required only cleanup actions). Since no release of spent fuel material has ever occurred, this assessment is consistent with historical events. Even though NUREG-0170 presumed the release of radioactive material under certain severe accident circumstances, the overall resulting radiological risk from transporting spent fuel under current regulations was calculated to be acceptable.

Nevertheless, because of the lack of actual data on the real effects of severe accidents on spent fuel casks, studies were initiated by the NRC prior to this work to define more precisely (1) the variability of mechanical and thermal loads which could be experienced by a cask in recorded severe railway and highway accidents, and (2) the degree to which these loads might exceed those implied by the hypothetical accident conditions.<sup>3</sup> In order to better understand the effectiveness of current regulations, this recorded severe accident information supplemented with other accident data has been used by the LLNL, working under contract to the NRC, to evaluate the responses of spent fuel casks exposed to severe highway and railway accident conditions. This report documents the work performed under this contract.

## 1.2 Regulations and Past Assessments

### 1.2.1 Title 10, Code of Federal Regulations, Part 71

To protect the public health and safety, commercial shipments of spent fuel are required to be made in spent fuel casks which are designed, fabricated, and operated in accordance with provisions of 10 CFR 71. The three basic safety requirements addressed by the regulations and which must be met when transporting spent fuel are:

1. Adequate containment of radioactive material
2. Adequate shielding of the radiation emitted by the radioactive contents
3. Prevention of nuclear criticality.

The containment requirements, as they apply to spent fuel shipments, impose a limit on radioactive material releases following the application of certain mechanical and thermal loadings on a spent fuel cask. The loadings are imposed by a series of test conditions called hypothetical accident conditions. The radioactive material release limits include a value for the relatively innocuous inert gas,  $^{85}\text{Kr}$ , ( $\leq 10,000$  curies in one week) and a separate limit on other releases over a 1-week period (called an  $A_2$  quantity). These limits on specific radioactive material releases are such that the doses to members of the public can be expected to be less than the allowable annual dose to individuals whose occupation involves potential exposure to radiation.

The shielding requirement following the application of the hypothetical accident condition is stated in terms of an external radiation dose rate at 1 meter from the external surface of the cask. This radiation level must not exceed one rem per hour.

The prevention of criticality under accident conditions is achieved by cask design features which assure subcriticality. This subcriticality must be achieved assuming (1) optimum (most reactive) configurations of the spent fuel consistent with the cask damage imposed by the hypothetical accident conditions and (2) most reactive conditions associated with the presence of water. (Water or other materials which act as neutron moderators or reflectors enhance criticality possibilities when in close contact with spent fuel.)

The safety requirements of 10 CFR 71 play an important role in this study because they provide a benchmark for relating a specific magnitude of mechanical or thermal loading (implied by the hypothetical accident conditions) to a specified level of cask response. For example, in practice, the containment limits are usually met by demonstrating that the cask containment experiences essentially no permanent deformations and the closure seals and penetration remain essentially leak tight (Fig. 1-1). The external dose rate limit is met by demonstrating that essentially no loss of the gamma shield occurs under accident conditions. Finally, the prevention of criticality requirement is typically met by demonstrating that essentially no deformation occurs to the basket, the structure within the cask which holds the spent fuel. These limits serve as benchmarks against which cask responses in real accident conditions can be compared.

One particular cask design feature is especially significant in ensuring that a spent fuel cask will meet the containment, shielding, and subcriticality requirements when the cask is subjected to the 30-foot drop onto the unyielding surface called for by 10 CFR 71. This feature is called an impact limiter (Fig. 1-1). Impact limiters reduce the mechanical loads to the main cask body under accident conditions.

Impact limiters are typically made of crushable material surrounding the extremities of a cask, but designs can also include the use of crushable exterior metal fins. In either case, the impact limiters are designed to absorb most of the energy generated in the regulatory-defined 30-foot drop onto the unyielding surface without causing any significant permanent damage to the cask containment or closure features.

The significant point is that, through the response of this design feature, a load level is defined which translates into no cask containment damage and, therefore, essentially no radiological hazard. For those real accidents which result in mechanical loads less than this limit, the radiological hazard is insignificant.

Similarly, protection against the regulatory-defined thermal loading conditions is typically provided by the use of thermal barriers. Thermal

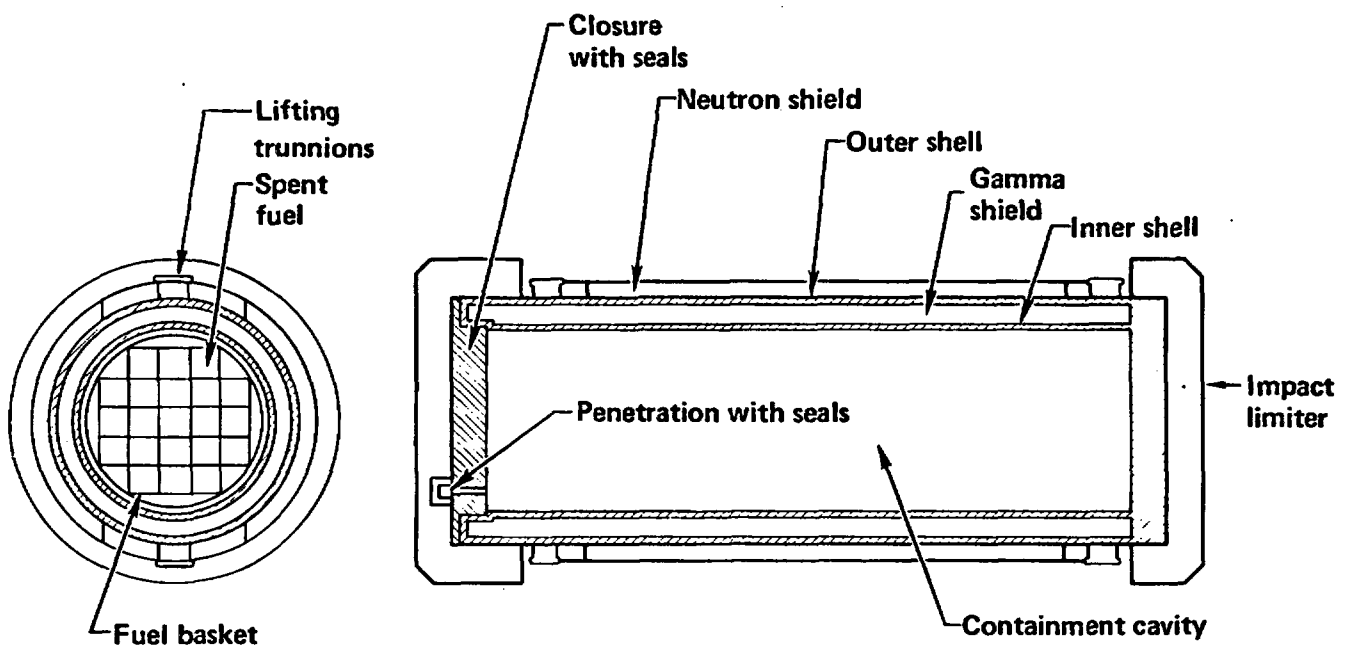


Figure 1-1 Schematic of a typical spent fuel cask.

barriers limit the heat transfer from a fire or thermal source external to the cask, to the cask containment structure, and to the contained spent fuel. Again, real world accidents involving fire can be compared with this defined thermal loading. These types of comparisons form the essence of the first-stage of a screening process used in this study.

### 1.2.2 Transportation of Radioactive Material - Environmental Statement (NUREG-0170)

In December 1977, the NRC published NUREG-0170, "Final Environmental Statement on the Transportation of Radioactive Material by Air and Other Modes".<sup>2</sup> The report included an assessment of the likelihood and magnitude of the radiological consequences associated with potential transportation accidents for all shipments of radioactive material. Most shipments consisted of medical and industrial isotopes, but spent fuel shipments were specifically addressed. The assessment indicated that the radiological risk involved in all shipments was small. This conclusion provided the technical basis for the Commission's decision that the existing 10 CFR 71 regulations are adequate and not in need of immediate change.

The NUREG-0170 analysis provides an additional benchmark for this study. Specifically, the radiological risk from spent fuel shipments reported in NUREG-0170 can be compared with the risk estimated in this study. In NUREG-0170, accident severities were divided into eight categories. For each category, the radiological hazards were assigned based on conservative engineering judgments. These hazards were measured in terms of the fraction of radioactive material released from the spent fuel and an equivalent fraction caused by shine from any unshielded fuel. For truck and rail accidents, the estimates in NUREG-0170 indicated that 91% of truck accidents and 80% of train accidents would result in no significant radiological hazard. In the remaining accidents, the radiological hazards increased as the accident severity increased. The increase is indicated in Table 1.1. As a point of reference, NUREG-0170 indicated that 0.4% of truck accidents and 0.2% of train accidents could involve a complete release from the cask of certain gaseous and volatile materials. These materials represent the radioactivity

Table 1.1  
Correlation of NUREG-0170 Accident Fractional Occurrence and  
Radiological Hazards as a Function of Accident Severity

Accident Severity Category	Truck Fractional Occurrences	Train Fractional Occurrences	Radiological Hazards	
			Fraction of Radioactive Material Released <sup>a/</sup>	Fraction of Equivalent Unshielded Fuel <sup>b/</sup>
I	0.55	0.50	0	0
II	0.36	0.30	0	0
III	0.07	0.18	0.01	0
IV	0.016	0.018	0.10	0
V	0.0028	0.0018	1	0
VI	0.0011	$1.3 \times 10^{-4}$	1	$3.18 \times 10^{-7}$
VII	$8.5 \times 10^{-5}$	$6.0 \times 10^{-5}$	1	$3.18 \times 10^{-5}$
VIII	$1.5 \times 10^{-5}$	$1.0 \times 10^{-5}$	1	$3.12 \times 10^{-3}$

a/ Radioactive gases and vapors

b/ Approximates the reduction in radiation shielding

which typically migrates from the fuel pellets to the fuel rod gap, the void space between the fuel pellets and the surrounding fuel rod. In this small percentage of accidents, all the fuel rods in the shipment were assumed to fail and to release their radioactivity.

Also, for accidents in Category VI and greater, a reduction of shielding was assumed. To provide a consistent measure of the radiological effects with cask damage, the radiological hazard due to the reduction in shielding was presented in terms of an equivalent fraction of unshielded fuel. The equivalent fraction of unshielded fuel is the ratio of that portion of the total spent fuel inventory that, if unshielded, would produce radiation levels equivalent to those being emitted from a damaged cask with reduced shielding.

The results of NUREG-0170 rely in part on the presumption that spent fuel casks have sufficient margins designed into them that major radioactive hazards will not occur even at loading conditions which exceed those specified in regulations. These margins of safety are included in all licensed cask designs through the use of established codes and standards which have margins of safety embedded in them.

The evaluation conducted in this study analyzes the response of representative shipping casks in severe accident environments. This evaluation uses representative cask designs that are likely to be licensed and have margins of safety included in their designs. The responses of the representative casks to all possible accident conditions are analyzed and categorized into cask response regions. For each cask response region, assessments are made of the potential for release of radioactive material and the potential for reducing the radiation shielding capabilities of the cask. This evaluation is the basis for a comparison with NUREG-0170; that is, what accident classes result in radiological hazards and how do those hazards and their likelihoods compare in terms of radiological risk to the public.

### 1.3 Objective and Approach

The objective of this study, the Shipping Container Response to Severe Highway and Railway Accident Conditions, is to estimate the adequacy of

radiological protection offered the public by the current NRC regulations when highway or railway accidents occur involving spent fuel shipments. The estimates are performed using data from real accident histories of similar types of vehicles and using models of cask designs that have a likelihood of meeting requirements for spent fuel shipments.

A two-stage screening process is used. The screening process is illustrated in Fig. 1-2. The first stage compares cask responses to accident loading conditions with those associated with the accident test conditions specified in 10 CFR 71. As an example of such a comparison, cask loadings from a class of accidents involving impacts exceeding 30 mph (the velocity reached in the 30-foot drop) are examined.

An example of such an accident class is the accident scenario involving a 60-mph collision with a highway sign pole. The cask loading in this scenario is such that no damage occurs to the containment, radiation shielding, or subcriticality assurance features of the cask, even though the accident velocity exceeds the regulatory-implied impact velocity. The reason is that although the accident velocity is twice the regulatory defined velocity, the loading imposed on the cask in the 30-foot drop test far exceeds the loading achieved on impact with the sign pole. The pole failure essentially limits the load to which the cask is exposed.

There are classes of accidents in which the loading can be conceived to approach or exceed the values imposed by the accident test conditions. Examples of these classes are high-speed impacts with massive bridge abutments and falls from great heights onto hard rocks. Sophisticated analysis can be used in many cases to demonstrate that the loadings on a cask are still less than those imposed by the regulation-defined hypothetical accident conditions. However, questions arise involving the specifics of a particular cask design and the orientation of impact (i.e., does the orientation assumed cause maximum damage). On the analysis side, the validity of analytical methods used to predict the cask response can be questioned. A major part of this report is directed toward demonstrating what broad classes of real-world accidents and their associated loadings are enveloped by the loadings implied

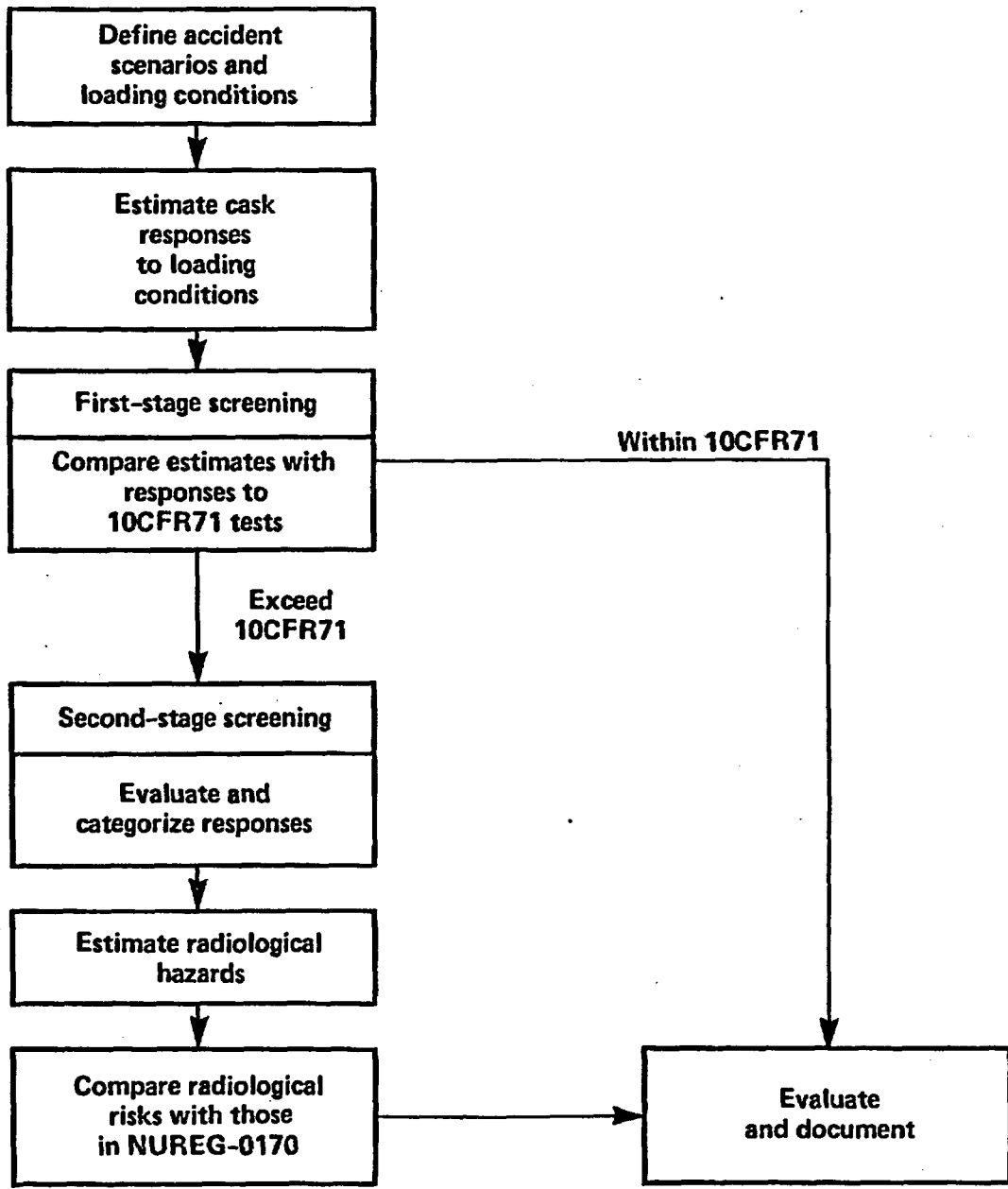


Figure 1-2 Two-stage screening process used in evaluating the regulations.

in the current regulatory standards. The first-stage screening envelopes accident loading conditions whose magnitudes do not exceed those defined by the accident test conditions and, therefore, the potential radiological hazards are less than those implied by regulations.

For those accident scenarios with loads and cask responses greater than those implied by the accident test conditions, a second-stage screening is performed. This screening evaluates the likelihood of the cask responses.

The potential radiological hazards associated with the cask responses are then determined. By summing all accident scenarios, the probability and magnitude of the radiological hazards is estimated and then compared with the risk evaluated in NUREG-0170.

Because of the numerous variables involved in defining cask loading and response, and because of the broad range of possibilities and interrelationships for each of the variables, a systematic scheme is developed to accomplish the two-stage screening process and to assess the effectiveness of 10 CFR 71 in assuring adequate radiological protection to the public. To describe this systematic process, this report is arranged into several sections. Many tasks are performed: model developments, data sources, data development, analysis of models, classification, and comparison of results. Although the tasks are described in the report by sections, the separate tasks are not developed independently, and they cannot be described without considering the interrelationship involved.

Figure 1-3 shows the interrelationship of the various tasks and how they influence the performance of the analysis. The initial tasks in this study involve developing models for casks and accident environments. Methods are also developed for evaluating how the cask models respond to accidents and for classifying their responses into response regions. The screening analyses are performed by subjecting the casks to the accident events identified in the accident scenarios, determining the predicted responses of the casks to these events, and classifying these predicted responses into the response regions. The cask physical responses are then related to any resulting radiological hazards. Because the likelihood or probability associated with an accident

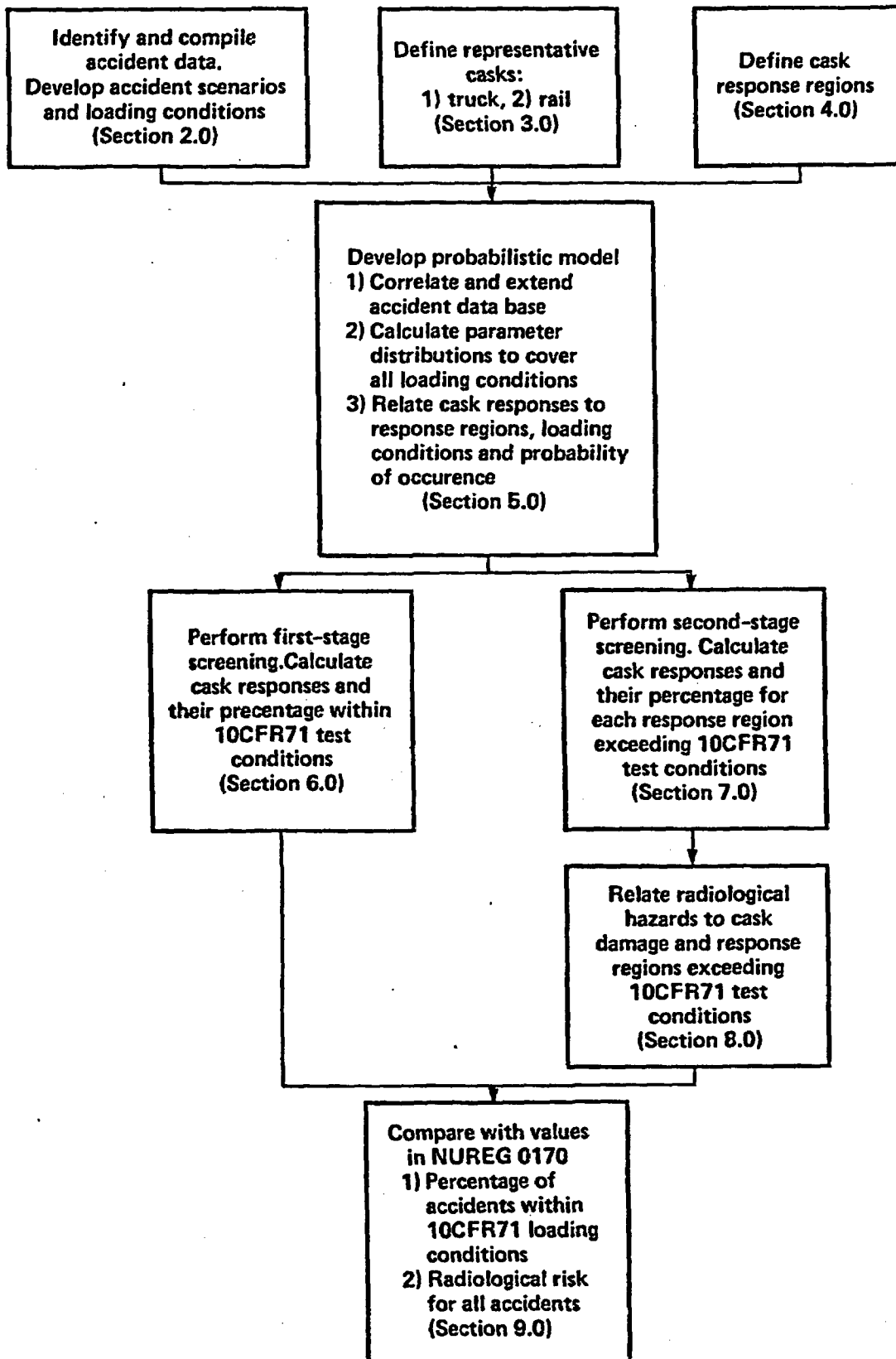


Figure 1-3 Schematic representation of the report.

event can be derived from accident data, the probability associated with the response and radiological hazard can be estimated.

In Section 2.0, the mechanical and thermal loads associated with real accidents are discussed. Also, accidents are classified into accident scenarios to systematize the analysis. Statistical accident data have been used and enhanced where necessary to establish likelihood estimates for the occurrence of those mechanical and thermal accident loads determined to be important to cask response. The mechanical loads are described in terms of parameters such as velocity of the cask, the hardness of the object that the cask hits, and whether the crash is head-on, glancing, or at some intermediate direction. The thermal loads are described in terms of location, temperature, and duration of a fire.

In Section 3.0, two casks are defined as representative of those used for ground transportation of spent fuel, one for highway and one for railway. The details and justification for selecting the representative cask designs are explained. The margins of safety included in their designs are discussed.

Cask response regions are specified in terms of the physical response of the cask to accident events. The response regions are described in Section 4.0; they are represented as strain for mechanical loads, and as temperature for thermal loads. The strains from mechanical loads and temperatures created by thermal loads which define the response regions are related to deformations and degradation of the cask's containment and shielding system. Deformation and degradation of the cask's containment and shielding systems can result in specific radiological hazards for each of the response regions. Details for relating radiological hazards to the response regions are found in Section 8.0.

In Section 5.0, the probabilistic model used in the analysis is described. The formulations used to relate cask responses to loading conditions, response regions, and the probability of occurrence are described. Techniques also are developed for calculating the probability for combined loading conditions for each accident scenario.

In Section 6.0, the first-stage screening process is described. The first step in this process is to subject the casks to each accident scenario identified in Section 2.0 and to estimate the responses. The responses are sorted into the response regions. The appropriate response region for the first-stage screening is the lowest response region since it is defined to encompass 10 CFR 71 accident test conditions. Since the accident rates are known, the fraction of accidents falling into each response region can be determined.

In Section 7.0, the second-stage screening process is described. The accidents not falling into the lowest response region are analyzed and the responses calculated. These responses are then categorized into the other response regions.

In Section 8.0, the radiological hazards associated with each cask response region are estimated. The radioactive material releases are estimated from laboratory test data. The radiation increases caused by lead slump are estimated from structural, thermal, and shielding calculations.

Finally, in Section 9.0, the results of the two-stage screening process are presented with respect to NUREG-0170. The conclusion reached is that at least 99.4% of truck and train accidents involving a spent fuel shipment will result in negligible radiological hazards which are less than those implied by the current 10 CFR 71 regulations. Of the remaining spent fuel shipment accidents, the overall radiological risk is less than the risk estimated in NUREG-0170.



## 2.0 ACCIDENT RATES, ACCIDENT SCENARIOS, AND LOADING PARAMETER DISTRIBUTIONS

### 2.1 Introduction

Severe accidents are typically characterized and reported by fatalities, injuries, property damage, transportation equipment damage, or a combination of these consequences. In this study, however, the characterization is in terms of the magnitude and frequency of loads that could be experienced by a spent fuel cask under accident conditions. Normally the higher the load on a cask, the higher the cask response and the greater the potential for radioactive release.

Both mechanical and thermal loads generate response states for a cask which could result in damage to the cask. High mechanical loads caused by impact can cause damage to the cask shielding or cause the cask containment to leak. High thermal loads caused by fires can cause the cask containment seals to deteriorate and leak or the lead shield to melt. In performing the two-stage screening process of accidents discussed in Sections 6.0 and 7.0, all possible accidents have to be included, especially those that could cause high mechanical and thermal loads on a cask.

Mechanical and thermal loads depend on the magnitudes of the accident loading parameters. Two examples of accident loading parameters and their magnitudes are a velocity of 50 mph and a fire duration of one hour. The same accident-caused load on a cask can occur for various combinations of loading parameters and loading magnitudes. For example, the same impact force on the cask can be generated by a low-velocity impact on a hard object or a high-velocity impact on a soft object. Also, the same heat load on a cask can occur for a short duration high-temperature fire or a long duration low-temperature fire. Consequently, specific mechanical and thermal loading conditions on the cask can occur under a variety of accident conditions.

Accident loading conditions must take into account many loading parameters and must include a wide range of values for each loading parameter. Accident scenarios can be derived from historical records. An accident scenario describes a sequence of events as they occur, allowing the

identification of possible loading conditions. For example, an accident scenario can involve a truck running off the highway, going over an embankment, and crashing into a rock. The loading conditions for this scenario primarily depend on the hardness of the rock, the velocity of the truck when it hits the rock, the direction of the truck velocity, and the orientation of the truck with respect to the rock. By varying these four parameters, thousands of loading conditions are possible for one accident scenario.

In order to evaluate all possible accident loading conditions on a cask, the following accident information is derived in this section:

- (1) Accident rates for spent fuel shipments are estimated from historical accident records for truck and train accidents for similar vehicles.
- (2) Accident loads that dominate the accident loading conditions and the structural and thermal responses of spent fuel casks are identified. The significant loading parameters for the dominant accident loads are identified.
- (3) Accident scenarios, to include all possible accident loading conditions for truck and train transport, are identified. Accident data, survey results, and engineering judgment are used to establish accident loading parameter distributions.

The accident information derived in this section is used with the probabilistic computer code called TASP (Transportation Accident Scenario Probabilities) described in Section 5.0 to calculate and screen the expected magnitude and frequency of cask responses to accident conditions.

In Sections 2.2 and 2.3, the expected accident rates for spent fuel shipments by highway and railway are estimated. In Section 2.4, the accident data required to estimate the accident loads on a cask are identified. In Sections 2.5 and 2.6, the accident scenarios and loading parameter distributions are discussed.

## 2.2 Highway Accident Rates

Highway accident rates depend on many elements including road type, vehicle type, regulations, and driving practices. The accident rate for all vehicles on California highways during 1981 through 1983 ranged from  $1 \times 10^{-6}$  accidents/vehicle-mile for freeways with limited access to  $5 \times 10^{-6}$  accidents/vehicle-mile for conventional four-lane highways.<sup>1</sup> Studies by the U.S. Department of Transportation (DOT) have indicated that accident rates are significantly lower for interstate federal highways (usually freeways) than for other road types. Routes for transport of spent fuel are selected in accordance with the DOT regulations to minimize the radiological risk. In general, the routes follow interstate federal highways.<sup>2</sup>

As discussed in Appendix B, two sources are used for estimating a typical accident rate for spent fuel transportation. An average accident rate of  $2.5 \times 10^{-6}$  accidents/vehicle-mile is derived from the data published by the Bureau of Motor Carrier Safety (BMCS) for all roadways.<sup>3-5</sup> Their data covered all truck and carrier type accidents from 1960 through 1972. The second data source is the American Petroleum Institute (API) for the period of 1968 through 1981 for all roadways.<sup>6-10</sup> The average accident rate is  $6.4 \times 10^{-6}$  accidents/vehicle-mile or approximately 2.5 times higher than that based on the BMCS data. For this study the API accident rate is used as the estimate for spent fuel truck accident rates because the data is judged to be more reliable, and trucks which transport hazardous petroleum materials are similar in size and weight to trucks that transport spent fuel casks. The use of the more conservative API value is not critical to the results of this study.

## 2.3 Railway Accident Rates

Train accident rates depend on many elements including the type of train, the type of track, and the reporting requirements. Freight trains are used to transport spent fuel over all track types and are subject to Federal Railroad Administration (FRA) reporting requirements. Because over 90% of all train mileage is attributed to freight trains, there is no significant difference in applying data based on all trains to freight trains in order to estimate accident rates, accident velocities, fire frequencies, etc.

Appendix C discusses the train accident rate selected for spent fuel shipments by train. Based on the FRA data for all train and track types, an accident rate of  $1.2 \times 10^{-5}$  accidents/train-mile is assumed for spent fuel rail shipments.<sup>11-17</sup>

#### 2.4 Accident Loading Data Requirements

Historical data bases on transportation accidents exist at all government levels. These data bases range from local accident records to state and national accident statistics. Typically, these records include many accident conditions and consequences that are not pertinent to this study, including weather conditions, fatalities, injuries, and property damage. However, some of the data are pertinent to this study; namely, data pertaining to accident loading conditions which could cause cask damage. Typical of such data are estimations of accident velocities, descriptions of objects impacted, and duration of fires. Most of these data bases are compiled to aid general transportation safety with the main focus on reducing injuries, fatalities, and property damage. They do not always include all the information necessary to define the loading a cask might experience. Therefore, specific data necessary to estimate accident loads on a cask are not always available.

Table 2.1 presents mechanical and thermal loads that can occur in an accident. The accident loading parameters that cause the loads and affect the response of the cask for various load types are also listed.

Mechanical loads include forces on the cask caused by impact with a surface or hard object, puncture by strong objects, and crushing by heavy objects. Based on the evaluation in Appendix E, it is concluded that impact loads are the dominant mechanical loads and have the greatest potential for causing significant structural damage to a spent fuel cask. Therefore, only impact loads and their associated loading parameters are used to perform the two-stage screening of accidents generating mechanical loads.

Mechanical loads from impacts can be analyzed using three loading parameters that affect the cask response and potential damage: impact velocity, orientation of the cask, and the hardness of the object impacted.

Table 2.1  
Accident Loads and Loading Parameters

Loading Parameter	Accident Loads					
	Mechanical Load Type			Thermal Load Type		
	Impact	Punch	Crush	Fire	Torch	Decay Heat <sup>a/</sup>
Object Hardness	X	X	X			
Impact Velocity	X	X				
Cask Orientation	X	X	X			
Object Weight	X	X	X			
Object Impact Area		X				
Flame Temperature				X	X	
Fire Duration				X	X	
Fire Location				X	X	
Flame Emissivity				X	X	
Convection Coefficient				X	X	
Surrounding Material						X

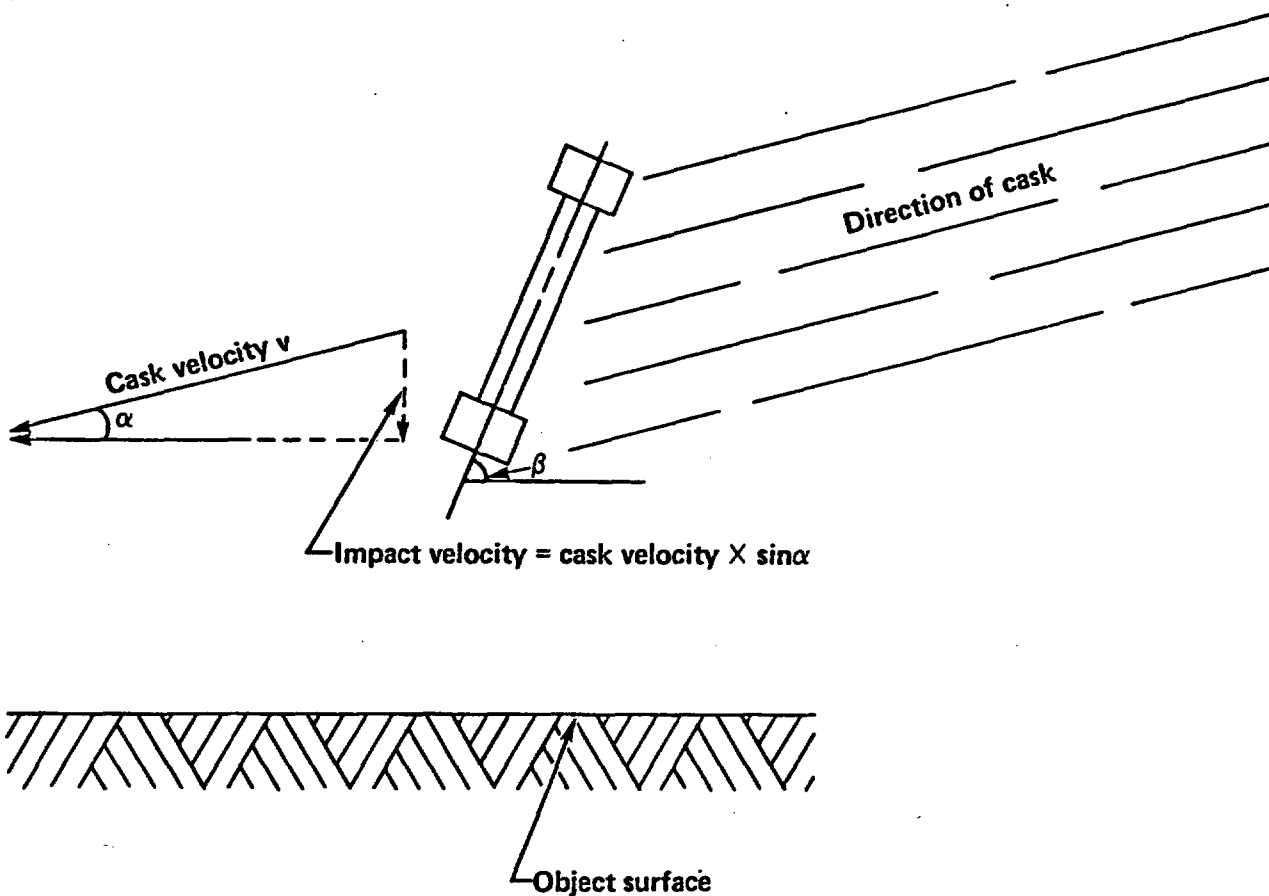
<sup>a/</sup> Decay heat from spent fuel cargo.

Figure 2-1 defines these three loading parameters. The impact velocity is the cask velocity perpendicular to the surface impacted. The angle of impact,  $\alpha$ , represents the angle between the cask velocity vector and the object's surface. When an accident occurs, the cask velocity vector can take any direction. However, it can always be decomposed into two components: one perpendicular to the impacted object surface and one parallel to it. The accident velocity is a function of reported vehicle velocity, braking effects, and fall heights from bridges or embankments. In the cask response calculations, only the velocity component perpendicular to the object surface is considered. The velocity component parallel to the object surface introduces a sliding-friction effect to the cask structure. The sliding-friction effect will not induce any significant structural deformation in the cask. In this study, the angle of impact is combined with the cask velocity to produce the cask impact velocity, i.e., impact velocity equals cask velocity times sine  $\alpha$  where  $\alpha$  is the angle of impact and the impact velocity is treated as a single loading parameter.

The angle defining the cask orientation,  $\beta$ , is the angle between the cask longitudinal axis and the object's surface. The cask orientation affects the cask response, particularly for endwise impacts ( $\beta = 90^\circ$ ) where lead slump can occur at high impact velocities.

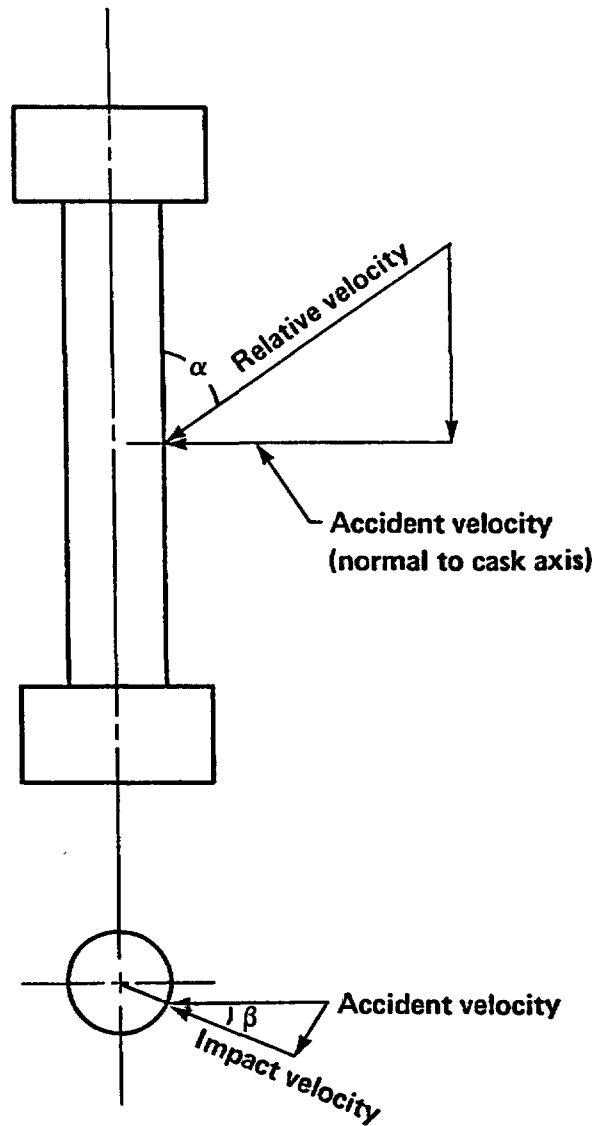
Object hardness needs to be considered because casks can strike objects such as concrete abutments, roadbeds, hard rock, soft rock, hard soil, and water. The hardness of the objects and the associated impact responses vary greatly. The weight of the object impacted can also affect the response of the cask. However, only massive objects can cause significant mechanical loads on a cask, hence the object hardness is the dominant parameter that is considered for objects impacted.

In some accidents, such as rail grade-crossing accidents, the impact limiters on the cask can be bypassed and the side of the cask can be struck directly. Once again the mechanical loads depend on the impact velocity, the orientation of the cask, and the hardness of the object struck. Figure 2-2 defines these three loading parameters for this type of accident. The impact



- o Object surface hardness
- o Impact velocity: Cask velocity component perpendicular to the object surface
- o Cask orientation is defined by angle  $\beta$ , the angle between the cask longitudinal axis and the object's surface

Figure 2-1 Three impact loading parameters considered in the response analysis for impacts on surfaces.



- o Object hardness
- o Impact velocity: Relative velocity component perpendicular to cask surface.
- o Cask orientation angle,  $\beta$ : the angle between the accident velocity and impact velocity.

Figure 2-2 Three impact loading parameters considered in the response analysis for impacts with objects such as train sills.

velocity is the component of the relative velocity of the cask and object that is perpendicular to the cask surface. The angle of impact,  $\alpha$ , represents the angle between the relative velocity direction and the cask axis. For the purpose of this study, the impact angle is conservatively assumed to be  $90^\circ$ , that is, perpendicular to the cask axis in all cases. Also, it is assumed that the impact occurs at the mid-plane of the cask to cause the most damage. The cask orientation angle,  $\beta$ , is the angle at which the impact occurs on the cask surface as shown in Fig. 2-2. In the worst case the cask is hit at  $0^\circ$  or head-on. For orientation angles near  $90^\circ$ , the cask is essentially not struck. The object hardness depends on the object hitting the cask, such as a train sill or a small bridge column.

The thermal loads identified in Table 2.1 include the heating of a spent fuel cask by large fires, both engulfing and non-engulfing; torch fires; and decay heat from the spent fuel, particularly when the cask is accidentally buried in debris. Based on the evaluation in Appendix F, it is concluded that heat loads from large fires, both engulfing and non-engulfing, have the greatest potential for causing significant damage to a spent fuel cask. Therefore, only heat loads from large fires and their associated loading parameters are used in the screening of accidents generating thermal loads.

Thermal loads from large fires depend on three loading parameters that affect the cask response and potential damage: fire duration, flame temperature, and fire location. The fire duration affects the amount of heat that is transferred into the cask--the longer the fire burns the greater the amount of heat that is absorbed by the cask. Higher flame temperatures cause greater amounts of heat to be transferred to the cask. As discussed in Appendix F, the flame temperature, assuming a flame emissivity of 0.9, is the single parameter used to characterize both radiation and convection heat transfer over a wide range of conditions. The location of the fire with respect to the cask affects the amount of heat that can be transferred to the cask. An engulfing fire would transfer the most heat to the cask, given the same flame temperature and fire durations, whereas less heat would be transferred from non-engulfing fires.

Accident records typically classify accidents into broad categories or types that describe, in general, the causes of the accidents. Examples are ran-off-the-road, overturn, and derailment. Accident scenarios describe a sequence of events and involve individual accidents that occur at specific velocities, impact specific objects at specific angles, and perhaps include a fire. For the purpose of this study, accident scenarios are specified and typically identified by the object impacted. By interpreting accident data bases in the context of these scenarios, the analysis is made manageable.

## 2.5 Highway Accident Loading Parameters

### 2.5.1 Mechanical Loading Parameters

Three mechanical loading parameters have been identified which can affect the structural response of a cask in a severe accident: object hardness, impact velocity, and cask orientation. The distribution functions for these parameters can differ with each specific accident scenario. The object hardness distribution is derived from the truck accident data base. For accident scenarios that could cause high mechanical loads on a cask, impact velocity distributions are estimated from truck and train accident velocity data, bridge height data, and engineering models. No specific data is available to estimate cask orientation on impacts; therefore, distributions are estimated from engineering models.

#### 2.5.1.1 Accident Scenarios and Object Hardness

Data from several sources are collected and combined in Appendix B to estimate the frequency of specific accident scenarios and potential impacts on specific objects of varying hardness. The accident scenarios are primarily based on truck accident data documented in the BMCS annual reports for the years 1973 through 1983.<sup>18-27</sup> The BMCS accident data are for all truck sizes and all roadways including city streets, county roads, state and interstate highways.

Figures 2-3 and 2-4 list the truck collision and non-collision accident scenarios used to categorize the response of spent fuel casks to accident loads. Thirty-one scenarios, each identified with an accident index number, are presented. By combining historical accident records with a survey of highway roadside structures, the probability associated with each accident scenario is estimated in percent. For example, a truck can be involved in a collision accident, hit a bridge railing, run over the bridge, and drop into water below (accident index 7 in Fig. 2-3). This scenario describes a sequence of events involving many different accident features such as collision objects, bridge railings, and water.

An example will be used to illustrate how this probability estimate is made. Figure 2-3 shows that 74.12% of truck accidents are collisions. Of these collision accidents, 11.95% involve hitting a roadside fixed object. The probability that the roadside object is a bridge railing is 5.77%. The probability that the truck, after hitting the bridge railing, breaks through the bridge railing and lands in the water is 20.34%. Therefore, the fractional occurrence for the example scenario is 0.104% given that a truck accident occurs. Multiplying this fractional occurrence by the assumed truck accident rate of  $6.4 \times 10^{-6}$  accidents/vehicle-mile gives the chance of this kind of accident occurring per mile traveled as  $6.7 \times 10^{-9}$ .

#### 2.5.1.1.1 Collision Accident Hardness Data

Figure 2-3 summarizes collision accident scenarios and the frequencies of collisions with moving objects such as trucks, autos, and trains as compiled from the BMCS data. Over 56% of the truck accidents involve collisions with another truck or auto. The BMCS accident data did not classify collisions with fixed objects, even though they ranged from stop signs to bridge columns. To classify fixed objects, highway accident data are obtained from the California Department of Transportation (CALTRANS) reports of stationary objects struck along state and interstate highways for the years 1975 through 1983.<sup>28-36</sup> Those objects in the CALTRANS survey are tabulated and a fraction calculated for each type of fixed object. These fractions are then applied to the fixed object collision accidents in the BMCS data to estimate the number of accidents involving each type of object, such as a bridge rail or column.

		Probability percent**	Accident index			
Truck accident $8.4 \times 10^{-6}$ per mi.	Collision 0.7412	'Soft objects' cones, animals, pedestrians 0.0521	3.4002 1			
		Motorcycle 0.0124	0.8093 2			
		Automobile 0.6612	43.1517 3			
		Truck, bus 0.2041	13.3201 4			
		Train 0.0118	0.7701 5*			
		Other 0.0584	3.8113 6			
		On road fixed obj. 0.1195	Bridge railing 0.0577	Water 0.20339	0.1039 7*	
				Railbed/roadbed 0.77965	0.3986 8*	
				Clay, silt 0.015486	0.0079 9*	
				Hard soil, soft rock 0.001262	0.0006 10*	
				Hard rock 0.000199	0.0001 11*	
				Column, abutment 0.0042	Small 0.8289	0.0299 12*
					Large 0.1711	0.0062 13*
				Abutment 0.0382	0.0011 14*	
				Concr. obj, bottom str. 0.0096	0.0850 15	
				Wall barrier, wall, post 0.4525	4.0079 16	
		Signs, cushions 0.0577	0.5111 17			
		Curb, culvert 0.4183	3.7050 18			
Non-collision 0.2588	See figure 2-4 for non-collision accidents →					

\* Potentially significant accident scenarios

\*\* Conditional probability which assumes an accident occurs

Figure 2-3 Truck collision accident scenarios and their percent probabilities.

Truck accident	Probability percent**	Accident index
Collision 0.7412	See figure 2-3 for collision accidents	
Non-collision 0.2588	Clay, silt 0.91370	2.3063 19*
	Into slope 0.2789	
	Hard soil/soft rock 0.07454	0.1881 20*
	Hard rock 0.01176	0.0297 21*
	Clay, silt 0.5654	1.3192 22*
	Off road 0.3497	
	Over embankment 0.2578	
	Hard soil/soft rock 0.0461	0.1076 23*
	Hard rock 0.007277	0.0170 24*
	Drain ditch 0.381223	0.8894 25
	Trees 0.1040	0.9412 26
	Other 0.3593	3.2517 27
	Impact roadbed 0.5336	
	Overturn 0.6046	8.3493 28
Jackknife 0.3954	5.4603 29	
Other-involving mech. loading 0.0792	2.0497 30	
Fire only 0.0375	0.9705 31	

\* Potentially significant accident scenarios

\*\* Conditional probability which assumes as accident occurs

Figure 2-4 Truck non-collision accident scenarios and their percent probabilities.

Based on the quasi-static screening analysis in Section 6.0 for mechanical loads and responses of the representative truck cask, only three significant accident scenarios can cause mechanical loads high enough to damage a spent fuel cask: collisions with trains and columns, trucks running off bridges and over embankments, and trucks running into slopes. Therefore, detailed accident loading information is compiled only for these significant scenarios.

Since collision accidents involving piers, columns, and abutments may lead to significant damage to a spent fuel cask, a survey is performed to differentiate among the various sizes of piers, columns, and abutments along state and interstate highways.<sup>37</sup> From the survey data, the fractional occurrence is determined for each pier, column, and abutment size and is used to estimate the probability of collision accidents involving piers, columns, and abutments. For example, the expected probability of collisions with large concrete abutments is estimated to be 0.0011% as given in Fig. 2-3.

In the event a truck runs off a bridge, the magnitude of the resulting impact load depends not only on the bridge height, but also on the surface being impacted below the bridge. A survey along Interstate 80 in California is performed to identify the types and frequency distributions of surfaces that could be impacted below the bridge.<sup>38</sup> These surfaces are classified into four categories: roadbeds, railbeds, water, and earth. The earth category is then subdivided into three sub-categories: soil, soft rock, and hard rock. The earth sub-category distributions are determined by the survey performed for "ran-off-the-road." Table 2.2 is a summary of the impact surface distribution under bridges.

#### 2.5.1.1.2 Non-Collision Accident Hardness Data

Non-collision accident scenarios include rollover, jackknifing, and running off the road. The accident scenarios judged to have greatest damage potential for a spent fuel cask are the ran-off-the-road scenarios. In these accidents, the truck could impact a slope or go over an embankment, with the possibility of hitting a hard rock such as granite.

**Table 2.2**  
**Fractional Occurrence of Surface Types below Bridges on**  
**Interstate 80 from Davis, California to Nevada Border**

Surface Type	Fractional Occurrence
Water	0.2034
Roads/Railways	0.7797
Earth	
Soil	0.0154
Soft Rock	0.0013
Hard Rock	0.0002

The hardness of earth surfaces adjacent to highways can vary over a wide range. This variability can have a significant effect on the loadings that could be imposed on a cask or any other impacting object. The water and land (hard rock, soft rock/hard soil, and tillable soil) distribution along proposed spent fuel shipment routes between the east coast and west coast is initially estimated using agricultural soil survey data and geological highway maps for the United States.<sup>39,40</sup> The initial distributions estimated from these sources are considered to be indicative of the types of surfaces which could be impacted along highways in the various regions of the United States. However, since highway construction and landscaping can greatly affect the adjacent surroundings, the initial distributions are used to select representative portions of Interstates 5 and 80 in California to perform detailed highway surveys and to establish final distributions along highways.

The types of earth adjacent to 133 miles of Interstate 5 through Orange and Los Angeles Counties in California are classified into three groups: tillable soil, non-tillable soil, and hard rock (Appendix D, Table D.2). Only tillable soil (92.8% fractional occurrence) and untillable soil, classified as soft rock (7.2% fractional occurrence), are identified on a total mileage basis. Although this survey included portions of the Santa Susana Mountain, no hard rock is identified in the survey.

A highway survey of soil types adjacent to the roadway is then performed on a section of Interstate 80 from Davis, California, to the Nevada border.<sup>38</sup> This 122 mile section of Interstate 80 crosses the Sierra where numerous outcroppings of granite rock occur. This survey (Appendix D, Table D.3) indicates the following earth distribution : tillable 90.2%, non-tillable 7.3%, hard rock 2.5%.

Based on the results of both highway surveys and the reviews of the agricultural soil surveys, the geological highway maps, and proposed spent fuel shipping routes, the representative earth distribution used in this study is tillable soil 91.4%, soft rock/hard soil 7.4%, hard rock 1.2%.

### 2.5.1.2 Impact Velocity

The impact velocity depends on the relative velocity of the cask and the angle of impact with respect to the object impacted. The distributions of these two variables are estimated from truck accident records, train accident records, highway surveys, and engineering judgments for the significant accident scenarios.

#### 2.5.1.2.1 Cask Velocity

The distribution of potential cask velocities can vary depending on the specifics of the accident scenario. Each accident scenario may have a different historically based velocity distribution. For example, the distribution of accident velocities experienced in truck-truck collisions differs from the distribution associated with accidents involving falls from bridges. In the truck-truck accidents, the distribution depends on the individual velocities of the trucks at collision. For accidents involving falls from bridges, the accident velocity is determined by the fall height. The accident velocity distribution for accident scenarios involving trucks running over or off embankments could, at worst, be represented by the vector sum of the vehicle velocity and the velocity attained in the resulting fall.

One of the following distributions of cask velocities at impact is considered applicable to a particular truck accident scenario:

V1: A distribution based on truck accident velocities with braking effects included,

V2: A distribution based on fall heights from bridges,

V3: A distribution based on truck accident velocities with braking effects and fall heights from bridges, or

V4: A distribution based on train accident velocities at grade crossings.

Reports record accident velocity data in many different forms. Most reports give the vehicle velocity prior to the accident. Therefore, it is difficult to estimate the actual velocity of impact which a cask can realistically experience.

Distribution V1 is determined by consideration of accident reports involving trucks/semitrailers. Table 2.3 gives the fraction of accidents occurring in the State of California for 1958 through 1967 for trucks/semitrailers as a function of truck velocity prior to the accident.<sup>41-51</sup> This accident data is derived from the California Highway Patrol's (CHP) annual report on fatal and injury motor vehicle traffic accidents. This data represents a sample of truck/semitrailer drivers involved in fatal and injury accidents and their estimated accident velocity without braking effects included. Approximately half of truck accidents occur at velocities greater than 30 mph. This velocity data is conservative because it does not include non-injury accidents, which typically occur at lower velocities.

Accident velocities for the State of California are compared with those in the states of Alabama, Texas, Virginia, and North Carolina.<sup>52-56</sup> The comparison is made for all vehicles because not all of the states had information on trucks. The comparison shows that the California accident velocities are comparable for the same conditions. Therefore, it is concluded that the accident velocities from California are representative of those in the nation and that the truck/semitrailer accident velocities for California provide a reasonable estimate of future accident velocities for spent fuel transport trucks. Accident data from North Carolina is used to estimate the effects of braking on the reduction of impact velocity. The method used to estimate the velocity reduction is described in Subsection 5.2.1.2.

Distribution V2, the velocity attained in falls from bridges is developed directly from a survey of bridge height data presented in Table 2.4.<sup>37</sup> This bridge height data is collected along Interstate 5 during the survey of bridge column sizes and types of soil along the highway. The bridge height distribution is reasonable for representing travel on interstate and state highways.

Table 2.3  
 Distribution of Velocities for Trucks/Semitrailers  
 Involved in Fatal and Injury Accidents in California, 1958-1967<sup>a/</sup>

Velocity (mph)	Number of Accidents	Fractional Percent (%)	Cumulative Percent (%)
0	1,774	6.41	6.41
1 - 10	4,143	14.96	21.37
11 - 20	4,122	14.89	36.25
21 - 30	4,248	15.34	51.59
31 - 40	4,733	17.09	68.69
41 - 50	7,264	26.23	94.92
51 - 60	1,173	4.24	99.15
61 - 70	171	0.62	99.77
>70	63	0.23	100.00
Subtotal	<u>27,691</u>	<u>100.00</u>	-
Not stated	2,834	-	-
Total	30,525	-	-

<sup>a/</sup>. Data derived from the 1958 to 1967 annual reports on fatal and injury motor vehicle traffic accidents, California Highway Patrol

Table 2.4  
 Distribution of Bridge Heights along Interstate 5  
 through Orange and Los Angeles Counties, California

Bridge Height (ft)	Number of Bridges	Fractional Percent (%)	Cumulative Percent (%)
0 - 10	5	4.13	4.13
11 - 20	22	18.18	22.31
21 - 30	74	61.16	83.47
31 - 40	14	11.57	95.04
41 - 50	3	2.48	97.57
51 - 60	1	0.83	98.34
61 - 70	1	0.83	99.17
71 - 80			
81 - 90	1	0.83	100.00
Total	<u>121</u>	<u>100.00</u>	-

Distribution V3 is developed for those accident scenarios in which the velocity is considered to be the vector sum of the accident velocity V1 and the fall velocity V2. This distribution is used for accidents that involve running off of embankments and into slopes.

Distribution V4 is used for accident scenarios involving train-truck collisions at grade crossings. The magnitude and frequency of the cask velocity is estimated from rail-highway grade-crossing accident velocity data. This accident data is derived from the FRA annual report on rail-highway grade-crossing accident/incident and inventory for the years 1975 through 1982.<sup>57-64</sup> Table 2.5 gives the fraction of rail-highway grade-crossing accidents as a function of train velocity. Fewer than 30% of the accidents occur at velocities greater than 30 mph.

#### 2.5.1.2.2 Impact Angle

The impact angle is the angle between the cask velocity and the plane of the surface struck. The damage caused in a transportation accident is not controlled solely by the vehicle(s) velocity at impact. A head-on impact is more severe than a sideswiping event, even though both accidents could involve similar accident velocities. The reason is that accident severity is most directly related to the vector component of the accident velocity perpendicular to the object being struck. The orientation of the vehicle, or in this case, cask motion relative to the plane or surface of the object impacted, is established by a parameter called the impact angle, depicted earlier as angle  $\alpha$  in Fig. 2-1. A  $90^\circ$ -impact angle defines the accident as head-on; that is, the impact velocity and accident velocity at impact are the same. An impact angle close to  $0^\circ$  defines the accident as a sideswiping impact; that is, the impact velocity is only a small fraction of the accident velocity. In mathematical terms the impact velocity is the accident velocity multiplied by the sine of the impact angle.

The distribution of impact angles can be expected to be a function of the accident scenario being considered. For example, if an accident involves a collision with another vehicle on the road, any impact angle is equally

Table 2.5  
 Train Velocity Distribution for Rail-Highway Grade-Crossing  
 Accident/Incidents Involving Motor Vehicles, 1975-1982<sup>a/</sup>

Velocity (mph)	Number of Accidents	Fractional Percent (%)	Cumulative Percent (%)
0 - 9	27,553	33.79	33.79
10 - 19	16,765	20.56	54.35
20 - 29	14,611	17.92	72.47
30 - 39	10,788	13.23	85.50
40 - 49	7,617	9.34	94.84
50 - 59	2,879	3.53	98.37
60 - 69	824	1.01	99.38
70 - 79	461	0.57	99.94
80 - 89	29	0.04	99.98
>90	17	0.02	100.00
Subtotal	81,544	100.00	-
Unknown	573	-	-
Total	82,117	-	-

<sup>a/</sup> Data derived from the 1975 to 1982 annual inventory on rail-highway grade-crossing accidents/incidents, Federal Railroad Administration

likely. Information on impact angle distributions is not readily available; however, three distributions are defined. The distributions include:

VV1: A uniform distribution in which any impact angle is equally likely,

VV2: A distribution which considers all impacts as  $90^{\circ}$  occurrences, and

VV3: A triangular distribution in which  $90^{\circ}$  impacts are most likely with other orientations decreasing in likelihood as the impact angle decreases.

### 2.5.1.3 Cask Orientation

Historical records do not contain significant information on the orientation of the cask with respect to the object impacted. For impacts on a surface  $0^{\circ}$  cask orientation defines a sidewise impact while a  $90^{\circ}$  cask orientation defines an endwise impact of the cask. Alternatively for impacts by train sills, a  $0^{\circ}$  cask orientation defines a head-on impact to the cask side while a  $90^{\circ}$  cask orientation indicates a near miss. Again, since the cask orientation distribution can be dependent on the accident scenario being considered, three cask orientation distributions are defined. The distributions include:

CT1: A uniform distribution in which all cask impact orientations are equally likely,

CT2: A triangular distribution in which end-on impacts on surfaces or head-on impacts to the side of the cask by train sills are most likely, with other orientations decreasing linearly in likelihood as the orientation angle approaches  $0^{\circ}$ , and

CT3: A triangular distribution in which impacts at  $45^{\circ}$  are most likely, with other orientations decreasing linearly in likelihood as the orientation angle approaches either  $0^{\circ}$  or  $90^{\circ}$ .

## 2.5.2 Thermal Loading Parameters

The thermal response of a cask, specifically the temperature reached within the gamma shield, is determined by three major thermal loading parameters: fire duration, flame temperature, and fire location with respect to the cask. The distribution functions for these parameters can be a function of the specific accident scenario being evaluated and can also vary from accident to accident within the same accident scenario (e.g., variations of fire locations with respect to the cask).

The BMCS reports and other sources provide information such as the accident type, the cause of fire property damage, and method of extinguishment.<sup>65</sup> This information is useful for defining actions to improve public safety. The sources, however, do not provide data on thermal loading parameters such as flame temperature and fire duration. Limited data on thermal loading parameters are sometimes included in the National Transportation Safety Board severe accident reports, but the data is not sufficient to adequately define thermal loads and their fractional occurrence.

A truck-fire accident has many variables that affect the fire and thermal loads. The variables include the involvement of the truck's fuel tank and its contents; the possibilities of a collision with an auto, another truck or a tanker truck; and the availability of fire fighting equipment. The many variables and the lack of specific data lead to the use of the Monte Carlo technique<sup>66</sup> and engineering models to determine the distribution functions for the thermal loading parameters.

### 2.5.2.1 Accident Scenarios and Fire Frequency

The accident scenario in which a truck is involved can affect the thermal loads on the truck and its cargo. Table 2.6 presents the accident type and the frequency of fires.<sup>66</sup> In Subsection 5.3 these accident fire frequencies are correlated with the accident scenarios in Figs. 2-3 and 2-4 to determine the probabilities of fire for each of the scenarios.

**Table 2.6**  
**Frequency of Fire for Truck Accident Types**

Accident Type	Fire Involved in Accident (%)	No Fire in Accident (%)
Collision with Auto	0.3	99.7
Collision with Truck	0.8	99.2
Collision with Fixed Object	0.4	99.6
Other Collision	0.9	99.1
Ran off Road	1.1	98.9
Overturns	1.2	98.8
Other Noncollision	13.0	87.0

### 2.5.2.2 Fire Duration

Since the available fire-accident data do not provide specific information on fire duration, the Monte Carlo method is used to derive the fire duration distribution for each accident scenario.<sup>66</sup> This method combines data on accident types, cause of the fire, availability of combustibles, and fire-fighting efforts with statistical engineering models on the burning of combustibles for various types of accidents. A Monte Carlo computer code is used as recommended<sup>66</sup> to analyze the interaction and probabilistic involvement of fuel tanks, tires, cargo, brakes, and electrical systems, as well as the effects of fire fighting efforts.

The Monte Carlo code is also used to predict fire duration distributions for each accident scenario in Figs. 2-3 and 2-4. As might be expected, there is a large variation in the fire duration distributions for the scenarios. In general, the fire durations following high impact loads on hard surfaces are shorter compared to those involving lower impact loads or collisions with other trucks, particularly tanker trucks.

### 2.5.2.3 Flame Temperature

Flame temperature depends on the burning materials and the amount of oxygen present in the flame. This study uses the flame temperature probability distribution from Sandia.<sup>66</sup> The fire distribution is primarily based on the open burning of hydrocarbon fuels such as diesel and gasoline in the temperature range of 1400 to 2400<sup>o</sup>F, but also includes other materials which tend to burn at lower temperatures.

The size of a fire affects both the radiation heat transfer capabilities and the duration of the fire. Fires with a flame that is at least four feet high radiate essentially as a blackbody with flame emissivity in the range of 0.9 to 1.0. Smaller fires have much lower emissivities and are usually of short duration, and would have little effect on a cask.

The convection heat transfer from a fire to a truck and its cargo is usually less than 10% of the radiation heat transfer. As discussed in Appendix F, an equivalent flame temperature for specific cask configurations

can be used to estimate the thermal loads for various combinations of flame temperatures, flame emissivities, and convection coefficients. In this study, it is conservatively assumed that all fires will have an emissivity of 0.9.

#### 2.5.2.4 Fire Location

The heat load to a cask varies with the location of the fire with respect to the cask. The heat load to the cask can decrease by a factor of 4 for a fire 20 feet from the cask compared with the heat load for an engulfing fire. As with other fire parameters, insufficient historical accident data exists to develop fire location distributions with respect to the cask. A uniform distribution for cask-to-fire location is assumed for all fire accident scenarios defined by:

L1: A uniform distribution in which any fire location relative to the cask is equally likely, in the interval between 0 and 31.5 feet. The cask is sidewise to the fire in all cases to maximize the heat load to the cask.

### 2.6 Railway Accident Loading Parameters

#### 2.6.1 Mechanical Loading Parameters

Types of train accidents are identified from FRA data, and supplemented by other sources to define accident scenarios used in this study. For some of the accident scenarios, loading parameter magnitudes and frequencies are estimated from highway data. In other cases, loading parameter data is derived from severe accident reports. In all cases, the selection of the data is justified as being suitably conservative. As with highway accident scenarios, the primary effort in obtaining railway accident data is placed on collecting information on those accident scenarios that could result in high loads to a cask. In this subsection the distribution functions are determined for three mechanical loading parameters: object hardness, impact velocity, and cask orientation.

### 2.6.1.1 Accident Scenarios and Object Hardness

Data is collated from several sources to derive accident scenarios and to estimate the cask impact frequency with a particular object. The combined data are presented in Fig. 2-4 for derailment, collision, and other accident types. The fraction of train accidents due to each type is estimated from the FRA data in Appendix C.<sup>11-17</sup> Derailment is the most common railway accident, accounting for 77.1%. Derailment involves a section or all of the train leaving the track. The section leaving the track separates from the preceding car as it leaves the track, causing the braking system to activate for all cars in the train. The lead car leaves the track at the highest speed, and the other cars follow at successively slower speeds. The average derailment involves approximately 10% of the cars in the train.

Collision accidents account for 13.4% of train accidents. The damage during a collision is usually limited to the cars near the impact point and involves less than 10% of the cars. For head-on collisions, damage is usually limited to the locomotive and the few cars that follow. For rear-end collisions, only the caboose and the few cars ahead of it are damaged.

Other accidents, including grade-crossing accidents, account for the remaining 9.5% of the accidents. These accidents usually do not cause serious impact forces to the train.

As shown in Fig. 2-5, collision accidents can result in derailments. In 64% of the collisions, the train remains on the tracks. In this case the cars may impact each other, but the forces would be relatively low or else the cars would have left the tracks. In 36% of the collisions, a derailment results and the cars leave the tracks. When considering the percentage of derailments occurring with collisions, the total percentage of train accidents that involve derailment is 82%.

The severe accident data in Appendix A is used in conjunction with the highway data to identify the objects and to estimate impact frequencies for the derailment accidents.<sup>67</sup> Owing to the limited amount of severe accident data and the nature of the reports, there is a high uncertainty in applying the data to the continuous spectrum of accidents.

		Probability percent**	Accident index
Rail-highway grade crossing		3.0400	1
0.0304			
Remain on track		8.5878	2
Collision			
0.1341			
Derailment			
0.3596			
Derailment			
0.7705			
Other			
0.0650			
Water		0.1615	3*
0.20339			
Clay, silt		0.0122	4*
0.015486			
Over bridge			
0.0097			
Hard soil/soft rock & concr. 0.001262		0.0010	5*
Hard rock		0.0002	6*
0.000199			
Railbed, roadbed		0.6192	7*
0.77965			
Drain ditch		0.3433	8
0.3812			
Over embankment			
0.0110			
Clay, silt		0.5092	9*
0.5654			
Hard soil/soft rock		0.0415	10*
0.04610			
Hard rock		0.0066	11*
0.007277			
Clay, silt		1.4437	12*
0.91370			
Derailment			
0.818722			
Into slope			
0.0193			
Hard soil/soft rock		0.1178	13*
0.07454			
Hard rock		0.0186	14*
0.01176			
Into structure			
0.2016			
Abutment			
0.0001		0.0017	17*
Other		16.4477	18
0.9965			
Locomotive		3.2517	19*
0.2305			
Coll.			
0.2272			
Car		10.0148	20
0.7099			
Coupler		0.8408	21*
0.0596			
Rollover			
0.7584			
Roadbed		15.9981	22
0.3334			
Non-coll.			
0.7728			
Earth		31.9865	23
0.6666			
Other		6.500	24

\*Potentially significant accident scenarios  
 \*\*Conditional probability which assumes an accident occurs

Figure 2-5 Train accident scenarios.

If a derailment accident occurs, the train can go off a bridge or an embankment, strike a slope, or rollover onto the adjacent ground. In this study, the percentage of accidents that go off a bridge or an embankment or onto a slope is estimated to be the same as those for highway accidents. For these types of accidents, the frequencies of impacting different soils, roadways, and water are also assumed to be the same as those used for highway accidents. These estimates and assumptions are made because of the lack of data on railway accidents and the fact that railways cross similar terrain as highways for similar routings. The remaining derailment accidents are assumed to be rollover-type accidents.

When a train derails in a rollover type of accident, it can (1) slide along the adjacent railbed or earth with relatively low damage occurring; (2) hit the superstructure of adjacent cars or locomotives; (3) strike couplers from adjacent cars; or (4) impact structures adjacent to the track. The severe accident data from Eggers<sup>67</sup> is used to estimate the frequencies for impact on railbed, earth, car superstructure, locomotive superstructures, car couplers, and adjacent structures. As shown in Fig. 2-5, it is estimated from the Eggers database that 0.8% of the train derailment accidents involve train couplers. The frequency for impacting large structures, such as columns and abutments, is estimated to be the same as the frequencies obtained from the CALTRANS highway data.

#### 2.6.1.2 Impact Velocity

The impact velocity of a cask involved in a train accident depends on the cask velocity and the impact angle. The cask velocity depends on the train velocity prior to collision or derailment and the height of any fall that might occur. The impact velocity distributions for a cask involved in train accidents are estimated from train accident records, surveys, and engineering judgments.

#### 2.6.1.2.1 Cask Velocity

For potential accidents in which the rail cask impacts an object, the magnitude and frequency of the impact velocity are estimated from the train accident velocity provided in Appendix C. This estimate conservatively disregards the fact that a reduction in impact velocity occurs because of energy absorption by the transporting car or the rest of the train. Tables 2.7 and 2.8 give the average frequencies of train collisions and derailments as functions of accident velocities, respectively, for the years 1979 through 1982. This accident data is derived from the FRA reports on train accidents.<sup>13-17</sup> The velocities for other accidents include grade-crossing incidents which are included in the truck data.

In the absence of a statistical data base on distance fallen by trains going off bridges and embankments in actual accidents, the highway survey bridge distribution in Table 2.4 is used to estimate distances fallen in this type of accident. Since specific train and truck routes for transporting spent fuel traverse similar terrain, the use of the highway bridge data for this study is reasonable.

In summary, the cask velocity distributions for each of the potentially significant train accident scenarios are:

- TV1: A distribution based on train collision accident velocities without braking,
- TV2: A distribution based on train derailment accident velocities without braking,
- TV3: A distribution based on fall heights from bridges, and
- TV4: A distribution based on the vector sum of train derailment velocities and fall heights from bridges.

Table 2.7  
 Railroad Accident Velocity Distribution, Collisions, Main Line, 1979-1982<sup>a/</sup>

Velocity (mph)	Number of Accidents	Fractional Percent (%)	Cumulative Percent (%)
1 - 10	392	46.12	46.12
11 - 20	182	21.41	67.53
21 - 30	117	13.76	81.29
31 - 40	92	10.82	92.12
41 - 50	47	5.53	96.65
51 - 60	14	1.65	99.29
61 - 70	3	0.35	99.65
71 - 80	2	0.24	99.88
81 - 90	0	0.00	99.88
>91	1	0.12	100.00
Subtotal	<u>850</u>	<u>100.00</u>	-
Unknown	8	-	-
Total	858	-	-

<sup>a/</sup> Data derived from Federal Railroad Administration reports on train accidents, 1979 - 1982.

Table 2.8  
 Railroad Accident Velocity Distribution, Derailments, Main Line, 1979-1982<sup>a/</sup>

Velocity (mph)	Number of Accidents	Fractional Percent (%)	Cumulative Percent (%)
1 - 10	4,394	40.42	40.42
11 - 20	2,250	20.70	61.12
21 - 30	2,183	20.08	81.21
31 - 40	1,091	10.04	91.24
41 - 50	659	6.02	97.30
51 - 60	239	2.20	99.50
61 - 70	41	0.38	99.88
71 - 80	10	0.09	99.97
81 - 90	3	0.03	100.00
>91	0	0.00	-
Subtotal	<u>10,870</u>	<u>100.00</u>	-
Unknown	76	-	-
Total	10,946	-	-

<sup>a/</sup> Data derived from Federal Railroad Administration reports on train accidents, 1979 - 1982.

#### 2.6.1.2.2 Impact Angle

As for highway accidents, there is insufficient historical accident data available to define distribution functions for the impact angle of a spent fuel cask onto an object. Three distribution functions for spent fuel cask impacts are assumed for train accidents, namely: (1) uniform distribution, (2) all impacts at  $90^{\circ}$ , and (3) triangular distribution in which  $90^{\circ}$  impacts are most likely.

#### 2.6.1.3 Cask Orientation

Since there is insufficient historical railway accident data available to define distribution functions for the cask orientation at the time of impact, three distribution functions are assumed for train accidents. The distribution functions are (1) uniform distribution, (2) all impacts endwise or head-on to the cask, and (3) triangular distributions in which  $45^{\circ}$  impacts are most likely.

#### 2.6.2 Thermal Loading Parameters

As with truck accidents, every train accident does not necessarily result in a fire. As indicated in Appendix C, approximately 1% of train collision and derailment accidents involves a fire. As for truck accidents, the train accidents have data on type of accident, frequency of fire, cause of fire, and property damage estimates. However, the accident records do not provide data on thermal loading parameters such as flame temperature and fire duration.

A train-fire accident has a large number of variables that affect the thermal loads. Such variables are (1) type of accident (collision, derailment, grade crossing, etc.), (2) type and amount of cargo (flammable or nonflammable), (3) involvement of locomotive fuel, (4) types of cars involved (box car, tanker, etc.), and (5) the availability of fire fighting equipment.

The same methods used in Subsection 2.5.2 to estimate the truck fire duration distribution are used here to estimate the distribution functions for the three thermal loading parameters: fire duration, flame temperature, and fire location.

### 2.6.2.1 Accident Scenarios and Fire Frequency

The type of railway accident can affect the thermal load on a train and its cargo. Table 2.9 presents the accident type and the frequency of fires, modified to include grade-crossing accidents which were separately identified beginning in 1978 (see Appendix C).<sup>66</sup> The fire frequency for "other" accidents is judged to be too high, but owing to the lack of consistent data, this conservative estimate is used.<sup>66</sup>

### 2.6.2.2 Fire Duration

Since the available fire-accident data do not provide specific information on fire duration for each of the railway accidents, the same method used in Subsection 2.5.2.2 to estimate truck fire duration distribution is used to estimate the fire duration distribution for trains. A Monte Carlo scheme is used in analyzing a large number of variables and their interactions.<sup>66</sup> The code can evaluate the interaction and involvement of locomotive fuel tanks, different types of rail cars and their flammability, and different types and amounts of flammable cargo, as well as the effects of fire fighting efforts. The code is used to predict the fire distributions for each of the accident types in Table 2.9 and the accident scenarios in Fig. 2-5.

### 2.6.2.3 Flame Temperature

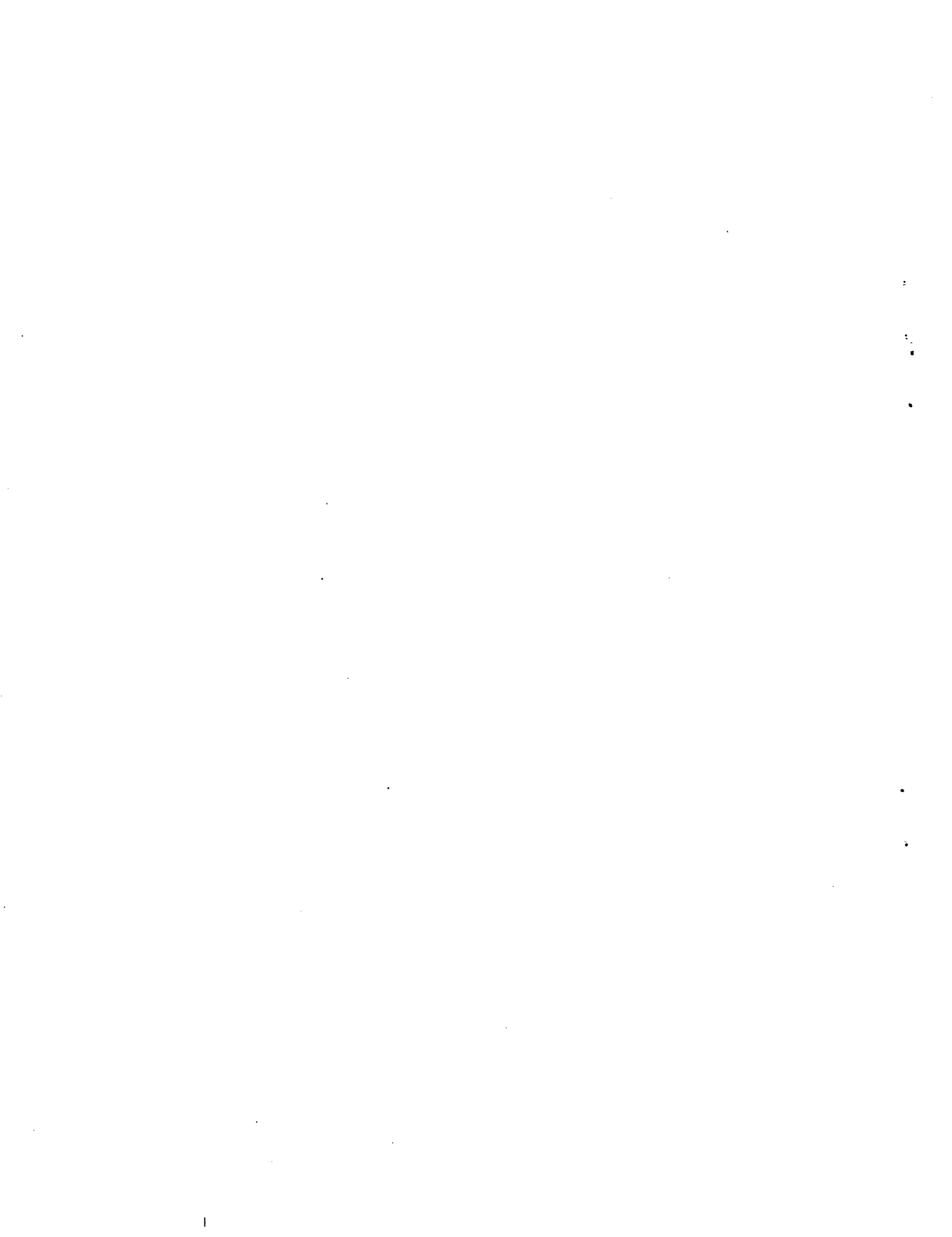
The thermal loads on a train and its cargo are affected by the flame temperature of the fire. They are primarily determined by the type of material involved in the fire, the oxygen supply, and geometric configuration. Train fires often include diesel fuel, flammable cargo, and flammable parts of the cars. The flame temperature for train fires are the same as those evaluated for truck fires in Subsection 2.5.2.3. For the purpose of this study, it is assumed that all train fires will have an emissivity of 0.9.

**Table 2.9  
Train-Fire Accident Types**

Accident Type	Fire Involved in Accident (%)	No Fire in Accident (%)
Collision	1	99
Derailment	1	99
Grade Crossing	1	99
Other	90	10

#### 2.6.2.4 Fire Location

As with other fire parameters, insufficient historical accident data exists to develop fire location distributions with respect to a spent fuel cask. As is done for the truck cask accident scenarios, uniform distributions (L1) are assumed for each of the fire accident scenarios for fire locations 0 to 43.0 feet from the cask.



### 3.0 SELECTION OF REPRESENTATIVE SPENT FUEL CASKS FOR EVALUATION

#### 3.1 Introduction

Casks currently certified for shipment of spent fuel from nuclear power reactors in the United States vary distinctly in design.<sup>1-4</sup> The most obvious difference between these casks is that they are designed to carry differing amounts of spent fuel. Casks weighing under 25 tons carry one or two fuel assemblies and can be transported by truck. Other casks can carry three to seven fuel assemblies and can also be carried by truck if appropriate highway overweight permits are secured. Finally, because railroads can carry greater loads, currently licensed rail casks can carry between 7 and 24 assemblies.

All of these casks must be designed to accomplish certain basic safety functions which are defined by a set of performance-oriented regulatory requirements.<sup>5</sup> In this regulatory approach, the cask design features which accomplish a specific safety function can vary, but the functional result must meet minimum specified requirements. In order to study the adequacy of the regulations to provide radiological protection, representative casks are defined which have design features likely to meet the regulations. Sufficient features must be defined to evaluate the protection provided by spent fuel casks involved in transportation accidents.

In addition, casks designed to meet regulatory requirements are usually designed and manufactured to code and standards which have margins of safety embedded in them. These margins of safety ensure that the spent fuel cask not only will meet the regulatory accident test conditions and radiation hazard limits but will survive loading conditions beyond the regulatory conditions.

The purpose of this section is to define the representative casks which are used in the accident response calculations described in later sections of this report. These representative casks are developed from current cask designs and technology. These representative casks include the necessary design features and safety margins for evaluating their response to accident conditions.

In Section 3.2, general safety functions for the cask are defined. The cask features needed to meet these functions are identified. Specific characteristics are determined for the various design features.

In Section 3.3, each design feature is evaluated from two standpoints: (1) the feature's susceptibility to damage under transportation accident conditions, and (2) the feature's ability to mitigate damage to other important cask features. Some features, e.g., impact limiters, are characteristically sacrificial and highly susceptible to damage, but are effective in mitigating further damage to the rest of the system. At the other extreme are features that are characteristically highly resistant to damage, but transmit damaging forces into other parts of the system with little mitigation.

In Section 3.4, six preliminary cask designs are evaluated on a comparative basis. From this comparison the gamma shielding material for the representative truck and rail cask designs is selected. The six designs include three truck casks and three rail casks which use the candidate shield materials: lead, depleted uranium, and steel.

Section 3.5 describes the two representative cask designs selected--one for truck shipments and the other for rail shipments. The physical and material specifications for the two designs are established. Those design features which are necessary to perform the evaluations in this study are identified. The rationale and the sensitivity studies used to define the required design features are also described.

Section 3.6 describes the typical safety margins that are included in licensed cask designs and the representative cask. These safety margins are embedded in the codes and standards used in designing and manufacturing casks.

### 3.2 Cask Functions and Design Features

Casks currently certified for shipment of spent fuel are relatively complex engineering structures designed to meet certain functional needs.<sup>1-4</sup> Many of these functional needs are dictated by the characteristics of the spent fuel being shipped. The spent fuel is a source of radioactivity and

heat, both originating within the fuel pellets which are contained within the rods of a fuel assembly. The primary cask functions include (1) containment of radioactive material, (2) shielding against the radiation emanating from the spent fuel, and (3) the assurance that subcriticality is maintained.

Containment is the retention of radioactive material within a closed vessel. Containment is provided to preclude any contact between people and radioactive material. Typically, containment is provided by the integrity of the spent fuel and by a cylindrical steel vessel (Fig. 3-1). The vessel is provided with a bolted end closure to accommodate spent fuel loading and unloading operations. The closure contains a seal to inhibit leakage between the cask containment and the environment. Piping penetrations of this containment are needed for operating purposes, and the associated closure valves are considered a part of the containment system. These penetrations are in the containment vessel for draining, filling, testing, etc. The containment cavity is filled with a non-oxidizing gas for shipments.

A radiation shield is a barrier which absorbs ionizing radiation or subatomic particles emanating from a radioactive source. Two types of radiation shielding are typically included in spent fuel cask design, gamma and neutron. The most important shielding provides protection against the highly penetrating gamma radiation. This protection is achieved through the use of dense materials such as lead, depleted uranium, or steel. These materials surround the containment vessel (Fig. 3-1) and are, in turn, enclosed within an outer steel shell. If steel is the shield material, this shield can be an integral part of the containment vessel. The second type of shielding is used to mitigate radiation caused by spent fuel emission of neutrons. This source of radiation is typically less significant than gamma radiation. Hydrogenous materials provide shielding against neutrons. The neutron shield, usually a water jacket, surrounds the cask on its exterior surfaces. The hazard associated with neutron radiation is such that loss of neutron shielding does not result in radiation levels that exceed regulations for accident situations. The regulations allow for higher external radiation levels following an accident than during normal transport.

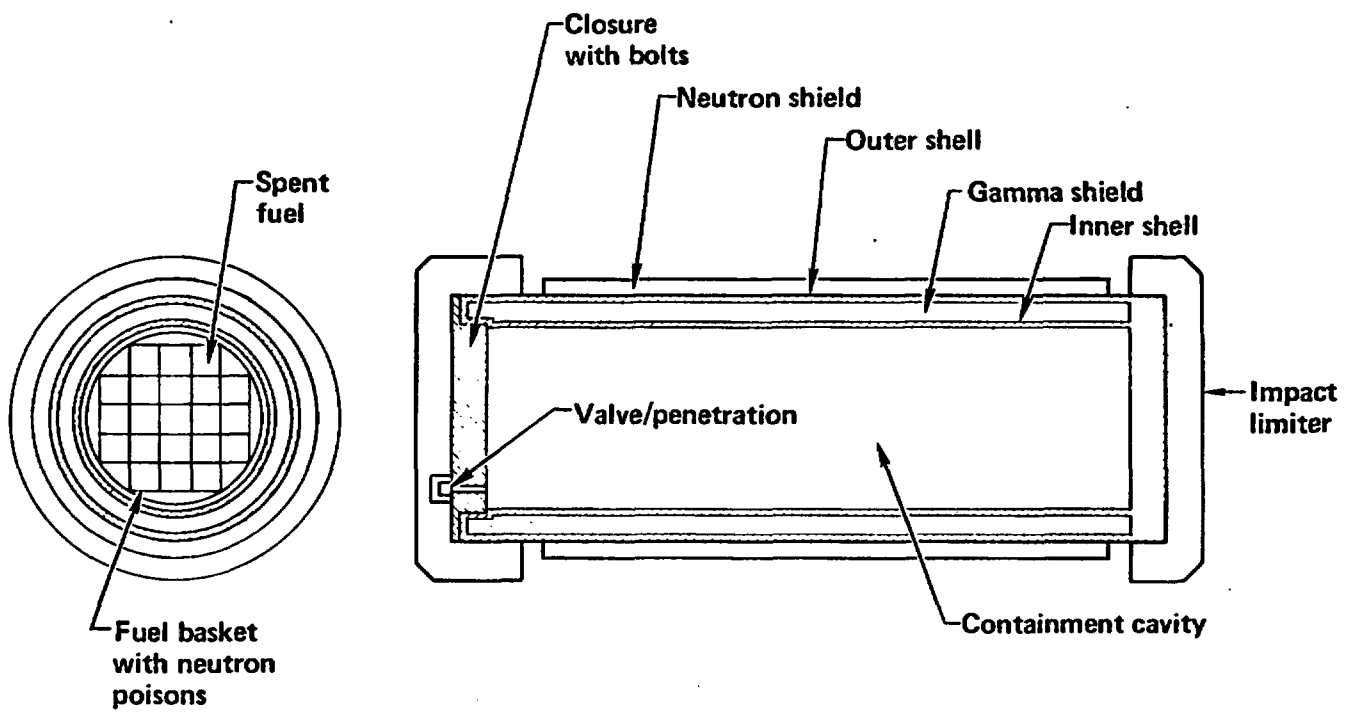


Figure 3-1 Spent fuel cask features important to safety.

Criticality is a self-sustained nuclear chain reaction which might result in high energy production and a radiation burst before self-termination. Spent fuel casks are designed to maintain a condition of subcriticality. The subcriticality assurance function, if not achieved by the physical limitation on the amount of spent fuel being shipped, is assured by maintaining geometric control of the spent fuel during shipment and by including neutron poisons in appropriate cask structural materials. Neutron fission interactions with spent fuel must attain a prescribed level before criticality can occur. The neutron poisons, which are typically included in the basket holding the fuel assemblies, absorb emitted neutrons to a sufficient degree to limit neutron fission interaction and thus assure subcriticality.

As the above discussions of containment, shielding, and subcriticality assurance indicate, two fundamentally different concepts are applied in the regulations: containment and shielding are limiting in nature while subcriticality is absolute.

In all casks, the design features used to meet each of the specific functional needs have many mutual dependencies. The containment shell, for example, must be designed to structurally support the heavy surrounding gamma shielding material. Also the geometry control achieved by internal cask features is dependent on the protection against deformations provided by the overall cask structure. These dependencies between specific design features are further described in Section 3.3 which discusses the performance requirements for the design features important to safety.

### 3.3 Cask Design Features Important to Safety

#### 3.3.1 Containment

This subsection describes several design features which basically compose the typical cask containment system: (1) the cylindrical steel containment shell, (2) the bolted end-closure, (3) the closure seal, and (4) the piping and valves associated with any containment system penetrations. The containment system must be designed so that when subjected to the hypothetical

accident conditions specified in existing regulations, the regulatory limits for radioactive material releases are met. In practice, the required function of the containment vessel is achieved by a combination of three factors: (1) the structural integrity of the individual containment system features, (2) the provision of external features such as energy-absorbing structures designed to protect the cask and its containment system against external forces, and (3) the integration of the containment features into an overall cask design which maximizes the protection provided against these external forces.

The steel containment is designed as a system and must support itself and the weight of the spent fuel and other internal structure under regulatory-defined normal and accident transport conditions. The steel containment shell provides a substantial resistance to any externally applied forces. To provide assurance that this shell maintains its integrity under potential transportation accident conditions, casks are designed with impact limiters. Impact limiting devices can take the shape of large end-caps made of a crushable material such as balsa wood or rigid foam, or they can be in the form of bendable metal fins or tubes which protrude from the outer cask body. In all cases, impact limiters are designed to limit, or reduce, the mechanical loads imposed on the cask containment shell. The impact limiters do this by deforming and sacrificially absorbing the energy of the accident. The containment shell is designed for the impact-limited loads which arise from the accident test conditions.

The bolted containment end closure and the closure seal are located within the envelope of protection provided by the impact limiting devices (Fig. 3-2). The bolted closure is typically recessed within the outer cask shell, and the closure seal is located between the end closure and the containment shell wall. These cask features are designed so that if the cask is subjected to accident conditions, the containment function is not compromised.

Piping and valves associated with subsystems that penetrate the containment are also located in protected recessed areas within the outer cask

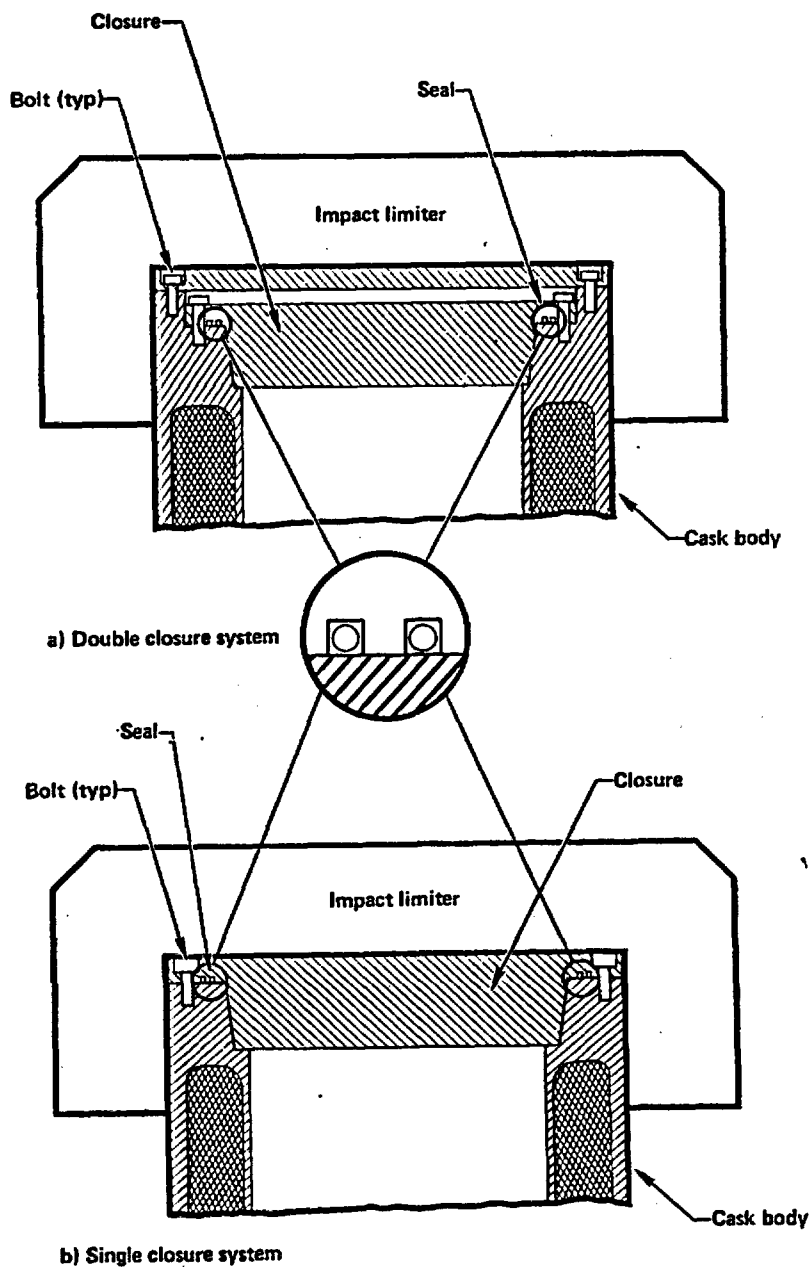


Figure 3-2 Typical closure designs for spent fuel casks.

structure (Fig. 3-3). As a result, this piping system and its related valves are also protected by the impact limiting devices. Again, this system is designed to withstand the accident conditions without compromising containment integrity.

### 3.3.2 Radiation Shielding

Shielding is provided in all cask designs to limit the gamma and neutron radiation which emanates from the spent fuel. The gamma shield is typically a dense metal, such as lead, depleted uranium, or steel. These materials surround the cask containment vessel and, in the case of lead and depleted uranium, are enclosed within an outer steel shell. The neutron radiation shield typically consists of hydrogenous compounds such as water. The neutron shield is generally located beyond the outer steel shell which encases the gamma shield. When water is used for neutron shielding, it is contained within a water jacket. The thicknesses of these shields are determined to ensure that the radiation levels external to the cask are within regulatory values which are specified for both normal transport and transportation accident conditions, (i.e.,  $\leq 200$  mrem/hr on the external surface and  $\leq 1$  rem/hr at 1 meter from the external surface, respectively).

In practice, the dose rate of  $\leq 1$  rem/hr at 1 meter from the external surface can be achieved by maintaining the integrity of the gamma shield. The magnitude of neutron radiation is intrinsically limited to levels that allow the loss of neutron shielding to be presumed in the event of a transportation accident. The gamma shielding is protected by both the outer steel shell of the cask and the cask's impact limiters. If the cask is subjected to the accident test conditions, the cask gamma shield is designed to assure that external radiation levels remain within regulatory limits.

### 3.3.3 Subcriticality Assurance

Subcriticality for one pressurized water reactor (PWR) assembly or two boiling water reactor (BWR) assembly shipments (typically made by truck) is assured because the amount of fissile material available in the  $UO_2$  fuel form

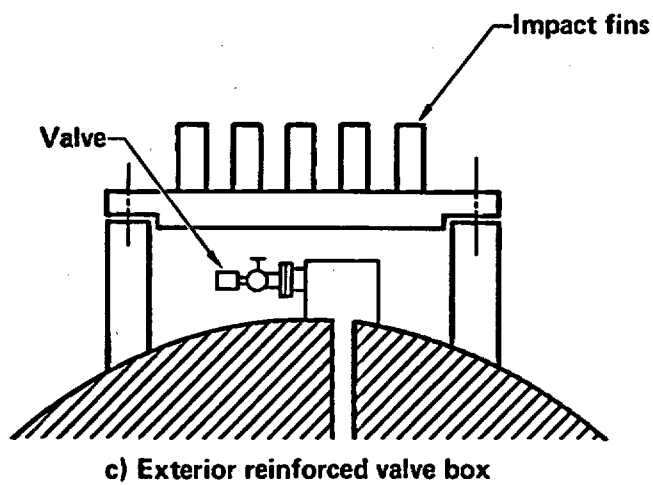
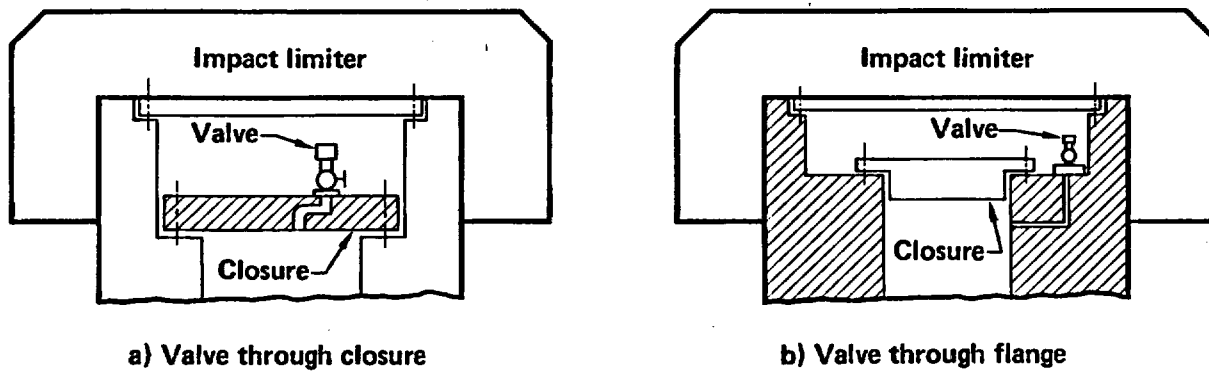


Figure 3-3 Typical cask penetration subsystems.

is insufficient to achieve criticality under any credible circumstances. Larger shipments, however, which are generally made by rail, do contain enough fissile material to make criticality a theoretical possibility if: (1) the material can be optimally rearranged geometrically, (2) a neutron reflecting material surrounds the fuel, and (3) a neutron moderating media such as water can be interspersed between fuel rods and assemblies. For these shipments, subcriticality assurance is achieved by geometry control features and the use of neutron poisons, materials which preclude a self-sustaining fission process.

A cask's capability to assure spent fuel subcriticality for these larger shipments is evaluated in an extremely conservative manner. The effectiveness of the geometry control provisions and the neutron poisons must be demonstrated not only under the specified accident test conditions but also under defined conditions which optimize the possibility for criticality. Among these other conditions, the larger shipments must be demonstrated to be subcritical when: (1) two similar casks are assumed to be stacked together in an arrangement which optimizes criticality potential, (2) the stacked casks are closely reflected on all sides by water, and (3) the fuel within each cask is subjected to optimum, interspersed hydrogenous moderation.

The assumed presence of the reflecting and moderating materials increases the possibility of achieving a critical configuration. The use of this conservative approach to assure subcriticality highlights the importance of cask features other than the spent fuel geometry control features and neutron poisons previously described. For example, if containment integrity is maintained, water or other hydrogenous material could not enter the cask containment vessel and the possibility of criticality would be precluded. Similarly, if the overall cask structure prevents gross internal distortions, then spent fuel geometry control and neutron poisons would be sufficient to assure subcriticality even if water or other hydrogenous material entered the cask containment vessel.

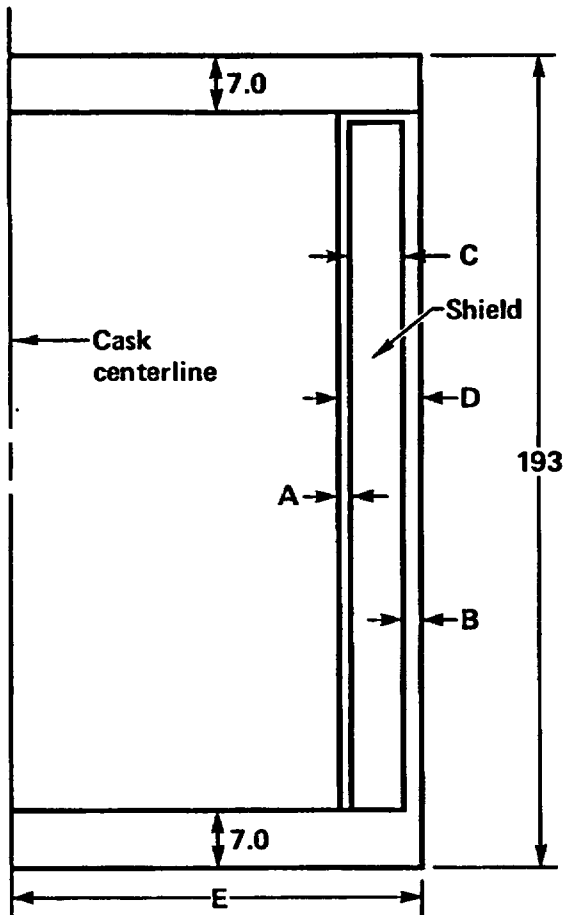
### 3.4 Selection of Cask Shielding Material

Shielding provides protection from both the neutron and gamma radiation emanating from spent fuel. The gamma shielding can be provided by several different materials, each with a distinct capability to withstand the mechanical and thermal loads associated with potential transportation accidents. The selection of the gamma shield material for a representative cask is based on an evaluation of the comparative performance of different preliminary cask designs: three each for truck and rail. The six preliminary designs shown schematically in Figs. 3-4 and 3-5 include consideration of sizing differences typical to truck and rail casks and the use of each of the three candidate gamma shield materials: lead, depleted uranium, and steel.

These six designs are evaluated against two quasi-static mechanical loading conditions, i.e., end-on and side loads. Then the magnitude of loads necessary to initiate yielding of the containment shell is determined. Static loads are applied to the end and side of the casks for this evaluation. The details of these evaluations are described in Appendix E. The results indicate that the lead shielded casks--both the railway and highway configurations--will begin to yield when subjected to a lower external force than the casks with steel or depleted uranium shields. From a structural standpoint, lead is the worst of the three candidate gamma shield materials and is, therefore, the material of choice.

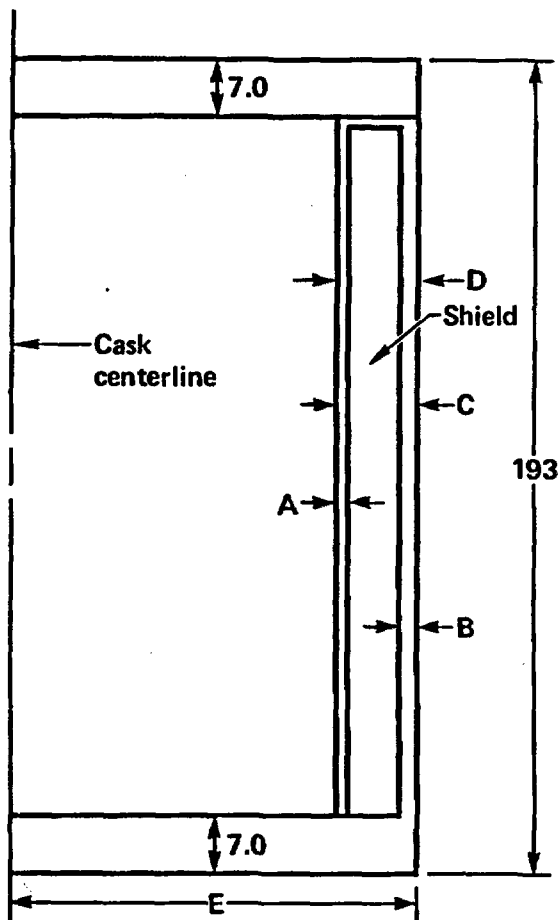
The six preliminary designs also are compared in terms of their capability to absorb thermal energy from potential fire environments. In terms of thermal capacities, the steel-shielded designs are capable of absorbing the most heat; the depleted uranium and lead designs have essentially equal capabilities. Lead has a melting temperature below the other cask shield materials, which is considered another factor significant to safety. The thermal expansion effect is also the most significant for lead shielded casks. From a thermal standpoint, lead is again the worst of the three candidate shield materials and is the material of choice.

Based on these structural and thermal evaluations, lead is selected as the gamma shield material for the representative cask designs.



Dim	Thickness (in.)	Material
<b>Truck Cask 1</b>		
A	0.5	304SS
B	1.25	304SS
C	5.25	Lead
E	13.75	304SS
<b>Truck Cask 2</b>		
A	0.5	304SS
B	1.25	304SS
C	4.25	Depleted uranium
E	12.75	304SS
<b>Truck Cask 3</b>		
D	12.25	Steel
E	19.00	Steel

Figure 3-4 Preliminary truck cask designs with three types of gamma shielding, used for quasi-static loading response studies only.



Dim	Thickness (in.)	Material
<b>Rail Cask 1</b>		
A	0.5	304SS
B	1.5	304SS
C	5.25	Lead
E	26.0	304SS
<b>Rail Cask 2</b>		
A	0.5	304SS
B	1.5	304SS
C	4.0	Depleted uranium
E	24.8	304SS
<b>Rail Cask 3</b>		
D	12.25	Steel
E	30.75	Steel

Figure 3-5 Preliminary rail cask designs with three types of gamma shielding, used for quasi-static loading response studies only.

### 3.5 Definition of Representative Cask Designs

Previous sections discuss the functions of a spent fuel cask which are important to safety in the event of a transportation accident. This section presents the basis for the selection of the representative spent fuel casks used in the response analyses. The response of these casks is evaluated when subjected to the forces of real world accident environments in later sections of this report. The definition of a representative cask involves the accomplishment of two major tasks: (1) a determination of what cask features important to safety require specific design definition, and (2) a selection of a design definition which considers the variety of design features that can accomplish a specific safety function.

The following subsections present the rationale for accomplishing these two tasks. Separate subsections consider features which are important to the containment, shielding, and subcriticality assurance functions of cask designs. An additional subsection considers the definition of those cask features whose principal purpose is to mitigate the damage to the cask caused by accident forces (principally the impact limiters).

#### 3.5.1 Shielding Features

Based on the evaluations in Section 3.4, lead is selected as the gamma shield material for the representative cask designs. Under impact conditions, lead is not self-supporting and can slump. A properly designed cask has adequate thickness in each steel shell as well as a soft impact limiter to prevent any significant lead slump from occurring under the 30-foot drop test conditions. Bonding of the lead to the inner shell of the cask can provide resistance to lead slump, but bonding varies significantly with the cask design and the fabrication process. Lead slump effects and damage to the cask are maximized when there is no bonding between the lead and the inner wall of the cask. Therefore bonding of the lead is not assumed.

The neutron shield design will not be expected to significantly affect cask response to the mechanical loads associated with severe transportation

accident environments. In fact, as indicated previously, the safety evaluations performed on all current casks presume that the capabilities of the neutron shield to reduce external radiation levels is lost as a result of the effects of transportation accident forces. On this basis, specifying the neutron shield design will not be necessary for the representative cask designs. However, this neutron shield, whether lost or maintained, will affect heat transfer. If a water neutron shield is maintained, it will exhibit high heat capacity as well as good heat transfer characteristics. If the water is lost, the empty tank containing air does not have high heat capacity, but provides an effective thermal barrier against heat from a fire. The post-fire effect of a neutron shield tank is to increase resistance to dissipation of internal heat, thereby increasing internal temperatures. Therefore, the volumetric characteristics of the neutron shield design must be considered in the definition of the representative casks.

### 3.5.2 Containment Features

The containment system includes the steel containment shell, the closure seal, the bolted-end closure, and the piping and valves in the containment-penetrating subsystems.

The steel shell is the containment feature most likely to be subjected to the full brunt of any severe transportation accident forces. The magnitude of any accident damage sustained by the shell provides a broad indication of the possibility and the magnitude of any resulting radiological hazard.

The containment seal can be subjected to damage by mechanical or thermal accident loads transmitted through the cask body to the seal region. However, the radiological hazard resulting from seal damage is limited to the spent fuel material which can escape from the confines of the cask through the damaged or deformed seal region. Rather than attempting to model one of several possible seal designs, a worst-case evaluation of seal performance can be made by presuming a loss of the seal functional capability and the release of radioactive material. Specific levels of damage to the cask must be exceeded as a result of accident forces.

The bolted cask end-closure can be subjected to damage by mechanical loads transmitted through the cask body. Damage can also result from the mechanical loads which can be caused by severe thermal environments associated with certain transportation accidents. The end-closure, however, is a massive structure highly resistant to mechanically imposed loads. Furthermore, the closure bolts are designed with sufficient strength to resist tensile forces from corner or end drops of the cask. The recessed characteristics of all current closure designs provide significant protection against shearing of the many large-diameter bolts typically used to secure the end-closure to the cask body. Forces sufficient to cause significant damage to the cask containment shell could occur in many of the conceived severe accident events without compromising the gross integrity of the bolted end-closure. The converse, that is, significant damage to the end-closure without similar containment shell damage is certainly conceivable, but far from likely. From an evaluation standpoint, the definition of a specific closure in a representative cask design will add considerable complexity to the calculations of cask response to severe accident environments. For the above reasons, although the mass and configuration of the closure requires definition, the details of the closure design are not included in the representative cask design(s). Again, a specific level of damage to the cask containment is used as a surrogate measure to indicate damage to, and the occurrence of radioactive material leakage from, the cask closure region.

The penetration subsystems are typically located within the confines of the cask body with exterior valves situated within heavily protected enclosures. These subsystems are easily protected by design features. Unless accident loads are highly localized, damage done to the cask shell will dominate overall cask damage. Notwithstanding, a highly localized load can violate the containment function by providing an opening from the cask containment to the environment through a failed penetration subsystem. Such a violation of containment will limit the escape of any spent fuel material to that which can migrate or be driven out through the small-diameter, tortuous passageways presented by the damaged penetration system.

As a result of the above considerations, the details of a penetration subsystem are not included in any representative cask design. Damage to the containment shell again is used to indicate the possibility of a failed or damaged penetration subsystem.

### 3.5.3 Subcriticality Assurance Features

Subcriticality assurance features, are provided in casks used for the shipment of larger numbers of spent fuel assemblies. The spent fuel geometry control features and the neutron poisons can be subjected to transportation-accident-induced mechanical forces transmitted through the cask body. These features form an integral part of the overall cask structure internal to the containment shell. Significant damage to these features requires that significant damage be incurred by the total cask structure including the containment shell. Physical damage, taken alone however, does not affect the cask's subcriticality assurance function. A hydrogenous material, such as water, must surround the cask and be interspersed between the individual fuel rods and fuel assemblies before criticality can become a credible possibility.

For these reasons, the subcriticality features are not specifically modeled in the representative cask designs. Instead, a maximum estimate of the likelihood of a criticality incident is provided in Section 9.0. This estimate considers those transportation accident events in which the structural damage is sufficiently severe to cause gross fuel assembly damage. The estimate then evaluates the likelihood that such an event will involve the intimate presence of hydrogenous material in the accident scenario.

### 3.5.4 Damage-Mitigating Features

The principal damage-mitigating features provided in cask designs are the impact limiters. These devices are designed to be sacrificial and can be of two general types, hard and soft. In either case, they absorb some of the energy of impact by deforming. The ratio of the energy absorbed by the impact limiter to that transmitted to the cask depends on the accident severity and

the type of impact limiter. The choice of an impact limiter is strongly affected by the choice of gamma shielding. If lead is the gamma shield material, soft impact limiters of balsa wood or rigid foam are typically used in cask designs. Soft impact limiters are designed to ensure that imposition of the accident test condition loads will not produce forces sufficient to cause lead slump.

Hard impact limiters in the form of bendable metal fins have been used in casks using depleted uranium as the gamma shield material. In these designs, the casks are more rigid. As a result, the forces transmitted through the cask body when the cask is subjected to the accident test conditions (specifically, the 30-foot cask drop onto an unyielding surface) are higher than those associated with casks using soft impact limiters. In either case, however, the cask design must meet the regulatory-defined post-test acceptance criteria.

A soft impact limiter is selected for the representative cask design for two major reasons. First, the soft impact limiter is consistent with the selection of the lead gamma shield. Second, and more significant, casks with soft impact limiters, if subjected to transportation accidents resulting in severe mechanical and thermal loads, will be more likely to incur damage.

### 3.5.5 Representative Cask Design Description

Two representative cask designs are developed: one for truck shipments and one for rail shipments of spent fuel. The representative truck cask design uses the same dimensions as the preliminary lead truck cask design (Fig. 3-4). The truck cask design allows transport of a single PWR fuel assembly. The representative rail cask design dimensions differ from the preliminary lead rail cask design (Fig. 3-5). The capacity of the rail cask is 21 PWR fuel assemblies which reflects the greater capacities of anticipated cask designs. Each design uses helium in the cask cavity.

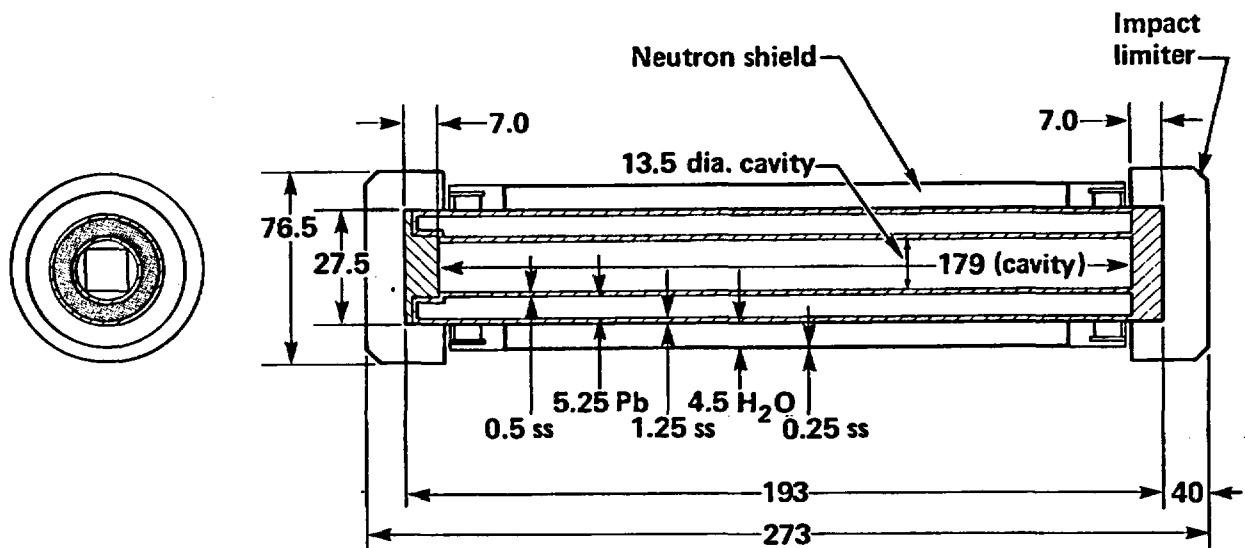
Both designs include a lead gamma shield sized to meet current regulatory requirements. The truck cask gamma shield of 5.25 inches is thicker than the rail cask gamma shield of 4.00 inches to allow for the possibility of shipping

fuel decayed less than 5 years by truck. The neutron shield dimensions reflect values typical of current cask designs. The cask shell structures, including the containment shell, are sized to support the lead shield. Specifically, the thickness of each cask steel shell is selected based on standard design practice; that is, the cask structure can withstand a force level typically generated from the accident test conditions. The resultant representative cask designs are indicative of current designs.<sup>1-4</sup>

The pertinent materials, weights, and dimensions of the representative truck and rail casks are shown in Figs. 3-6 and 3-7, respectively. The structural shell material is type 304 stainless steel. The lead shield is assumed to be unbonded to the steel shells. This fabrication assumption maximizes the potential for lead slump during transportation accidents involving impacts. Cask resistance to accident forces is thereby minimized, which introduces an element of conservatism to the results of this study. The impact limiters are made from balsa wood or rigid foam. Figure 3-8 shows the force deflection characteristics of the representative limiter design as a function of the presumed angle of impact between a cask and an impact surface. The impact limiter is sized to transmit a force of approximately 40 g if the cask is subjected to the impact environment specified by the accident test conditions.

### 3.6 Margins of Safety

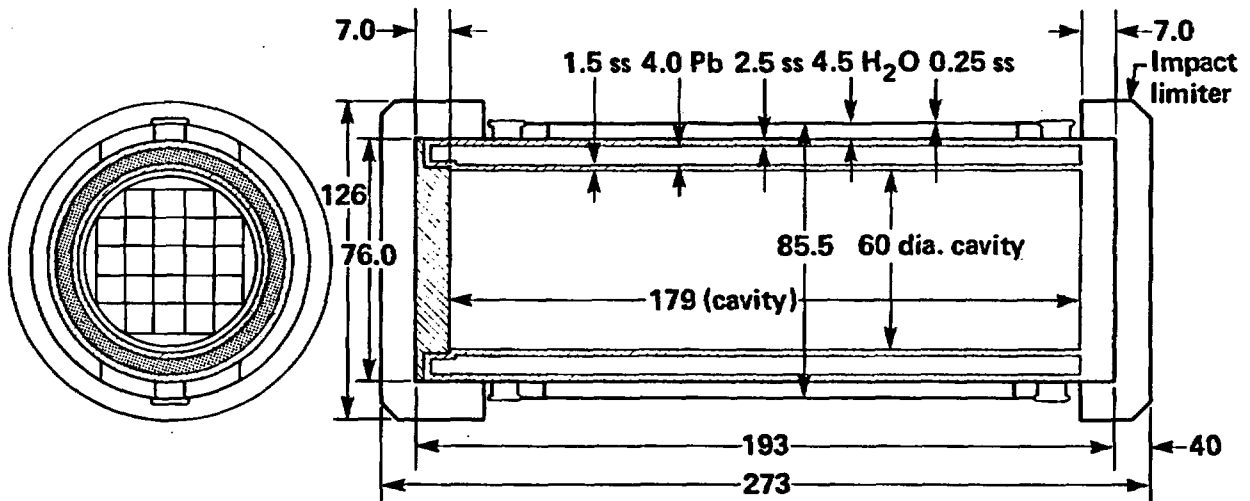
The representative casks are designed to meet the regulatory accident test conditions. However, before a cask is allowed to transport spent fuel, it must be certified by the U.S. Nuclear Regulatory Commission (NRC). The certification process requires that all activities related to the design, manufacture, use, and maintenance of the cask be documented in a Safety Analysis Report (SAR). The SAR is submitted to the NRC for review and approval. The analyses and evaluations in the SAR must demonstrate that the spent fuel cask meets all 10 CFR 71 requirements and has sufficient margins of safety included to protect the public from undue risk. In general, margins of safety are included by using established practices, codes, and standards such as the American Society of Mechanical Engineers (ASME) Code and the American



All dimensions in inches

<u>Item</u>	<u>Weight, lbs</u>
Body	32,000
Limiter	4,500
Contents	<u>2,500</u>
	39,000

Figure 3-6 Representative truck cask design used for dynamic structural and thermal response studies.



All dimensions in inches

<u>Item</u>	<u>Weight, lbs</u>
Body	122,500
Limiter	22,500
Contents	52,000
	<u>197,000</u>

Figure 3-7 Representative rail cask design used for dynamic structural and thermal response studies.

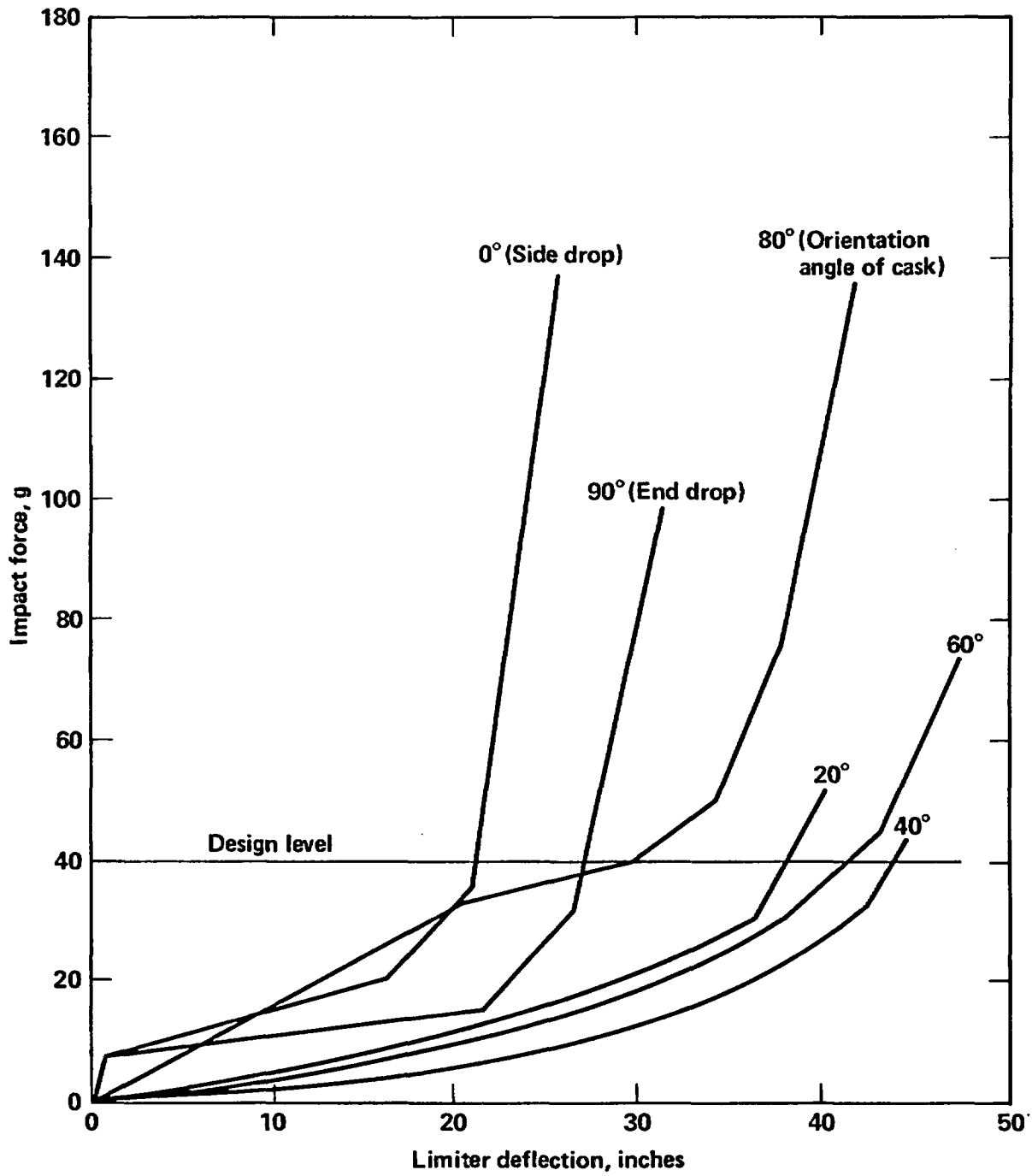


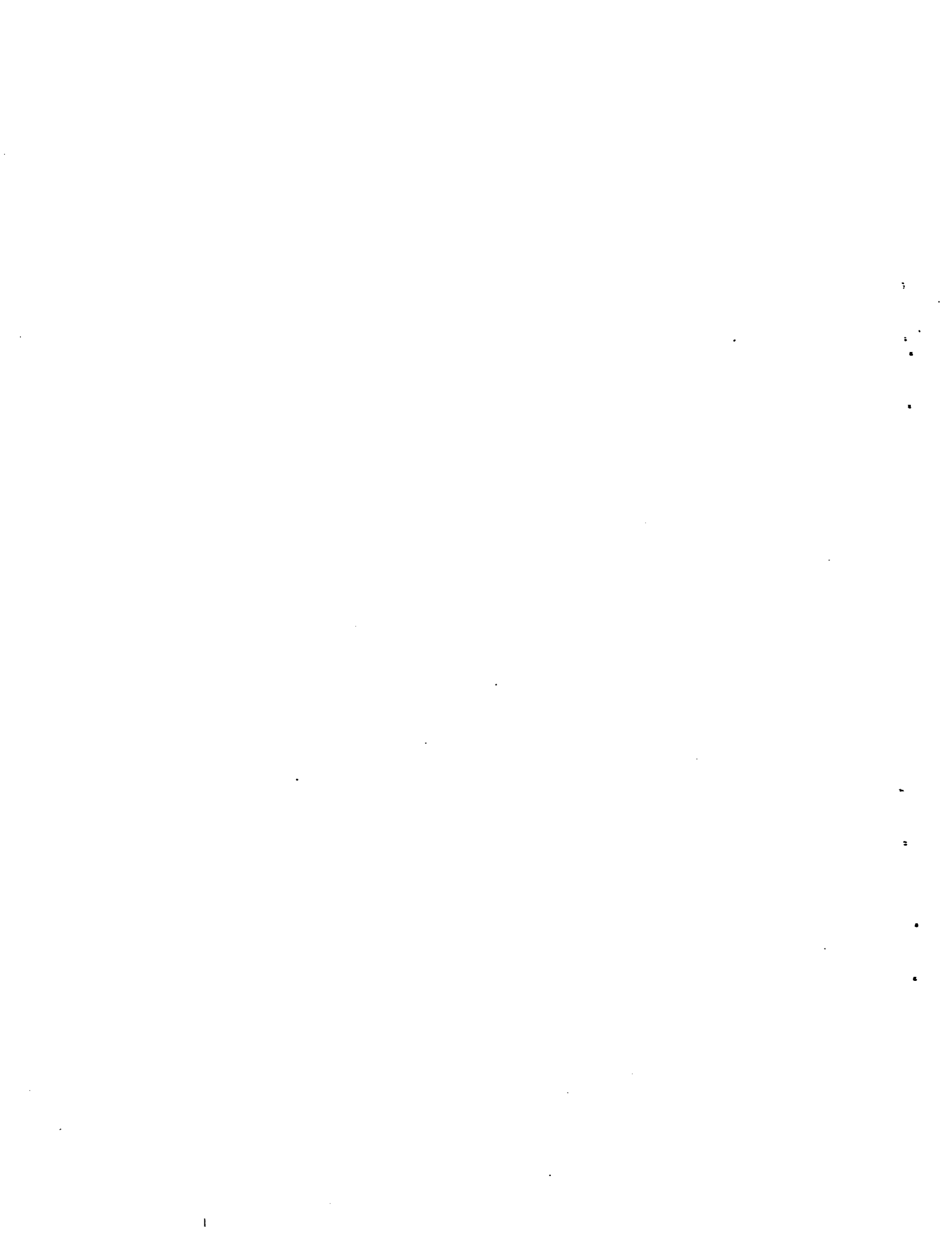
Figure 3-8 Force-deflection characteristics of the limiter design as a function of cask orientation at impact.

National Standards Institute (ANSI) Standards, and Regulatory Guides, all of which must be identified in the SAR.

Regulatory Guides are written by the NRC to provide guidance in many areas of licensing that result in acceptable margins of safety. For example, Regulatory Guide 7.6 adapts portions of the ASME Code, Section III to the design of spent fuel casks and recommends that elastic methods of structural analysis be used in the containment design.<sup>6</sup> Other Regulatory Guides relating to spent fuel casks are 7.4 (Leak Testing), 7.8 (Load Combinations), 7.9 (SAR Format), and 7.10 (Quality Assurance).<sup>7-10</sup>

Although there is no specific section in the ASME Code applicable to spent fuel casks, the ASME Code has been used extensively in designing, manufacturing, using, and maintaining spent fuel casks.<sup>11</sup> In general, materials adopted by the ASME Code provide a large margin of safety against rupture because the materials have high ductility. Also the use of elastic analysis for structural design usually results in a large margin of safety. For example, cask containments using 304 stainless steel are designed for the accident test conditions to ASME stress intensity limits that result only in slight yielding of the cask structure. In most cases, depending on the limiter design, the 304 stainless steel material can experience an off-set strain less than 1% under accident test conditions but rupture of 304 stainless steel occurs at strains greater than 30%. Therefore, large amounts of energy can be absorbed by the cask structure though large deformations under loading conditions exceeding the accident test conditions without catastrophic rupture occurring. To preclude brittle fracture failure from occurring at low temperatures, only materials with adequate toughness can be used in the structural design of spent fuel casks.<sup>12,13,14</sup>

In this study it is assumed that the representative casks have been properly designed and manufactured to appropriate codes and standards.<sup>15,16</sup> The representative cask designs are based on currently licensed cask designs and are likely to be certified if a SAR were prepared and submitted to the NRC. The margins of safety included in the cask design are representative of those included in currently licensed casks.



## 4.0 REPRESENTATIVE CASK RESPONSE STATES, LEVELS, AND REGIONS

### 4.1 Introduction

If a shipping container is involved in an accident, a cask response is generated and damage can occur. The response depends on many elements, such as the magnitude of the loadings generated by the accident impact velocity, the object struck, and if a fire is involved, the flame temperature and the duration of the fire. The response can be different at different locations or by various components within a cask. Different cask designs can have different magnitudes and types of responses when subjected to the same accident conditions. The actual response is a result of the combined effect of all these factors. Normally, the higher the response, the greater the damage to the cask and, therefore, the greater the potential for an event with a radiological significance.

In order to determine the response, three methods are commonly used: analytical, experimental, and a combination of the two. In this study, the analytical method is used to estimate responses. Many different computer codes are used to perform the analyses. These computer codes, as pointed out throughout the report, are benchmarked against closed-form solutions and experimental data. Appendix H discusses benchmarking for some of these codes.

In order to calculate response by analysis, a proper selection of computer codes is essential. Every computer code has limitations. The proper selection of a code requires a thorough understanding of its limitations. Sections 6.0 and 7.0 discuss the method of analysis, including the assumptions used in the analysis and the modeling technique by which the cask structures are represented. Individual analyses and their results are also presented.

The purpose of estimating the response is to determine the degree of structural damage. Certain types of damage, such as damage at specific locations or to certain components within the cask structure, can result in radiological hazards. Other types of damage may appear to be large, but result in essentially no radiological hazards. In order to evaluate the consequences resulting from structural damage, it is necessary to relate the

potential radiological hazard to the type of damage and cask response. Sections 4.2 and 4.3 qualitatively discuss the association between the structural and thermal damages and the potential radiation hazard. Section 8.0 provides a detailed discussion that relates the level of response to the level of potential radiological hazard.

Defining a specific response state is a very complex problem because response varies with different cask designs, severity of accidents, and location within the cask structure. In order to evaluate the level of damage between one response state and another, it is essential to establish some kind of measurement scale.

Response can be expressed in terms of many parameters, such as force, moment, displacement, stress, strain, and temperature. To establish a measuring scale with too many different types of response parameters will make any assessment unmanageable. The most effective approach is to identify one response parameter which provides both an adequate indication of cask structural damage and also an easy linkage to a radiological hazard estimate. This section discusses the selection of the parameters to represent the structural and thermal responses for the representative cask designs, the justification of the selections, and the discretized levels of response states used in this study.

#### 4.2 Response States and Levels for Mechanical Loads

Various types of damage can occur to casks subjected to mechanical loads. The most important types of damage to a lead shielded cask are yielding, large dimensional changes, and rupture of the cask structure. Any parameter selected to represent the structural response state of the representative casks should indicate these types of structural damage.

Three engineering response parameters--stress, strain, and displacement--are considered as candidates for the single parameter to represent the response state for mechanical loads.

Stress is commonly used in structural analysis to represent the state of response. Both the American Society of Mechanical Engineers and the American

Institute of Steel Construction use stress as the parameter to define acceptance design limits in terms of yield and ultimate stress.<sup>1,2</sup> It is a good parameter for design within the elastic range of the material. When the response is beyond the elastic range, however, large dimensional changes can occur with only small changes in the stress level. The purpose of this study is to estimate the damage and consequence to the representative casks when subjected to severe accident conditions in which the response could exceed the elastic range. Therefore, stress is not the best parameter to represent the response state for mechanical loads applied to the representative casks.

Displacement is a parameter for measuring the dimensional change of structural elements. It is capable of describing the deformation shape for both small and large loading conditions. The deficiency in using displacement is that it cannot provide direct comparison with the design acceptance limits. Displacement cannot indicate directly when the structure has yielded or ruptured.

Strain is the most appropriate single parameter to represent the response state for mechanical loads. For a given material, dimensional changes occurring with loading conditions are directly related to strain. Strain can also indicate yielding and rupture when responses reach strain limits. Therefore, strain is selected for mechanical load responses of the representative casks.

Strain will most likely vary according to location within the structure. Under one specific accident load, strain at the inner shell is different from that at the outer shell, at the bolts, and at the enclosures. Sensitivity studies are conducted using the representative casks to find out the relationship between the strains at different locations or on different components inside the cask structure. This relationship helps to estimate the total cask damage level when strain at a particular component is identified. The strain on the inner shell of the cask structure is selected as the best single parameter to characterize mechanical load response states for the representative casks.

Although the response of a cask is continuous over a loading range, three discrete response levels are defined to relate ranges of response states and mechanical loads to potential radiological hazards. The response levels are defined as discrete levels of maximum effective strain on the inner shell of the representative cask structure. The maximum effective strain of the representative truck and rail cask impacting an unyielding surface can be significantly different as shown schematically in Fig. 4-1. The three discrete response levels or strain levels that bound the response state ranges are identified on the figure.

#### 4.2.1 Structural Response Level, $S_1$

The first response level,  $S_1$ , is defined to be 0.2% strain at the inner shell. This level of strain is selected for the first response level because the structural material of the representative casks is 304 stainless steel which has a 0.2% offset yield point. For strains within the 0.2% yield strain ( $S_1$ ), shown as range A in Fig. 4-1, the response of the structure is elastic and there is no permanent dimensional change after the loading is removed. This characteristic assures that little, if any, radiation release occurs when the cask is subjected to accident loads that are within range A because the seal and bolts remain functional. At 0.2% strain ( $S_1$ ), the representative lead cask designs experience less than 40 g axial force on the lead for all orientations of impact. No lead slump occurs. The fuel basket remains functional. Up to 3% of the fuel rods can release limited amounts of radioactive material into the cask cavity under these loading conditions. Essentially all of the impact loads on the casks are absorbed by their impact limiters. These loads and releases are within the regulatory design conditions and release limits.

#### 4.2.2 Structural Response Level, $S_2$

The second response level,  $S_2$ , is defined to be 2% plastic strain at the inner shell. For strains between 0.2% ( $S_1$ ) and 2% ( $S_2$ ), shown as range B in Fig. 4-1, the response of the structure is plastic, and small permanent dimensional changes occur. The dimensional changes can affect the cask

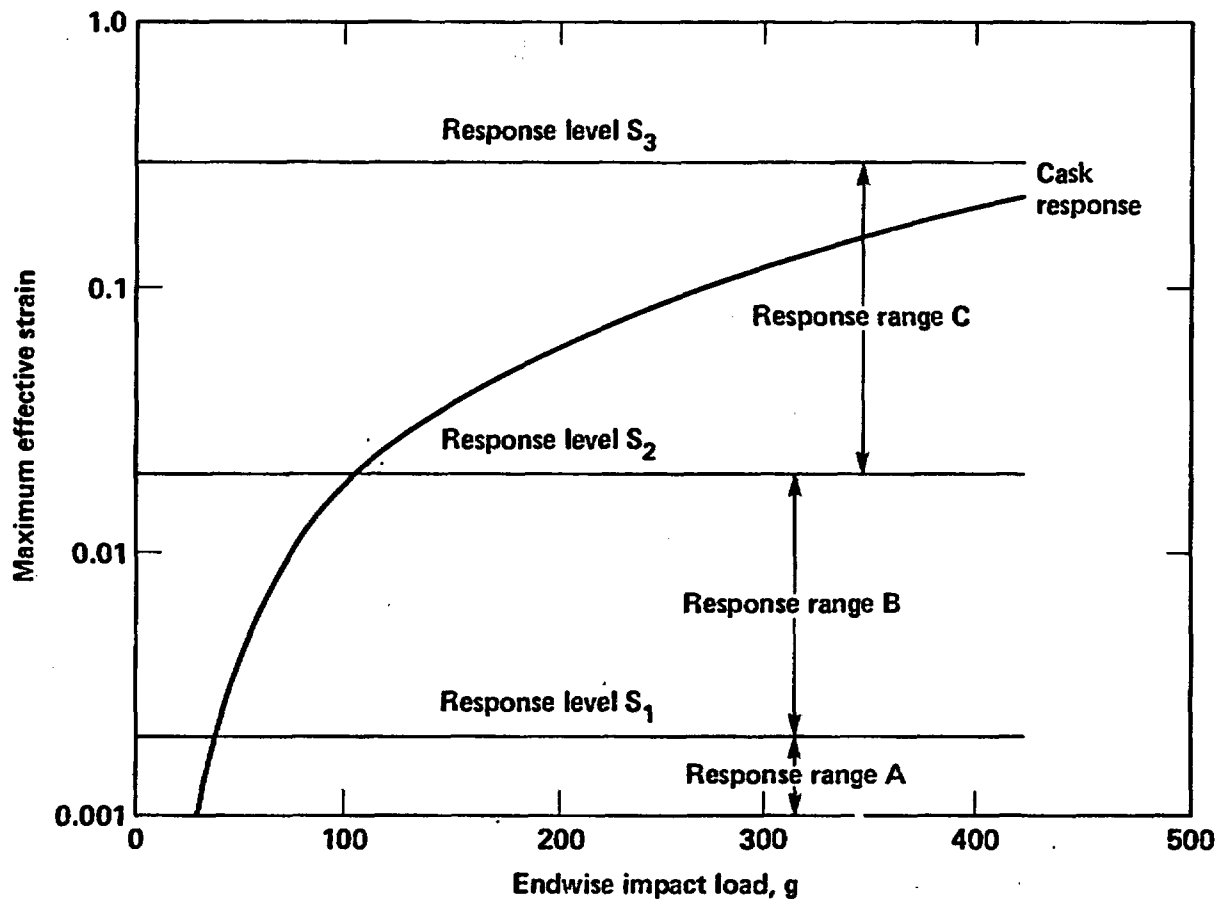


Figure 4-1 Schematic representation of cask response state for mechanical load.

closure seals and result in limited radioactive material releases. Also, a small dimensional change can result from limited lead slump which can result in an increase of radiation emanating from the cask. Up to 10% of the fuel rods can leak into the cask cavity under these loading conditions. The radiation hazards caused by seal leakage and lead slump in range B are near regulatory limits. The loads that produce the second response state are near the loads imposed by the accident test conditions. In this range, the impact loads on the representative casks are absorbed mostly by their impact limiters, but part of the loads are absorbed by the cask structure.

#### 4.2.3 Structural Response Level, $S_3$

The third response level,  $S_3$ , is defined to be 30% plastic strain at the inner shell. The 30% strain ( $S_3$ ) level is below the fracture strain of 304 stainless steel, but the large distortions occurring with this strain level can cause local cracking in the welded regions. For strains between 2% ( $S_2$ ) and 30% ( $S_3$ ), shown as range C in Fig. 4-1, the response is plastic deformation with large dimensional changes occurring, particularly for strain near 30% ( $S_3$ ). Any large distortions of the cask will likely cause seal leakage in the closure region, lead slump, localized weld cracking, and some crushing of the cask contents. All of the fuel rods are expected to release limited amounts of radioactive material into the cask cavity under these extreme loading conditions. The radiological hazards associated with this response can be outside of regulatory limits; however, there will not be any failure that will result in release of solids from fuel rods, except very small particles that may escape to the environment. In this response range, an increasing amount of the impact force is absorbed by the cask compared to the force absorbed by the limiter. In fact, at the 30% strain ( $S_3$ ) level, the energy absorption by the representative casks may be eight times higher than the energy absorbed by the limiter.

#### 4.2.4 Application of Response States and Levels

Each response state implies a force on the cask as a result of impacts upon various objects. The force is primarily determined by the impact

velocity and the hardness of the object, but various combinations of velocity and object hardness can result in the same force. Consequently, the force associated with each structural response state can be related to various accident scenarios. Furthermore, the potential radiation hazard associated with these response states can be related to these same accident conditions.

Figure 4-2 shows schematically the structural response state of a representative cask in terms of strain as a function of both impact velocity and surface hardness for endwise impacts. The combination of impact velocity and surface hardness for the strain levels 0.2% ( $S_1$ ), 2% ( $S_2$ ), and 30% ( $S_3$ ) are also shown on the plot. For example, the impact velocities required to reach the 0.2% strain ( $S_1$ ) level, will be 30 mph for an unyielding object, 60 mph for an object of medium hardness, and 90 mph for a soft object. For very soft objects, the 0.2% strain ( $S_1$ ) level can never be attained. Limiting the velocities impacting various objects can similarly be obtained corresponding to the 2% ( $S_2$ ) and 30% ( $S_3$ ) strain levels.

#### 4.3 Response States and Levels for Thermal Loads

Various types of damage can occur to the representative casks subjected to thermal loads. The most important types of damage are degradation of the closure seal material, melting of the lead shield, dimensional changes to the structure, and alloying of the lead with the nickel in the 304 stainless steel structural material. Any parameter selected to represent the thermal response state of the cask should indicate the various types of thermal damage that can occur.

Two engineering response parameters, strain (thermally-induced) and temperature, are considered as candidates for the single parameter to represent the response state for thermal loads.

In Section 4.2, mechanical strain is selected as the single parameter to represent the response state for mechanical loads. Thermally induced strain provides a good indication of dimensional changes to the cask structure, but does not provide any indication of seal deterioration, melting of lead, or alloying of lead with the nickel in stainless steel. Therefore strain is

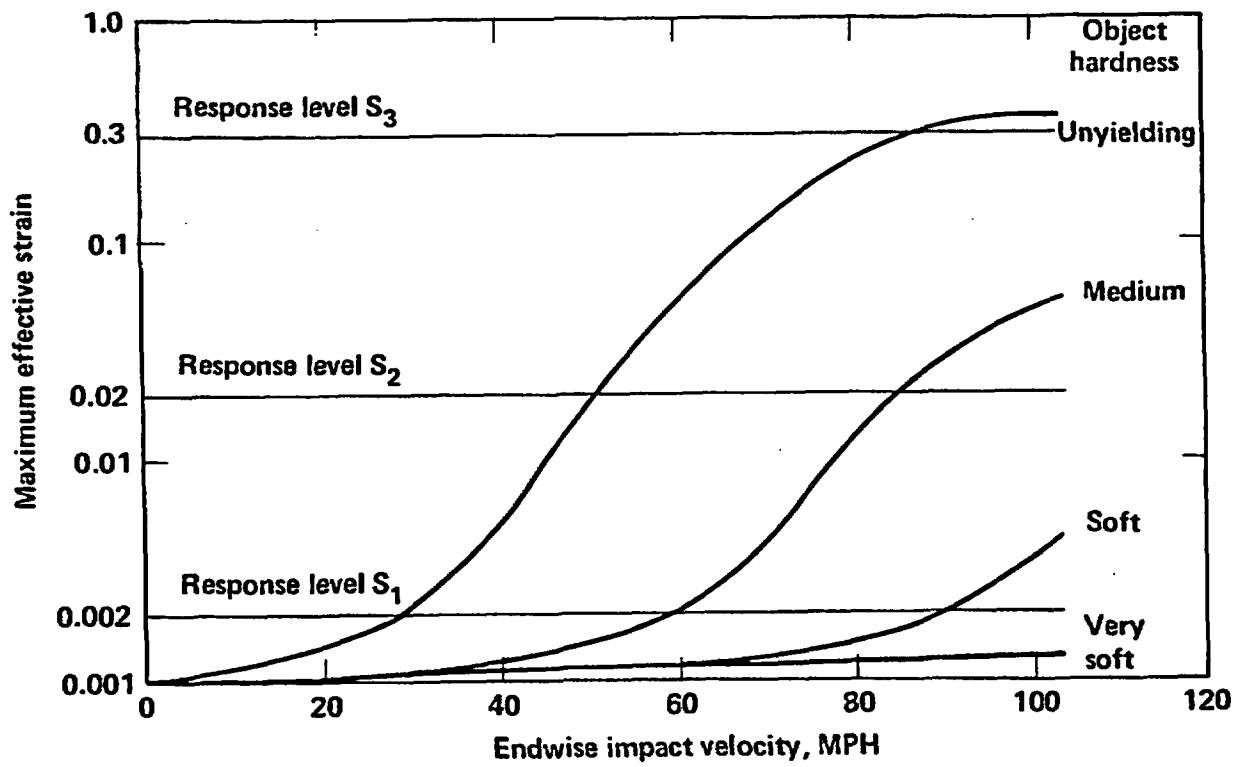


Figure 4-2 Schematic representation of cask structural response for various surface hardness and impact velocities.

determined not to be the best parameter to represent the response state for thermal loads.

Temperature is the best single parameter to represent the response state for thermal loads. Temperature provides an indication of seal deterioration, melting of lead, and alloying of lead with the nickel in stainless steel. It also provides an indirect measure of dimensional changes with lead melt. Therefore, temperature is selected for thermal load responses.

Temperature varies from location to location within the cask. For any specific fire-accident, the temperature at the inner shell is different from that at the outer shell, at the bolts, and at the enclosures. Sensitivity studies are conducted to find out the relationship between the temperatures at different locations and on different components inside the cask structure. This relationship provides a means to estimate the total cask damage level when the temperature at a particular component is identified. The temperature at the middle of the lead shield thickness is selected as the appropriate single parameter to characterize thermal load response states.

Although the response of a cask is continuous over a loading range, four discrete response levels are defined to relate ranges of response states and thermal loads to radiological hazard. The response levels are defined in terms of the temperature at the middle of the lead shield thickness. As an illustration of a cask exposed to a regulatory fire, Fig. 4-3 shows schematically the lead mid-thickness temperatures as a function of the thermal loads to the cask. The four discrete response levels, or lead mid-thickness temperatures, that bound the response state ranges are identified on the figure.

#### 4.3.1 Thermal Response Level, $T_1$

The first response level,  $T_1$ , is defined as a temperature of 500°F at the middle of the lead shield thickness. This temperature is selected because the cask seals are below temperatures that can cause degradation of properties to such materials as silicon and fluorocarbons. Also, there is a significant margin between 500°F ( $T_1$ ) and the melting point of lead at 621°F. For

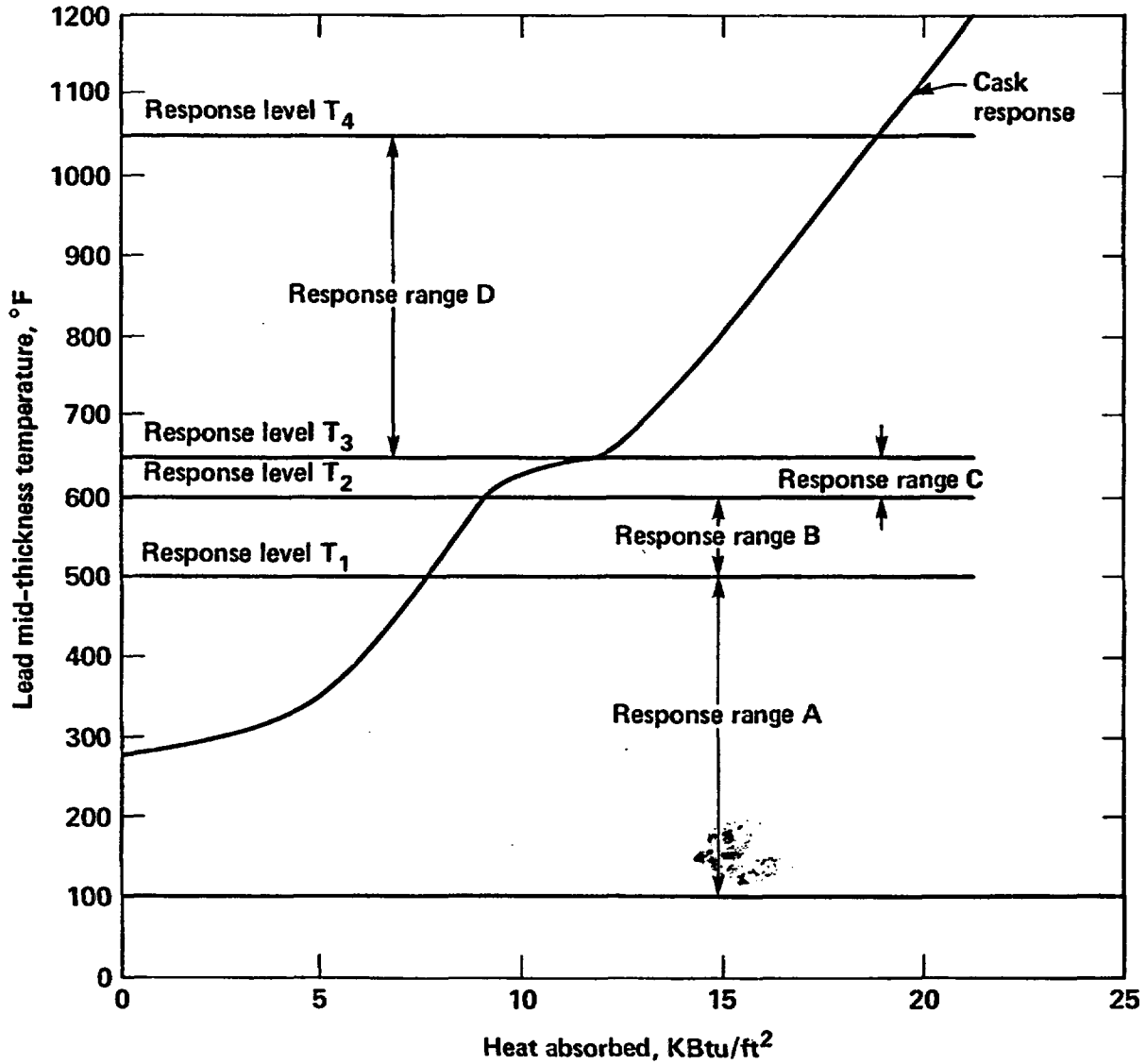


Figure 4-3 Schematic representation of cask response state for thermal load.

temperatures less than 500°F ( $T_1$ ), shown as range A in Fig. 4-3, there is no significant damage to the cask due to thermal loads. However, it is assumed that the water in the neutron shield is released before the 500°F temperature ( $T_1$ ) is reached. The release of the water forms a thermal barrier between the neutron shield wall and the cask outer wall which protects the cask from any fire. The release of the water also increases the neutron radiation surrounding the cask; however, all radiological hazards are within regulatory limits below this first level thermal response.

#### 4.3.2 Thermal Response Level, $T_2$

The second response level,  $T_2$ , is defined as a temperature of 600°F at the middle of the lead shield thickness. Temperatures between 500°F ( $T_1$ ) and 600°F ( $T_2$ ) are shown to be in range B in Fig. 4-3. In this temperature range, the lead at the outer stainless steel wall of the cask is still below 621°F, the melting point of lead. Even though the lead does not melt, the cask closure seals can degrade and potentially release limited radioactive material. Any radiological hazards caused by seal leakage and the loss of the neutron shield are likely to be within regulatory limits.

#### 4.3.3 Thermal Response Level, $T_3$

The third response level,  $T_3$ , is defined as a lead mid-thickness temperature of 650°F. For temperatures between 600°F ( $T_2$ ) and 650°F ( $T_3$ ), shown as range C in Fig. 4-3, melting of the lead shield occurs. Lead melt results in a phase change with a lead density decrease of approximately 10%. The density change results in an increase in the lead volume and significant plastic straining of the inner cask wall. After the cask cools, the lead returns to its original density, and voids can occur in the lead shield owing to the increased volume from the plastic strain of the inner cask wall. The cask closure seals are assumed to leak. The increase in radiation level from the lead shield reduction and any radioactive material releases will likely be outside of regulatory limits.

#### 4.3.4 Thermal Response Level, $T_4$

The fourth response level,  $T_4$ , is defined as a lead mid-thickness temperature of 1050°F. For temperatures in the range of 650°F ( $T_3$ ) to 1050°F ( $T_4$ ), shown as range D in Fig. 4-3, the lead shield thickness is reduced further due to differential thermal expansion between the liquid lead and stainless steel structural material. The fuel rods can also increase in temperature and begin to burst. For temperatures above 1050°F ( $T_4$ ), the alloying of the lead with the nickel in the stainless steel structure can become significant and result in stress corrosion cracking.<sup>3-5</sup> In this response range, the further reduction in shielding and possible bursting of fuel rods increases the radiological hazards.

#### 4.3.5 Application of Response States and Levels

Each response state implies a thermal load applied to the cask as a result of various fire conditions. The thermal load is determined by the fire characteristics. However, various fire characteristics can result in the same thermal load. Consequently, the thermal load associated with each thermal response state can be related to various accident conditions involving fires. Furthermore, the potential radioactive hazards associated with these response states can also be related to the same accident conditions.

Figure 4-4 schematically presents the thermal response of a cask in terms of the lead mid-thickness temperature as a function of both fire duration and fire location. The combination of fire duration and location for the temperature levels 500°F ( $T_1$ ), 600°F ( $T_2$ ), 650°F ( $T_3$ ), and 1050°F ( $T_4$ ) is also shown on the plot. For example, for a fire with a flame temperature of 1700°F, the time duration to reach the 500°F temperature ( $T_1$ ) level, will be 1.3 hours for an engulfing fire, 2.3 hours for a fire tangent to the cask, and 3.6 hours for a fire 20 feet from the cask. For fires greater than 50 feet away, the 500°F temperature ( $T_1$ ) level can never be attained. Fire durations for the various fire locations can similarly be estimated corresponding to the 600°F ( $T_2$ ), 650°F ( $T_3$ ), and 1050°F ( $T_4$ ) temperature levels.

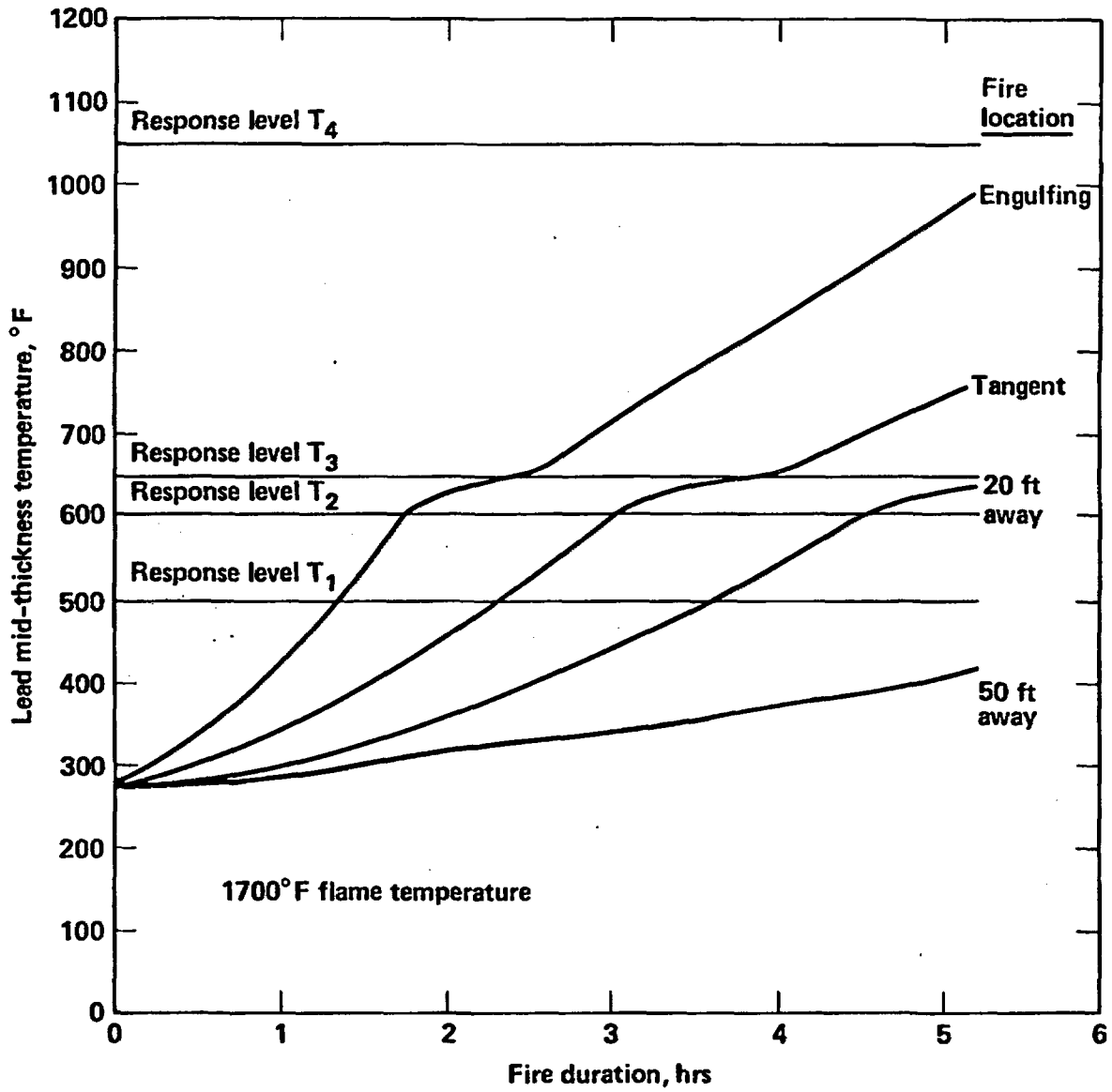


Figure 4-4 Schematic representation of cask response for various fire locations and fire durations.

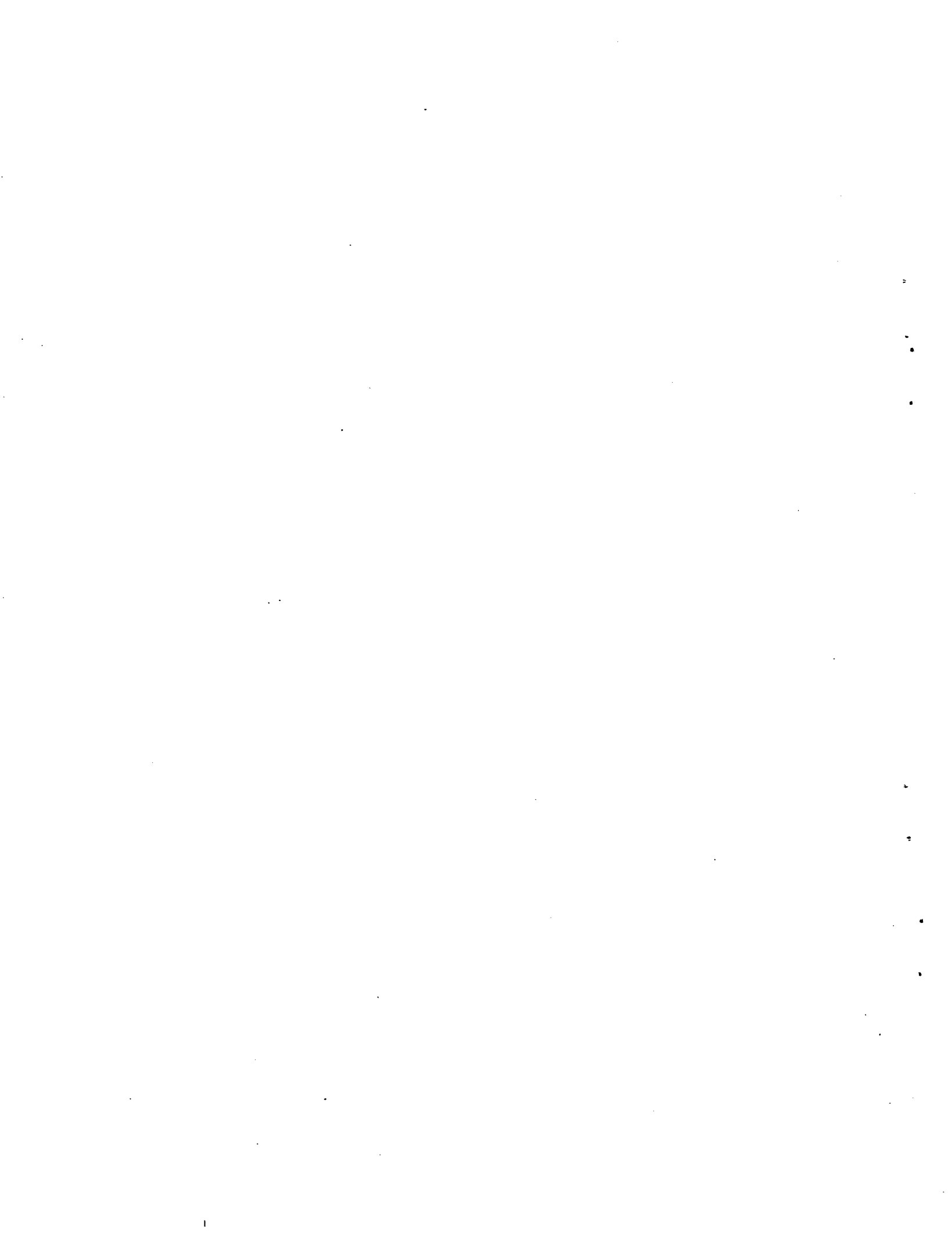
#### 4.4 Cask Response Regions

In some cases, a cask will be exposed to both mechanical and thermal loads. A range of combined structural and thermal responses for a cask can be represented by the response matrix shown in Fig. 4-5. The ordinate of the response matrix represents the structural response states; the abscissa represents the thermal response states; and the boundaries of the response regions are defined by the structural and thermal response levels.

There are 20 response regions denoted by  $R(S_i, T_j)$  where  $S_i$  is the structural response level and  $T_j$  is the thermal response level. Although only three discrete structural response levels are defined, a fourth unbounded level exists that consists of cask strain responses greater than 30% ( $S_3$ ). Similarly, a fifth unbounded thermal response level exists which consists of cask temperature responses greater than 1050<sup>0</sup>F ( $T_4$ ). The first region,  $R(1,1)$ , represents the cask response to combined mechanical and thermal loads within the 0.2% strain ( $S_1$ ) and 500<sup>0</sup>F temperature ( $T_1$ ) levels. Radioactive releases, if any, for cask responses in  $R(1,1)$  will be within regulatory limits. The twentieth region,  $R(4,5)$ , represents the most extreme combined response state in which the potential radiological hazards will be a maximum. In general, the probability of occurrence of a particular combination of mechanical and thermal loadings decreases with the severity of these loads. The probabilities associated with each region of the load matrix are discussed in more detail in Section 5.0.

Structural response (maximum strain on inner shell, %)	$S_3$ (30)	R (4,1)	R (4,2)	R (4,3)	R (4,4)	R (4,5)
	$S_2$ (2)	R (3,1)	R (3,2)	R (3,3)	R (3,4)	R (3,5)
	$S_1$ (0.2)	R (2,1)	R (2,2)	R (2,3)	R (2,4)	R (2,5)
		R (1,1)	R (1,2)	R (1,3)	R (1,4)	R (1,5)
		$T_1$ (500)	$T_2$ (600)	$T_3$ (650)	$T_4$ (1050)	
		Thermal response (lead mid-thickness temperature, °F)				

Figure 4-5 Matrix of cask response regions for combined mechanical and thermal loads.



## 5.0 PROBABILITY ANALYSIS

### 5.1 Introduction

The emphasis of the discussion in Sections 6.0 and 7.0 is on the physical loads, both mechanical and thermal, which a spent fuel cask can experience in a transportation accident. Specifically, cask response states, evaluated in terms of containment vessel strains and lead shield temperatures, are related to basic accident parameters such as impact velocities and fire duration.

The relationships between cask responses to mechanical loads and the impact velocity of the cask are derived for several cask impact orientations involving interactions with objects of differing hardness. The effect of cask orientation on the strain-impact velocity relationship for an unyielding object is shown in Fig. 5-1 for the truck cask. The impact velocity, defined as the cask velocity in the direction perpendicular to the object impacted, is determined by the velocity of the cask due to the accident and the impact angle.

The thermal loading to a cask depends on the flame temperature and fire location as well as the duration of a fire. Thus, the relationship between cask response to thermal loads and the duration of a fire is affected by the flame temperature and location of the fire with respect to the cask. The effects of these parameters are illustrated in Fig. 5-2.

In summary, the following accident parameters, which affect the cask response to mechanical and thermal loads, are identified and are considered in the probability analysis:

- o Mechanical loads
  - impact velocity
    - cask velocity
    - impact angle
  - cask orientation
  - hardness of the impacted object

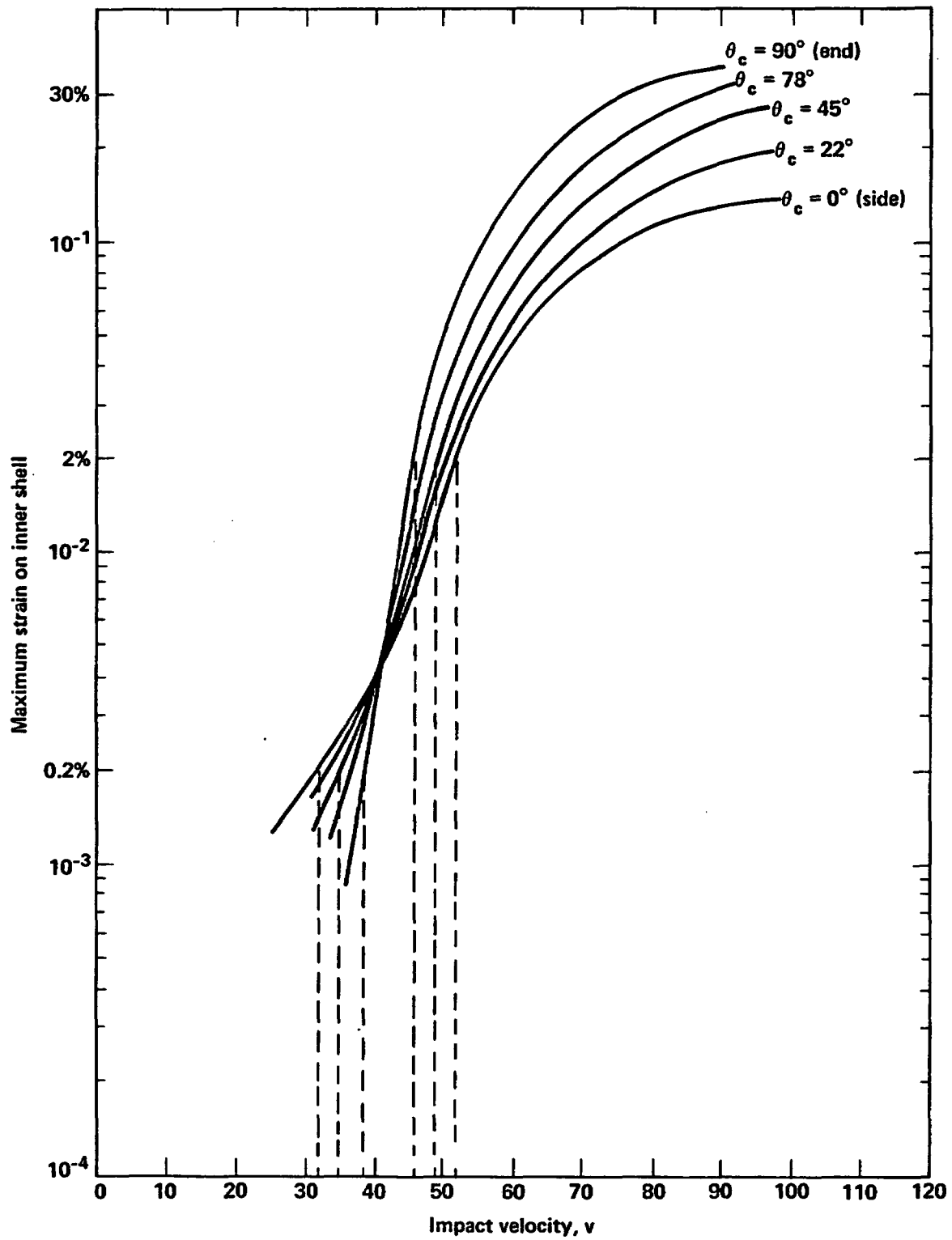


Figure 5-1 Effect of cask orientation on the strain-impact velocity relationship for a truck cask impacting an unyielding object.

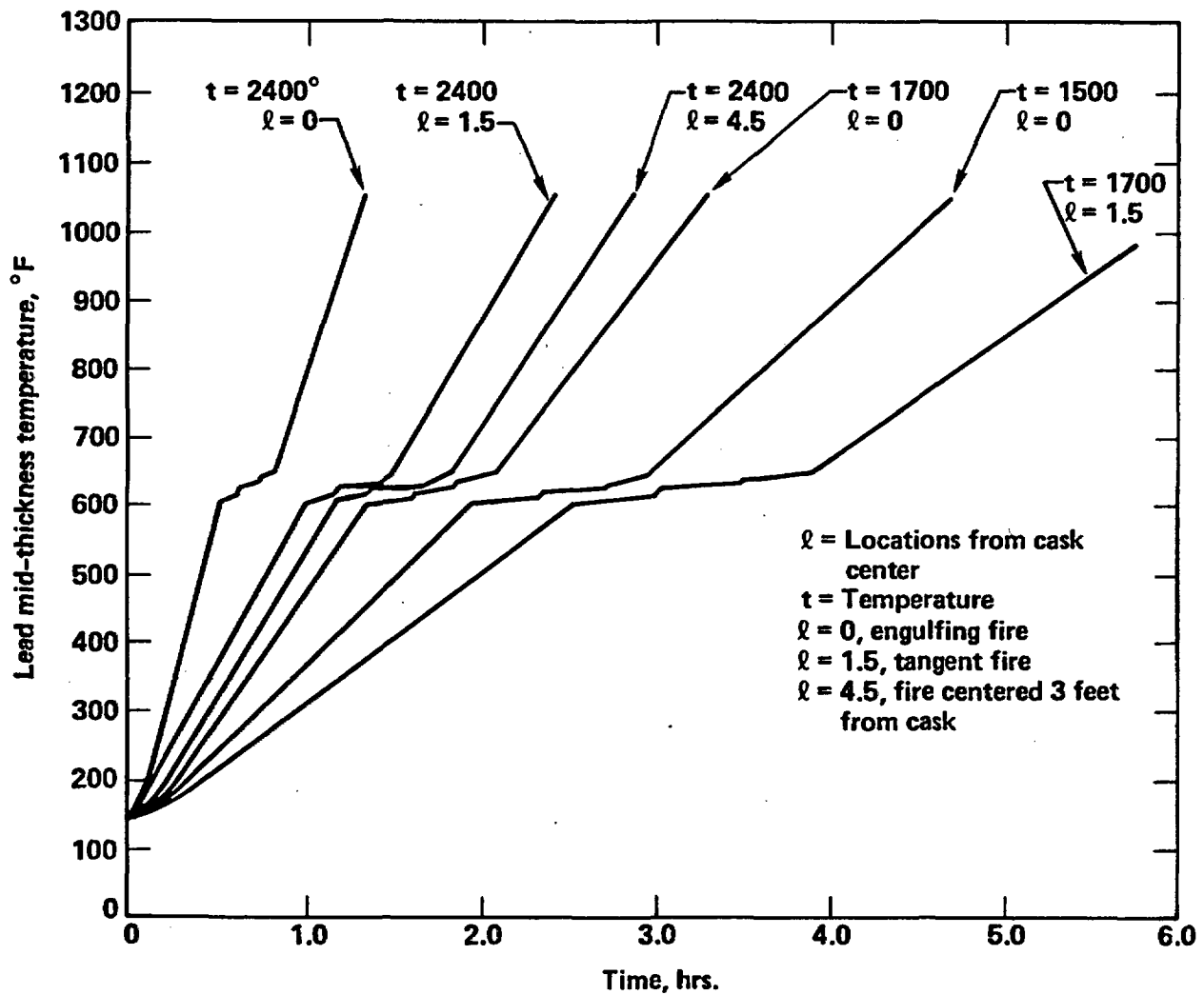


Figure 5-2 Effect of flame temperature and fire location on lead-temperature-time relationship for a truck cask.

- o Thermal loads
  - fire duration
  - flame temperature
  - fire location with respect to the cask.

Because future accident conditions are unpredictable, i.e., random, the response state of a spent fuel cask cannot be predicted deterministically. Assessment of the response states and the subsequent damage and release of radioactive materials due to transportation accidents can only be expressed probabilistically.

The purpose of this section is to describe the probability analysis developed to estimate the likelihood that a spent fuel cask will attain various response states during a transportation accident. Section 5.2 catalogs the probability distributions used to describe the random variation associated with the accident parameters. The probability calculations are outlined in Section 5.3.

## 5.2 Probabilistic Inputs

Estimation of the likelihood of various cask response states, represented by the containment vessel strain and the lead mid-thickness temperature, is based on estimates of the distributions of the accident parameters which affect the response of the cask during a transportation accident. The distributions of the accident parameters are described in terms of a cumulative distribution function,  $F(x)$ , if the parameter is quantitative, or a probability function,  $h(\theta)$ , if the parameter is qualitative, e.g., the object impacted. The cumulative distribution function describes the likelihood that the parameter value is less than or equal to  $x$ , the argument of  $F(\cdot)$ , i.e.,

$$F(x) = P_r(X \leq x) \quad (5.1)$$

where  $X$  denotes the accident parameter. The probability function describes the likelihood of each  $\theta$  or object, i.e.,

$$h(\theta) = P_r(\theta) \quad (5.2)$$

where  $\theta$  denotes the qualitative object.

The distributions of the accident parameters used to estimate the likelihood of cask response states are presented in this section. Development of these distributions was discussed in Section 2.0. The data used to estimate accident rates and velocity distributions is summarized in Appendixes B and C. The method of estimation is discussed in Appendix G.

### 5.2.1 Mechanical Loading Parameter Distributions

Object hardness, impact velocity, and cask orientation are three mechanical loading parameters which have a significant influence on a cask's structural response in a transportation accident.

#### 5.2.1.1 Object Hardness Distributions

Each of the accident scenarios, described in Section 2.0 and shown in Figs. 2-3, 2-4, and 2-5, identifies a type of accident, e.g., a collision, and the object or surface which a cask could impact, e.g., a truck, bridge abutment, or embankment. From these descriptions, object hardness is estimated. Thus, the distribution of hardness of the impacted object is described in terms of the probabilities of the accident scenarios. These are included in Figs. 2-3, 2-4 and 2-5 for highway and railway accidents.

#### 5.2.1.2 Impact Velocity Distributions

##### 5.2.1.2.1 Cask Velocity

The distribution of cask velocity during a transportation accident varies between accident scenarios. For example, the distribution of cask velocity experienced in truck-truck collisions is expected to differ from the distribution associated with accidents involving falls from bridges. In truck-truck accidents, the distribution depends on the speeds of the individual trucks at the time of the collision. For accidents involving falls from bridges, the cask impact velocity is determined by the fall height.

The following distributions of cask velocities are applicable to highway accidents:

- V1: The truck velocity, adjusted for braking, prior to an accident
- V2: The velocity due to bridge heights
- V3: The vector sum of truck velocity, adjusted for braking, and velocity due to bridge heights
- V4: The train velocities at grade crossing accidents.

As discussed in Subsection 2.5.1.2.1, the primary source of truck velocities is based on accident reports that estimate velocities prior to an accident. The observed data does not account for any reduction in velocity at impact due to braking efforts by the drivers. However, a North Carolina study provides data which allow for braking effects.<sup>1</sup> These results are used to adjust the basic cumulative distribution function of truck velocities as shown in Fig. 5-3. The adjustment is based on the identity

$$F_{V1}(s) = F_I[s/\delta(s)] \quad (5.3)$$

where

$$\delta(s) = \begin{cases} 0.65 + \frac{0.35}{78} s & 0 \leq s \leq 78 \\ 1.0 & s \geq 78 \end{cases} \quad (5.4)$$

and  $F_{V1}(\cdot)$  and  $F_I(\cdot)$  denote the adjusted and initial truck velocity cumulative distribution functions, respectively. At velocities greater than 78 mph no credit for braking is assumed. As velocity decreased, the effect of braking increased, e.g., a 40 mph velocity is reduced to 33 mph, whereas a 10 mph velocity is reduced to 7 mph.

The four cumulative distribution functions used for the velocity of highway accidents are presented in Table 5.1. They are estimated from historical accident data using the method of estimation described in Appendix G.

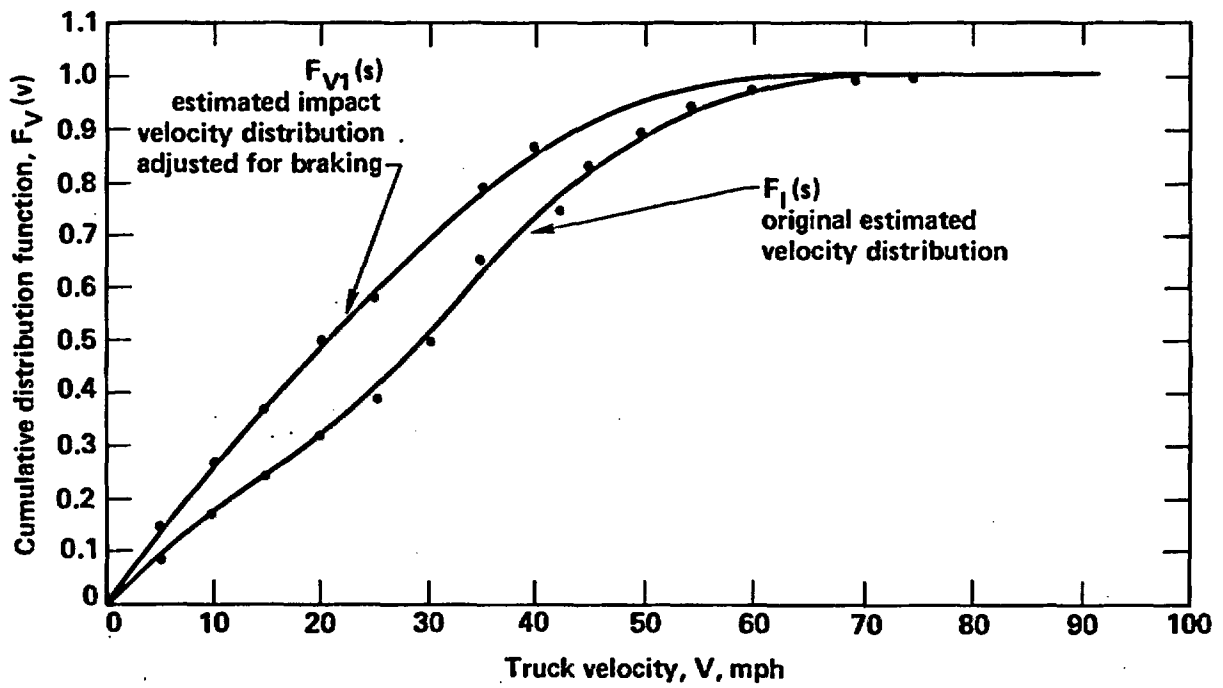


Figure 5-3 Distribution of vehicle velocities adjusted for braking.

Table 5.1  
Cumulative Cask Velocity Distributions for Highway Analysis

Distributions							
<u>V1</u>		<u>V2</u>		<u>V3</u>		<u>V4</u>	
Cask Velocity,s (mph)	$F_S(s)$	Cask Velocity,s (mph)	$F_S(s)$	Cask Velocity,s (mph)	$F_S(s)$	Cask Velocity,s (mph)	$F_S(s)$
0.	0.	0.	0.	0.	0.	0.	0.
2.0	0.03834	7.74	0.00621	5.0	0.	2.0	0.06014
6.0	0.12916	10.94	0.01550	10.0	0.00141	6.0	0.17906
10.0	0.23508	15.48	0.04754	15.0	0.00821	10.0	0.29398
14.0	0.34886	18.95	0.1051	20.0	0.03387	14.0	0.40255
18.0	0.46237	21.89	0.1952	25.0	0.11129	18.0	0.50280
22.0	0.56877	24.47	0.3178	30.0	0.28292	22.0	0.59331
26.0	0.66345	26.81	0.4629	35.0	0.51279	26.0	0.67319
30.0	0.74353	28.95	0.6124	40.0	0.70110	30.0	0.74210
34.0	0.80877	30.95	0.7464	45.0	0.81951	34.0	0.80022
38.0	0.86020	32.83	0.8508	50.0	0.89168	38.0	0.84814
42.0	0.89961	34.61	0.9217	55.0	0.93543	42.0	0.88676
46.0	0.92881	36.29	0.9635	60.0	0.96178	46.0	0.91718
50.0	0.95009	37.91	0.9849	65.0	0.97751	50.0	0.94062
54.0	0.96547	39.46	0.9945	70.0	0.98680	54.0	0.95826
58.0	0.97634	41.67	0.9991	75.0	0.99227	58.0	0.97125
62.0	0.98383	43.08	0.9998	80.0	0.99547	62.0	0.98060
66.0	0.98908	44.45	0.9999	85.0	0.99766	66.0	0.98717
70.0	0.99261	56.86	1.0	90.0	0.99901	70.0	0.99169
74.0	0.99503			95.0	0.99961	74.0	0.99473
78.0	0.99670			100.0	0.99985	78.0	0.99672
82.0	0.99825			105.0	0.99995	82.0	0.99800
86.0	0.99910			110.0	0.99998	86.0	0.99881
90.0	0.99956			115.0	0.99999	90.0	0.99930
94.0	0.99979			150.0	1.0	94.0	0.99960
98.0	0.99990					98.0	0.99977
102.0	0.99995					102.0	0.99987
106.0	0.99998					106.0	0.99993
110.0	0.99999					110.0	0.99996
150.0	1.0					114.0	0.99998
						118.0	0.99999
						150.0	1.0

$F_S(s)$  - Probability that cask velocity is less than or equal to cask velocity listed.

V1: The truck velocity, adjusted for braking, prior to an accident

V2: The velocity due to bridge heights

V3: The vector sum of truck velocity adjusted for braking and velocity due to bridge heights

V4: The train velocities at grade crossing accidents

The following distributions of cask velocities are considered applicable to railway accidents:

- TV1: The train velocities in collision accidents without braking
- TV2: The train velocities in derailment accidents without braking
- TV3: The velocities due to bridge heights
- TV4: The vector sum of train velocities in derailment accidents and velocities due to bridge heights.

The cumulative distribution functions are presented in Table 5.2.

#### 5.2.1.2.2 Impact Angle

The damage resulting from an accident is not controlled solely by the cask velocity at impact. A head-on impact is more severe than a sideswiping accident, even though both accidents can involve similar velocities. The reason is that accident severity is most directly related to the impact velocity, the component of the cask velocity vector perpendicular to the object impacted. The orientation of the cask motion, relative to the surface of the object impacted is called the impact angle,  $\alpha$ . A  $90^\circ$  impact angle defines a head-on impact, i.e., the impact velocity and cask velocity at impact are the same. An impact angle close to  $0^\circ$  defines a sideswiping impact. In this case the impact velocity is a small fraction of the cask velocity. Mathematically, the impact velocity is the cask velocity times  $\sin \alpha$ .

As for cask velocities, the distribution of impact angle can depend on the accident scenario. For example, if the accident involves a collision with another vehicle on the highway, any impact angle is likely. Three impact angle distributions are used:

VV1: Uniform ( $0^\circ, 90^\circ$ ) - any impact angle is equally likely

$$F(x) = x/90 \qquad 0^\circ \leq x \leq 90^\circ \qquad (5.5)$$

Table 5.2  
Cumulative Cask Velocity Distributions for Railway Analysis

Distributions							
TV1		TV2		TV3		TV4	
Cask Velocity,s (mph)	F <sub>S</sub> (s)						
0.	0.	0.	0.	0.	0.	0.	0.
2.0	0.09385	2.0	0.07543	7.74	0.00621	5.0	0.
6.0	0.26286	6.0	0.22036	10.94	0.01550	10.0	0.00232
10.0	0.40788	10.0	0.35480	15.48	0.04754	15.0	0.01244
14.0	0.53042	14.0	0.47634	18.95	0.1051	20.0	0.04814
18.0	0.63240	18.0	0.58341	21.89	0.1952	25.0	0.14919
22.0	0.71598	22.0	0.67534	24.47	0.3178	30.0	0.35837
26.0	0.78345	26.0	0.75225	26.81	0.4629	35.0	0.60624
30.0	0.83709	30.0	0.81495	28.95	0.6124	40.0	0.77834
34.0	0.87908	34.0	0.86477	30.95	0.7464	45.0	0.87230
38.0	0.91147	38.0	0.90385	32.83	0.8508	50.0	0.92649
42.0	0.93606	42.0	0.93246	34.61	0.9217	55.0	0.95855
46.0	0.95446	46.0	0.95386	36.29	0.9635	60.0	0.97727
50.0	0.96801	50.0	0.96920	37.91	0.9849	65.0	0.98792
54.0	0.97784	54.0	0.97991	39.46	0.9945	70.0	0.99379
58.0	0.98486	58.0	0.98720	41.67	0.9991	75.0	0.99692
62.0	0.98980	62.0	0.99204	43.08	0.9998	80.0	0.99852
66.0	0.99323	66.0	0.99516	44.45	0.9999	85.0	0.99932
70.0	0.99557	70.0	0.99713	56.86	1.0	90.0	0.99970
74.0	0.99714	74.0	0.99834			95.0	0.99987
78.0	0.99818	78.0	0.99906			100.0	0.99995
82.0	0.99886	82.0	0.99948			105.0	0.99998
86.0	0.99929	86.0	0.99972			110.0	0.99999
90.0	0.99957	90.0	0.99985			150.0	1.0
94.0	0.99974	94.0	0.99992				
98.0	0.99985	98.0	0.99996				
102.0	0.99991	102.0	0.99998				
106.0	0.99995	106.0	0.99999				
110.0	0.99997	150.0	1.0				
114.0	0.99998						
118.0	0.99999						
150.0	1.0						

F<sub>S</sub>(s) - Probability that cask velocity is less than or equal to cask velocity listed.

TV1: The train velocities in collision accidents without braking

TV2: The train velocities in derailment accidents without braking

TV3: The velocities due to bridge heights

TV4: The vector sum of train velocities in derailment accidents and velocities due to bridge heights

VV2: Degenerate ( $90^0$ ) - impact is head-on only

$$F(x) = \begin{cases} 0 & x < 90^0 \\ 1 & x = 90^0 \end{cases} \quad (5.6)$$

VV3: Triangular ( $0^0, 90^0$ ) - head-on impact is most likely

$$F(x) = x^2/90^2 \quad 0^0 \leq x \leq 90^0 \quad (5.7)$$

The cumulative distribution functions are presented in Table 5.3.

### 5.2.1.3 Cask Orientation Distributions

The orientation of the cask with respect to the object impacted is called the orientation angle,  $\beta$ . It affects the severity of the cask response to mechanical loads. As described in Subsection 2.5.1.3 for impacts on surfaces, a  $0^0$  cask orientation defines a sidewise impact while a  $90^0$  cask orientation indicates impact of the cask on its end. Alternatively for impacts by train sills, a  $0^0$  cask orientation defines a head-on impact to the cask side while a  $90^0$  cask orientation indicates a near miss. Again, the cask orientation distribution can depend on the accident scenario, thus three distributions are used:

CT1: Uniform ( $0^0, 90^0$ ) - all cask orientation angles equally likely

$$F(x) = x/90 \quad 0^0 \leq x \leq 90^0 \quad (5.8)$$

CT2: Triangular ( $0^0, 90^0$ ) - end orientation impact on surfaces or head-on impact to side of cask by train is most likely

$$F(x) = x^2/90^2 \quad 0^0 \leq x \leq 90^0 \quad (5.9)$$

Table 5.3  
Cumulative Impact Angle Distributions

Impact Angle, $\alpha$ ( $^{\circ}$ )	Distributions		
	VV1 $F_A(\alpha)$	VV2 $F_A(\alpha)$	VV3 $F_A(\alpha)$
0.	0.	0.	0.
5.0	0.05556	0.	0.00309
10.0	0.11111	0.	0.01235
15.0	0.16667	0.	0.02778
20.0	0.22222	0.	0.04938
25.0	0.27778	0.	0.07716
30.0	0.33333	0.	0.11111
35.0	0.38889	0.	0.15123
40.0	0.44444	0.	0.19753
45.0	0.50000	0.	0.25000
50.0	0.55556	0.	0.30864
55.0	0.61111	0.	0.37346
60.0	0.66667	0.	0.44444
65.0	0.72222	0.	0.52160
70.0	0.77778	0.	0.60494
75.0	0.83333	0.	0.69444
80.0	0.88889	0.	0.79012
85.0	0.94444	0.	0.89198
90.0	1.0	1.0	1.0

- $F_A(\alpha)$  - Probability that impact angle is less than or equal to impact angle stated in left-hand column.
- VV1: Uniform ( $0^{\circ}, 90^{\circ}$ ) - any impact angle is equally likely
- VV2: Degenerate ( $90^{\circ}$ ) - impact is head-on only
- VV3: Triangular ( $0^{\circ}, 90^{\circ}$ ) - head-on impact is most likely

CT3: Triangular (0°,90°) - 45° orientation impact on surface or 45° impact on side of cask by train is most likely

$$F(x) = \begin{cases} x^2/2(45)^2 & 0^\circ \leq x \leq 45^\circ \\ 1 - [(90-x)^2/2(45)^2] & 45^\circ \leq x \leq 90^\circ \end{cases} \quad (5.10)$$

The cumulative distribution functions are presented in Table 5.4.

### 5.2.2 Thermal Loading Parameter Distributions

The thermal response of a cask, represented by the temperature reached at the middle of the lead shield thickness, is determined by three major thermal loading parameters: fire duration, flame temperature, and fire location with respect to the cask.

#### 5.2.2.1 Fire Duration Distributions

The duration of a fire occurring during a transportation accident depends on a number of factors including

- o the amount and type of fuel, combustibles, and other volatile materials available
- o the availability and feasibility of fire fighting support.

The first factor is influenced by the type of accident. For example, a single truck accident is likely to involve a different fire environment than a truck-truck or truck-auto collision. Similarly, a truck hitting a bridge abutment is likely to cause a different type of fire than a truck jackknifing or overturning along the roadbed. To accommodate these possibilities, several fire duration distributions are considered in the analysis of both highway and railway accident fires. These distributions are generated using the simulation code developed at Sandia<sup>2</sup>.

Table 5.4  
Cumulative Cask Orientation Angle Distributions

Cask Orientation Angle, $\beta$ ( $^{\circ}$ )	Distributions		
	CT1 $F_B(\beta)$	CT2 $F_B(\beta)$	CT3 $F_B(\beta)$
0.	0.	0.	0.
5.0	0.05556	0.00309	0.00617
10.0	0.11111	0.01235	0.02469
15.0	0.16667	0.02778	0.05556
20.0	0.22222	0.04938	0.09877
25.0	0.27778	0.07716	0.15432
30.0	0.33333	0.11111	0.22222
35.0	0.38889	0.15123	0.30246
40.0	0.44444	0.19753	0.39506
45.0	0.50000	0.25000	0.50000
50.0	0.55556	0.30864	0.60494
55.0	0.61111	0.37346	0.69753
60.0	0.66667	0.44444	0.77778
65.0	0.72222	0.52160	0.84568
70.0	0.77778	0.60494	0.90123
75.0	0.83333	0.69444	0.94444
80.0	0.88889	0.79012	0.97531
85.0	0.94444	0.89198	0.99383
90.0	1.0	1.0	1.0

$F_B(\beta)$  - - Probability that cask orientation angle is less than or equal to cask orientation angle stated in left-hand column.

CT1: Uniform ( $0^{\circ}, 90^{\circ}$ ) - all cask orientation angles equally likely

CT2: Triangular ( $0^{\circ}, 90^{\circ}$ ) - end orientation impact is most likely

CT3: Triangular ( $0^{\circ}, 90^{\circ}$ ) -  $45^{\circ}$  orientation impact is most likely

The following fire duration distributions are used in the analysis of highway accident fires:

- F1: Non-collision accident fires
- F2: Off-road (or collision with fixed objects) accident fires
- F3: Truck/truck collision accident fires
- F4: Truck/automobile collision accident fires
- F5: Truck/train collision accident fires.

These distributions are presented in Table 5.5. The distributions for accidents involving a truck colliding with a fixed object and a truck running off the highway are simulated separately but result in the same output.

The following train fire duration distributions are presented in Table 5.6 for analyzing railway accident fires:

- TF1: Collision accident fires
- TF2: Derailment accident fires
- TF3: Other accident fires.

#### 5.2.2.2 Flame Temperature Distributions

Flame temperature and fire duration are often correlated. Highly volatile and chemically reactive substances exhibit high reaction rates and high intensity (temperature), while substances with low reaction rates are consumed slowly and exhibit low intensity. However, information about the joint probability distribution of temperature and duration is not available. Also, the distribution of flame temperature can vary between accident scenarios due to several factors, including the likely amount of fuel available. This information is also not available, thus a simple flame temperature distribution is used in the probability analyses. This distribution,  $T_1$ , is based on a Weibull function for flame temperatures between 1400<sup>0</sup>F and 2400<sup>0</sup>F:

$T_1$ : Weibull (1400<sup>0</sup>F, 2400<sup>0</sup>F)

Table 5.5  
Cumulative Fire Duration Distributions for Truck Cask Analysis

Fire Duration, d (hours)	Distributions				
	F1 $G_D(d)$	F2 $G_D(d)$	F3 $G_D(d)$	F4 $G_D(d)$	F5 $G_D(d)$
0.	0.	0.	0.	0.	0.
0.083	0.3311	0.0321	0.0035	0.0131	0.00238
0.167	0.6596	0.2821	0.0451	0.1653	0.07222
0.250	0.8551	0.5860	0.1572	0.4179	0.16427
0.333	0.9625	0.7754	0.3488	0.6516	0.31099
0.417	0.9801	0.8769	0.5001	0.7878	0.43757
0.500	0.9897	0.9358	0.6034	0.8725	0.54957
0.583	0.9944	0.9643	0.6771	0.9161	0.64690
0.667	0.9970	0.9800	0.7322	0.9456	0.73075
0.750	0.9985	0.9902	0.7750	0.9662	0.80265
0.833	0.9992	0.9949	0.7960	0.9761	0.86416
0.917	0.9996	0.9973	0.8123	0.9838	0.87612
1.0	0.9998	0.9989	0.8257	0.9898	0.88589
1.083	0.99991	0.9995	0.8367	0.9936	
1.167	0.99996	0.9998	0.8459	0.9964	0.89828
1.250	0.99999	0.99995	0.8535	0.9984	
1.333	1.0	0.99998	0.8596	0.9993	0.90934
1.417		0.99999	0.8652	0.9997	
1.500		1.0	0.8696	0.9999	0.91874
1.583			0.8737	0.99996	
1.667			0.8779	0.99997	0.92730
1.750			0.8812	0.99999	
1.833			0.8847	1.0	0.93452
1.917			0.8882		
2.0			0.8917		0.94126
3.0			0.9287		0.96792
4.0			0.9503		0.98247
5.0			0.9641		0.99056
6.0			0.9773		0.99643
7.0			0.9905		1.0
8.0			1.0		

$G_D(d)$  = Probability that fire duration is less than or equal to fire duration stated in left-hand column.

- F1: Non-collision accident fires
- F2: Off-road (or collision with fixed objects) accident fires
- F3: Truck/truck collision accident fires
- F4: Truck/automobile collision accident fires
- F5: Train collision accident fires

Table 5.6  
Cumulative Fire Duration Distributions for Rail Cask Analysis

Fire Duration, d (hours)	Distributions		
	TF1 $G_D(d)$	TF2 $G_D(d)$	TF3 $G_D(d)$
0.	0.	0.	0.
0.083	0.00238	0.01009	0.00943
0.167	0.07222	0.09213	0.09180
0.250	0.16427	0.17603	0.17574
0.330	0.31099	0.29164	0.29183
0.417	0.43757	0.39717	0.39789
0.500	0.54957	0.49517	0.49648
0.583	0.64690	0.58120	0.58291
0.667	0.73075	0.65917	0.66075
0.750	0.80265	0.72958	0.73139
0.833	0.86416	0.79154	0.79373
0.917	0.87612	0.80544	0.80765
1.0	0.88589	0.81870	0.82036
1.167	0.89828	0.83308	0.83454
1.333	0.90934	0.84752	0.91874
1.500	0.91874	0.86071	0.86292
1.667	0.92730	0.87388	0.87564
1.833	0.93452	0.88537	0.88704
2.0	0.94126	0.89665	0.89792
3.0	0.96792	0.94290	0.94342
4.0	0.98247	0.96790	0.96821
5.0	0.99056	0.98166	0.98239
6.0	0.99643	0.98868	0.98941
7.0	1.0	0.99380	0.99403
8.0		0.99702	0.99754
9.0		0.99910	0.99928
10.0		0.99978	0.99985
11.0		1.0	1.0

$G_D(d)$  - Probability that fire duration is less than or equal to fire duration stated in left-hand column.

TF1: Collision accident fires  
 TF2: Derailment accident fires  
 TF3: Other accident fires

$$F(x) = \left[ 1 - e^{-\left(\frac{x-1400}{550}\right)^{1.83}} \right] / \left[ 1 - e^{-\left(\frac{1000}{550}\right)^{1.83}} \right] \quad 1400^{\circ}\text{F} \leq x \leq 2400^{\circ}\text{F} \quad (5.11)$$

This distribution covers the range of flame temperature achievable in typical hydrocarbon fires.<sup>2</sup> These types of fires constitute the majority of fires which occur in transportation accidents. The cumulative distribution function is presented in Table 5.7.

### 5.2.2.3 Fire Location Distributions

The location of a fire has a significant affect on the heat flux to which a cask is exposed and hence on the temperature attained at the middle of the lead shield thickness. An engulfing fire typically produces a greater heat flux exposure to the cask and results in higher cask temperatures than a fire of the same temperature, size, and duration that is adjacent to the cask. The greater the distance of the fire from the cask, the less the thermal interaction and effective exposure.

As with the other fire parameters, no historical data is available for developing a distribution of fire location with respect to the cask. In lieu of such information, a uniform distribution of cask to fire location is assumed. The fire locations are varied between the truck and rail casks in proportion to the size differences between the two casks. The fire location distributions,  $L_1$ , used are:

Truck fires - Uniform (0 ft, 30.75 ft)

$$F(x) = x/30.75 \quad 0 \text{ ft} \leq x \leq 30.75 \text{ ft} \quad (5.12)$$

Train fires - Uniform (0 ft, 43 ft)

$$F(x) = x/43 \quad 0 \text{ ft} \leq x \leq 43 \text{ ft} \quad (5.13)$$

Table 5.7  
Cumulative Flame Temperature Distribution

Flame Temperature, t (°F)	$G_T(t)$
1400	0.
1500	0.04551
1600	0.15306
1700	0.29588
1800	0.45059
1900	0.59847
2000	0.72714
2100	0.83069
2200	0.90849
2300	0.96342
2400	1.0

$G_T(t)$  = Probability that flame temperature is less than or equal to temperature stated in left-hand column.

The cumulative distribution functions are presented in Table 5.8. A fire is considered engulfing if it is within 1/4 foot of the center of a truck cask or within one foot of the center of a rail cask.

### 5.3 Probability Calculation

The purpose of the probability calculation is to estimate the likelihood that specified sets of cask responses will be realized if an accident occurs. The calculation is based on combining the probabilistic information about the accident parameters with the probabilities of the various accident scenarios. The probability estimate is then combined with an estimate of the expected accident rate/truck or train-mile to estimate the expected frequency/mile of cask response in specified response regions. Once the radiological hazards for each cask response region are characterized, the risk, i.e., probability times hazard, associated with transporting spent fuel is estimated.

As described in Section 4.0, the potential cask response represented by the containment vessel strain and the lead mid-thickness temperature due to a transportation accident are partitioned into 20 response regions  $R(i,j)$ ,  $i=1,\dots,4$ ,  $j=1,\dots,5$ , consisting of the combination of 4 structural response regions and 5 thermal response regions:

Structural	
<u>Response Region</u>	<u>Condition</u>
i-1	Less than 0.2% strain ( $<S_1$ )
2	Between 0.2% ( $S_1$ ) and 2% ( $S_2$ ) strain
3	Between 2% ( $S_2$ ) and 30% ( $S_3$ ) strain
4	Greater than 30% strain ( $>S_3$ )

Table 5.8  
Cumulative Fire Location Distributions

Fire Location, $l$ (feet)	Distributions	
	Truck $G_L(l)$	Train $G_L(l)$
0.	0.	0.
1.0	0.03175	0.02326
2.0	0.06349	0.04651
6.0	0.19048	0.13953
10.0	0.31746	0.23256
14.0	0.44444	0.32558
18.0	0.57143	0.41860
22.0	0.69841	0.51163
26.0	0.8455	0.60465
30.00	0.9756	0.69767
30.75	1.0	
34.0		0.79070
38.0		0.88372
42.0		0.97674
43.0		1.0

$G_L(l)$  - Probability that fire location is less than or equal to fire location stated in left-hand column.

Thermal	
<u>Response Region</u>	<u>Condition</u>
j-1	Less than 500 <sup>0</sup> F lead mid-thickness temperature ( $<T_1$ )
2	Between 500 <sup>0</sup> F ( $T_1$ ) and 600 <sup>0</sup> F ( $T_2$ ) lead mid-thickness temperature
3	Between 600 <sup>0</sup> F ( $T_2$ ) and 650 <sup>0</sup> F ( $T_3$ ) lead mid-thickness temperature
4	Between 650 <sup>0</sup> F ( $T_3$ ) and 1050 <sup>0</sup> F ( $T_4$ ) lead mid-thickness temperature
5	Greater than 1050 <sup>0</sup> F lead mid-thickness temperature ( $>T_4$ )

The probabilities estimated in the probability analysis are the likelihood of the cask response being in each one of the response regions.

The initial step in modeling the probability calculations is to relate the containment vessel strain to impact velocity and the lead mid-thickness temperature to effective fire duration. The first part is done by developing strain-impact velocity curves for several object hardnesses. Similarly, the lead mid-thickness temperature-fire duration models are developed for several fire locations and a 1700<sup>0</sup>F flame temperature.

Given a fixed impact angle and cask orientation, the probability that containment vessel strain is within a given region is derived from the distribution of the impact velocity via the strain-impact velocity curves. For example, given a truck cask, using Fig. 7-3 and assuming an unyielding object and an end-on cask orientation, a strain between 0.2% ( $S_1$ ) and 2% ( $S_2$ ) corresponds to an impact velocity between 38 mph and 46 mph. Thus, assuming a head-on impact, i.e., 90<sup>0</sup> impact angle, the probability of the containment vessel strain being between 0.2% ( $S_1$ ) and 2% ( $S_2$ ), denoted  $P(0.2 \leq S_t \leq 2)$ , is equal to the probability that the cask velocity is between 38 mph and 46 mph. Recognizing the fact that the relationships between strain and cask velocity are conditional on the impact angle, cask orientation, and object hardness, the identity involving the strain and cask velocity probabilities can be written mathematically as:

$$P(0.2 < S_t \leq 2 | \text{head-on, end-on impact with unyielding object}) = F_S(46) - F_S(38) \quad (5.14)$$

where  $F_S(\cdot)$  denotes the appropriate cumulative distribution function of cask velocity.

Taking into consideration the fact that the impact angle and cask orientation are variable, and recognizing that the hardness of the object impacted is identified by an accident scenario, the probability of the containment vessel strain given a specific accident scenario is obtained by averaging the probability in Equation 5.14 with respect to the appropriate distributions for impact angle and cask orientation. Mathematically,

$$P(0.2 < S_t \leq 2 | A_k) = \int_{\alpha} \int_{\beta} \{F_S[s_2(\alpha, \beta, A_k) | A_k] - F_S[s_{0.2}(\alpha, \beta, A_k) | A_k]\} \\ \times dF_A(\alpha | A_k) dF_B(\beta | A_k) \quad (5.15)$$

where  $A_k$  identifies an accident scenario and  $F_S(\cdot)$ ,  $F_A(\cdot)$  and  $F_B(\cdot)$  are the cumulative distribution functions for cask velocity, impact angle, and cask orientation, respectively. Equation 5.15 recognizes that the cask accident velocity corresponding to 0.2% ( $S_1$ ) and 2% ( $S_2$ ) strain depends on the impact angle, cask orientation, and hardness of the object impacted, i.e., the accident scenario.

As illustrated in Fig. 5.1, changing the cask orientation corresponds to varying the strain-impact velocity curve. This change is included in the probability analysis by developing strain-impact velocity curves for  $0^\circ$ ,  $45^\circ$ , and  $90^\circ$  cask orientation for each level of hardness of the impacted object. It is assumed, given a fixed impact angle, that the impact velocities for intermediate angles can be approximated by:

$$v_{\%}(\beta) = \begin{cases} v_{\%}(0^\circ) + \frac{\beta}{45} [v_{\%}(45^\circ) - v_{\%}(0^\circ)] & 0^\circ < \beta \leq 45^\circ \\ v_{\%}(45^\circ) + \frac{(\beta-45)}{45} [v_{\%}(90^\circ) - v_{\%}(45^\circ)] & 45^\circ \leq \beta < 90^\circ \end{cases} \quad (5.16)$$

That is, a linear interpolation is assumed between the 0° and 45° curves and between the 45° and 90° curves. Notationally,  $v_{\%}(\beta)$  denotes the impact velocity corresponding to strain percent, %, for cask orientation angle,  $\beta$ . The corresponding strain-impact velocity curves for several  $\beta$ 's are illustrated in Fig. 5-1.

The impact angle  $\alpha$  relates the cask impact velocity to the cask accident velocity. If the impact is head-on, i.e.,  $\alpha=90^\circ$ , then the impact velocity equals the accident velocity. On the other hand, if  $\alpha$  is less than  $90^\circ$ , then the impact velocity is less than the accident velocity. Since the velocity distributions V1 through V4 and TV1 through TV4 are distributions for accident velocities, it is necessary to transform the impact velocity corresponding to a strain level to an accident velocity. This transformation, for a fixed cask orientation angle,  $\beta$ , is given by

$$s_{\%}(\beta, \alpha) = v_{\%}(\beta) / \sin \alpha \quad (5.17)$$

where  $v_{\%}(\beta)$  represents impact velocity and  $s_{\%}(\beta, \alpha)$  is the corresponding accident velocity for the given impact angle.

To illustrate how cask orientation and impact angle are handled in the calculations, we consider structural response region i=2, i.e., between 0.2% ( $S_1$ ) and 2% ( $S_2$ ) strain, being attained when a cask hits a concrete object at a  $45^\circ$  orientation angle and a  $35^\circ$  impact angle. From Table 5.9 for accident scenario No. 8 the impact velocities for 0.2% ( $S_1$ ) and 2% ( $S_2$ ) strain are  $v_{0.2\%}(45^\circ) = 35$  mph and  $v_{2\%}(45^\circ) = 49$  mph. (Note: for other orientation angles  $\beta$ , Equation 5.16 would be used to evaluate  $v_{\%}(\beta)$ .) Using Equation 5.17, the vehicle velocities necessary to result in impact velocities of 35 mph and 49 mph, if the angle of impact is  $35^\circ$ , are (since  $\sin 35^\circ = 0.57378$ ):

$$\begin{aligned} s_{0.2\%}(45^\circ, 35^\circ) &= v_{0.2\%}(45^\circ) / 0.57378 \\ &= 61 \text{ mph} \end{aligned}$$

**Table 5.9**  
**Probability Inputs for Highway Analysis**

Accident Index	Probability $\times 10^{-3}$	P(fire)	Fire duration	Temperature	Location	Distributions					Damage state upper boundaries								
						Cask orientation	Impact angle	Speed	Strain-impact velocity curve	<0.2%			<2%			<30%			
										0°	45°	90°	0°	45°	90°	0°	45°	90°	
1	34.002	0.004	F1	T1	L1	CT1	VV1	V1		150	150	150	150	150	150	150	150	150	150
2	8.093		F2																
3	431.517		F4																
4	133.201	0.008	F3																
5	7.701	0.011	F5			CT3	VV2	V4	5	9	14	150	20	27					
6	38.113	0.009	F2			CT1	VV1	V1		150	150	150	150	150					
7	1.039	0.004				CT3	VV2	V2	4	42	150	38	59	150	64				
8	3.986								2	32	35	38	51	49	46				
9	0.079								3		58	84		101	150				
10	0.006								2		35	38		49	46				
11	0.001								1										
12	0.299					CT2	VV3	V1	2								113	76	
13	0.062																150	150	
14	0.011																		
15	0.850					CT1	VV1			150	150	150	150	150	150				
16	40.079																		
17	5.111																		
18	37.050																		
19	23.063	0.011	F1						3	32	58	84	51	101	46				
20	1.981								2		35	38		49	46				
21	0.297								1								113	76	
22	13.192					CT2	VV3	V3	3	32	58	84		101	150		150	150	
23	1.076								3		35	38		49	46				
24	0.170								2								113	76	
25	8.894					CT1	VV1	V1	1	150	150	150	150	150	150		150	150	
26	8.412																		
27	32.517																		
28	83.493	0.012																	
29	54.603	0.130																	
30	20.497	1.0																	
31	9.705																		

$$\begin{aligned}
 s_{2\%}(45^{\circ}, 35^{\circ}) &= v_{2\%}(45^{\circ}) / 0.57378 \\
 &= 85.40 \text{ mph}
 \end{aligned}$$

Given a fire, the thermal response of the cask, represented by the lead mid-thickness temperature is related to the duration of the fire. This relationship, illustrated in Fig. 5-2, depends on both flame temperature and fire location. Using an argument analogous to the development of the probability corresponding to a structural response region, the probability that the cask thermal response is in a specific region, for example, between 600°F ( $T_2$ ) and 650°F ( $T_3$ ) or thermal response region  $j=3$ , is given by

$$\begin{aligned}
 P(600 < T < 650 | A_k \text{ with a Fire}) &= \int_{t_1}^{\infty} \int_{l_1}^{\infty} \{G_D[d_{650}(t, l) | A_k] - G_D[d_{600}(t, l) | A_k]\} \\
 &\quad \times dG_T(t) dG_L(l) \quad (5.18)
 \end{aligned}$$

where  $G_D(\cdot)$ ,  $G_T(\cdot)$ ,  $G_L(\cdot)$  denote the fire duration, flame temperature, and fire location cumulative distribution functions, respectively. Again, the fire duration,  $d_{T_{OF}}(t, l)$ , corresponding to a lead mid-thickness temperature,  $T_{OF}$ , depends on the flame temperature and fire location. This is denoted in the argument of the fire duration distribution function. Also, the fire duration distribution varies with the accident scenario.

The basic mid-thickness temperature of the lead shield-fire duration curve is based on a 1700°F real engulfing fire. The effects of the other fire parameters are included in the analyses by adjusting this basic curve. For fires that deviate from a 1700°F fire, the same temperature is reached within the shield, but the time to reach this temperature is shorter or longer depending on the flame temperature. If the flame temperature is greater than 1700°F, the same lead mid-thickness temperature is reached in a shorter time; whereas if the flame temperature is below 1700°F, it takes longer to produce the same temperature in the middle of the lead shield thickness. Thus, for a given lead mid-thickness temperature, the effects of different flame temperatures for an engulfing fire are modeled by the identity

$$d_{oF}(t,0) = \delta(t) d_{oF}(1700^0, 0 \text{ ft}) \quad (5.19)$$

A list of the factors  $\delta(t)$  is presented in Table 5.10.

For fire location, as the distance between the fire and the cask increases, heat exposure decreases, and a longer duration fire is needed to produce the same temperature in the middle of the lead shield thickness as an engulfing fire. Thus, the effect of fire location on the lead shield temperature-fire duration relationship is modeled by a multiplicative factor. The model used is

$$\begin{aligned} d_{oF}(t,l) &= \delta(l) d_{oF}(t^0, 0 \text{ ft}) \\ &= \delta(l) \delta(t) d_{oF}(1700^0, 0 \text{ ft}) \end{aligned} \quad (5.20)$$

where the factor  $\delta(l)$  is given by

$$\delta(l) = 0.78e^{(0.7732+0.06287l)} \quad l > 1.5 \text{ ft} \quad (5.21)$$

for a truck cask and

$$\delta(l) = 0.78e^{(0.62874 + 0.08471l)} \quad l > 4 \text{ ft} \quad (5.22)$$

for a rail cask. In both cases, location is measured from the center of the cask, which is mathematically assumed to represent the location of an engulfing fire. Development of the flame temperature and fire location models in Equations 5.19 through 5.22 is discussed in Subsections 2.5.2.3 and 2.5.2.4. The effect on the basic lead mid-thickness temperature-fire duration curve for a truck cask is shown in Fig. 5-2.

Equations 5.15 and 5.18 are expressions for estimating the probability that the containment vessel strain is within a given structural response region, e.g., between 0.2% ( $S_1$ ) and 2% ( $S_2$ ) strain, and the probability, given a fire, that the lead mid-thickness temperature is within a given thermal response region, e.g., between 600<sup>0</sup>F ( $T_2$ ) and 650<sup>0</sup>F ( $T_3$ ), respectively. Both expressions are conditional on a given accident scenario. A cask response

Table 5.10  
Heat Flux Factors for Flame Temperatures  
(Engulfing Fire)

Flame Temperature, t (°)	$\delta(t)$
1400	1.72
1500	1.43
1600	1.21
1700	1.0
1800	0.86
1900	0.73
2000	0.64
2100	0.56
2200	0.49
2300	0.44
2400	0.39

expressions are conditional on a given accident scenario. A cask response region involves a combination of structural responses and thermal responses. Assuming that strain is independent of the lead shield temperature, these probabilities can be multiplied to estimate the probability associated with a response region. For example, for response region R(2,3), i.e., strain between 0.2% ( $S_1$ ) and 2% ( $S_2$ ) and lead mid-thickness temperature between 600°F ( $T_2$ ) and 650°F ( $T_3$ ), the probability, given accident scenario  $A_k$  is:

$$P[R(2,3)|A_k] = P(\text{Fire}|A_k) \left[ \int_{\alpha} \int_{\beta} \{F_S[s_2(\alpha, \beta, A_k)|A_k] - F_S[s_{0.2}(\alpha, \beta, A_k)|A_k]\} \right. \\ \left. \times dF_A(\alpha|A_k) dF_B(\beta|A_k) \right] \left[ \int_t \int_l \{G_D[d_{650}(t, l)|A_k] - G_D[d_{600}(t, l)|A_k]\} \right. \\ \left. \times dG_T(t) dG_L(l) \right] \quad (5.23)$$

where the probability of a fire is included in the expression. Similar expressions hold for each of the response regions R(i,j).

Two response regions correspond to accidents involving either no fire or fire only. In these cases, it is assumed that there is no cask thermal response and no cask structural response. For no fire, the response regions are denoted R(i,0), and the probabilities are

$$P[R(i,0)|A_k] = [1 - P(\text{Fire}|A_k)] P[s_{l,i} \leq S \leq s_{u,i} | A_k] \quad (5.24)$$

where  $s_{l,i}$  and  $s_{u,i}$  denote the lower and upper strain limit for the ith region, respectively. For fire only, the response regions are denoted R(0,j), and the probabilities are

$$P[R(0,j)|\text{Fire only}] = P[d_{l,j} \leq T \leq d_{u,j} | \text{Fire only}] \quad (5.25)$$

where  $d_{l,j}$  and  $d_{u,j}$  denote the lower and upper shield temperature for the jth region, respectively.

The final step in the probability calculation is to combine the probabilities over all accident scenarios. Thus, for response region R(i,j),

$$P[R(i,j)] = \sum_{A_k} P(A_k) P[R(i,j)|A_k] \quad (5.26)$$

where  $P(A_k)$  is the likelihood of accident scenario  $A_k$  given an accident. Tables 5.9 and 5.11 summarize the value of  $P(A_k)$ ;  $P(\text{Fire}|A_k)$ ; choice of distributions for each accident scenario; and the structural response region limits for  $0^\circ$ ,  $45^\circ$ , and  $90^\circ$  cask orientation for a truck cask and rail cask, respectively.

The actual probability calculations described in Equations 5.23 and 5.26 are done by a computer code, called TASP (Transportation Accident Scenario Probabilities). The inputs into the code are appropriate distributions for the accident parameters. These are combined for each accident scenario using Equation 5.23 and averaged over accident scenarios using Equation 5.26. The integration in Equation 5.23 is based on approximating the integrals by sums. Details of the integration are discussed in Appendix G. A flow chart of TASP is given in Fig. 5-4.

The results of the probability calculations are presented and discussed in Section 9.0.

**Table 5.11  
Probability Inputs for Railway Analysis**

Accident Index	Probability $\times 10^{-2}$	P(fire)	Fire duration	Temperature	Location	Distributions					Damage state upper boundaries										
						Cask orientation	Impact angle	Speed	Strain-impact velocity curve	<0.2%			<2%			<30%					
										0°	45°	90°	0°	45°	90°	0°	45°	90°			
1	3.0400	0.01	TF1	T1	L1	CT1	VV1	TV1		150	150	150	150	150	150	150	150	150	150	150	
2	8.5678		TF1																		
3	0.1616		TF2			CT3	VV2	TV3	4	65	150	38	72	150	60	150	150	150	150	150	
4	0.0122								3		47	40		69	66						
5	0.0010								2			38		60	48	150	128	105			
6	0.0002								1												
7	0.6192					CT1	VV1	TV1	2												
8	0.3433					CT2	VV3	TV4	3	150	150	150	150	150	150	150	150	150	150	150	
9	0.5092								1	55	47	40	72	69	66	150	150	150	150	150	
10	0.0416								2			38	56	60	48	150	128	105			
11	0.0066					CT1	VV1	TV2	1												
12	1.4437								3			40	60	69	66	150	150	150	150	150	
13	0.1178								2			38	56	60	48	150	128	105			
14	0.0186					CT2	VV3		1												
15	0.0465								2												
16	0.0096					CT1	VV1	TV1	1												
17	0.0017								2												
18	16.4477					CT1	VV1	TV1		150	150	150	150	150	150	150	150	150	150	150	
19	3.2517																				
20	10.0148																				
21	0.8408						VV2	TV2	5	11	16	150	27	49	150						
22	15.9981						VV1	TV1		150	150	150	150	150	150						
23	31.9865																				
24	6.5000	0.90	TF3																		

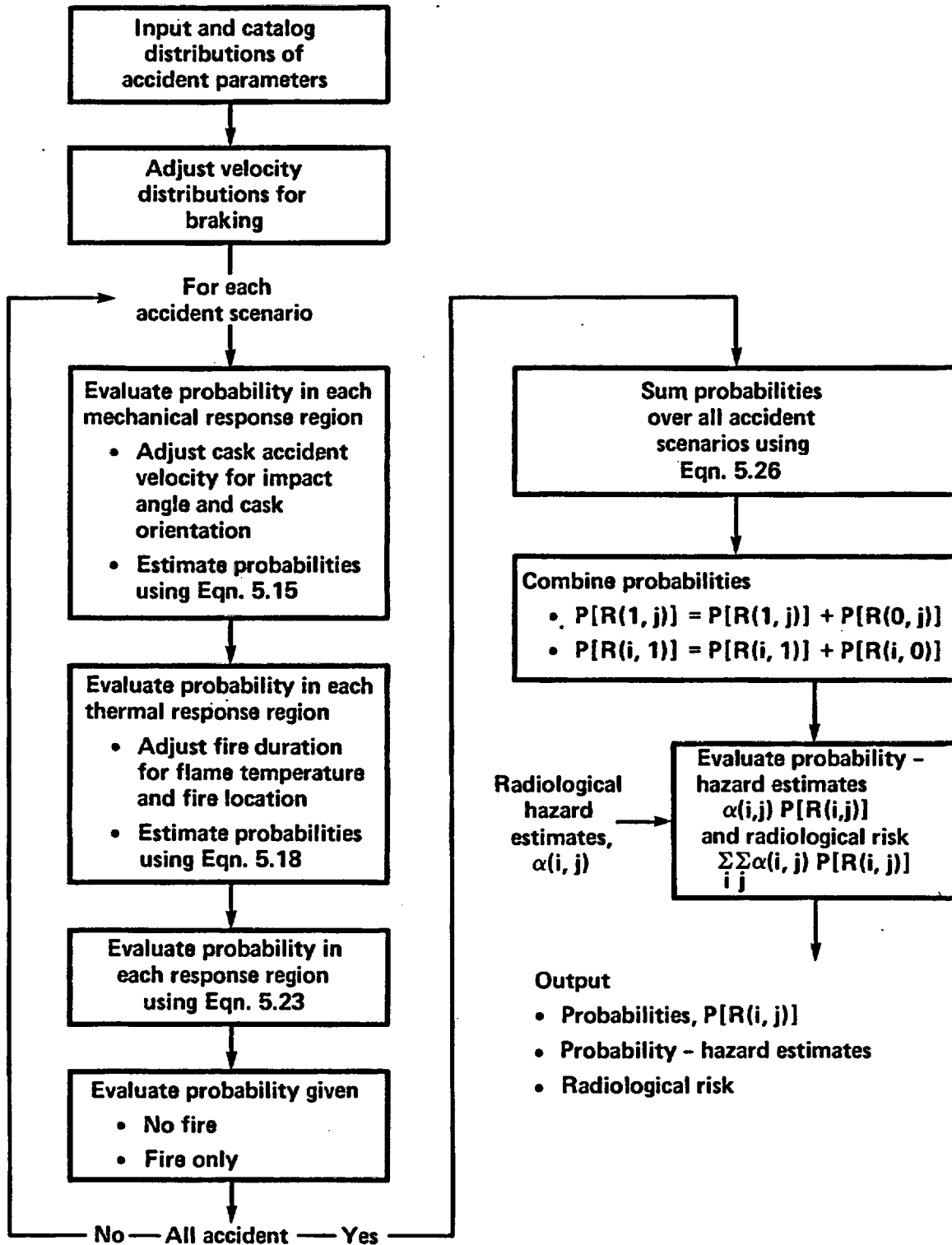


Figure 5-4 Flow chart of TASP computer code.

## 6.0 FIRST-STAGE SCREENING ANALYSIS

### 6.1 Introduction

A two-stage screening process is used to evaluate the level of protection provided by licensed fuel casks against real accident loading conditions. Response regions are developed on the basis of cask performance and are described in terms of damage. The response regions are used to sort or screen accident events in terms of the analytically predicted performance of the representative casks. Figure 6-1 shows the 20 response regions defined in Section 4.0. In the first-stage screening, the intent is to determine by analysis which accident-caused loading conditions can result in cask responses that will fall within the first response region R(1,1). Cask responses in this region are less than or equal to responses implied by the 10 CFR 71 accident test conditions.<sup>1</sup> The second-stage screening analysis identifies accidents which produce loading conditions that can cause cask responses outside the R(1,1) region. The first-stage screening analysis is discussed in this section; the second-stage screening analysis is discussed in Section 7.0.

Within the R(1,1) region, the cask structural response does not exceed a strain level of 0.2% ( $S_1$ ) on the inner shell of the cask. The cask thermal response does not exceed a temperature level of 500°F ( $T_1$ ) at the middle of the lead shield thickness. Within the R(1,1) region, all the major cask components important to safety during transportation accidents are expected to remain fully functional, and the cask meets regulatory requirements. The cask responses within the R(1,1) region do not exceed the responses that would be expected if the cask were subjected to the accident test conditions of 10 CFR 71. Since cask responses within the R(1,1) region do not result in any significant damage to the cask, no radiological release beyond the regulatory limit is expected from the accident causing this level of damage. In fact, in most cases, releases, if any, would be much less than regulatory limits.

The first-stage screening analysis follows this procedure:

- o For each representative cask, dynamic structural and transient thermal analyses are performed to calculate responses to a range of loading

Structural response (maximum strain on inner shell, %)	$S_3$ (30)	R (4,1)	R (4,2)	R (4,3)	R (4,4)	R (4,5)
	$S_2$ (2)	R (3,1)	R (3,2)	R (3,3)	R (3,4)	R (3,5)
	$S_1$ (0.2)	R (2,1)	R (2,2)	R (2,3)	R (2,4)	R (2,5)
	First Screen R (1,1)	R (1,2)	R (1,3)	R (1,4)	R (1,5)	
		$T_1$ (500)	$T_2$ (600)	$T_3$ (650)	$T_4$ (1050)	
		Thermal response (lead mid-thickness temperature, °F)				

- Note:
- o The radiological hazard of cask responses falling in region R(1,1) are negligible and less than limits specified in existing regulations (10 CFR 71).
  - o The radiological hazard of cask responses falling outside region R(1,1) can exceed the limits specified in existing regulations (10 CFR 71).

Figure 6-1 Identification of first-stage screening.

conditions for the accident scenarios identified in Section 2.0. The loading conditions for the accident scenarios are defined by three mechanical loading parameters and three thermal loading parameters. The mechanical loading parameters are impact velocity, object hardness, and cask orientation. The thermal loading parameters are fire duration, flame temperature, and fire location with respect to the cask.

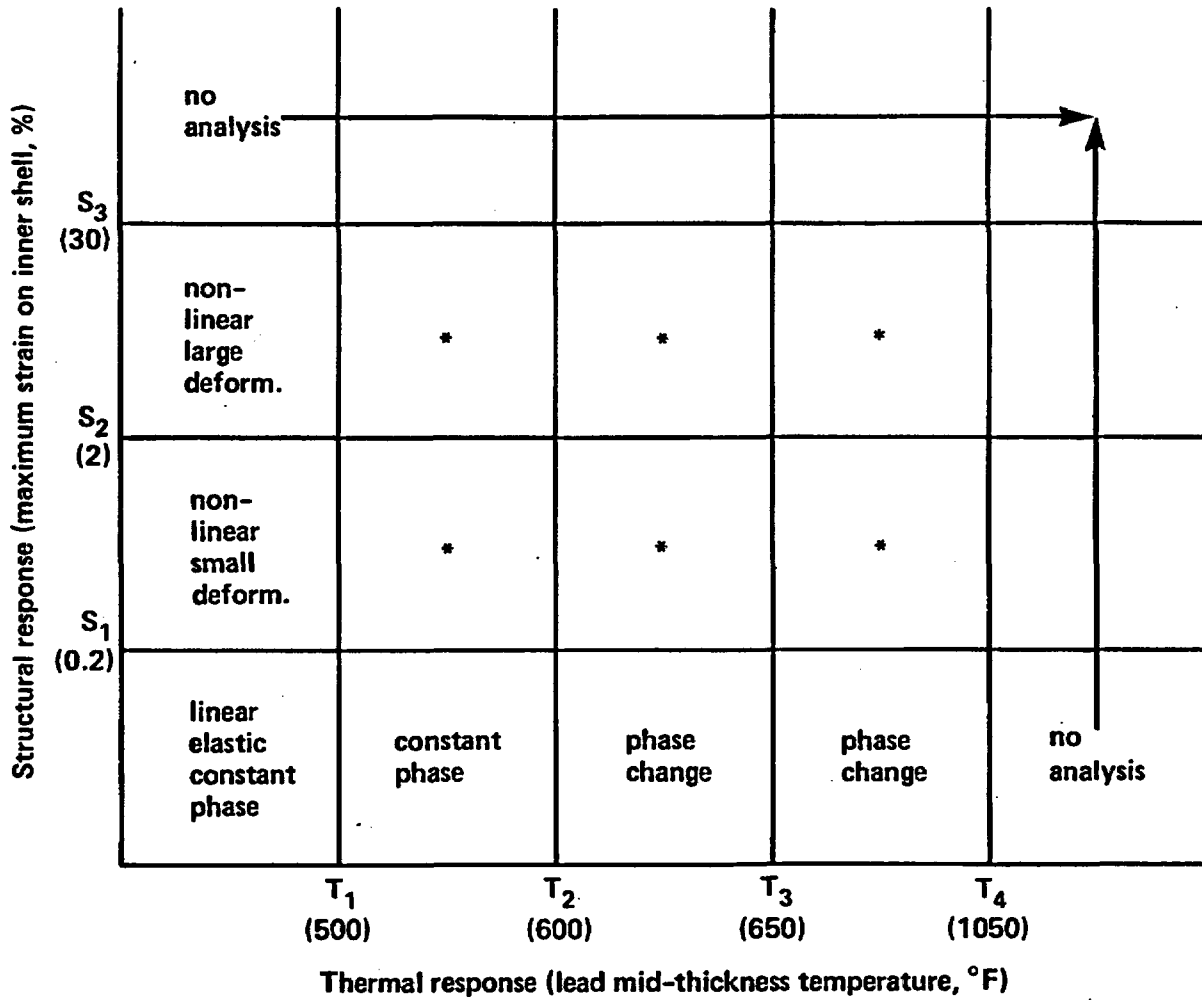
- o The structural response is calculated for various impact velocities. The impact velocity is equal to the component of the accident velocity perpendicular to the surface impacted. It is arrived at by multiplying the accident velocity by the sine of the impact angle. Since the impact angle is not precisely known, it is assumed to follow selected probability distributions depending on the accident scenario under study.
- o For each accident scenario, the loading conditions that result in cask responses within the R(1,1) region are determined by comparing the cask response with the response levels of 0.2% strain ( $S_1$ ) on the inner shell for mechanical loads and 500°F ( $T_1$ ) at the mid-thickness of the lead for thermal loads.
- o For each accident scenario, the probability of occurrence of the specific loading conditions that could result in cask responses within the R(1,1) region is estimated as described in Section 5.0, using the data bases identified in Section 2.0.
- o The fraction of accidents with loading conditions that could result in cask responses within the R(1,1) region is calculated by summing the individual occurrence probabilities associated with each accident scenario.

The major differences between the first-stage and second-stage screening analyses involve the methods used in the structural and thermal analyses. For

the first-stage screening analysis, less sophisticated methods of analysis can be reliably used. For structural responses below the 0.2% strain ( $S_1$ ) level, dynamic linear elastic analysis can be used with high confidence to evaluate mechanically induced structural responses. For responses beyond the 0.2% strain ( $S_1$ ) level, 2% strain ( $S_2$ ) and 30% strain ( $S_3$ ), dynamic nonlinear analysis is required. For thermal responses below the 600°F temperature ( $T_2$ ) level, standard transient heat transfer analysis methods can be used. These methods include transient heat transfer by conduction, radiation, and convection. Responses beyond the 600°F temperature ( $T_2$ ) level include melting of the lead shield, which requires that the transient analysis method include the consideration of phase changes of materials. Figure 6-2 is a schematic diagram showing the general methods of analysis used in the cask response calculations for each of the response regions. Analyses are not performed to calculate responses beyond the 30% strain ( $S_3$ ) and 1050°F temperature ( $T_4$ ) levels since the uncertainties in calculational results would be large. However, in Section 8.0, the potential radiological significance is estimated for responses beyond these levels.

In order to consolidate the many variables and analyses required to cover the wide range of potential accident situations, the following approaches and assumptions are used in this study.

- (1) Casks used for spent fuel shipments are assumed to be properly designed, fabricated, maintained, and operated in accordance with regulations. The intent of this evaluation is not to assess the probability and potential effects of cask defects or deficient or misapplied operational procedures.
- (2) The accident loading parameter distributions in Section 5.0 are generated from the accident data identified in Section 2.0 and are assumed to represent loadings which could be experienced by a spent fuel cask. These accident data are derived from several broad data bases and are independent of any specific transportation route. The frequency of occurrence of certain accident scenarios and their loading conditions can



\*Combined analysis

Figure 6-2 Methods of analysis used in cask response determinations.

experience some variations depending on the specific routing selected. These variations are considered minor for purposes of this study.

- (3) In evaluating highway and railway accidents involving impacts, any damage done to the cask is assumed to result from striking a single object. Real accidents can involve impact with multiple objects; however, for impacts into the harder objects of interest, almost all of the energy involved in the accident is associated with the initial impact. In certain cases, such as accident scenarios involving impacts with bridge railings, conservative assumptions are made. In this scenario, it is assumed that the bridge railing does not cause the transport vehicle to stop but instead allows the cask to fall off the bridge and onto the surface below. The cask response is calculated for falling off the bridge and striking the surface below. Damage to the cask caused by hitting the bridge railing is not significant to the overall evaluation. Conservatism is further introduced in the probability portion of the evaluation because a cask is assumed to fall off a bridge whenever the truck hits the bridge railing.
- (4) The representative truck and rail casks selected for this study and described in Section 3.0 are defined to meet regulatory requirements and generally reflect the designs of casks on the roads and railways today. In actual shipments there will be a variety of cask designs. For all of the accident conditions analyzed, most, if not all, would be expected to exhibit degrees of damage equal to or less than those calculated for the representative casks. Ideally the screening analyses would have used a variety of cask designs with their commensurate variety of potential responses. The results of using a representative cask design for the screening process undoubtedly results in an underestimate of the fraction of accidents leading to cask responses in the R(1,1) region. Conversely, the fraction of accidents leading to cask responses in the other regions is most likely overstated.

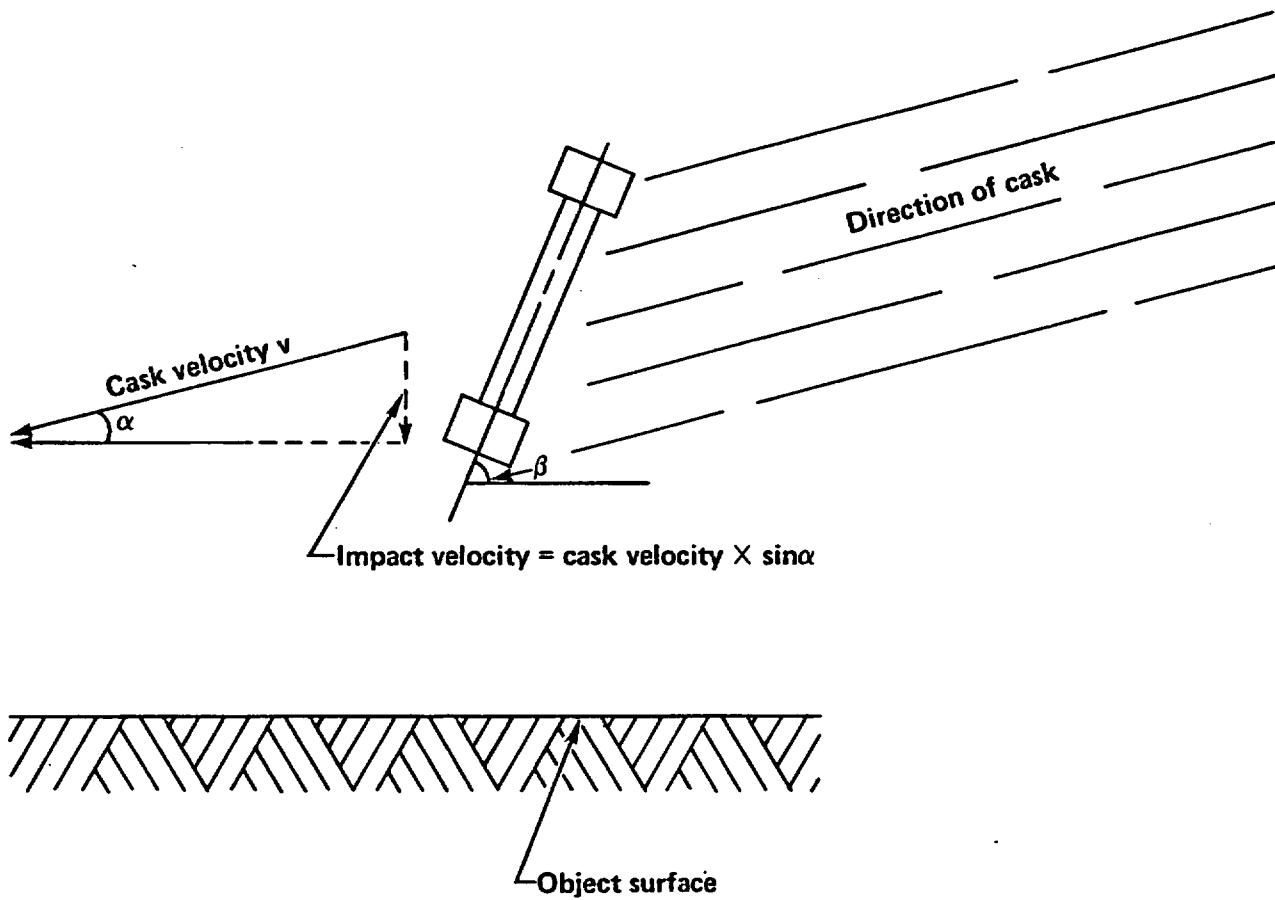
- (5) If there is a lack of data or any unknown factors involved in the structural and thermal analyses or in the accident definition, one of two approaches is followed. Either reasonable assumptions are made from sensitivity study results, or conservative assumptions are made. This approach reduces the need to significantly expand the current data base or unnecessarily complicate the analysis.

Section 6.2 discusses the structural response analysis for impact loads on the representative truck casks. The response analysis determines which accident loading conditions can result in responses that are less than the 0.2% strain ( $S_1$ ) level within the inner shell of the cask. Section 6.3 discusses the thermal response analysis for thermal loads on the cask that result in responses within the 500°F temperature ( $T_1$ ) level at the mid-thickness of the lead shield. In Section 6.4 the probabilities of occurrence are estimated for highway and railway accident loading conditions that could result in cask responses falling in the R(1,1) region.

## 6.2 Structural Response Analysis

Impact loads dominate the structural evaluation. Other loads such as crushing and projectile loads are determined to have little effect on the structural screening analysis. The significance of these loads is discussed in Appendix E. Many accident loads are easily screened out. Minor accidents involving low impact loads, like a rollover or impact with low-resistance objects such as a cask hitting a tree, motorcycle, or automobile, are screened out because the maximum forces generated in these impacts cannot cause significant damage to the cask.

The structural response of a cask to loads generated by potentially significant accidents involving impacts with harder objects at high velocities are calculated. There are three parameters that are considered in estimating structural response. These are shown in Figure 6-3 for impacts on surfaces as impact velocity, cask orientation angle,  $\beta$ , and object hardness. Response calculations are made for various impact velocities and cask orientation angles. The impact velocity is the component of the cask velocity vector



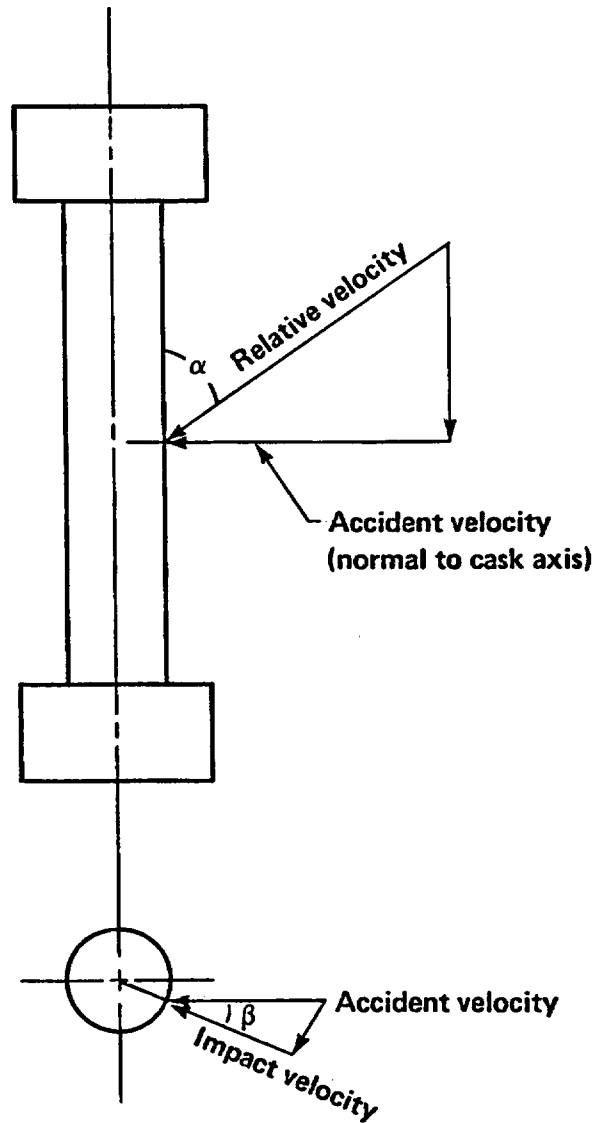
- o Object surface hardness
- o Impact velocity: Cask velocity component perpendicular to the object surface is defined as impact velocity.
- o Cask orientation is defined by angle  $\beta$ , the angle between the cask longitudinal axis and the surface of the object struck

Figure 6-3 Three impact loading parameters considered in the response analysis for impacts on surfaces.

perpendicular to the surface impacted. The angle of impact,  $\alpha$ , represents the angle between the cask velocity direction and the surface of the impacted object. When an accident occurs, the cask velocity vector can be in any direction. However, it can always be decomposed into two components: one perpendicular to the impacted object surface and one parallel to it. In the cask response calculation, only the velocity component perpendicular to the object surface is considered. The velocity component parallel to the object surface introduces a sliding-friction effect to the cask structure. The sliding-friction effect will not produce any significant structural deformation to the cask; therefore, it is ignored. The angle defining the cask orientation is the angle between the cask longitudinal axis and the surface of the object struck. Object hardness needs to be considered because casks can strike objects such as concrete abutments, roadbeds, hard rock, soft rock, hard soil, and water. The hardness of the objects and their responses to impact vary over a wide range.

In some accidents, such as rail grade crossing accidents, the impact limiters on the cask can be bypassed and the side of the cask can be struck directly. Once again the mechanical loads depend on the impact velocity, the orientation of the cask and the hardness of the object struck. Figure 6-4 defines these three loading parameters for this type of accident. The impact velocity is the component of the relative velocity of the cask and object that is perpendicular to the cask axis. The angle of impact,  $\alpha$ , represents the angle between the relative velocity direction and the cask axis. For the purposes of this study, the impact angle is conservatively assumed to be  $90^\circ$ , that is perpendicular to the cask axis in all cases. Also, it is assumed that the impact occurs at the mid-plane of the cask to cause the most damage. The cask orientation angle,  $\beta$ , is the angle at which the impact occurs on the cask surface. In the worst case the cask is hit at  $0^\circ$  or head-on. For orientation angles near  $90^\circ$ , the cask is essentially not struck. The object hardness depends on the object hitting the cask, such as a train sill or a small bridge column.

Two methods of analysis are used in performing the first-stage screening: quasi-static and linear elastic dynamic. The quasi-static method is used to screen out minor accidents involving low-resistance objects such as poles and



- o Object hardness
- o Impact velocity: Relative velocity component perpendicular to cask surface.
- o Cask orientation angle,  $\beta$ : the angle between the accident velocity and impact velocity.

Figure 6-4 Three impact loading parameters considered in the response analysis for impacts with objects such as train sills.

automobiles. A variety of tools are used to accomplish the quasi-static evaluation, including engineering formulas, impact test data, and a computer code called NIKE 2-D, the 2-D designation indicating the two-dimensional modeling option.<sup>2</sup> The linear elastic method is used to perform a dynamic response analysis of the cask structure for accidents involving impacts with hard, massive objects in which cask damage cannot be ruled out by the quasi-static evaluations.

The IMPASC code is a linear elastic dynamic code within the SCANS computer program that can be operated on a personal computer.<sup>3</sup> IMPASC is developed specifically for analyzing dynamic impacts of shipping casks when the casks are subjected to loadings generated as a result of imposition of 10 CFR 71 accident test conditions. The code which is inexpensive to run can be used to analyze oblique impacts and to analyze non-linear behavior of an impact limiter. The deficiency is that IMPASC can model only collisions with unyielding surfaces and cannot handle real surfaces, such as soil or concrete. Also, IMPASC cannot assess lead slump.

In order to perform the dynamic response calculations, the IMPASC code is used in conjunction with two other codes called NIKE 2-D/3-D and DYNA 2-D/3-D; the 2D/3-D designation indicating that either two- or three-dimensional modeling can be performed.<sup>2,4</sup> The NIKE 2-D/3-D and DYNA 2-D/3-D codes are powerful finite element codes suitable for dynamic impact analysis. IMPASC is used to evaluate cask responses for impacts on an unyielding surface for various cask orientations. DYNA and NIKE are used to evaluate cask responses for endwise and sidewise impacts on unyielding and real surfaces. IMPASC is benchmarked against NIKE as discussed in Appendix E.

A cost-effective equivalent damage technique is used to estimate the response of the representative casks impacting real surfaces. The basic assumption in the equivalent damage technique involves conservation of energy; that is, the total energy of the falling cask is absorbed by deformation of the cask and the surface that it hits. In order to estimate the energy absorbed by the surface, the cask is first modeled as a rigid body and the impact surface as deformable and energy-absorbent. This model is used to

establish the force on a rigid cask generated by a real surface and the deformation of the real surface for several impact velocities. Next, calculations are made with the representative cask impacting an unyielding surface at different impact velocities. This establishes the impact forces on the cask and the corresponding cask deformations.

In order to account for the energy absorbed by an actual surface, the force determined from the first analysis, i.e., a rigid cask hitting a deformable surface, is applied to the representative cask to determine a corresponding cask deflection and an associated velocity. By summing both the cask and surface deflections and again considering the defined force level, an equivalent impact velocity on an unyielding surface can be estimated for a representative cask impacting a real surface. Figure 6-5 illustrates this analysis process for the case of a vertical end-drop of a cask without impact limiters. The process is discussed in detail, including the benchmark calculation, in Appendix E.

Three surfaces are used to represent the range of credible impact surfaces. These surfaces simulate hard rock, soft rock/hard soil, and tillable soil. Soft rock and hard soils are similar for impact and are represented as a single surface. Real surfaces exhibit complex response characteristics but can be considered to deform elastically during the early part of an impact, with a subsequent energy dissipation phase. The exact nature of the energy dissipation mechanism is not well known; therefore, for simplicity, an elastic-plastic formulation is used. The parameters used in this formulation, namely, the initial elastic modulus, the poisson ratio, and the yield stress are calibrated to approximate an equivalent energy-absorbent medium. To provide the calibration, penetration data<sup>5</sup> are used as discussed in Appendix E. Reasonable predictions of penetration are possible using the approximate elastic-plastic formulation. The resulting calibrated parameters are listed in Table 6.1 for each surface.

Subsection 6.2.1 describes the structural response analysis for highway accidents. The 31 accident scenarios identified in Section 2.0 are individually analyzed to determine the loading conditions that could cause

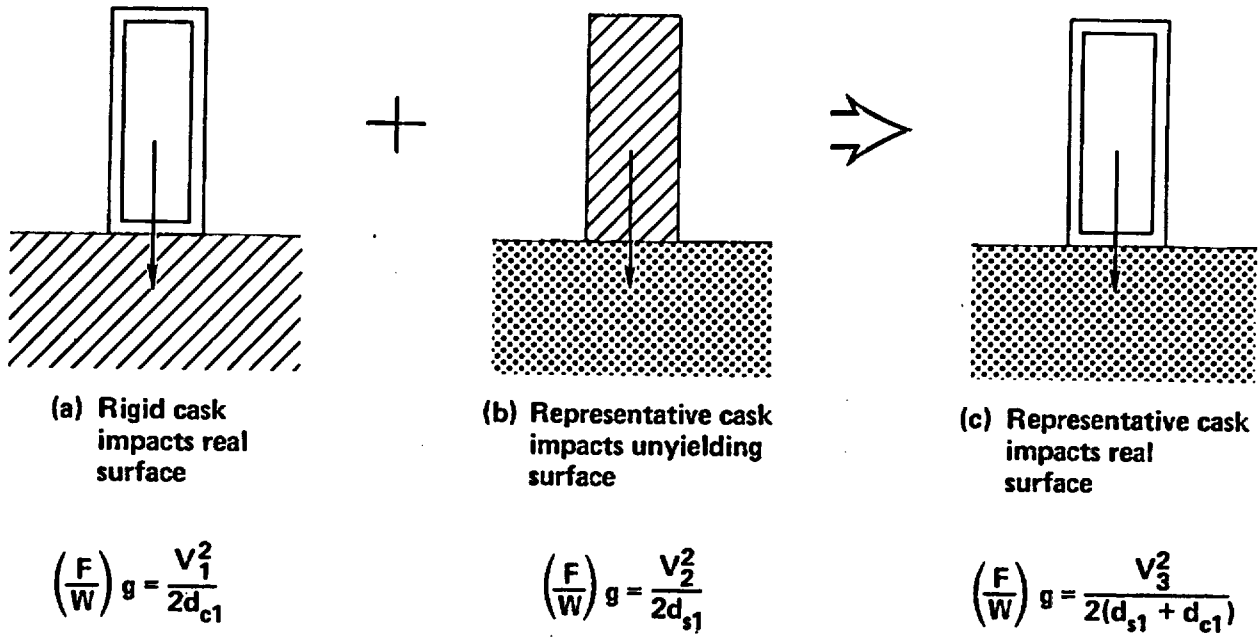


Figure 6-5 Equivalent damage technique.

Table 6.1  
Material Parameters Selected for Real Surfaces

Surface type	Young's Modulus (psi)	Poisson Ratio	Yield Stress (psi)
Hard Rock	7,000,000	0.28	25,000
Soft Rock/Hard Soil	3,640,000	0.2	4,000
Tillable Soil	6,000	0.4	1,000

cask responses of 0.2% strain ( $S_1$ ) or less. Subsection 6.2.2 describes a similar response analysis performed for 24 railway accident scenarios. Subsection 6.2.3 discusses the structural response results.

### 6.2.1 Cask Response Analysis for Highway Accidents

The representative truck cask described in Section 3.5 is used to perform the highway accident response analysis. Appendix E discusses the computer models of the cask and the detailed structural calculations used in the analysis. The structural evaluations use the highway accident scenarios presented in Figs. 2-3 and 2-4. The results of the response evaluations are described in Subsection 6.2.1.1 for accidents involving minor forces and in Subsection 6.2.1.2 for accidents in which the forces are potentially significant.

#### 6.2.1.1 Response to Minor Accidents

Accident scenarios which result in minor forces are determined with an evaluation of cask performance under static loads. A static crushing force of 1.6 million pounds is applied to the cask side. The resulting strain calculated at the inner shell is less than 0.2% ( $S_1$ ). When crushing the cask from the end, 3.2 million pounds of force generates a strain of less than 0.2% ( $S_1$ ). Assuming that the sidewise impact force is linearly applied, the force/unit length that could cause local deformation can be estimated. The representative cask can resist a linear force of 100,000 pounds/foot, generating a strain of less than 0.2% ( $S_1$ ). The linear force required to crush objects in many accidents is much less than 100,000 pounds/foot, and thus these accidents are screened out (placed in the R(1,1) response region).

The maximum force that an object generates during a high velocity impact can be estimated using quasi-static methods. By substituting equivalent static forces for inertial forces due to deceleration, calculations indicate that objects such as automobiles or truck trailers cannot generate forces greater than 100,000 pounds/foot-of-contact, even at high impact velocities. The automobile, as this calculation indicates, is a relatively soft object

when compared with the massive steel cask and is severely damaged. The energy generated by the high-velocity impact of the automobile is almost totally absorbed in the destruction of the automobile, and no impact force greater than 10,000 pounds/foot is applied to the shipping cask. Also, for such a relatively light object (<5,000 pounds), the massive cask (50,000 pounds) will accelerate the object, hence reducing the impact forces to values significantly less than the 10,000 pounds/foot.

Many other low-resistance objects, such as trees, road signs, utility poles, motorcycles, trailers, and trucks, are also in this relatively soft object category. All these objects pose no threat to the cask and require no further analysis. Table 6.2 identifies all objects that can generate a maximum quasi-static force less than 100,000 pounds/foot at any velocity. The percentage of accidents involving these objects is 94.7%.

The remaining highway accidents involve stronger and more massive objects, such as trains, bridge columns, abutments, and certain real surfaces such as roadbeds. The analysis of these accidents is described in the next subsection.

#### 6.2.1.2. Response to Other Accidents

Truck accident scenarios involving impacts with trains, running off bridges or over embankments, and running into slopes or massive concrete structures require dynamic structural analysis. The cask dynamic response is analyzed for impacts with the principal objects involved in these accidents.

Figure 6-3 shows the variables considered in the dynamic response analysis: cask orientation, object hardness, and impact velocity. The IMPASC code is used only for unyielding targets. Different methods of analysis are used for soft objects, depending on their hardness. Hard objects are considered unyielding surfaces. The impact analysis application for these objects is presented in Subsection 6.2.1.2.1. Cask responses for relatively soft objects are discussed in Subsection 6.2.1.2.2

Table 6.2  
Evaluation of Quasi-Static Force for Minor Highway Accidents<sup>a/</sup>

Accident Scenario	Frequency	Total Force (lb)	Linear Force (lb/ft)
1. Soft objects (cones, animals, etc.)	0.034	<1,000	< 1,000
2. Motorcycle	0.008	<20,000	<10,000
3. Automobile	0.432	<50,000	<10,000
4. Truck, bus	0.133	<400,000	<70,000
5. Train	0.008		b/
6. Other (rocks, furniture, etc.)	0.038	<50,000	<10,000
7-11 Bridge railing	0.005		b/
12-14 Columns, abutments	<0.001		b/
15. Bridge bottom structure	<0.001	<100,000	<30,000
16. Wall barrier, post	0.040	<50,000	<50,000
17. Signs, cushions	0.005	<10,000	<10,000
18. Curb, culvert	0.037	<10,000	<10,000
19-21 Into slope	0.025		b/
22-24 Over embankment	0.014		b/
25. Over embankment (draining ditch)	0.009		c/
26. Trees	0.009	<100,000	<70,000
27. Other (fences, bushes, etc.)	0.033	<50,000	<10,000
28. Overturn	0.083		c/
29. Jackknife	0.055		c/
30. Other (cargo shift, etc.)	0.020	<1,000	<1000
31. Fire only	0.010		No load
	<u>1.000</u>		

<sup>a/</sup> Accident scenarios are screened out as minor except those designated for dynamic analysis.

<sup>b/</sup> Linear force may exceed 100,000 lb/ft. Dynamic analysis is required.

<sup>c/</sup> Fall impact distance is <15 ft.; therefore the linear force is <100,000 lb/ft.

#### 6.2.1.2.1 Response for Impacts with Unyielding Surfaces

This subsection assesses cask response during impact with objects such as hard rock, which have a hardness close to the unyielding surface specified in regulations. The analysis considers variations in two parameters: cask orientation angle and impact velocity. IMPASC is used to calculate the cask response for cask orientation angles,  $\beta$ , of  $0^\circ$ ,  $10^\circ$ ,  $30^\circ$ ,  $50^\circ$ ,  $70^\circ$ , and  $90^\circ$  and impact velocities of 30 mph, 38 mph and 45 mph. The  $0^\circ$  cask orientation angle represents an impact to the side of the cask, whereas the  $90^\circ$  cask orientation angle is an impact to the end of the cask.

For the  $90^\circ$  angle case, the effects of truck cab crushing and lead slump pressures are considered. The sensitivity study results are given in Fig. 6-6. The results indicate that, for the representative truck cask, a line connecting the endwise and sidewise strain responses conservatively bounds the strain responses for all other cask impact orientations. Therefore, for cask orientations from  $0-90^\circ$ , the structural strain responses can be linearly interpolated between the sidewise and endwise strain responses. The strain in the inner cask shell can reach 0.2% ( $S_1$ ) at an impact velocity of 32 mph for sidewise impacts and an impact velocity of 38 mph for endwise impacts.

#### 6.2.1.2.2 Response for Real Objects

The equivalent damage technique estimates the representative truck cask response for endwise impacts on real surfaces. A rigid body with the outer dimensions and weight of the truck cask is dropped onto various surfaces from heights up to 480 feet and with equivalent velocities up to 120 mph. Figure 6-7 plots the interface forces for endwise impacts of the rigid body on tillable soil, soft rock/hard soil, and hard rock.

The impact force exceeds 1000 g for hard rock and 200 g for soft rock/hard soil. By comparison, an impact force of 40 g is presumed to cause a 0.2% strain ( $S_1$ ) at the inner shell of the representative truck cask. For impact forces up to 40 g, the kinetic energy of the representative cask will be almost entirely absorbed by the cask's impact limiter. Above this force level, cask deformation will begin. Because  $40 \text{ g} \ll 200 \text{ g}$ , soft and hard rock

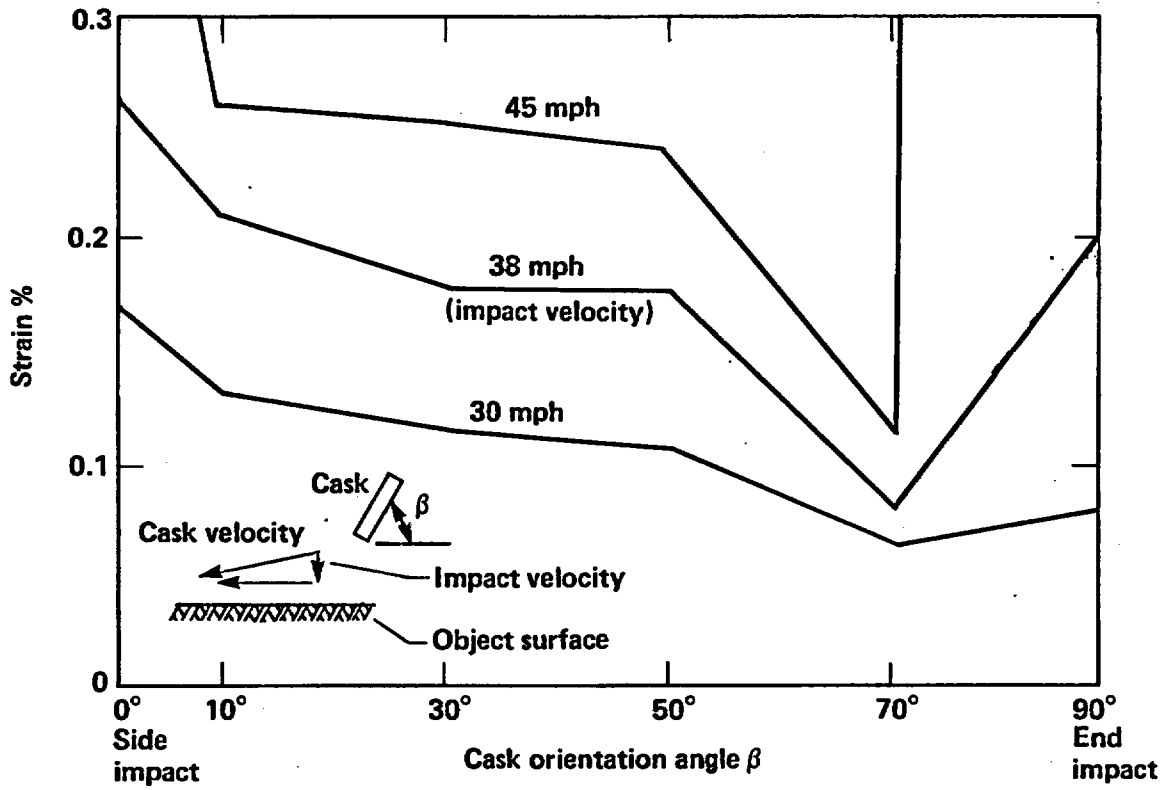


Figure 6-6 Strain versus impact velocity and cask orientation for the representative truck cask impacting an unyielding surface.

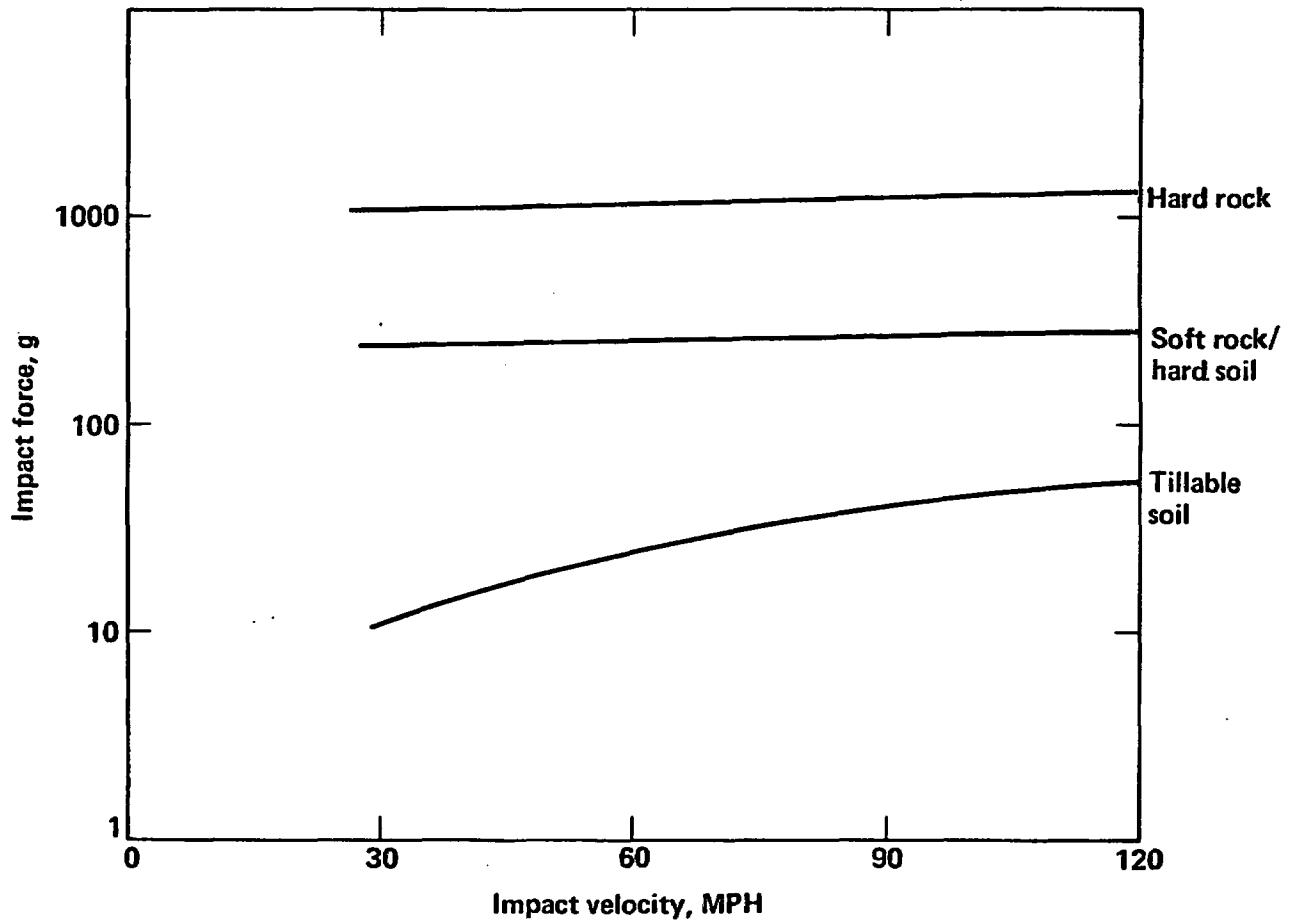


Figure 6-7 Impact force for a rigid truck cask dropped endwise onto real surfaces.

are treated as an unyielding surface. For impacts on tillable soils, the results shown in Fig. 6-7 indicate that significant energy can be absorbed by the soil at an impact force of 40 g. In this case, the representative cask can impact soil surfaces endwise at velocities up to 84 mph without exceeding the 0.2% strain ( $S_1$ ) level.

A similar equivalent damage evaluation is performed for sidewise drops onto various surfaces. To evaluate grade-crossing accidents, sidewise impacts by train sills are also analyzed to determine conditions which could cause 0.2% strain ( $S_1$ ) at the inner shell. Table 6.3 summarizes the impact velocities needed to attain the 0.2% strain ( $S_1$ ) level for sidewise and endwise impacts on various surfaces, including water.

At the 0.2% strain ( $S_1$ ) level and below, representative truck cask responses to impacts on hard or soft rocks are essentially equivalent to impacts on an unyielding surface for all orientation angles. Endwise and sidewise impact velocities of 38 mph and 32 mph respectively produce 0.2% strain ( $S_1$ ) levels. For endwise impacts on soil, significant energy is absorbed by the soil, which allows the maximum impact velocity to increase to 84 mph.

For cask impacts on water at a  $45^\circ$  orientation, an impact velocity of 150 mph will not cause the strain to exceed the 0.2% ( $S_1$ ) level. One-hundred-fifty mph is defined as the maximum credible impact velocity that can be attained based on review of the historical data base. This velocity corresponds to a drop height of 750 feet.

Head-on impact by locomotive sills at velocities greater than 9 mph can cause the 0.2% strain ( $S_1$ ) level to be exceeded. The train sill goes between the impact limiters and strikes the side of the cask.

#### 6.2.2 Cask Response Analysis for Railway Accidents

The representative rail cask described in Section 3.5 is used to perform the railway accident response analysis. The computer model of the cask and the detailed structural calculations used in the response analysis are discussed in Appendix E. The railway accident scenarios in Fig. 2-5 are used

Table 6.3  
Impact Velocities Required to Reach the 0.2% Strain ( $S_1$ ) Level  
for Objects Impacted in Highway Accidents

Object Impacted	Impact Velocity at 0.2% Strain (mph)		
	Cask Orientation Angle ( $^{\circ}$ )		
	0	45	90
Hard Rock	32	35 <sup>a/</sup>	38
Soft Rock	32	35 <sup>a/</sup>	38
Tillable Soil	32	58 <sup>a/</sup>	84
Water	42	150	38
Train Sill	9	14	150

<sup>a/</sup> Impact velocities at these orientation angles are linearly interpolated between the two bounding values.

as the basis for the structural evaluations. The results of the response evaluations are provided in Subsection 6.2.2.1 for minor accidents and in Subsection 6.2.2.2 for accidents in which the damage to a cask could be significant.

#### 6.2.2.1 Response to Minor Accidents

Train accidents are primarily derailments or collisions with other trains. Collisions not involving derailment are usually minor. In non-derailment cases, the only events that must be considered are those in which the coupler of one rail car can override the impacted car and cause damage to a rail car or cask. Rail cars specially designed for casks place the cask in the center of the car. In general, collisions not involving derailment do not generate enough force for the coupler of an adjacent car to penetrate a rail cask because the coupler is too short, as shown in Fig. 6-8. In those cases where the force is great enough for the coupler to strike the cask, it is assumed that the cars derail and the coupler strikes the side of the cask. Impacts with small structures such as poles and retaining walls or impacts with the superstructure of locomotives or other cars cannot significantly damage a cask.

A rail cask is larger than a truck cask and requires greater forces to damage it. A 1.6-million-pound static crush (100,000 pounds/foot) is required on the side of the representative rail cask to cause a 0.2% strain ( $S_1$ ) at the inner shell; whereas a 13.0-million-pound static force is required on the end of the cask to cause a similar level of strain. Based on the first-stage screening of the truck cask, dynamic impact analysis of the rail cask has to be considered only for derailment-caused impacts with massive objects or surfaces adjacent to railroad right-of-ways. Derailments that result in rollovers onto the adjacent railbed involve falls that are less than 15 feet and impact velocities less than 22 mph. These impact velocities can partially crush the rail cask impact limiters but cannot cause any significant damage to the cask.

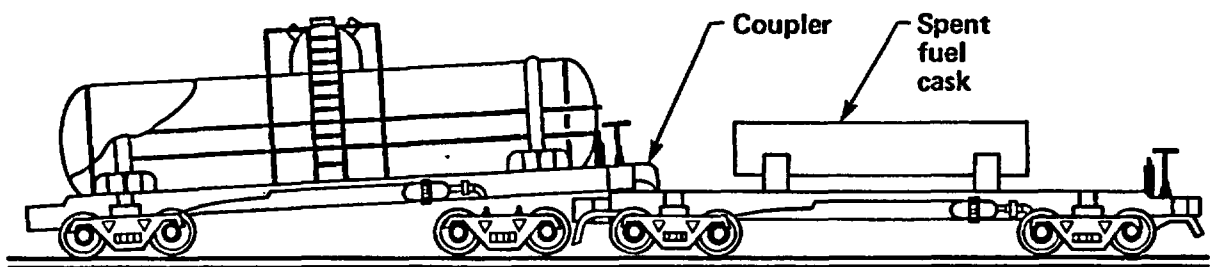


Figure 6-8 Rail car coupler override of spent fuel cask car.

Table 6.4 summarizes the 24 railway accident scenarios with their frequencies of occurrence. Those accident scenarios that can cause only minor cask damage are identified. The total fraction of minor accidents is calculated by summing the individual frequencies. The percentage of accidents screened out as minor is 96.1%. The remaining accidents involve derailments and impacts with massive objects such as train couplers, bridge columns, and abutments, and with surfaces such as rock. Subsection 6.2.2.2 discusses the analyses performed on the representative rail cask for these accidents.

#### 6.2.2.2 Response to Other Accidents

Railway accident scenarios involving derailments and falls off bridges or run-offs over embankments or into slopes or massive concrete structures require dynamic analysis. These accidents may involve impacts with a variety of surfaces: hard rock, soft rock/hard soil, and tillable soil. The dynamic response of the cask for impacts with each of these objects is analyzed.

Three parameters are considered significant in the dynamic response analysis as shown in Figs. 6-3 and 6-4: cask orientation, object hardness, and impact velocity. Again, different methods of analysis are used to analyze objects of different hardness. Hard objects are considered unyielding surfaces and the impact analysis applicable for these objects is presented in Subsection 6.2.2.2.1 below. Cask responses for relatively soft objects are discussed in Subsection 6.2.2.2.2.

##### 6.2.2.2.1 Response for Impacts with Unyielding Surfaces

This subsection assesses cask response during impact with objects such as rock that has a hardness close to the unyielding surface specified in regulations. The analysis considered variations in two parameters: cask orientation angle and impact velocity. IMPASC is used to calculate the cask response for cask orientation angles,  $\beta$ , of  $0^\circ$ ,  $10^\circ$ ,  $30^\circ$ ,  $50^\circ$ ,  $70^\circ$ , and  $90^\circ$  and impact velocities of 30 mph, 45 mph, and 60 mph. The  $0^\circ$  cask orientation angle represents an impact to the side of the cask, whereas the  $90^\circ$  cask orientation angle is an impact to the end of the cask.

Table 6.4  
Evaluation Summary of Minor Railway Accidents<sup>a/</sup>

Accident Scenario	Frequency	Total Force (lb)	Linear Force (lb/ft)
1. Grade crossing	0.030	<400,000	<70,000
2. Non-derailment	0.086	<500,000	<62,500
3-7 Over bridge	0.008		b/
8. Over embankment - ditch	0.003		c/
9-11 Over embankment - other	0.006		b/
12-14 Into slope	0.016		b/
15-17 Columns, abutments	<0.001		b/
18. Other structures	0.164	<500,000	<62,500
19. Locomotive superstructure	0.033	<500,000	<62,500
20. Rail car superstructure	0.100	<500,000	<62,500
21. Coupler/sill	0.008		b/
22. Roadbed	0.160		c/
23. Earth	0.320		c/
24. Other, fire cargo shift	0.065	<10,000	<10,000
Total	<u>1.000</u>		

<sup>a/</sup> Accident scenarios are screened out as minor except those designated as significant for dynamic analysis.

<sup>b/</sup> Linear force may exceed 100,000 lb/ft. Dynamic Analysis is required.

<sup>c/</sup> Fall impact distance is <15 ft; therefore the linear force is <100,000 lb/ft.

The sensitivity study results are given in Fig. 6-9. For the 90° angle case, the effects of lead slump pressure and the crushing of the front end of the rail car are included. The results indicate that, for the representative rail cask, a line connecting the endwise and sidewise strain responses conservatively bounds the strain responses for all other cask orientations. Therefore, for cask orientations from 0-90°, the structural strain responses can be linearly interpolated between the sidewise and endwise strain responses. The strain in the inner cask shell can reach 0.2% ( $S_1$ ) at an impact velocity of 55 mph for sidewise impacts and an impact velocity of 38 mph for endwise impacts.

#### 6.2.2.2.2 Response for Real Objects

The equivalent damage technique estimates the representative rail cask response for endwise impacts on real surfaces. A rigid body with the outer dimensions and weight of the rail cask is dropped onto various surfaces from heights up to 480 feet and with equivalent velocities up to 120 mph. Figure 6-10 plots the interface forces for endwise impacts on tillable soil and soft rock/hard soil. Calculations are not performed for impacts on hard rock. It is apparent from the soft rock/hard soil cask results that a hard rock surface is essentially an unyielding surface with respect to the representative rail cask.

The impact force exceeds 400 g for soft rock/hard soil. The impact forces required for significant energy absorption by tillable soil exceed 40 g at velocities above 40 mph. Since the cask is designed to withstand an impact force of 40 g, it is presumed that such a force causes less than a 0.2% strain ( $S_1$ ) at the inner shell of the representative rail cask. For impact forces up to 40 g on hard or soft rock surfaces, the kinetic energy of the representative cask will be almost entirely absorbed by the cask's impact limiter. For soil impacts, the kinetic energy will be absorbed by both the soil and the cask impact limiter.

A similar equivalent damage evaluation is performed for sidewise drops onto various surfaces. Table 6.5 summarizes the impact velocities needed to

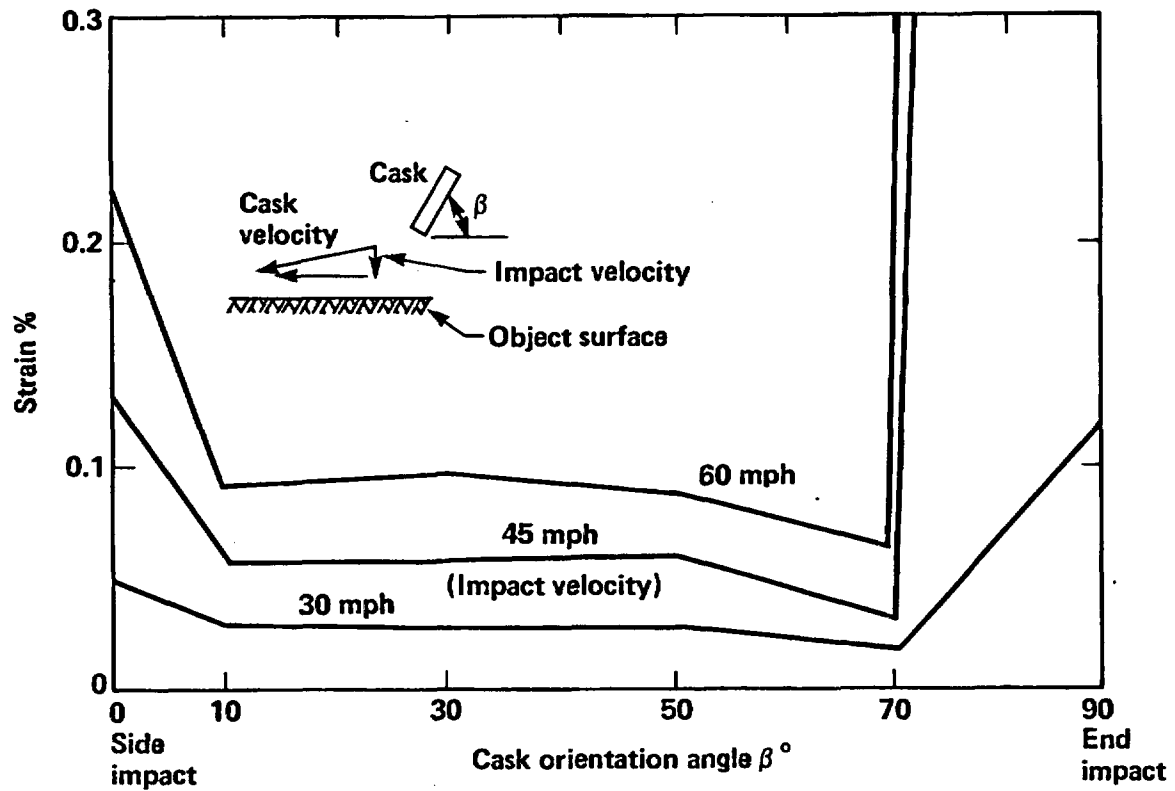


Figure 6-9 Strain versus impact velocity and cask orientation for the representative rail cask impacting an unyielding surface.

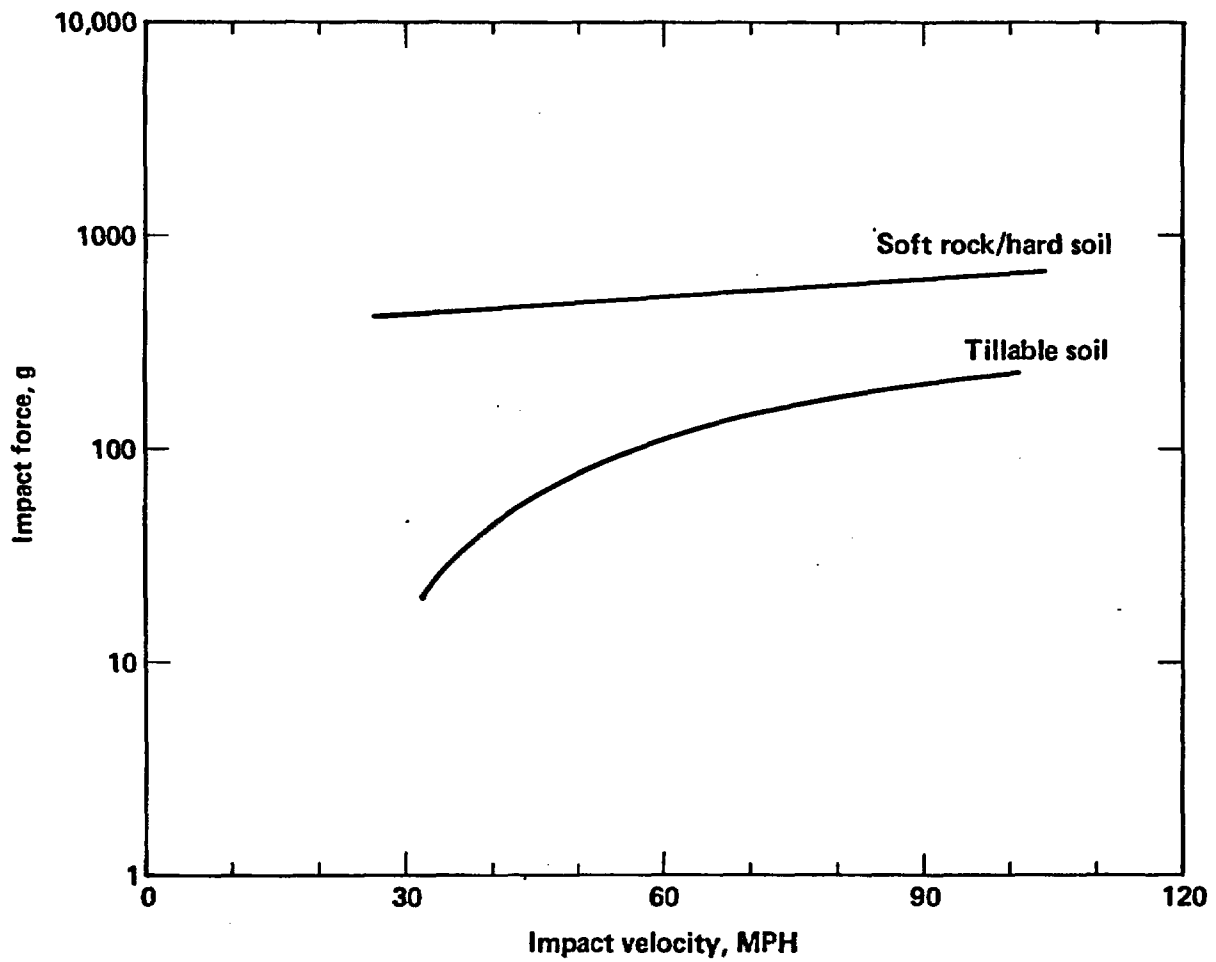


Figure 6-10 Impact force versus impact velocity for a rigid rail cask dropped endwise onto real surfaces.

Table 6.5  
Impact Velocities Required to Reach the 0.2% Strain ( $S_1$ ) Level  
for Objects Impacted in Railway Accidents

Object Impacted	Impact Velocity at 0.2% Strain (mph)		
	Cask Orientation Angle ( $^{\circ}$ )		
	0	45	90
Hard Rock	55	47	38
Soft Rock	55	47	38
Tillable Soil	55	47	40
Water	55	150	38
Train Sill	11	16	150

a/ Impact velocities at these orientation angles are linearly interpolated between the two bounding values.

attain the 0.2% strain ( $S_1$ ) level for sidewise and endwise impacts on various surfaces, including water.

At the 0.2% strain ( $S_1$ ) level and below, the representative rail cask responses to impacts on hard rock, soft rock, or soil are essentially equivalent to impacts on an unyielding surface for all orientation angles. For cask impacts on water at a  $45^\circ$  orientation, an impact velocity of 150 mph can be reached without exceeding the 0.2% strain ( $S_1$ ) level.

Head-on impacts by locomotive sills at velocities greater than 11 mph could cause the 0.2% strain ( $S_1$ ) level to be exceeded. The train sill goes between the impact limiters and strikes the side of the cask.

### 6.2.3 Discussion of Structural Analysis Results

This section has thus far addressed highway and railway accidents that can generate structural cask responses less than the 0.2% strain ( $S_1$ ) level. Cask structural responses within the 0.2% strain ( $S_1$ ) level are in the elastic range and would not lead to any significant radiological releases. Cask response within these constraints will meet requirements imposed by existing regulations.

For those accidents requiring a dynamic structural calculation, the dynamic structural response of the cask is calculated using primarily elastic analysis methods. Dynamic elastic response methods are routinely used to analyze structures, and the results can be used with confidence.

Current and future cask designs are expected to be stronger than the selected representative cask designs and would be able to withstand higher mechanical loads before the 0.2% strain ( $S_1$ ) level is reached. If a higher mechanical loading is required to cause the cask containment shell to reach the elastic limit, then a higher fraction of accidents will be screened out or shown to result in radiological hazards less than those in current regulations.

In July 1984, in Old Dalby, England, the United Kingdom Central Electricity Generating Board performed a train crash test with a steel spent

fuel cask.<sup>6</sup> The 100-mph train crash subjected the cask to a force greater than 8 million pounds but caused only minor deformation to the outside of the cask. The primary response of the cask structure was elastic. In fact, the force the train applied to the steel cask was less than 40% of the International Atomic Energy Agency test condition loads,<sup>7</sup> which are similar to the test conditions specified in 10 CFR 71. Therefore, the actual percentage of highway and railway accidents that are within the envelope of current accident test conditions and radiation hazard limits specified in regulations, are likely to be higher than the percentages indicated in Section 6.4.

### 6.3 Thermal Response Analysis

Thermal loads due to large fires dominate the thermal evaluation. Other thermal loads due to torch fires or cask burial in debris that result from self-heating are insignificant and are eliminated in the thermal screening analysis. Each type of accident is evaluated for its potential for causing damage to a spent fuel cask, such as melting of the lead shield or damage to the cask seal. Even accidents involving only impact of a spent fuel transport truck with small objects or the adjacent roadbed can result in a fire that could burn up to an hour because of the diesel fuel being carried by the truck. Other accidents involving impacts with tanker trucks, locomotives, and tank cars, each of which carry considerable amounts of fuel, can cause fires that could last for a few hours.

The intent of this section is to determine the fraction of accidents that will not cause a temperature exceeding 500<sup>o</sup>F ( $T_1$ ) at the middle of the lead shield thickness of the representative casks. Heating the cask structure to 500<sup>o</sup>F ( $T_1$ ) does not result in any significant deterioration of the cask components. This statement applies to cask seals, which are the component whose failure could signify the earliest onset of a potential radioactive release.

A finite element computer code called TACO 2-D is used to perform the thermal analysis of the cask.<sup>8</sup> Sensitivity studies indicate that a one-dimensional (1-D) heat transfer model can be used, which simplifies the

analysis, reduces computing time, and provides suitably conservative results. In all of the analyses, the representative casks neutron shield tank water is lost prior to the fire. The thin outer shell of the remaining neutron shield tank provides a thermal barrier to the fire. Loss of the shield water reduces heat transfer into the cask; it also removes a significant heat absorber, water.

Currently licensed cask designs are reviewed to relate the temperatures at the mid-plane of the cask to the temperatures at other locations, particularly the closure seals. Valve boxes located where they can be exposed to heat loads and temperatures approaching those in the middle portion of the cask are also considered. These sensitivity studies confirm the selection of the lead shield temperature as the most appropriate and conservative measure of cask thermal response.

Fire accidents have three loading parameters that can affect the response of a spent fuel cask: fire duration, flame temperature, and fire location. These loading parameters vary widely when considering all fire accidents. Longer fire durations and higher flame temperatures increase the thermal loads to the cask and affect temperature responses. The proximity of the cask to a fire is also important. The closer a cask is to a fire, the higher the thermal load; the worst case is a cask being engulfed by a fire.

In order to reduce the large amount of analysis otherwise required to cover a wide range of fire accidents, a simplified calculational method is developed. The method includes the following steps:

1. A reference fire condition is established to perform the thermal response analysis for the representative truck and rail casks. The first step in accomplishing this task is to relate the thermal condition specified in 10 CFR 71 to real fire conditions. As shown in Fig. 6-11, a cask is completely surrounded by fire in the accident test conditions used to guide design; whereas the cask would most likely be only partially surrounded by a fire in a real situation because of the shielding effects of the ground, transport vehicle, or other cask-supporting surfaces. For

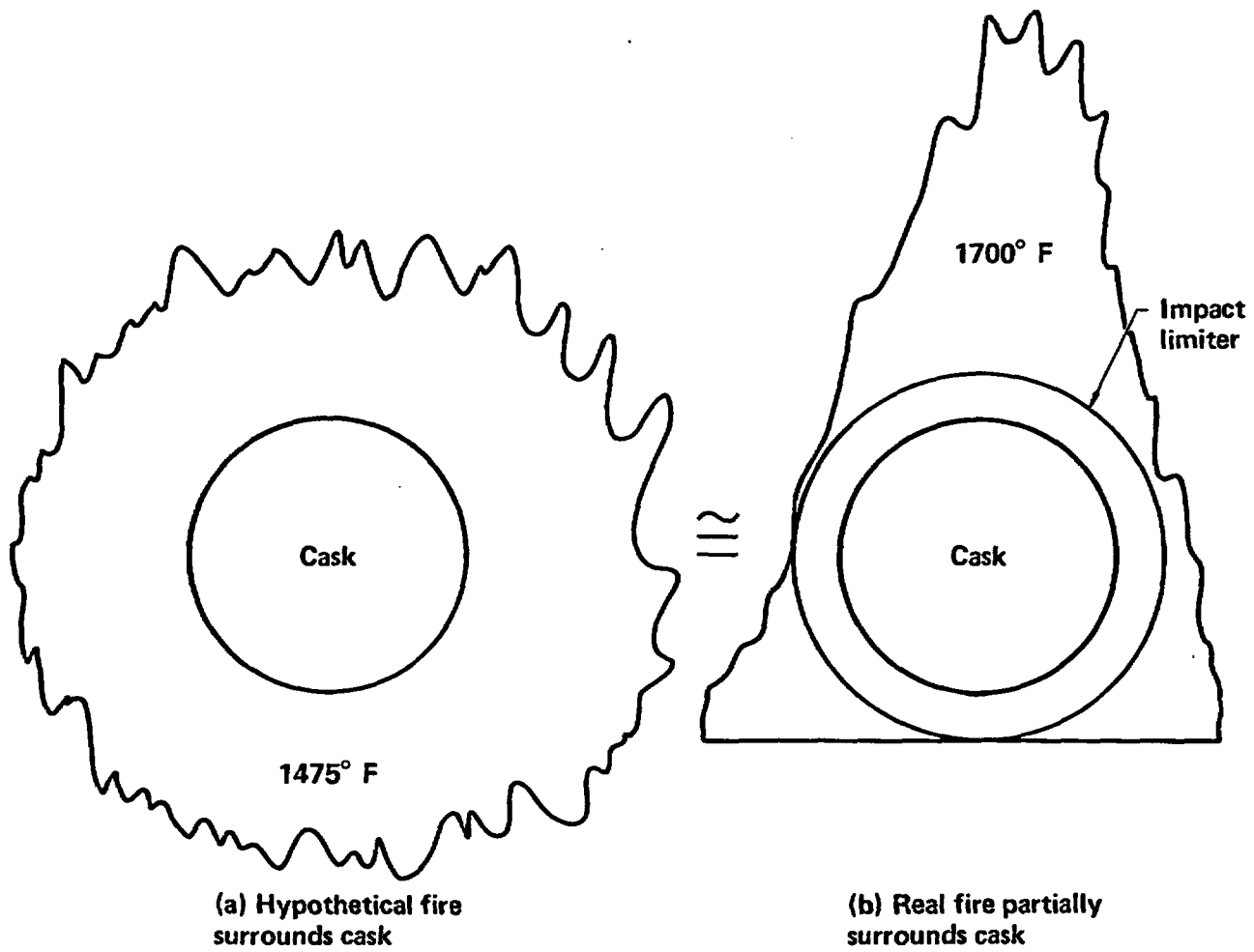


Figure 6-11 Comparison of an engulfing hypothetical fire and a real fire.

the same flame temperature, the average heat flux into the cask in a real engulfing fire is 0.78 of the heat flux on the cask in the hypothetical engulfing fire. A flame temperature of 1700<sup>0</sup>F is required for a real engulfing fire, including ground or transport vehicle shielding effects, to provide the same average heat flux and temperature response as the 1475<sup>0</sup>F hypothetical engulfing fire. The 1700<sup>0</sup>F real engulfing fire is the reference fire condition.

2. The heat fluxes and temperature responses of the truck and rail casks are calculated as a function of fire duration. These evaluations are performed using a 1-D model and the thermal parameters for the accident test conditions.
3. Based on sensitivity studies in Appendix F, the time to reach a specific temperature is approximately proportional to the incident heat flux on the cask caused by the fire. A fire that causes a heat flux twice that of the reference fire can heat a cask to a specified temperature in one-half the time. Conversely, a fire that causes a heat flux one-half the amount takes twice as long to heat the cask to a specified temperature. Using this correlation and the results from step 2, the fire durations required to reach the 500<sup>0</sup>F temperature ( $T_1$ ) level are calculated for a range of heat fluxes that cover a wide range of real fire conditions.
4. The variation of heat loads on the representative casks is determined as a function of the flame temperature and location. The heat load variations are normalized to the engulfing real fire condition and defined as flux factors for flame temperature and load factors for fire location.
5. Using the fire duration results from step 3 and the heat flux factors from step 4, the fire duration required to reach the 500<sup>0</sup>F temperature ( $T_1$ ) level is derived for a wide range of flame temperatures and locations.

The thermal response analysis of highway fire accidents is performed based on the above calculational method. The analysis appears in Subsection 6.3.1. The 31 highway accident scenarios are analyzed to determine the thermal loading conditions that can cause a temperature response of 500°F ( $T_1$ ) or less at the mid-thickness of the lead shield of the representative truck cask. Subsection 6.3.2 describes a similar response analysis performed for 24 railway fire accident scenarios that could involve the representative rail cask. The thermal response results are discussed in Subsection 6.3.3.

### 6.3.1 Cask Response Analysis for Highway Fire Accidents

The representative truck cask described in Section 3.5 is used to perform the highway accident response analysis. Appendix F discusses the cask model and the detailed thermal calculations used in the response analysis.

The temperature response of the representative truck cask is calculated for a hypothetical engulfing fire with a 1475°F flame temperature. A flame emissivity of 0.9 is assumed. The temperature at the middle of the lead shield thickness is plotted in Fig. 6-12 as a function of fire duration. The lead mid-thickness temperature reaches 500°F ( $T_1$ ) in 1.08 hours which is twice the regulatory fire duration. The total heat absorbed by the cask in reaching the 500°F temperature ( $T_1$ ) is 5,000 Btu/ft<sup>2</sup> which results in an average thermal flux of approximately 4,630 Btu/hr-ft<sup>2</sup> compared with the initial rate of 17,000 Btu/hr-ft<sup>2</sup>. The average thermal flux is lower because the thermal barrier formed by the water jacket rapidly reduces the heat flow into the cask during the first 10 minutes as shown in Fig. 6-13. These heat fluxes are equivalent to those on a cask in a real engulfing fire with a flame temperature of 1700°F.

For engulfing fires, the heat flux from the fire onto the surface of the truck cask depends on radiation heat transfer caused by the flame temperature. The average heat flux on the representative truck cask is calculated as a function of flame temperature for a hypothetical engulfing fire. The heat flux is then reduced by a factor of 0.78 to adjust the results

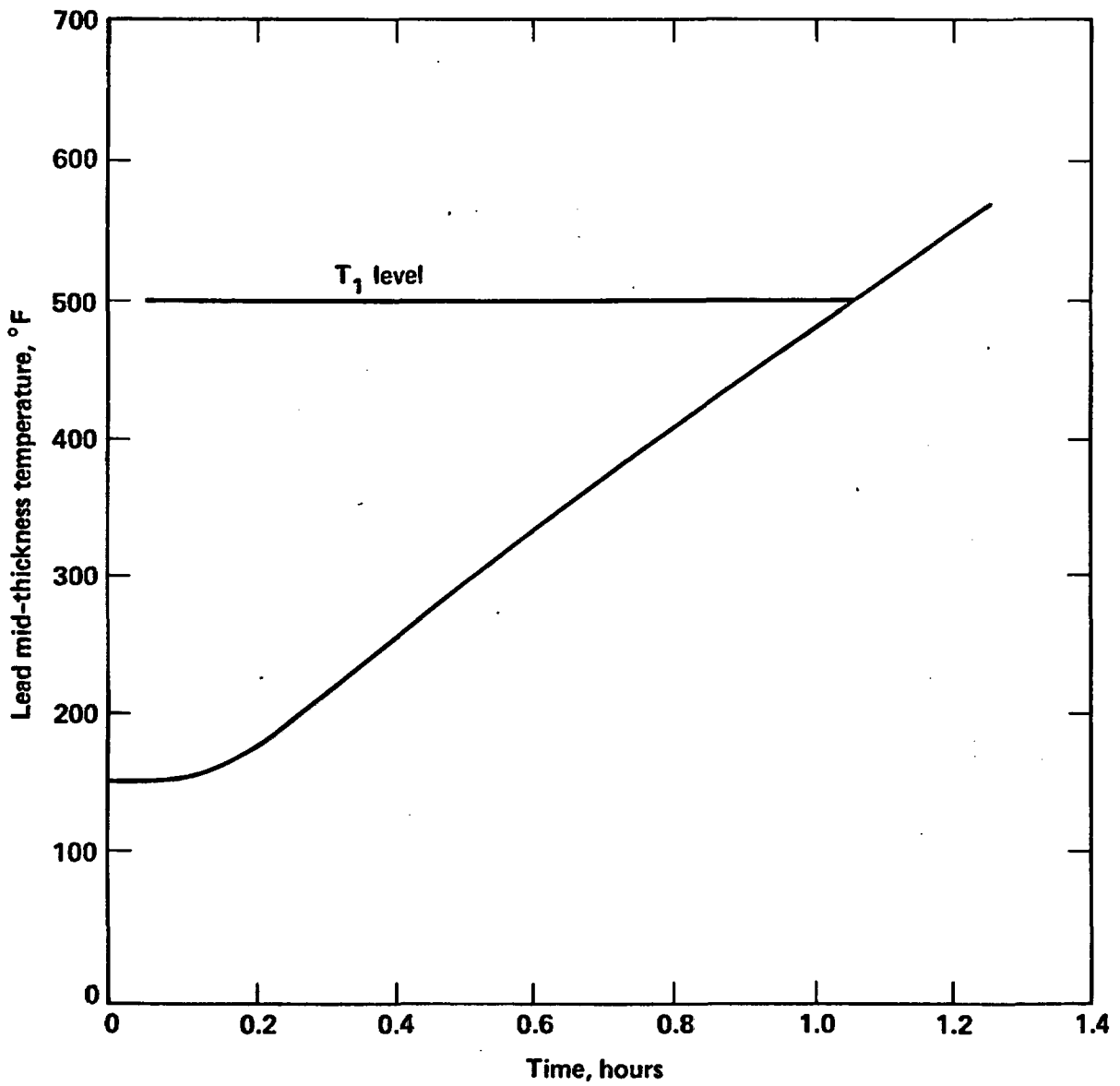


Figure 6-12 Representative truck cask temperature response to a hypothetical 1475<sup>o</sup>F (equivalent to a real 1700<sup>o</sup>F) fire versus fire duration.

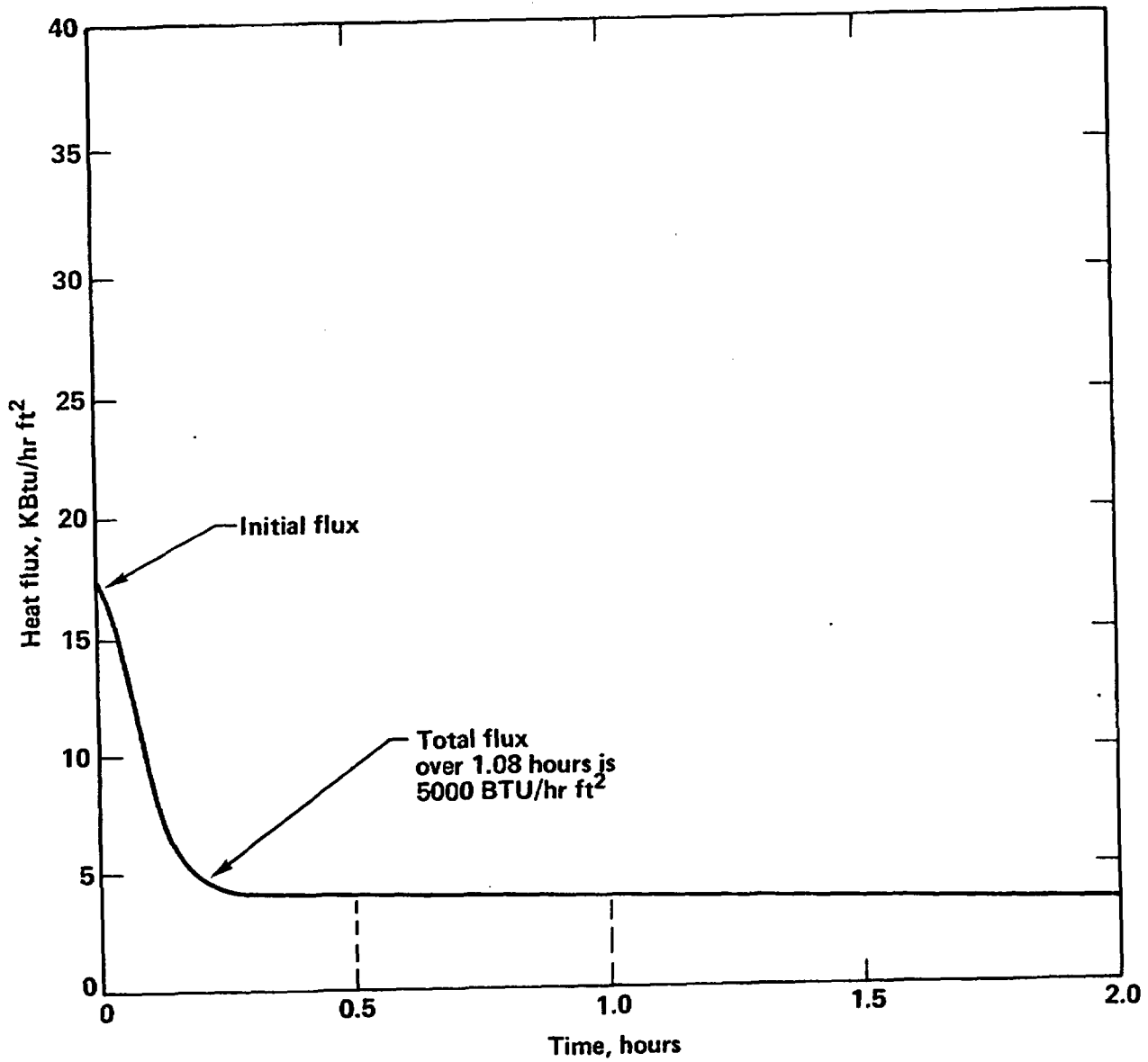


Figure 6-13 Heat flux versus fire duration for the representative truck cask exposed to the regulatory 1475<sup>o</sup>F fire.

for real fire conditions. This normalized heat flux factor is plotted in Fig. 6-14 as a function of flame temperature. For a 1700°F real fire, the average thermal flux on the representative cask is 4,630 Btu/hr-ft<sup>2</sup> and the heat flux factor is 1.0. As the flame temperature increases, the thermal flux increases, and the fire duration required to reach the 500°F temperature (T<sub>1</sub>) level decreases.

The heat load to the truck cask also depends on the location of the fire with respect to the cask. In terms of location, an engulfing fire provides the maximum heat load to the cask. The heat load decreases rapidly as the distance between the fire and the cask increases. Figure 6-15 shows the effect of distance between cask and fire for the truck cask where the heat load factor is normalized with respect to a real engulfing fire.

The heat flux and load factors are used to calculate the change required in the 1.08 hour reference fire to reach the 500°F temperature (T<sub>1</sub>) level for a variety of flame temperatures and durations. The fire durations for the wide range of fire conditions are calculated using the probabilistic code described in Section 5.0.

### 6.3.2 Cask Response Analysis for Railway Fire Accidents

The representative rail cask in Section 3.5 is used to perform the railway fire accident response analysis. The computer analysis of the cask and the detailed thermal calculations are provided in Appendix F.

The temperature response of the representative rail cask is calculated for a hypothetical engulfing fire with a flame temperature of 1475°F and flame emissivity of 0.9. The temperature at the middle of the lead shield thickness is plotted in Fig. 6-16. The lead mid-thickness temperature reaches 500°F (T<sub>1</sub>) in 1.35 hours which is more than twice the regulatory fire duration. The total heat absorbed by the cask in reaching the 500°F (T<sub>1</sub>) level is approximately 6,000 Btu/ft<sup>2</sup> which results in an average heat flux of approximately 4,445 Btu/hr-ft<sup>2</sup>. These heat fluxes are equivalent to those on a cask in a real engulfing fire with a flame temperature of 1700°F.

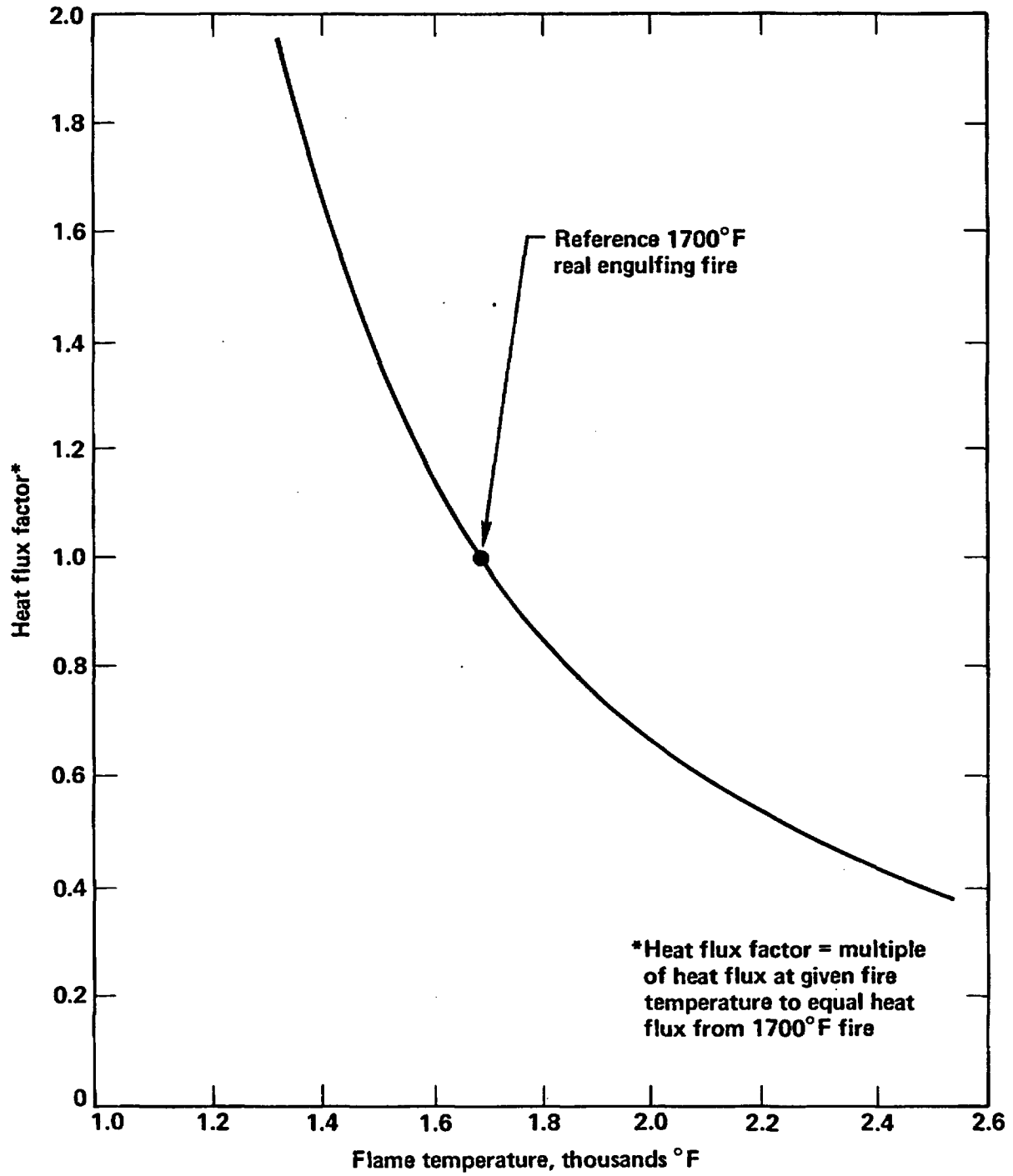


Figure 6-14 Average heat flux factor versus temperature for the representative truck cask.

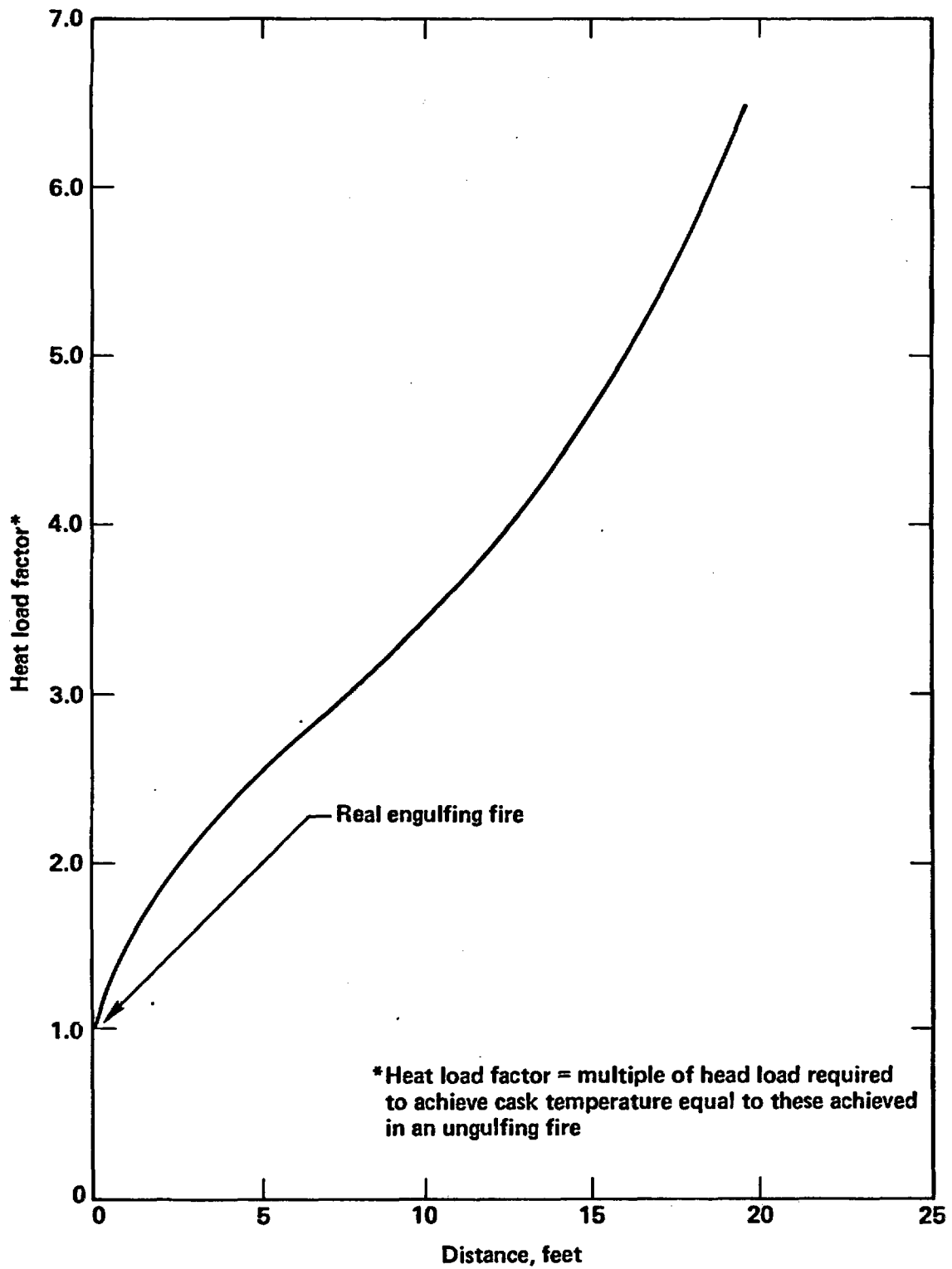


Figure 6-15 Heat load factor for real fire versus location of representative truck cask.

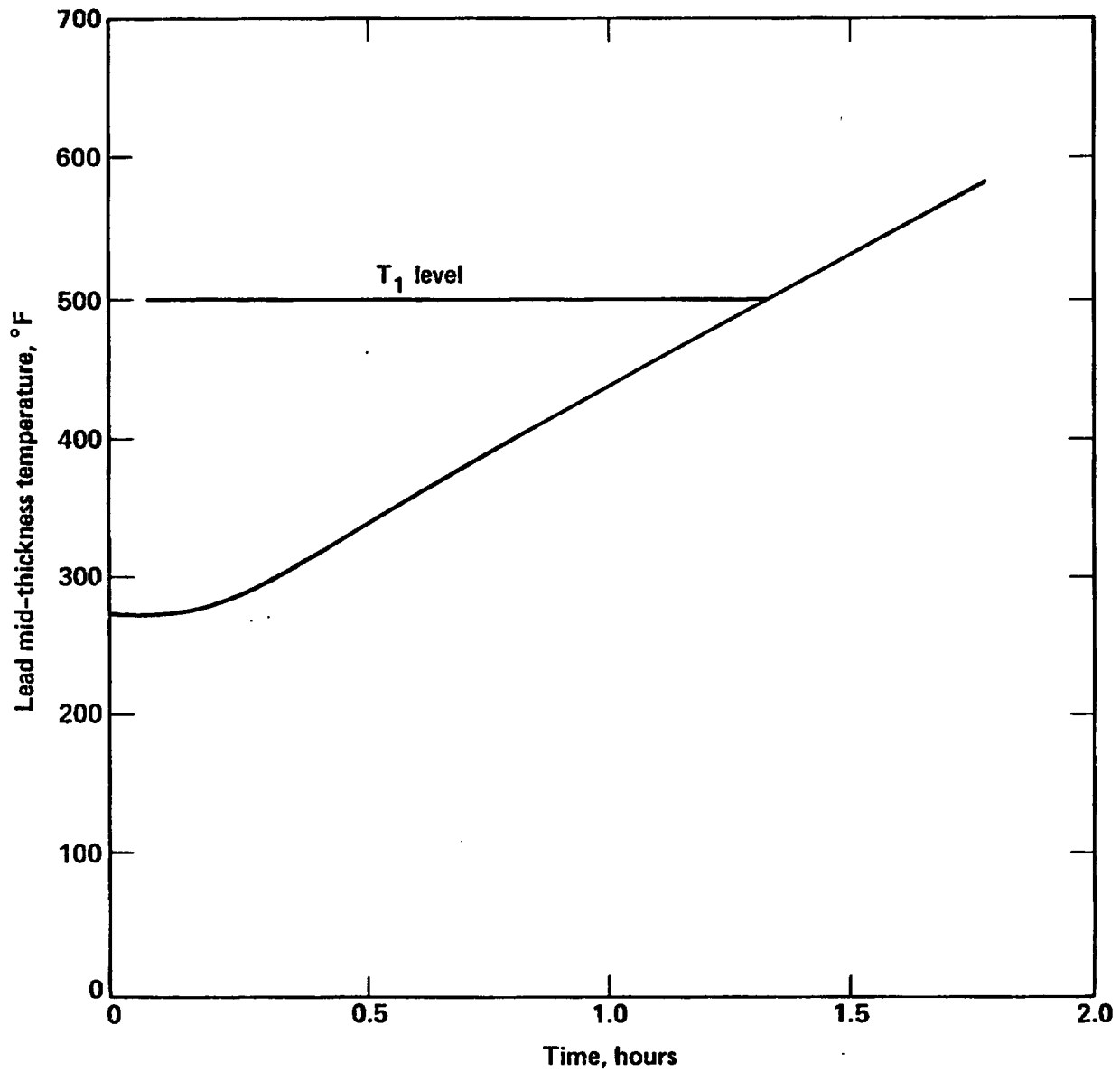


Figure 6-16 Representative rail cask temperature response to a hypothetical 1475°F (equivalent to a real 1700°F) fire versus fire duration.

For engulfing fires, the heat flux from a fire to the surface of the rail cask depends primarily on radiation heat transfer and is determined by the flame temperature. The heat flux dependency on the flame temperature is essentially the same as that for the truck cask discussed in Subsection 6.3.1. The average heat flux factors in Fig. 6-14 are used to adjust for flame temperature for the rail cask.

The heat load to the rail cask also depends on the location of the fire with respect to the cask. An engulfing fire provides the maximum heat load to the cask. The heat load decreases rapidly as the distance between the fire and the cask increases. Figure 6-17 shows the effect of distance between the cask and fire for the representative rail cask. The heat load factor is normalized with respect to an engulfing fire.

The heat flux and load factors are used to calculate the change required in the 1.35 hour reference fire to reach the 500°F temperature ( $T_1$ ) level for a variety of flame temperatures and durations. The fire durations are calculated using the probabilistic code described in Section 5.0 for the wide range of fire conditions.

### 6.3.3 Discussion of Thermal Analysis Results

This section addresses highway and railway fire accidents which generate cask temperature responses less than or equal to the 500°F temperature ( $T_1$ ) level. These accidents result in heating the cask structure to temperatures at which no significant deterioration of the cask components is expected. As a result, the radiological significance of such events is negligible.

The results indicate that the representative truck and rail casks can be exposed to a regulatory fire (1475°F, engulfing, etc.) for over 1 hour before the 500°F temperature ( $T_1$ ) limit is reached. This fire duration is approximately twice as long as that specified in the regulations for the accident test conditions; hence, the representative cask designs have considerable margin with respect to the fire duration. This margin is due to the high heat capacity and thermal resistance inherent in the casks. The massiveness of spent fuel casks due to shielding and mechanical strength contributes significantly to the thermal response characteristics.

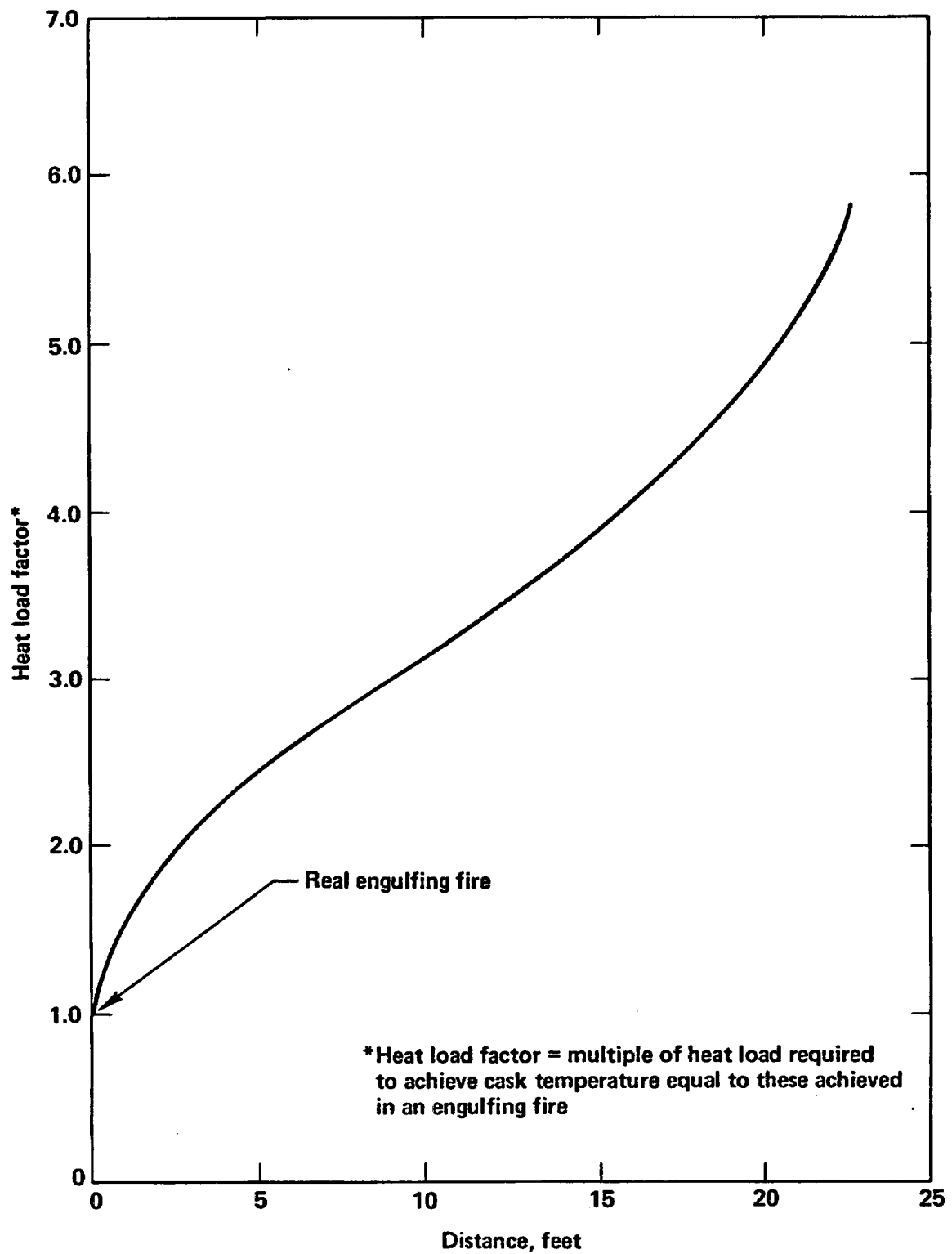
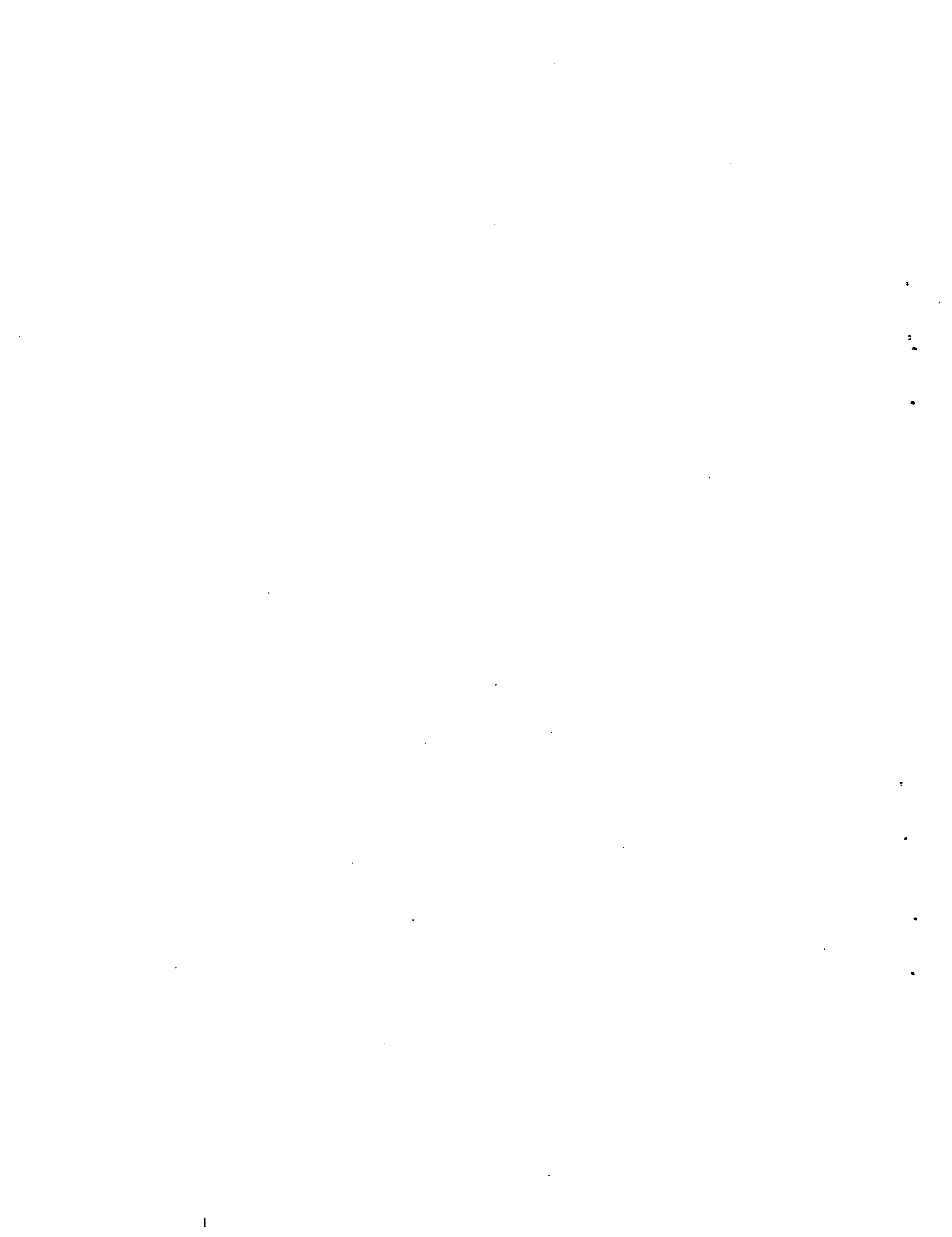


Figure 6-17 Heat load factor for real fire versus location of representative rail cask.

In reality, many currently licensed casks use components and seals that can reliably function at temperatures exceeding those associated with a 500°F (T<sub>1</sub>) lead mid-thickness temperature for long periods of time without being damaged. Therefore, the actual percentage of highway and railway accidents that are within the thermal loading envelope of the accident test conditions is significantly higher than those documented in this study. The radiological hazards for these events are expected to be negligible.

#### 6.4 Accident Screening Analysis

Section 5.0 provides the detailed probabilistic calculations performed in the accident screening analysis. From that analysis, approximately 99.4% of both highway and railway accidents leads to cask responses within the R(1,1) response region. At this level of damage, no radiological hazards of significance are expected; therefore, all are within the stated regulatory limits for radioactive releases and direct exposures. These results are discussed in detail in Subsection 9.2.1.



## 7.0 SECOND-STAGE SCREENING ANALYSIS

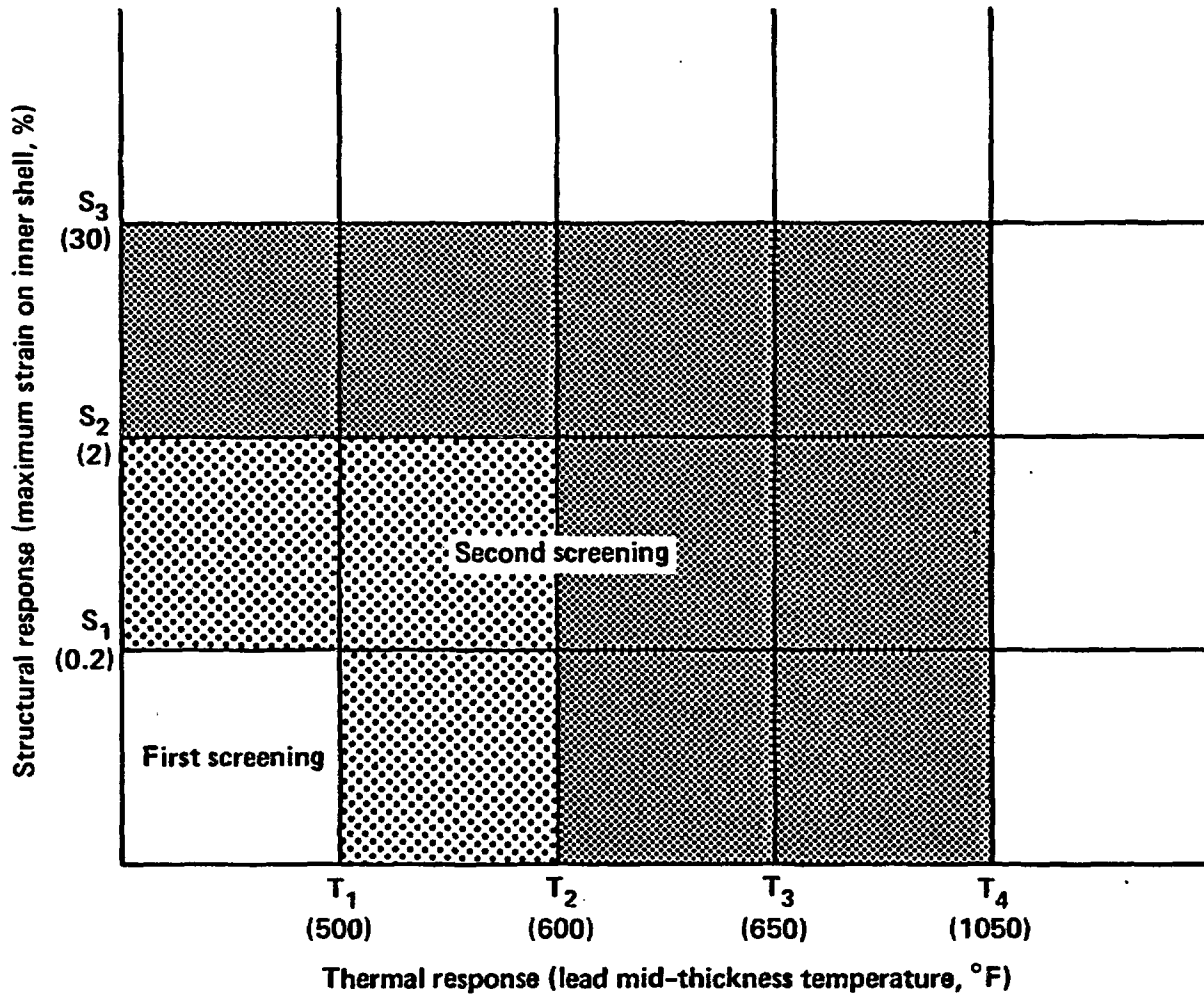
### 7.1 Introduction

The first-stage screening analyses identify classes of accidents in which the responses generated by the mechanical and thermal loadings are within the R(1,1) response region. At levels of response within the R(1,1) region, the accident event would not be expected to have any radiological significance. Approximately 99.4% of highway and railway accidents are expected to cause cask response states within the R(1,1) region.

The residual 0.6% of highway and railway accidents which could cause cask responses outside the R(1,1) region are addressed in this section. The intent of the second-stage screening is to determine what fractions of these residual accidents can be categorized into regions bounded by 30% strain ( $S_3$ ) in the inner cask containment shell and by a lead mid-thickness temperature of 1050°F ( $T_4$ ). These regions are shown in Fig. 7-1.

The light stippled area in Fig. 7-1, which covers regions R(1,2), R(2,1), and R(2,2), represents cask responses between the 0.2% ( $S_1$ ) and 2% ( $S_2$ ) strain levels and between the 500°F ( $T_1$ ) and 600°F ( $T_2$ ) temperature levels. These cask responses exceed the responses that would be generated if a shipping cask were subjected to the 10 CFR 71 accident test conditions.<sup>1</sup> Responses in this light stippled area can result in minor damage to the cask and could result in small radioactive releases or small increases in the direct radiation levels external to the cask. The radiological hazards associated with these cask responses could approach or slightly exceed the regulatory limits specified in 10 CFR 71 for transportation accidents.

The remaining eight regions, beyond the 2% strain ( $S_2$ ) and 600°F temperature ( $T_2$ ) levels, represent individual or combined cask responses between the 2% ( $S_2$ ) and 30% ( $S_3$ ) strain levels and between the 600°F ( $T_2$ ) and 1050°F ( $T_4$ ) temperature levels. For clarity, they are darkly shaded in Fig. 7-1. These responses are significantly greater than the responses expected after exposing the representative casks to the accident test conditions. Responses within the darkly shaded area in Fig. 7-1 can result in



- o First-stage screening analysis radiological hazards are negligible and less than 10 CFR 71 limits.
- o Second-stage screening analysis radiological hazards can be less than, equal to, or greater than 10 CFR 71 limits.
  - Light stippled area - minor damage to cask, with consequent radiological hazards approaching or slightly exceeding 10 CFR 71 limits.
- o - Dark shaded area - more substantial cask damage, with radiological hazards probably exceeding 10 CFR 71 limits.

Figure 7-1 Second-stage screening analysis relationship with response regions.

significant permanent deformation of the cask structure and melting of the lead shielding. Any radioactive material releases or increase in the direct radiation levels that could result from these cask responses are probably greater than the regulatory limits specified in 10 CFR 71 for transportation accidents.

The second-stage screening analysis involves calculations similar to those performed in the first-stage screening. The major difference between the two screening evaluations involves the calculational methods used. Nonlinear small-deformation analysis methods are needed to analyze the cask structure for deformations having strain levels within the 2% strain ( $S_2$ ) limit. For strain levels beyond the 2% ( $S_2$ ) limit, nonlinear, large deformation methods are needed. Thermal analysis methods account for the melting of the lead shield in the 600°F ( $T_2$ ) to 1050°F ( $T_4$ ) temperature range.

Section 7.2 discusses the structural response of the representative casks to mechanical loads; Section 7.3 addresses response to thermal loads. In Section 7.4, the results of both structural and thermal response are combined to estimate the fraction of accidents that fall within each of the response regions.

## 7.2 Structural Response Analysis

The classes of accidents requiring structural analysis in the second-stage screening typically involve impacts with massive objects or hard surfaces. In these accidents, dynamic forces greater than 400,000 pounds can be generated. The computer codes selected to perform the required analysis include two established codes called DYNA 2-D/3-D and NIKE 2-D/3-D; the 2-D/3-D designation indicating that either two- or three-dimensional modeling can be performed.<sup>2,3</sup> Two-dimensional calculations are much simpler and faster to run and are used whenever possible. The applicability of the 2-D modeling is verified through the performance of sensitivity studies which compared results of 2-D and 3-D modeling. The calculation methods and assumptions used in the 2-D modeling are discussed in further detail in Appendix E. The most significant aspects include the following:

1. For cask orientations between sidewise and endwise in the range of  $0^{\circ} < \beta < 90^{\circ}$ , the structural strain responses for the representative casks impacting solid surfaces are linearly interpolated from the results of sidewise,  $\beta=0^{\circ}$ , and endwise,  $\beta=90^{\circ}$ , impacts.
2. Two-dimensional plane strain analyses without impact limiters or end enclosures are performed for high velocity sidewise impacts,  $\beta=0^{\circ}$ , on hard rock, soft rock, and soil surfaces. This elimination of impact limiters overestimates strain responses of the representative casks, particularly for impact velocities less than 60 mph and for impacts on soft surfaces such as soil. The 2-D method is benchmarked with a 3-D impact analysis that modeled the representative truck cask with the inclusion of the impact limiters and end closures.
3. The strain responses of the representative casks impacting real surfaces are estimated using the equivalent damage technique discussed in Section 6.2 and in Appendix E.

The structural response analysis of highway accidents is in Subsection 7.2.1. Highway accident scenarios, in which the first-stage screening indicates the possibility of cask response outside the R(1,1) region, are evaluated. The fraction of these accidents causing responses within the 0.2% ( $S_1$ ) to 2% ( $S_2$ ) and 2% ( $S_3$ ) to 30% ( $S_3$ ) strain levels on the inner shell of the representative truck cask is determined. Subsection 7.2.2 describes a similar structural response analysis performed for the railway accidents. In Subsection 7.2.3 the overall structural analysis results are discussed.

#### 7.2.1 Cask Response Analysis for Highway Accidents

The representative truck cask described in Section 3.5 is used in the second stage screening analysis for highway accidents. Appendix E discusses the computer models of the cask, material properties, and the detailed structural evaluations used in the response analysis.

The highway accident scenarios involve impacts by train sills and impacts occurring as a result of a truck running off a bridge, over an embankment, into a slope, or into a massive concrete structure.

In this evaluation, the maximum strain at the inner wall of the representative truck cask is calculated as a function of the impact velocity for both endwise and sidewise impacts with real surfaces.

#### 7.2.1.1 Endwise Impacts

Since the representative truck cask is axi-symmetric along its length, a 2-D cask model with impact limiters is used to evaluate the response of the representative truck cask for endwise impacts on an unyielding surface. Figure 7-2 shows the strain response for the representative truck cask impacting an unyielding surface at 45 mph. The maximum strain of 3.63% occurs on the inner shell of the cask at the bottom junction with the end-cap, near the point of impact. The lead slumps to the impacted end of the cask, causing a 4-inch gap in the lead shield at the opposite end.

The cask impact calculations are performed, assuming impacts on an unyielding surface, over a range of velocities from 30 to 90 mph. As discussed in Appendix E, the energy absorption effects of crushing the transport truck cab are included in the analysis. The resultant impact force, maximum plastic strain at the inner shell of the cask, and the amount of lead slump are plotted as functions of impact velocity in Fig. 7-3. The 2% strain ( $S_2$ ) level occurs when a cask impacts an unyielding surface at a velocity of 46 mph. At this velocity the impact force is 80 g, and the lead slump is about 3 inches. The 30% strain ( $S_3$ ) level occurs when a cask impacts an unyielding surface at a velocity of 76 mph. The resultant impact force is 300 g and the lead slump is 16 inches. In both cases, the maximum strains occur because of lead slump at the bottom of the cask on the inner shell.

The equivalent damage technique, discussed in Section 6.2 and Appendix E, is used to estimate the cask response for endwise impacts on real surfaces. A rigid body with the outer dimensions and weight of the truck cask impacts varying surfaces at velocities up to 120 mph. The resultant interface forces

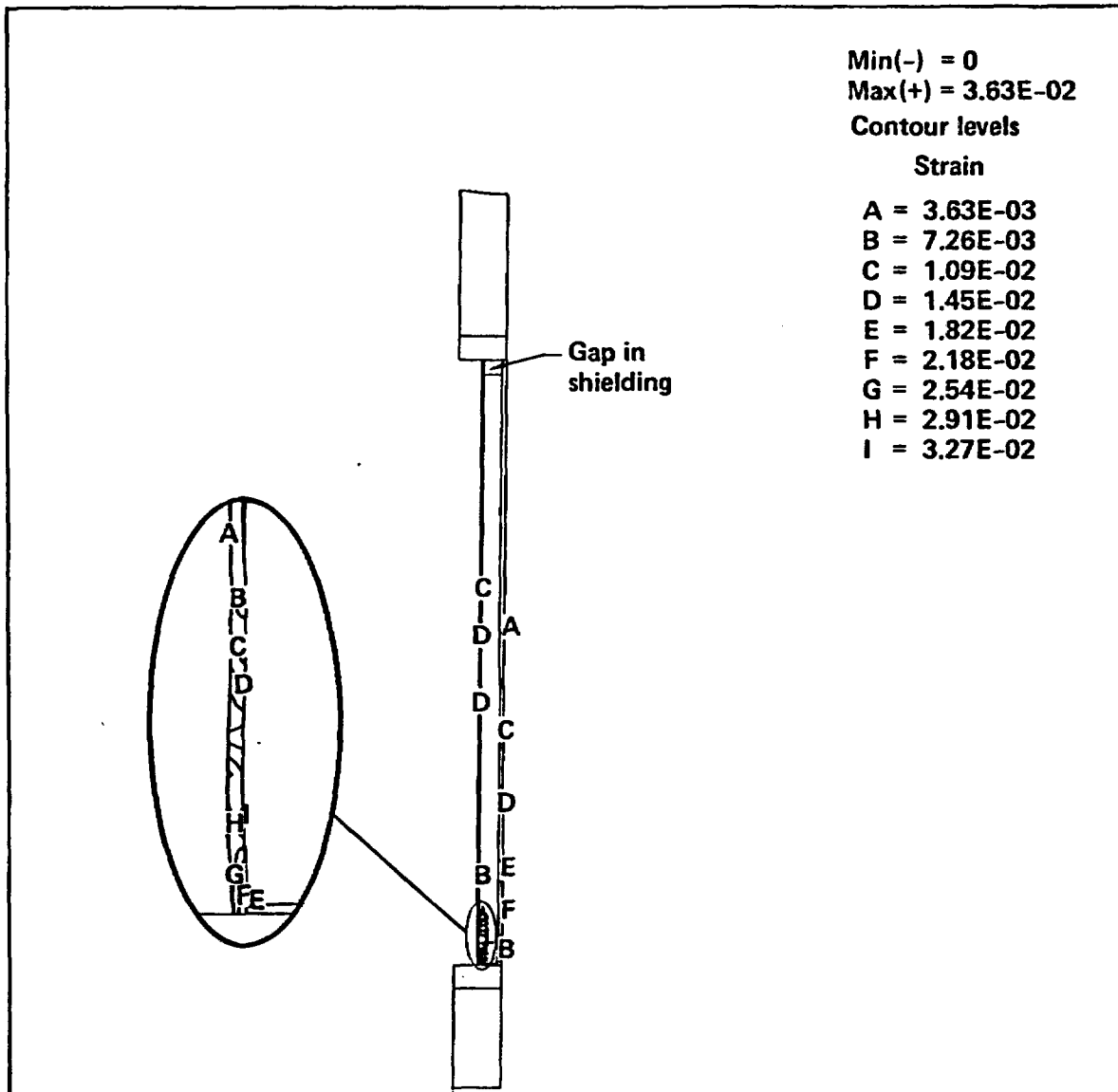


Figure 7-2 Example showing strain response of the representative truck cask for 45 mph endwise impact on an unyielding surface (2-D model with impact limiters) without any truck cab crushing included.

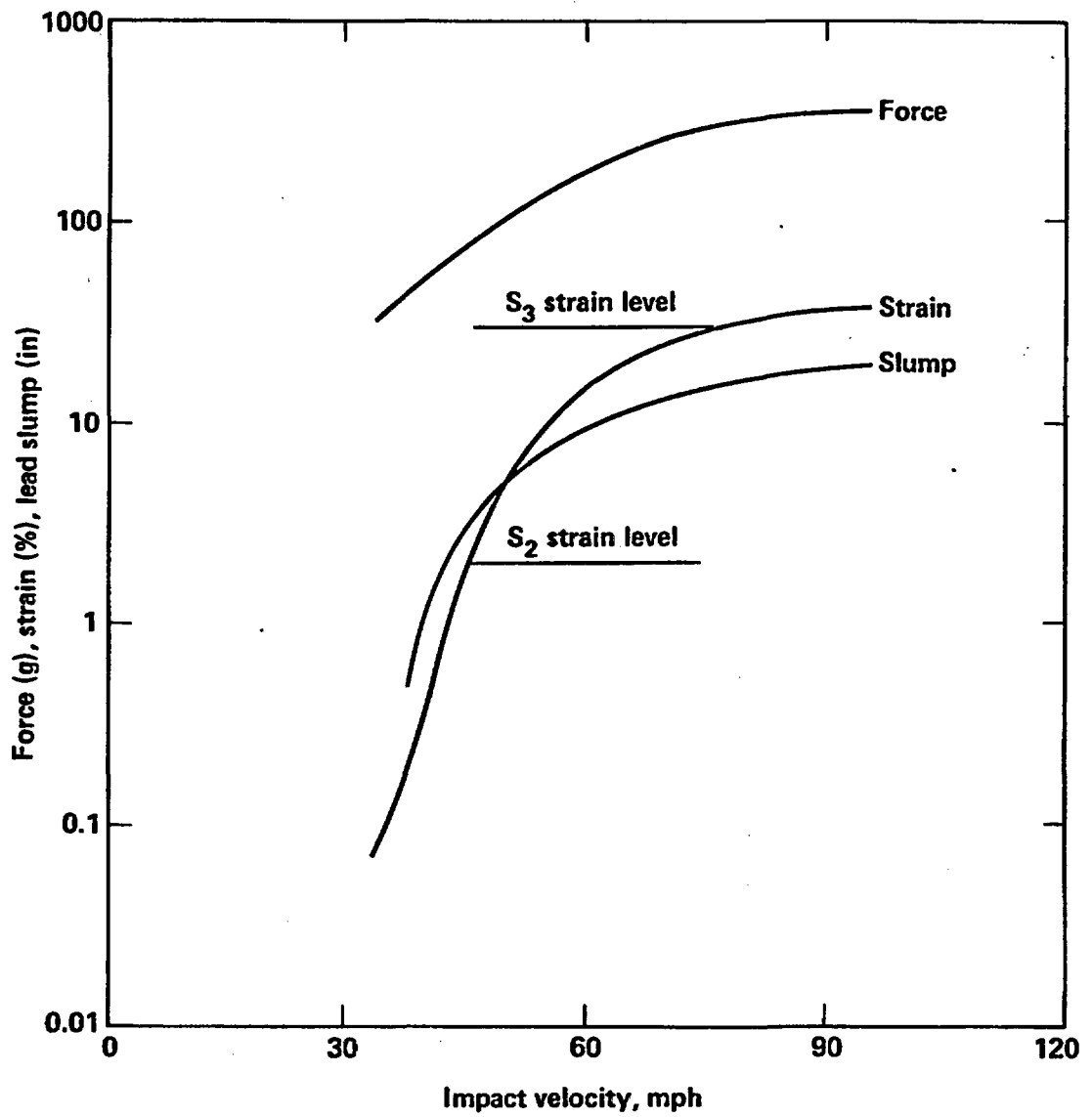


Figure 7-3 Response of the representative truck cask to endwise impacts on an unyielding surface (2-D model with impact limiters and cab crush).

were calculated in the first-stage screening and are plotted in Fig. 6-7. Using the equivalent damage technique, the 2% strain ( $S_2$ ) level is reached at impact velocities of 46 mph for impacts on hard and soft rocks but is never reached for impacts on soil. The 30% strain ( $S_3$ ) level is reached only for impacts on hard rocks at impact velocities exceeding 76 mph.

#### 7.2.1.2 Sidewise Impacts

An approximate 2-D plane strain model is used to calculate the response for high-velocity sidewise impacts on soil, soft rock, and hard rock. Figure 7-4 shows the strain response for the representative truck cask without an impact limiter impacting tillable soil at 60 mph. The maximum strain of 8.47% occurs at the inner shell. During impact, the cask inner diameter decreases by 50% in the impact direction and collapses onto any spent fuel being transported.

In Fig. 7-5, the maximum plastic strain at the inner wall is plotted as a function of impact velocity for impacts on hard rock, soft rock, and tillable soil. In the approximate 2-D model, the strains calculated for a specific impact velocity are essentially the same for sidewise impacts regardless of the surface impacted. The 2% strain ( $S_2$ ) level occurs at a velocity of 51 mph for impacts on all of the surfaces considered. The 30% strain ( $S_3$ ) level does not occur because the representative cask walls collapse together or onto the spent fuel contents before the limit is reached.

#### 7.2.1.3 Impact Response Summary

Table 7.1 summarizes the impact velocities at the 2% ( $S_2$ ) and 30% ( $S_3$ ) strain levels for sidewise,  $\beta = 0^\circ$ , and endwise,  $\beta = 90^\circ$ , impacts on hard rock, soft rock, and soil surfaces. Impacts of the cask on water and by a train sill are also included. In general, the endwise impacts result in higher strains to the cask than sidewise impacts for the same impact conditions on surfaces. The cask attains the 30% strain ( $S_3$ ) level only at high-velocity endwise impacts on hard rock.

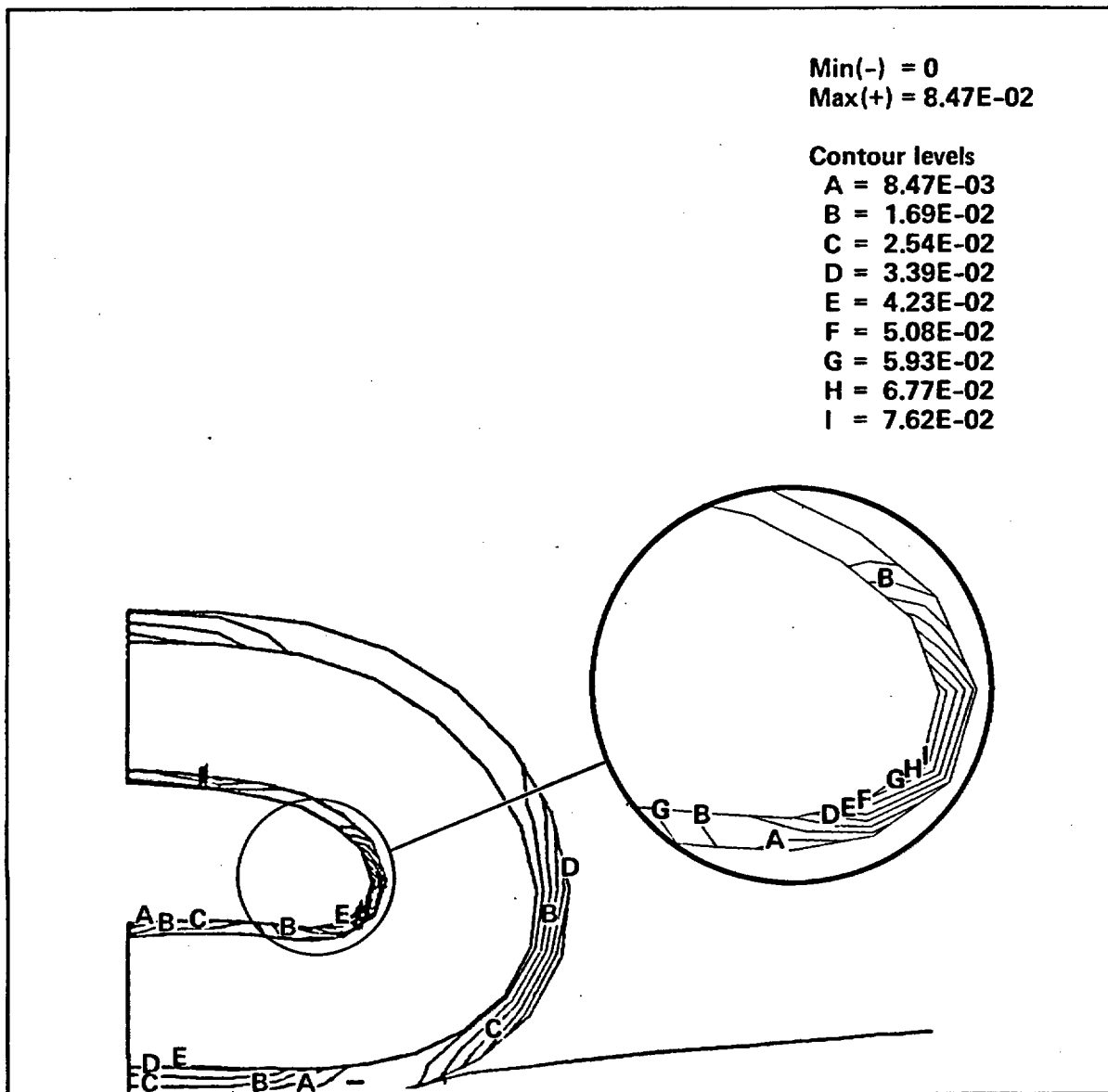


Figure 7-4 Example showing strain response of the representative truck cask for 60 mph sidewise impact on soil (2-D model without impact limiters) with strain exceeding the 2% ( $S_2$ ) limit.

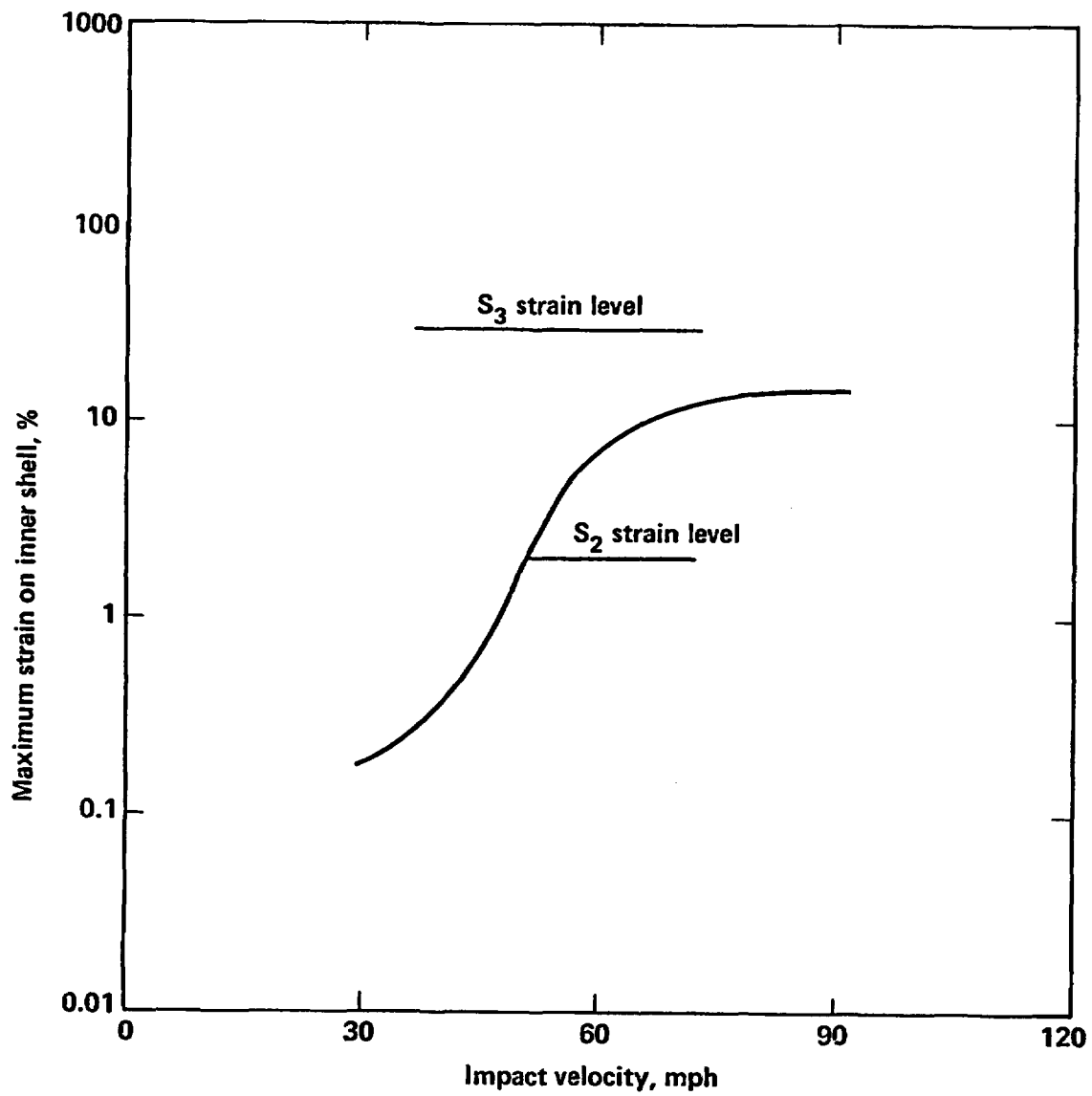


Figure 7-5 Response of the representative truck cask to sidewise impacts on various surfaces.

Table 7.1  
Impact Velocities Required to Attain 2% ( $S_2$ ) and 30% ( $S_3$ ) Strain Levels  
for Objects Impacted in Highway Accidents

Object Impacted	Impact Velocity $\underline{a/}$ at 2% Strain ( $S_2$ ) (mph)			Impact Velocity $\underline{a/}$ at 30% Strain ( $S_3$ ) (mph)		
	Cask Orientation Angle ( $^\circ$ )			Cask Orientation Angle ( $^\circ$ )		
	0	45	90	0	45	90
Hard Rock	51	49 $\underline{b/}$	46	>150	113 $\underline{b/}$	76
Soft Rock	51	49 $\underline{b/}$	46	>150	>150 $\underline{b/}$	150
Tillable Soil	51	101 $\underline{b/}$	>150	>150	>150 $\underline{b/}$	>150
Water	59	>150	64	>150	>150	>150
Train Sill	20	27	>150	>150	>150	>150

$\underline{a/}$  Impact velocity of >150 mph means that the strain level is not reached.

$\underline{b/}$  Impact velocities at these orientation angles are linearly interpolated between the two bounding values.

## 7.2.2 Cask Response Analysis for Railway Accidents

The representative rail cask described in Section 3.5 is used in the railway accident response analysis. Appendix E discusses the computer models of the cask, the material properties, and the detailed structural evaluations use in the cask response analysis.

The railway accident scenarios of interest are those involving falls from bridges; drops over embankments; and impacts into slopes, train couplers, or massive concrete structures. Again, the maximum strain at the inner wall of the representative rail cask is calculated as a function of the impact velocity for both endwise and sidewise impacts with real surfaces.

### 7.2.2.1 Endwise Impacts

As was done in the truck cask analysis, a 2-D model is used to evaluate the response of the representative rail cask for endwise impacts on an unyielding surface. The cask impact calculations cover a range of velocities from 30 to 90 mph. Figure 7-6 shows the resultant impact force, maximum plastic strain at the inner shell of the cask, and the amount of lead slump as functions of impact velocity. The 2% strain ( $S_2$ ) level occurs when a cask impacts an unyielding surface at a velocity of 48 mph. At this velocity the impact force is 102 g, and the lead slump is 6 inches. The 30% strain ( $S_3$ ) level occurs when a cask impacts an unyielding surface at a velocity of 105 mph. The resultant impact force at this velocity is 500 g and the lead slump is 28 inches. In both cases the maximum strain occurs at the bottom of the cask on the inner shell.

The equivalent damage technique is used to estimate the cask response for endwise impacts on real surfaces. A rigid body with the outer dimensions and weight of the rail cask impacts various surfaces at velocities up to 120 mph. The resultant interface forces for these impacts are calculated in the first-stage screening and are plotted in Fig. 6-10. Using the equivalent damage technique, the 2% strain ( $S_2$ ) level is reached at impact velocities of 48 mph for impacts on hard and soft rocks, and 65 mph for impacts on soil. The 30% strain ( $S_3$ ) level is reached only for impacts on hard and soft rocks at an impact velocity of 105 mph.

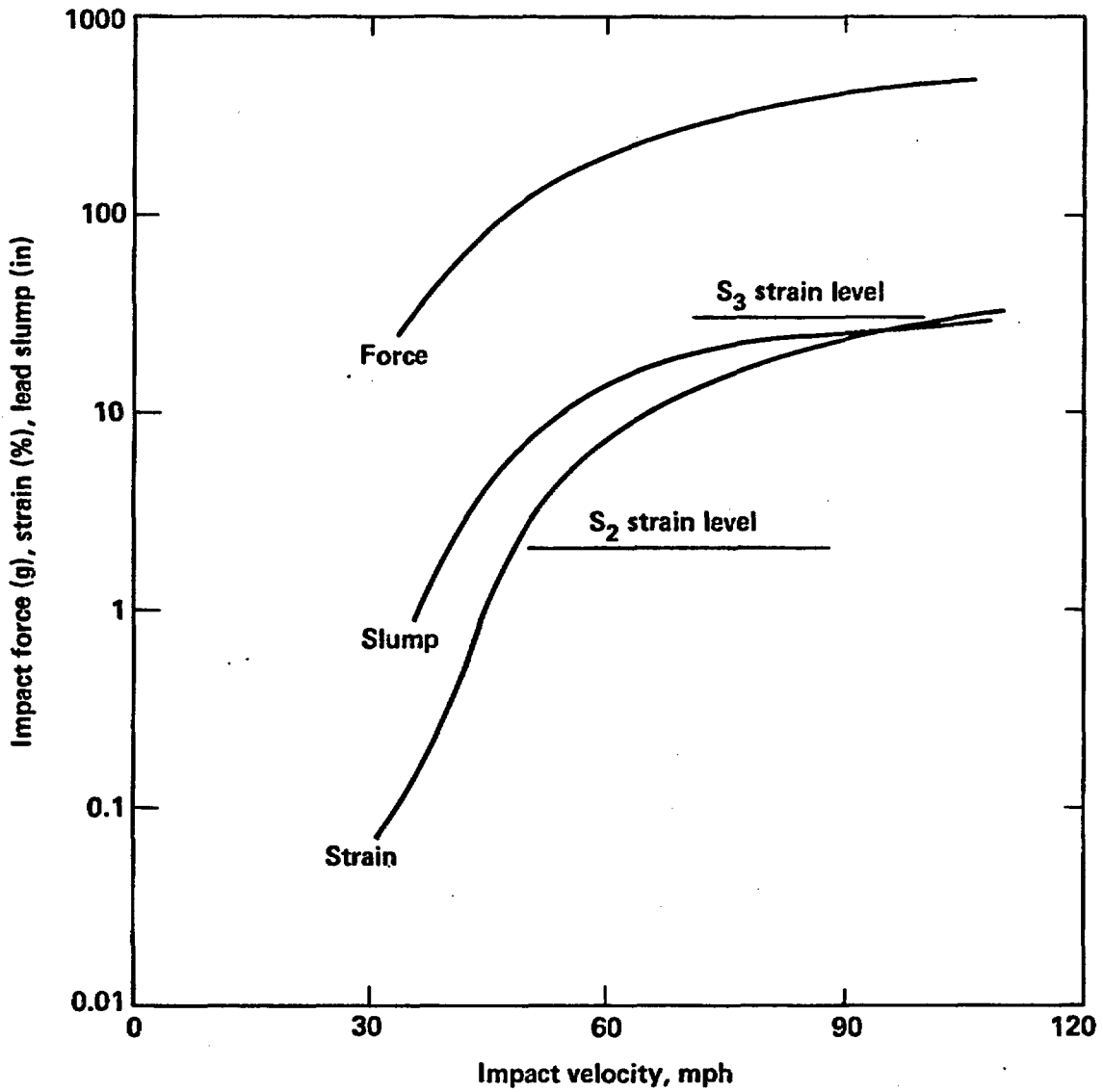


Figure 7-6 Response of the representative rail cask to endwise impacts on an unyielding surface (2-D model with impact limiters and railcar crush).

#### 7.2.2.2 Sidewise Impacts

As done in the truck cask, a 2-D model of the rail cask is used to calculate the response for high-velocity sidewise impacts on soil, soft rock, and hard rock. In Fig. 7-7, the maximum plastic strain at the inner wall is plotted as a function of impact velocity. The 2% strain ( $S_2$ ) level occurs at a velocity of 72 mph for impacts on hard and soft rock and on soil. The 30% strain ( $S_3$ ) level can never occur because the representative cask walls collapse together or onto the spent fuel contents before the limit is reached.

#### 7.2.2.3 Impact Response Summary

Table 7.2 summarizes the impact velocities at the 2% ( $S_2$ ) and 30% ( $S_3$ ) strain level for sidewise,  $\beta = 0^\circ$ , and endwise,  $\beta = 90^\circ$ , impacts on hard rock, soft rock, and soil surfaces. Impacts of the cask on water and by a train sill are also included. In general, the endwise impacts result in higher strains to the cask than sidewise impacts for the same impact conditions.

#### 7.2.3 Discussion of Structural Analysis Results

This section has thus far addressed highway and railway accidents that can generate cask responses within the 2% ( $S_2$ ) and 30% ( $S_3$ ) strain levels. Cask structural responses at these levels result in permanent deformations to the cask and potential radioactive material releases or increases in direct radiation exposure levels which could approach or exceed the limits specified in 10 CFR 71.

The dynamic response of the cask is calculated using the DYNA and NIKE families of elastic-plastic finite element computer codes.<sup>2,3</sup> These codes were developed at the Lawrence Livermore National Laboratory (LLNL) around 1979, and their predicted results were extensively benchmarked. Appendix H, for example, discusses the capability of these computer codes to calculate the dynamic responses of a cylinder impacting a rail, a nose cone impacting a rigid wall, and a rod impacting a rigid wall obliquely.

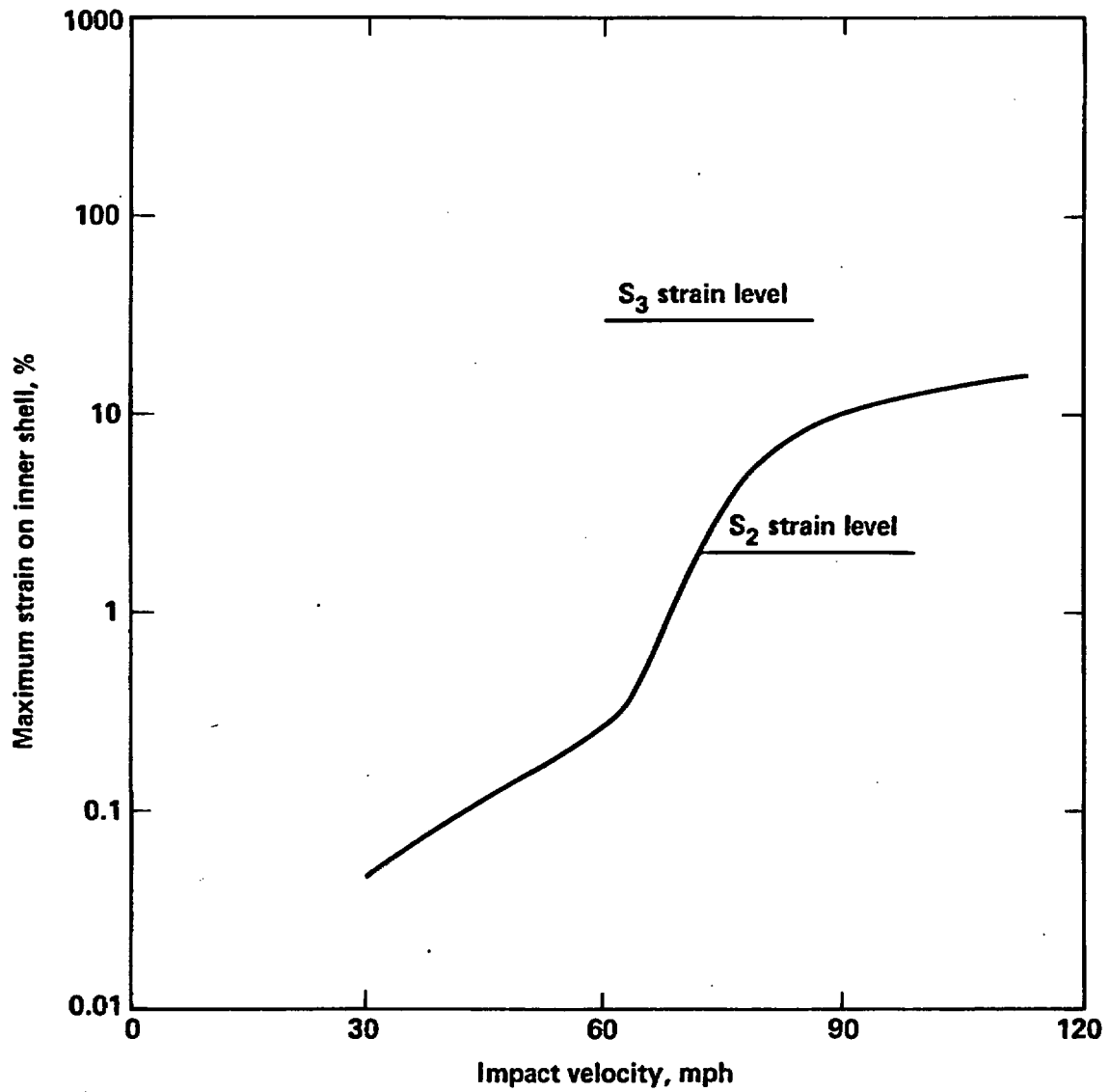


Figure 7-7 Response of the representative rail cask to sidewise impacts on various surfaces.

Table 7.2  
Impact Velocities Required to Attain 2% ( $S_2$ ) and 30% ( $S_3$ ) Strain Levels for  
Objects Impacted in Railway Accidents

Object Impacted	Impact Velocity <u>a/</u> for 2% Strain (mph)			Impact Velocity <u>a/</u> for 30% Strain (mph)		
	Cask Orientation Angle (°)			Cask Orientation Angle (°)		
	0	45	90	0	45	90
Hard Rock	72	60 <u>b/</u>	48	150	128 <u>b/</u>	105
Soft Rock	72	60 <u>b/</u>	48	150	128 <u>b/</u>	105
Tillable Soil	72	69 <u>b/</u>	65	150	150 <u>b/</u>	150
Water	72	150	60	150	150	150
Train Sill	27	49	150	150	150	150

a/ Impact velocity of 150 mph means that the strain level is not reached.

b/ Impact velocities at these orientation angles are linearly interpolated between the two bounding values.

These benchmark cases demonstrate the capabilities of the codes to calculate the dynamic response of objects which, when subjected to impact, can experience large permanent deformations. In all three cases, the computer predictions were within a few percent of the deformations measured in the tests.

Benchmark tests of DYNA 3-D have also been performed in the United Kingdom. Excellent agreement was obtained in predicting the dynamic response of a missile impacting a pipe.<sup>4</sup> DYNA 3-D was also used to predict the high deformation characteristics and response of a metal fin on the MAGNOX spent fuel cask when subjected to a 30-foot drop onto an unyielding surface.<sup>5</sup> Again there was a good comparison between the test results and the computer predictions.

The Sandia National Laboratory (SNL) used scale model tests and a computer code similar to DYNA 2-D to predict the dynamic response and deformations of full-scale casks used in a series of crash tests. The full-scale tests included a 25-ton truck cask being struck by a 100-ton locomotive at 80 mph.<sup>6</sup> Following the high-velocity impact, the cask was dented at the points of impact on the side, was slightly bowed along the length, and had a small leak at the closure. In another test, a similar truck cask was carried at 80 mph on a truck which crashed into a huge unyielding concrete abutment.<sup>7</sup> The endwise impact resulted in some lead slump and a small leak at the closure. The results of both of these tests were in good agreement with the computer predictions.

These benchmark tests of the computer codes support their use in conservatively predicting the damage to a spent fuel cask which is subjected to severe accident conditions. In many cases in this study, conservative modeling assumptions are made to simplify the cask response evaluation over a wide range of accident conditions. Examples include the 2-D modeling of 3-D sidewise impacts, the use of elastic-plastic soil modeling, the use of the equivalent damage technique for estimating strain, and the assumption of no bonding between the lead shield and the inner shell of the cask. All these assumptions result in overpredicting the cask damage response to real accident

conditions. In addition, the representative cask is structurally weaker than current casks. Again, for the same impact conditions, damage to the representative casks will be greater than that which would be incurred by real casks.

### 7.3 Thermal Response Analysis

Many of the accident scenarios involving fire led to a cask response well within the R(1,1) region associated with the first-stage screening. This observation is true for both truck and rail casks, but more prevalent for truck casks.

The accidents of interest in this section involve fires of approximately 1-hour duration and longer. These fire accidents have three loading parameters that can affect the response of a spent fuel cask: fire duration, flame temperature, and fire location. Longer fire durations and higher flame temperatures increase the thermal loads to the cask and increase its temperature responses. Also, the closer the cask is to the fire, the better the thermal interaction and the higher the thermal load. In the worst case, the cask is submerged or engulfed by the fire.

The thermal screening analysis in this section compares the truck and rail cask responses to the three temperature response levels of 600°F ( $T_2$ ), 650°F ( $T_3$ ), and 1050°F ( $T_4$ ) at the middle of the lead shield thickness. Since lead melts at 621°F, the calculation of the responses between 600°F ( $T_2$ ) and 650°F ( $T_3$ ) has to include the melting of the lead shield. The computer code TACO 2-D used in the first-stage screening has the capability of handling lead melt. TACO 2-D is used with the same one-dimensional (1-D) thermal models to perform the second-stage screening.<sup>8</sup> In other words, the thermal analysis is a continuation of the analysis performed for the first-stage screening, but includes consideration of lead melt.

The calculational method relies on the concept that the time to reach a specific cask temperature is approximately proportional to the incident heat flux on the cask caused by the fire. A fire that causes a heat flux twice the heat flux of a reference fire can heat a cask to a specified temperature in

one-half the time it takes the reference fire. Conversely, a fire that causes one-half the heat flux takes twice as long to heat the cask in comparison to a reference fire. For details on the calculational method, refer to Section 6.3.

The thermal response analysis of highway fire accidents is provided in Subsection 7.3.1. Subsection 7.3.2 describes a similar response analysis performed for the railway fire accidents. In Subsection 7.3.3, the overall thermal screening results are discussed.

### 7.3.1 Cask Response Analysis for Highway Fire Accidents

The representative truck cask described in Section 3.5 is used in the highway fire accident response analysis. Appendix F discusses the computer analysis model, the cask material properties, and the detailed thermal calculations. All highway accident scenarios are evaluated for cask responses to fire because in all scenarios, possibilities exist that a fire can occur and last longer than 1 hour.

The temperature response of the representative truck cask is calculated for a hypothetical engulfing fire with a flame temperature of 1475<sup>0</sup>F and flame emissivity of 0.9. This hypothetical fire approximates a real engulfing fire with a 1700<sup>0</sup>F flame temperature. The temperature at the middle of the lead shield thickness is plotted in Fig. 7-8 as a function of time. The lead mid-thickness temperature reaches 600<sup>0</sup>F ( $T_2$ ) in 1.35 hours for the specified heat flux conditions. The total heat absorbed by the cask in reaching the 600<sup>0</sup>F temperature ( $T_2$ ) level is approximately 6,000 Btu/ft<sup>2</sup> which results in an average thermal flux of approximately 4,450 Btu/hr-ft<sup>2</sup>. As the lead mid-thickness temperature increases beyond the 600<sup>0</sup>F ( $T_2$ ) level, the lead at the outer shell starts to melt. The lead melts at the inner shell in 2.1 hours as the mid-thickness temperature reaches 650<sup>0</sup>F ( $T_3$ ). The 1050<sup>0</sup>F temperature ( $T_4$ ) level is reached in 3.3 hours.

These temperature response and heat flux results from the hypothetical fire are used to evaluate real fires. For an engulfing fire, the heat flux from the fire onto the surface of the truck cask depends on radiation heat

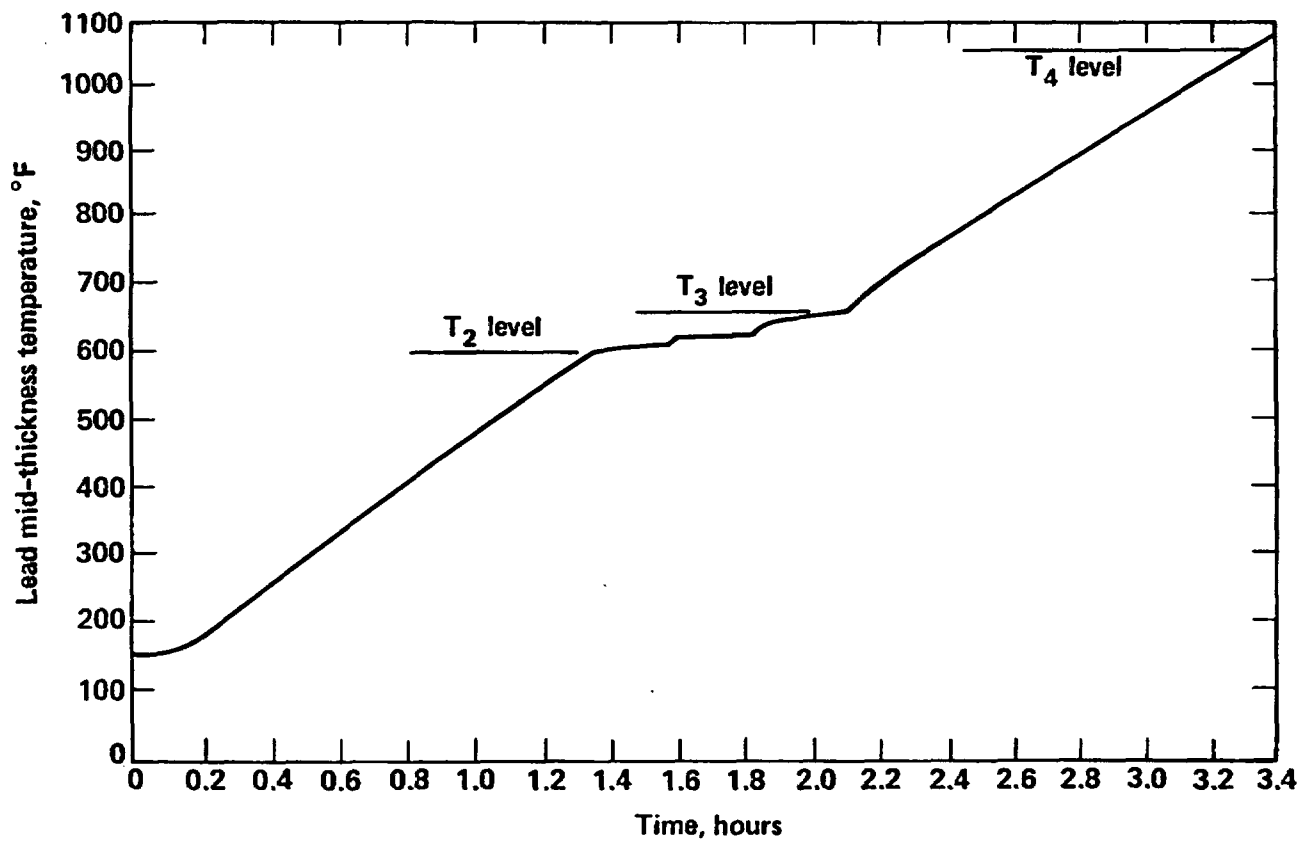


Figure 7-8 Representative truck cask temperature response to a hypothetical 1475°F (equivalent to a real 1700°F) fire versus fire duration.

transfer which is strongly dependent on the flame temperature. The average heat flux on the representative truck cask is calculated as a function of flame temperature for a hypothetical engulfing fire. The heat flux is then reduced by a factor of 0.78 to adjust the results to real engulfing fire conditions. The heat flux factors are derived in the first-stage screening evaluations, and the results are plotted in Fig. 6-14 as a function of flame temperature. For a 1700°F fire, the average thermal flux on the representative cask is 5,000 Btu/hr-ft<sup>2</sup> and the heat flux factor is 1.0.

The heat flux to the truck cask also depends on the location of the fire with respect to the cask. An engulfing fire provides the maximum heat flux to the cask. The heat flux decreases rapidly as the distance between the fire and the cask increases. As discussed in Subsection 6.3.2 and plotted in Fig. 6-15, the heat load factor is normalized with respect to a real engulfing fire.

As the flame temperature increases, the thermal flux to the cask increases, and the fire duration required to reach the 600°F (T<sub>2</sub>), 650°F (T<sub>3</sub>), and 1050°F (T<sub>4</sub>) temperature levels decreases proportionally. On the other hand, as the cask distance from the fire increases, the thermal flux decreases and the duration time increases proportionally to reach the same temperature levels.

The heat flux and load factors are used to determine the amounts of increase or decrease required in each of the fire duration times to reach the 600°F (T<sub>2</sub>), 650°F (T<sub>3</sub>), and 1050°F (T<sub>4</sub>) temperature levels for a variety of flame temperatures and fire locations.

### 7.3.2 Cask Response Analysis for Railway Fire Accidents

The representative rail cask described in Section 3.5 is used in the railway fire accident response analysis. Appendix F discusses the computer analysis model of the cask, the material properties, and the detailed thermal calculations used in the response analysis.

All railway accident scenarios are evaluated for cask responses to fire because in all scenarios, possibilities exist that a fire can occur and can last longer than 1 hour.

The temperature response of the representative rail cask is calculated for a hypothetical engulfing fire with a flame temperature of 1475°F and flame emissivity of 0.9. The temperature at the middle of the lead shield thickness is plotted in Fig. 7-9 as a function of fire duration. The lead mid-thickness temperature reaches 600°F temperature ( $T_2$ ) in 1.8 hours for the specific thermal flux conditions. The total heat absorbed by the cask in reaching the 600°F temperature ( $T_2$ ) level is approximately 7,900 Btu/ft<sup>2</sup> which results in an average thermal flux of approximately 4,400 Btu/hr-ft<sup>2</sup>. As the lead mid-thickness temperature increases beyond the 600°F ( $T_2$ ) level, the lead at the outer shell starts to melt. The lead melts at the inner shell in 2.6 hours as the lead mid-thickness temperature reaches 650°F ( $T_3$ ). The 1050°F temperature ( $T_4$ ) level is reached in 5.1 hours. These final temperature response and heat flux results are used to evaluate real fires.

As is done for the truck cask, heat flux and load factors are calculated for the rail cask, as plotted in Figs. 6-14 and 6-17. These factors are used to determine the amounts of increase or decrease in each of the fire duration times necessary to reach the 600°F ( $T_2$ ), 650°F ( $T_3$ ), and 1050°F ( $T_4$ ) temperature levels for a variety of flame temperatures and fire locations.

### 7.3.3 Discussion of Thermal Analysis Results

Cask responses at the 600°F ( $T_2$ ), 650°F ( $T_3$ ), and 1050°F ( $T_4$ ) temperature levels can involve deterioration of safety components and melting of the lead shield. Consequently, radioactive material releases and increases in direct radiation exposures are possible and could equal or exceed regulatory limits specified in 10 CFR 71 for transportation accidents.

The TACO 2-D code used to perform the thermal analysis was developed about 1978 at the LLNL and was benchmarked against proven engineering solutions for various thermal conditions.<sup>8</sup> The benchmark cases demonstrate the code's capability to calculate the temperature response for objects heated under steady state and transient conditions.<sup>8</sup> In all cases, TACO 2-D calculates temperature results, which are within a few percent of the exact solution.

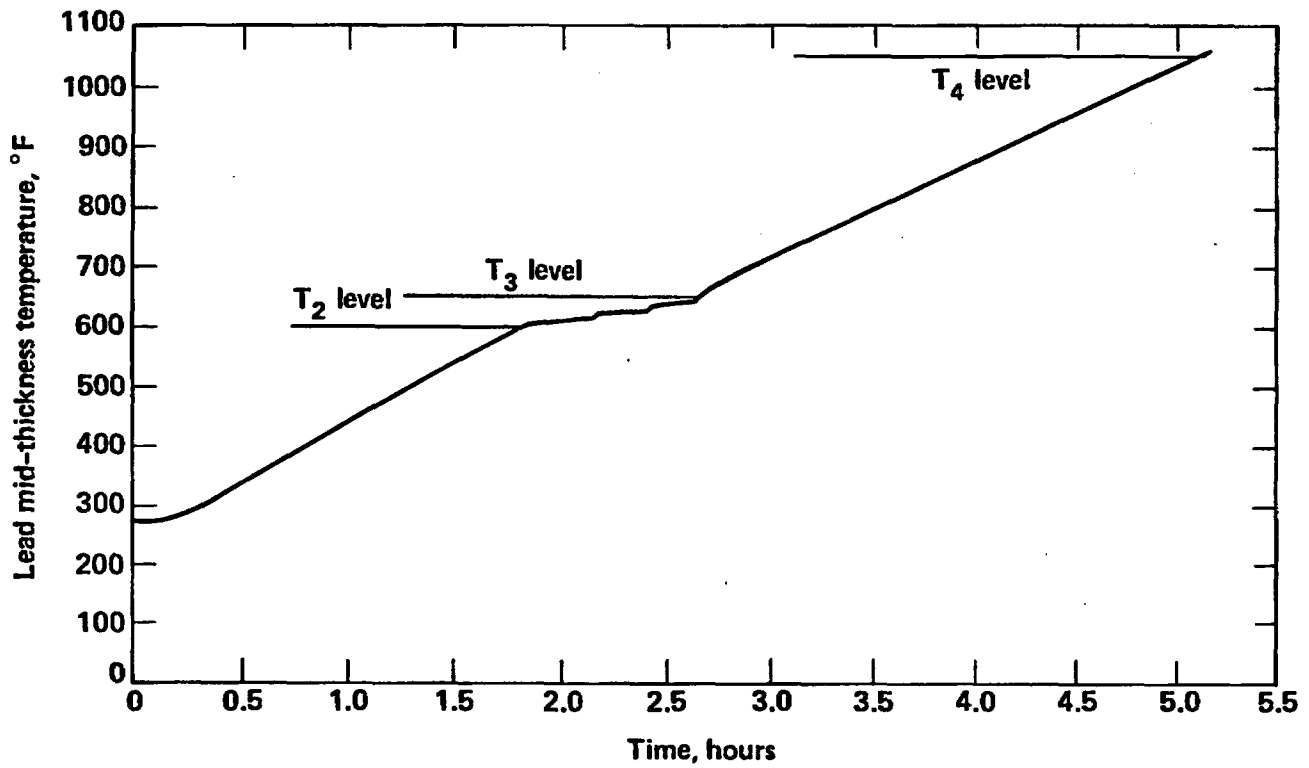


Figure 7-9 Representative rail cask temperature response to a hypothetical 1475°F (equivalent to a real 1700°F) fire versus fire duration.

In 1978, the SNL used similar computer codes to analyze temperatures from a test involving a spent fuel cask suspended over a pit filled with burning jet fuel.<sup>9,10</sup> Under these test conditions, the temperature measurement instruments and the code predictions showed that the environment in a real fire varies significantly along the length of the cask and as a function of time. The thermal flux varies with the wind and ventilation conditions surrounding the cask. Sandia concluded that the regulatory thermal test conditions (1475°F hypothetical engulfing fire) are equivalent to a real engulfing fire with much higher flame temperatures.

Both the benchmark computer code calculations and the Sandia fire test support the use of computer code modeling to evaluate the temperature response of a cask to a real fire accident. In this study, conservative modeling techniques are introduced to simplify the cask response evaluation over a wide range of fire accident conditions. A 1-D model of a hypothetical engulfing fire with a nominal flame temperature of 1475°F is used in lieu of a 2-D model with variable flame temperatures. In addition, no inclusion of heat loss with cask location is considered. These modeling assumptions overpredict the cask temperature response to fires. In addition, casks that use shielding material other than lead cannot incur damage due to melting.

#### 7.4 Accident Screening Analysis

Section 5.0 discusses how the detailed probabilistic calculations are performed by the (Transportation Accident Scenario Probabilities) TASP code in the accident screening analysis. The fraction of accidents calculated by the TASP code is summarized in Figs. 7-10 and 7-11 respectively for the truck and train accidents for each response region. Assuming that an accident occurs, the percentage of both truck and train accidents within the 2% strain ( $S_2$ ) and 600°F temperature ( $T_2$ ) levels is about 99.8%. Fewer than 0.001% of truck accidents and 0.013% of rail accidents fall outside of the 30% strain ( $S_3$ ) and 1050°F temperature ( $T_4$ ) levels for which the cask structural and thermal analyses are performed.

Structural response (maximum strain on inner shell, %)	$S_3$ (30)	1.532E-7	3.926E-14	1.495E-14	7.681E-16	<E-16
	$S_2$ (2)	1.7984E-3	1.574E-7	2.034E-7	1.076E-7	4.873E-8
	$S_1$ (0.2)	3.8192E-3	2.330E-7	3.008E-7	1.592E-7	7.201E-8
		0.994316	1.687E-5	2.362E-5	1.525E-5	9.570E-6
		$T_1$ (500)	$T_2$ (600)	$T_3$ (650)	$T_4$ (1050)	
		Thermal response (lead mid-thickness temperature, °F)				

Note:  
E + x = 10<sup>x</sup>

Figure 7-10 Fraction of truck accidents that could result in responses within each response region, assuming an accident occurs.

Structural response (maximum strain on inner shell, %)	$S_3$ (30)	1.786E-9	3.290E-13	2.137E-13	1.644E-13	3.459E-14
	$S_2$ (2)	5.545E-4	1.021E-7	6.634E-8	5.162E-8	5.296E-8
		2.7204E-3	5.011E-7	3.255E-7	2.531E-7	1.075E-8
	$S_1$ (0.2)	.993962	1.2275E-3	7.9511E-4	6.140E-4	1.249E-4
		$T_1$ (500)	$T_2$ (600)	$T_3$ (650)	$T_4$ (1050)	
		Thermal response (lead mid-thickness temperature, °F)				

Note:  
E + x = 10<sup>x</sup>

Figure 7-11 Fraction of rail accidents that could result in responses within each response region, assuming an accident occurs.

The significance of these screening results is discussed in detail in Section 9.0 with respect to the existing regulatory requirements and the risk evaluations performed in NUREG-0170.<sup>11</sup>



## 8.0 POTENTIAL RADIOLOGICAL SIGNIFICANCE OF TRANSPORTATION ACCIDENTS

### 8.1 Introduction

The purpose of this section is to estimate the potential radiological hazards of various classes of transportation accidents involving a spent fuel shipment. Any significant radioactive material release or increase in the radiation levels from a cask following an accident will originate with the spent fuel. As the cask damage and response increase, the radiation hazard will also increase.

In the previous section, the specific levels of damage that a cask might experience in transportation accidents are categorized in terms of cask response regions. In this section, the potential radiological hazards from accident effects are estimated for each cask response region in terms of: (1) releases of spent fuel material, and (2) levels of radiation from the cask contents. Comparisons are then made in Section 9.0 with the release and radiation limits defined in 10 CFR 71<sup>1</sup> and the radiological risk estimates evaluated in the NUREG-0170, "Final Environmental Statement on the Transportation of Radioactive Material by Air and other Modes".<sup>2</sup>

### 8.2 Description of Spent Fuel

The characteristics of spent fuel strongly influences the potential radiological hazards of transportation accidents involving shipment. The level of radioactivity and the heat generated within the spent fuel depend on the amount of fission energy extracted from the fuel during its use in a power reactor. However, after the fuel is removed from the reactor, the total radioactivity decays or drops about 80 fold within 1 year and about 340 fold within 5 years. The radioactivity and thermal power in the spent fuel is produced, for the most part, by decay of radioactive isotopes residing within the solid fuel pellets. However, a small amount of gaseous and volatile radioactive material also migrates from the fuel pellets to the fuel rod gap. The radioactive inventory and thermal power of a typical spent fuel assembly is shown in Table 8.1 as a function of decay time.<sup>3</sup> The table

Table 8.1  
PWR Fuel Assembly Decay Heat and Radioactivity<sup>a/</sup>

Radioisotopes	Radioactivity (Ci)		
	Decay Time (years)		
	1	5	10
<sup>60</sup> Co <sup>b/</sup>	3.57x10 <sup>1</sup>	2.11x10 <sup>1</sup>	1.09x10 <sup>1</sup>
<sup>85</sup> Kr	3.99x10 <sup>3</sup>	3.08x10 <sup>3</sup>	2.23x10 <sup>3</sup>
<sup>90</sup> Sr	3.42x10 <sup>4</sup>	3.10x10 <sup>4</sup>	2.75x10 <sup>4</sup>
<sup>90</sup> Y	3.41x10 <sup>4</sup>	3.09x10 <sup>4</sup>	2.73x10 <sup>4</sup>
<sup>106</sup> Ru	1.21x10 <sup>5</sup>	7.79x10 <sup>3</sup>	2.52x10 <sup>2</sup>
<sup>129</sup> I	1.48x10 <sup>-2</sup>	1.48x10 <sup>-2</sup>	1.48x10 <sup>-2</sup>
<sup>134</sup> Cs	1.00x10 <sup>5</sup>	2.60x10 <sup>4</sup>	4.85x10 <sup>3</sup>
<sup>137</sup> Cs	4.73x10 <sup>4</sup>	4.32x10 <sup>4</sup>	3.85x10 <sup>4</sup>
<sup>137m</sup> Ba	4.47x10 <sup>4</sup>	4.07x10 <sup>4</sup>	3.62x10 <sup>4</sup>
<sup>144</sup> Ce	2.19x10 <sup>5</sup>	6.86x10 <sup>3</sup>	9.01x10 <sup>1</sup>
<sup>238</sup> Pu	1.46x10 <sup>3</sup>	1.41x10 <sup>3</sup>	1.36x10 <sup>3</sup>
<sup>239</sup> Pu	1.67x10 <sup>2</sup>	1.67x10 <sup>2</sup>	1.67x10 <sup>2</sup>
<sup>240</sup> Pu	2.06x10 <sup>2</sup>	2.06x10 <sup>2</sup>	2.06x10 <sup>2</sup>
<sup>241</sup> Pu	6.64x10 <sup>4</sup>	5.49x10 <sup>4</sup>	4.32x10 <sup>4</sup>
<sup>244</sup> Cm	9.72x10 <sup>2</sup>	8.34x10 <sup>2</sup>	6.90x10 <sup>2</sup>
Total Activity <sup>c/</sup>	1.12x10 <sup>6</sup>	2.66x10 <sup>5</sup>	1.82x10 <sup>5</sup>
Decay Heat, KBtu <sup>c/</sup>	16.42	3.02	1.93

<sup>a/</sup> Assumed burnup is 33,000 megawatt-days/metric ton of uranium<sup>3</sup>.

<sup>b/</sup> The <sup>60</sup>Co source is not a direct result of the fission process. It is produced from neutron activation of non-radioactive elements contained in structural materials and appears as crud on the fuel assembly surfaces<sup>4</sup>.

<sup>c/</sup> Includes all radioisotopes.

Note: Boxed column represents decay heat and radioactivity levels assumed for the fuel in this study.

identifies only the specific isotopes that are important in performing a radioactive release evaluation.

Different fuel assembly designs are used in nuclear power reactors. There are two major types of fuel assemblies used for the two principal reactor design concepts currently operating in this country--pressurized water reactors (PWRs) and boiling water reactors (BWRs). For purposes of this study, a typical PWR fuel assembly, shown in Fig. 8-1, is considered most representative for the following reasons. First, this assembly is most prevalent and typically contains the highest levels of radioactivity. Second, in terms of resistance to transportation accident loads, no significant difference can be identified in the gross structural response of the various fuel assembly designs. Finally, previous studies indicate that PWR fuel rods may be more susceptible to creep rupture than BWR fuel rods if subjected to high temperatures (1200°F) for a long period of time (e.g., ≥ 11 hours).<sup>5</sup>

The radioactive inventory of the reference PWR fuel assembly is based on an assumed burnup of 33,000 megawatt-days/metric ton of uranium and a decay time of 5 years. This burnup level is typical of current PWR fuel. Variations in burnup occur and increases in burnup are expected in future reactor operations. The effect of burnup level on the potential radiological significance of transportation accidents will not be large, i.e., less than a factor of 2. The 5-year decay time is selected because the vast majority of all spent fuel shipments, namely those expected to be made to the Federal repository, will have experienced at least this period of decay.<sup>6</sup> Spent fuel with minimum decay times of 4 to 5 months can be shipped in licensed casks; however, such shipments are expected to be rare. The boxed column in Table 8.1 shows the general radioactive characteristics of the spent fuel assembly considered representative for this study.

### 8.3 Measures of Radiological Significance

The general description of the reference spent fuel assembly, shown in Table 8.1, identifies the radioactivity level in terms of curie content. The curie content is important to radiological significance from two

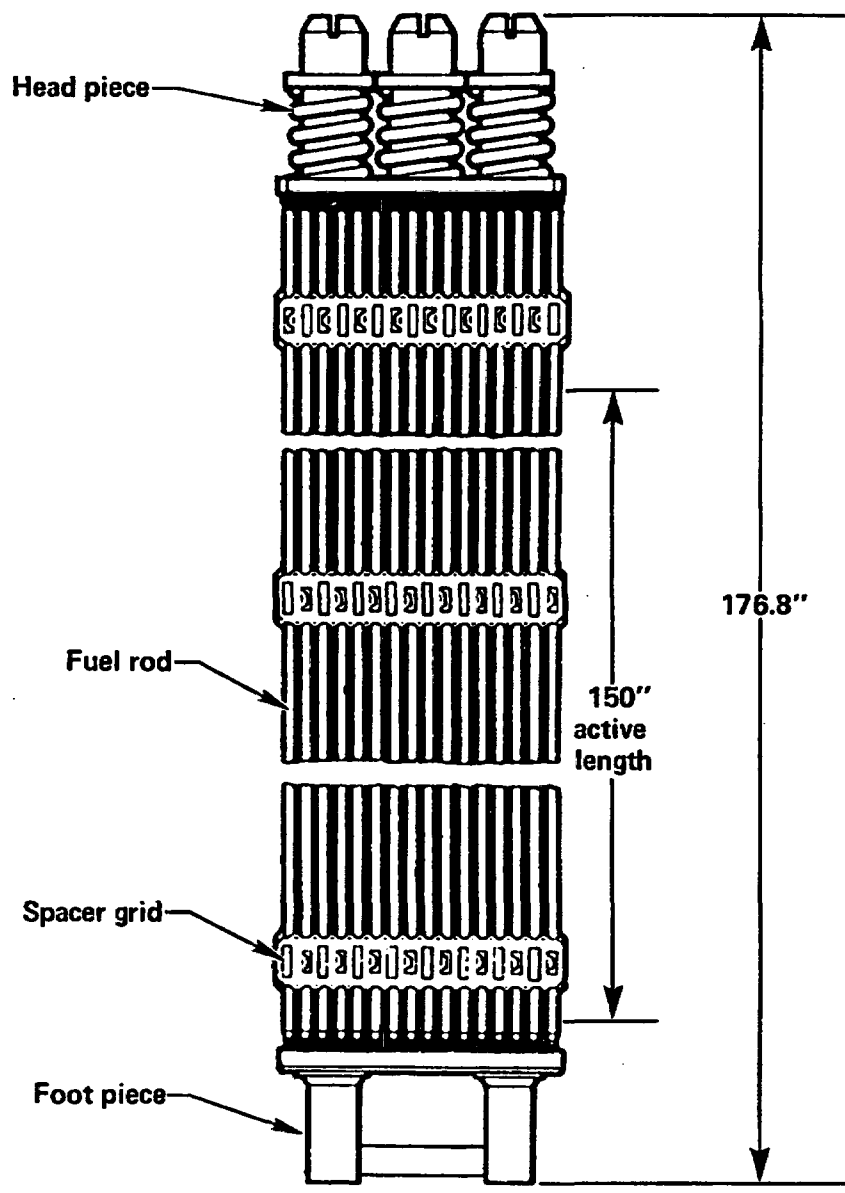


Figure 8-1 PWR fuel bundle.

standpoints. First, the curie content provides a starting point for establishing which isotopes should be evaluated for potential release from the containment barriers provided during the spent fuel shipment. These containment barriers include the fuel pellet itself, the fuel rod cladding, and the cask containment shell. Second, the curie content of each isotope indicates the magnitude of the radioactive source for determining the direct radiation level.

The potential for release of radioactive material from a cask depends heavily on the physical form of the radioactive material. Certain radioisotopes, such as  $^{85}\text{Kr}$ , are in gaseous form. Elements such as cesium, ruthenium, iodine, and their compounds may be volatile at temperatures that can be achieved by the fuel during transportation accidents but will condense to solids at ambient temperatures. However, the vast majority of the radioactive material is in solid and relatively immobile form. The material release estimates made in the next section take into account the physical form of specific isotopes.

The radiological significance of any release is dependent not only on the total radioactivity or number of curies released but also on the hazard posed by a particular isotope. Krypton-85, for example, does not present a significant health hazard. On the other hand, particles of plutonium can be extremely hazardous. The potential radiological hazard of a particular radioisotope is implied by the release limits specified in 10 CFR 71. The 10 CFR 71 release limits for the radioisotopes of interest are listed in Table 8.2. The relative hazards of any two radioisotopes are roughly estimated by comparing their release limits. For example, the release limits for  $^{85}\text{Kr}$  and  $^{134}\text{Cs}$  are 10,000 and 10 curies, respectively; therefore,  $^{134}\text{Cs}$  releases, on a radioactivity basis, are approximately 1,000 times as hazardous as  $^{85}\text{Kr}$ . This report differs from other reports<sup>2,7-10</sup> in that it does not include detailed discussion of the radiological consequences or public health impacts created by the release of specific isotopes. Rather, the releases associated with each cask response region are compared to those releases estimated in NUREG-0170.<sup>2</sup> Each cask response region, therefore, requires a separate estimate of the release of gaseous, volatile, and solid radioactivity

Table 8.2  
10 CFR 71 Release Limits for Radioisotopes

Radioisotope	Release Limit (Ci)
$^{60}\text{Co}$	7
$^{85}\text{Kr}$	10,000
$^{90}\text{Sr}$	0.4
$^{90}\text{Y}$	10
$^{106}\text{Ru}$	7
$^{129}\text{I}$	2
$^{134}\text{Cs}$	10
$^{137}\text{Cs}$	10
$^{137\text{m}}\text{Ba}$	40
$^{144}\text{Ce}$	7
$^{238}\text{Pu}$	0.003
$^{237}\text{Pu}$	0.002
$^{240}\text{Pu}$	0.002
$^{241}\text{Pu}$	0.1
$^{244}\text{Cm}$	0.01

from the shipping cask to the environment. Section 9.0 uses the results of NUREG-0170 to relate the release magnitudes to potential public health impacts which can be associated with these releases.<sup>2</sup>

The radiological significance of the direct radiation emanating from a cask as a result of shield degradation is typically controlled by those isotopes emitting high energy gamma rays. The potential for direct radiation exposure is presented for each cask response region in terms of an equivalent unshielded spent fuel radioactivity. This radioactivity represents the amount of material which, if no shielding were present, will lead to external radiation levels equal to those resulting from the calculated degradation in shielding associated with a specific cask response region.

#### 8.4 Estimates of Radiological Hazards

##### 8.4.1 Potential Radioactive Material Releases to the Environment

The potential for release of radioactive material to the environment from a spent fuel shipment requires consideration of three mechanisms for establishing a release path. These mechanisms are shown schematically in Fig. 8-2.

Under normal conditions, certain radioactive material contained in the ceramic fuel matrix migrates to the fuel rod gap. The migration involves radioactive gas and vapors formed during the fission process in the reactor. Since the claddings of most of the fuel rods are intact before the fuel is shipped, this cladding must be breached during transport before radioactive material is released into the cask cavity. A fuel rod's cladding can be breached by high impact forces or high thermal loads. The number of rods breached by mechanical forces is estimated by considering the rod responses over the range of impact forces that the cask might experience in a transportation accident. End-on impact is conservatively assumed since the almost 15-foot-long (0.4 inch diameter) rods are most susceptible to breaching by buckling. Figure 8-3 shows the percentage of fuel rods breached due to end-on impacts as a function of impact force on a cask.

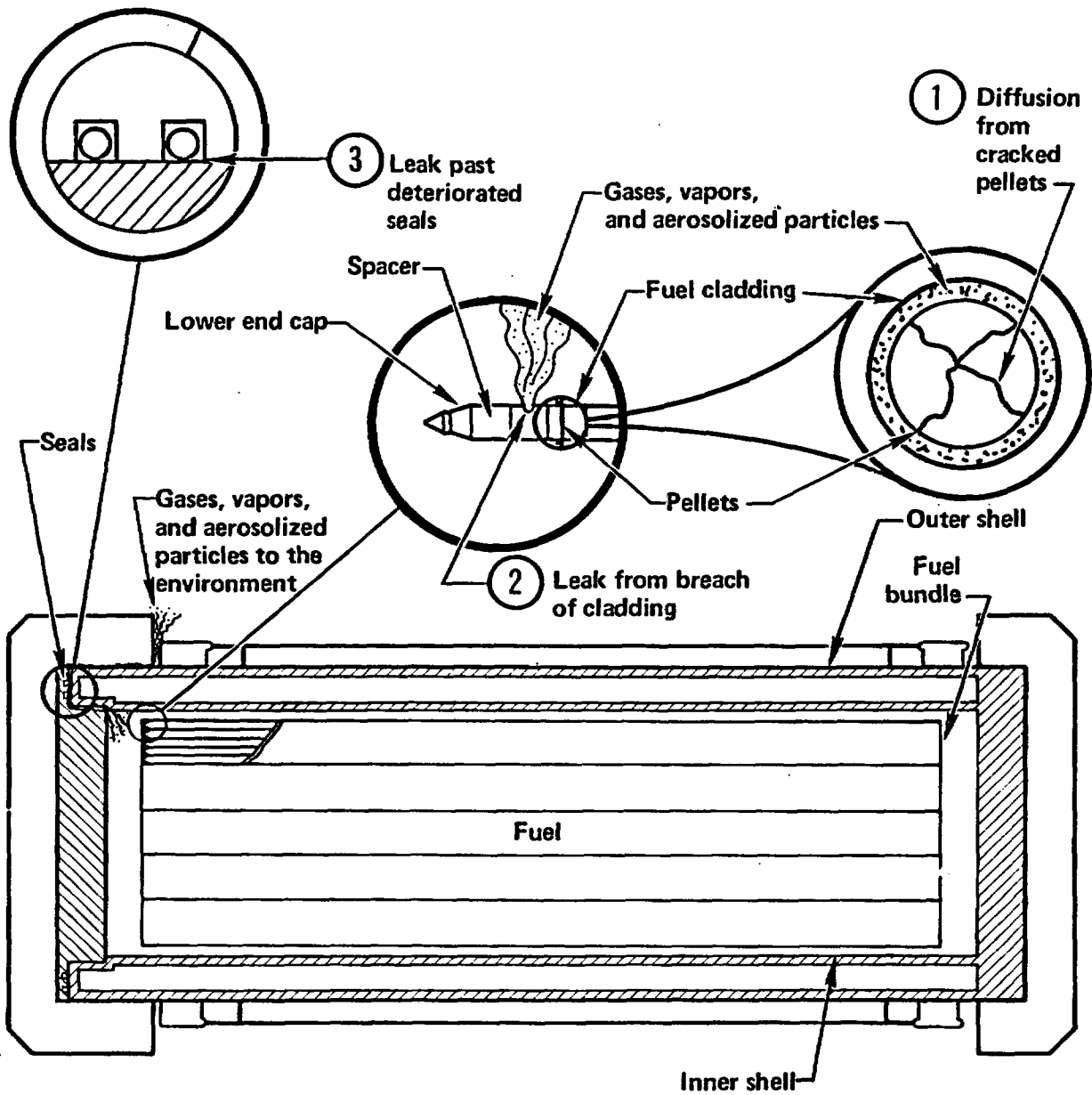


Figure 8-2 Three mechanisms required to establish a radioactive material release path.

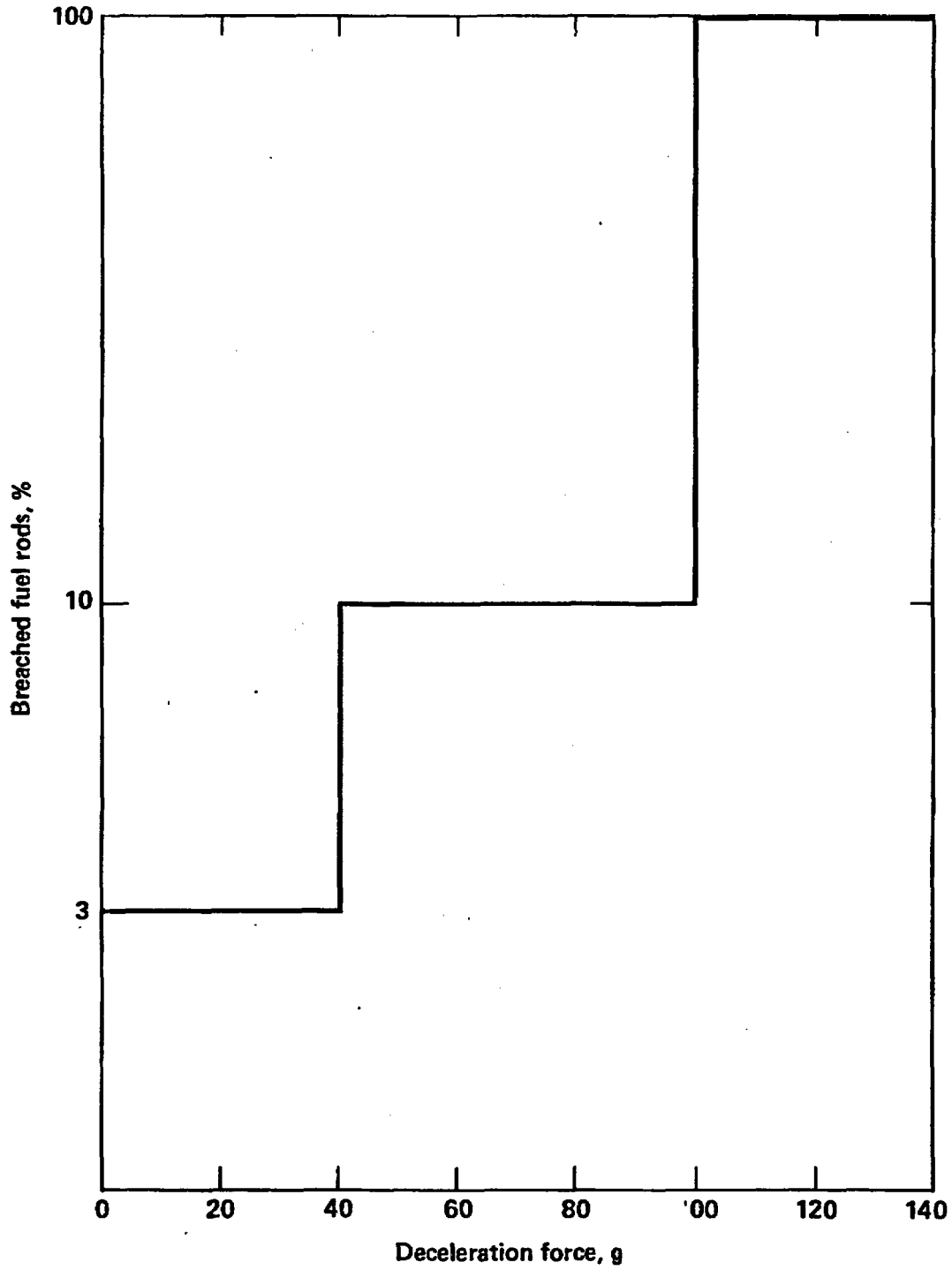


Figure 8-3 Percentage of fuel rods breached as a function of force for endwise impacts.

Cask impact forces are related to forces on the fuel rods necessary to achieve 0.2% ( $S_1$ ), 2% ( $S_2$ ), and 30% ( $S_3$ ) maximum effective strain on the inner containment shell of the cask. Three percent of the rods are assumed to be breached if the cask containment shell experiences maximum effective strains equal to or less than 0.2% ( $S_1$ ). Similarly, 10% of the rods are assumed to be breached for any transportation accident situation in which the containment shell experiences between 0.2% ( $S_1$ ) and 2% ( $S_2$ ) effective strain. Beyond 2% ( $S_2$ ) effective strain, all rods are presumed to be breached. These results are shown in Fig. 8-4.

Fuel rod cladding response to thermal loads is also evaluated. In transportation accidents involving fires, heat may be absorbed by the cask and its spent fuel contents. The resulting temperature increase of the fuel rod cladding can cause an effect called thermal creep. This effect coupled with pressures generated within the rods can cause a breaching of the cladding. If the cask temperature level is 650°F ( $T_3$ ) or less at the mid-thickness of the lead shield, no breaching is expected to occur because the fuel rod temperatures are too low to cause creep rupture. Beyond this thermal response level, temperatures at the center of the cask and at the center of the fuel assemblies are conservatively estimated to reach values which can breach up to 100% of the fuel rods for both the representative truck and rail casks. The results presented in Fig. 8-4 include response to both mechanical and thermal loads.

If a rod is breached, radioactive gases, volatiles, and solids can potentially escape from the fuel rods into the cask containment. Experimental information indicates that this escape involves three release mechanisms. The first mechanism is associated with the actual breaching of the rod and is referred to as the rod burst phenomenon. Pressure generated inside the fuel rods by both non-radioactive and radioactive gases and vapors cause an ejection of material to occur when the rod is breached. A temperature-controlled diffusion process is the second mechanism. Third, a chemical oxidation process involving the uranium fuel takes place if fuel temperatures exceed 400°F and air enters the cask cavity, thus replacing the normally inert containment vessel atmosphere. This process, which involves a change in the

Structural response (maximum strain on inner shell, %)	$S_3$ (30)	100%	100%	100%	100%	100%
	$S_2$ (2)	100%	100%	100%	100%	100%
	$S_1$ (0.2)	10%	10%	10%	100%	100%
		3%	3%	3%	100%	100%
		$T_1$ (500)	$T_2$ (600)	$T_3$ (650)	$T_4$ (1050)	
		Thermal response (lead mid-thickness temperature, °F)				

Figure 8-4 Percentage of fuel rods breached per fuel assembly in each cask response region.

chemical form or phase of the uranium oxide, causes further radioactive material releases.

Material release fractions for the significant radioisotopes are estimated using the results of experiments conducted at the Oak Ridge National Laboratories.<sup>11</sup> Table 8.3 summarizes these release fractions for the truck and rail cask response regions. The rod burst and oxidation mechanisms are the dominant mechanisms which control radioactive material release fractions. Thus, only the releases occurring as a result of these mechanisms are tabulated.

Once the radioactive material has entered the cask containment volume, a release to the environment can occur only through a leak or accident-caused breach of the cask containment boundary. Several processes, which are difficult to quantitatively analyze, will be expected to mitigate radioactive material releases. Particles released from the rods will tend to settle within containment without the presence of some driving force to promote their release. Even if such a force exists, particles can become lodged in leak passageways. Vapors released from the fuel rods will be cooled as they move to the cask walls in most accident events, and the vaporous material will tend to plate-out on all cask interior surfaces. These processes are expected to limit essentially all environmental releases to those materials existing in gaseous forms. In this study, however, because of the difficulty in quantifying these processes, any radioactive material released from the fuel rods is presumed to be released from the spent fuel cask if a leak path exists in the containment vessel. This leak path is presumed to exist for any transportation accident event resulting in (1) a maximum strain in the inner containment shell greater than 0.2% ( $S_1$ ), or (2) lead mid-thickness temperatures exceeding 500°F ( $T_1$ ).

#### 8.4.2 Potential Radiation Increases from Shielding Reduction

Under accident conditions, a reduction can occur in the radiation shielding provided by the shipping cask. Both neutron and gamma radiation shielding can be affected. Typical cask designs can lose the effectiveness of

Table 8.3  
Material Release Fractions from Breached Fuel Rods  
Occurring over 1 Week Following Rod Burst<sup>a/</sup>

Cask Response Regions	Release Mechanism	Release Fraction to Cask Cavity				
		Gas	Vapors			Particles
		Kr	I	Cs	Ru	
R(1,1)-R(3,1)	Rod Burst	$2.0 \times 10^{-1}$	$3.0 \times 10^{-4}$	$2 \times 10^{-4}$	$2.0 \times 10^{-5}$	$2 \times 10^{-6}$
R(1,2)-R(3,2)	Oxidation	$1.3 \times 10^{-1}$	$2.2 \times 10^{-3}$	$1 \times 10^{-6}$	$6.7 \times 10^{-6}$	0
R(1,3)-R(3,3)		$3.3 \times 10^{-1}$	$2.5 \times 10^{-3}$	$2 \times 10^{-4}$	$2.7 \times 10^{-5}$	$2 \times 10^{-6}$
R(1,4)-R(3,4)	Rod Burst	$2.0 \times 10^{-1}$	$3.0 \times 10^{-4}$	$2.0 \times 10^{-4}$	$2.0 \times 10^{-5}$	$2 \times 10^{-6}$
	Oxidation	$1.7 \times 10^{-1}$	$4.0 \times 10^{-3}$	$8.0 \times 10^{-6}$	$2.8 \times 10^{-5}$	0
		$3.9 \times 10^{-1}$	$4.3 \times 10^{-3}$	$2.0 \times 10^{-4}$	$4.8 \times 10^{-5}$	$2 \times 10^{-6}$

<sup>a/</sup> Approximately the same fractional release for truck and rail cask.

neutron shields and still meet existing standards for allowable external radiation levels. In this study, the neutron shielding is presumed lost in all transportation accidents. Of greater concern is the effectiveness of the gamma radiation shield. This type of shielding is provided by dense materials, with lead being the material of choice in the representative cask designs.

High-impact loads can cause the lead shielding to slump towards the impacting side of the cask, e.g., to the bottom of the cask for the impact orientation illustrated in Fig. 8-5. Shielding voids can be created and, in Fig. 8-5, this void is shown near the top of the cask.

The gamma dose versus lead slump is calculated for the rail cask for endwise impacts. The highest radiation increase occurs when the top of the rail cask impacts a surface and the lead slumps towards the cask closure region. In Table 8.4, the gamma dose is tabulated for various amounts of lead slump as a function of distance from the cask surface to the receptor. The dose from a truck cask with similar amounts of lead slump will be approximately 21 times lower than the rail cask, because the truck cask contains only 1 PWR assembly in comparison to 21 assemblies for the rail cask.

High thermal loads can cause the lead shield to melt and expand. The lead expansion can cause the inner wall of the cask to move inward. Upon cooling, the lead shrinks and creates a void along the length of the cask as illustrated in Fig. 8-6, causing the radiation level external to the cask to increase. As it turns out, thermal loads can cause only minor lead voids and increases in the local radiation.

To provide a consistent measure of radiological effects with cask damage, the radiological hazard created by a gamma shielding reduction is presented in terms of an equivalent inventory of unshielded spent fuel. This amount of spent fuel, if unshielded, will produce radiation levels equivalent to those emanating from the damaged cask. As an example of the calculation process, a transportation accident which leads to 2% maximum effective strain ( $S_2$ ) in the cask shell is presumed. The measure of the resulting radiation level is calculated through the following steps: (1) the deceleration force necessary

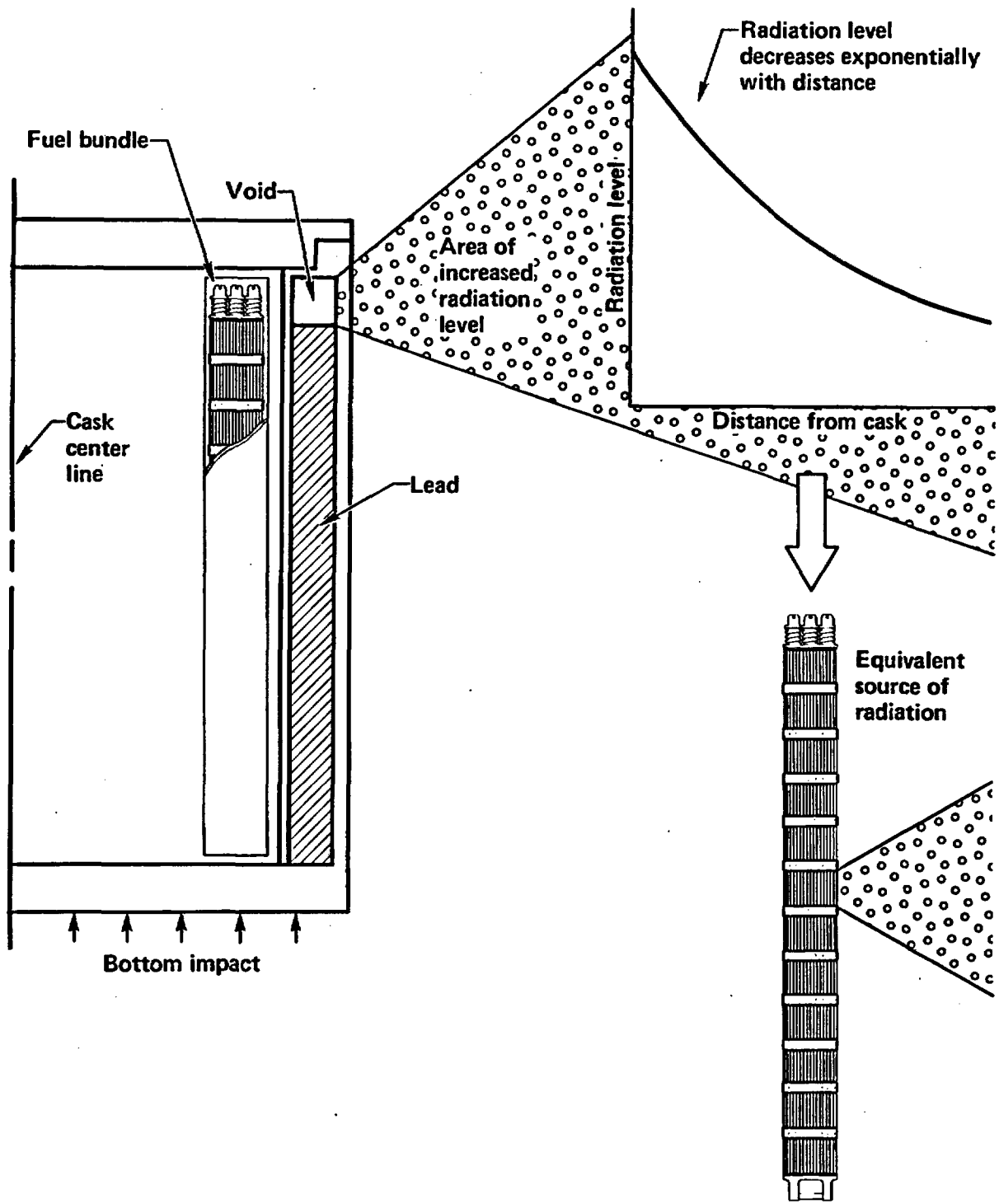


Figure 8-5 Lead voiding due to lead slump resulting from endwise impact of cask

Table 8.4  
Gamma Dose Summary for Lead Slump in a Rail Cask<sup>a/</sup>  
for Impacts on Closure Region

Gap at Cask Bottom Caused by Lead Slump (inches)	Dose Rate (mrem/hr)				
	Distance from Cask Surface to Receptor (ft)				
	3	10	30	300	3000
5.0	$1.02 \times 10^3$	$1.93 \times 10^2$	$2.38 \times 10^1$	$1.65 \times 10^{-1}$	$8.03 \times 10^{-6}$
10.0	$8.64 \times 10^3$	$1.30 \times 10^3$	$1.53 \times 10^2$	$9.13 \times 10^{-1}$	$2.71 \times 10^{-5}$
15.0	$1.65 \times 10^4$	$2.80 \times 10^3$	$2.88 \times 10^2$	$1.70 \times 10^0$	$4.72 \times 10^{-5}$

<sup>a/</sup> Truck cask dose is reduced by approximately the ratio of fuel assemblies or a factor of 21.

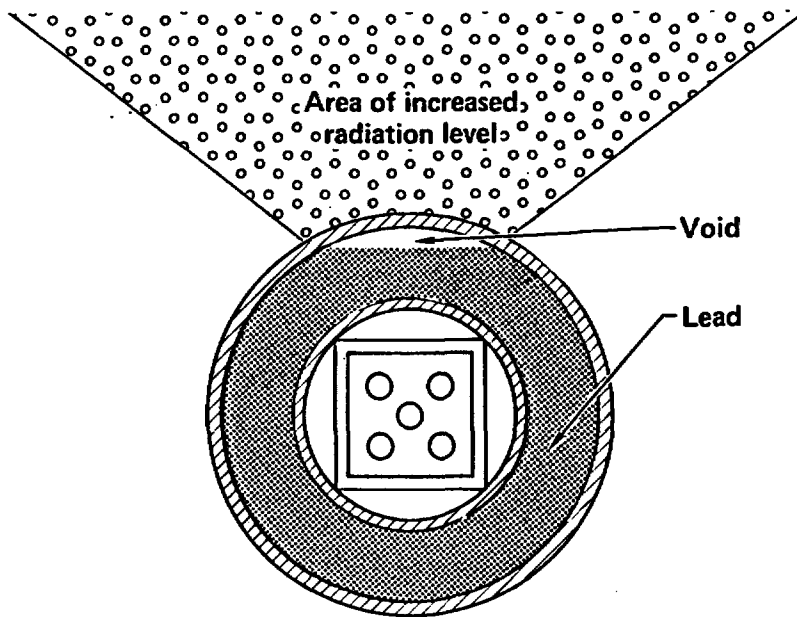
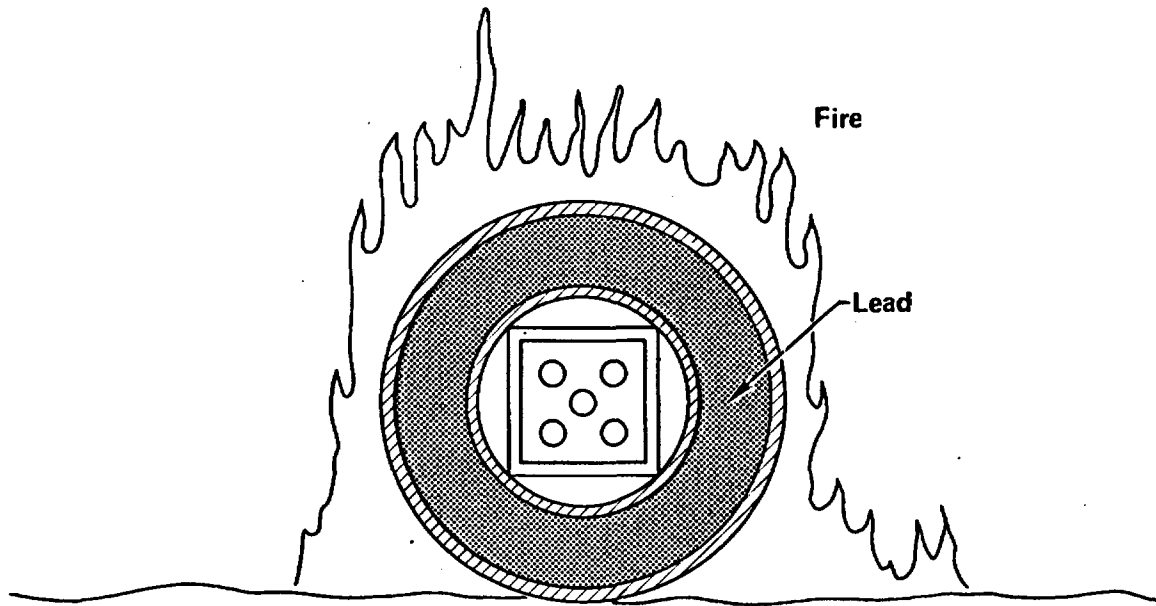


Figure 8-6 Lead voiding due to high thermal loads and lead melting.

to achieve the 2% maximum effective strain ( $S_2$ ) level is determined, (2) the lead slump level caused by this deceleration force is evaluated, (3) the radiation level resulting from the lead slump is calculated, and (4) the amount of unshielded spent fuel contents which will result in equivalent radiation levels is determined.

#### 8.5 Radiological Effect Estimates for Response Regions

The preceding evaluation provides the information necessary to estimate the radiological effects in each response region. The measures involve four parameters that can result in radiological hazards. The first three relate to potential releases of radioactive material from the cask to the environment, expressed in curies, and include: (1) the amount of radioactive gases, (2) the amount of volatiles (isotopes weighted for health hazards), and (3) the amount of solids (isotopes weighted for health hazards). The fourth measure relates to the potential for increased external cask radiation levels occurring as a result of losses or degradations in the cask shielding capabilities. This measure is the equivalent amount of the total spent fuel contents which, without shielding, will produce the calculated level of external cask radiation. These measures are shown in Figs. 8-7 and 8-8 and indicate the four types of radiological hazards estimated for the truck and rail cask response regions.

Radiological hazards beyond the 30% strain ( $S_3$ ) and 1050°F temperature ( $T_4$ ) levels are not calculated. They are assigned values 10 times those for region R(3,4) except for  $^{85}\text{Kr}$  gas. The values assigned for  $^{85}\text{Kr}$  gas are 1.62 times the region R(3,4) values because a high percentage of the gas is already released for states in the R(3,4) region.

Structural response (maximum strain on inner shell, %)	$S_3$ (30)	(G)1.95E+3 (V)1.41E+2 (P)7.22E-2 (E)8.60E+1	1.95E+3 1.41E+2 7.22E-2 8.60E+1	1.95E+3 1.41E+2 7.22E-2 8.60E+1	1.95E+3 1.41E+2 7.22E-2 8.60E+1	1.95E+3 1.41E+2 7.22E-2 8.60E+1
	$S_2$ (2)	(G)1.02E+3 (V)1.41E+1 (P)7.22E-3 (E)8.40E+0	1.02E+3 1.41E+1 7.22E-3 8.40E+0	1.02E+3 1.41E+1 7.22E-3 8.60E+0	1.20E+3 1.42E+1 7.22E-3 8.60E+0	1.95E+3 1.41E+2 7.22E-2 8.60E+1
	$S_1$ (0.2)	(G)1.02E+2 (V)1.41E+0 (P)7.22E-4 (E)3.60E-1	1.02E+2 1.41E+0 7.22E-4 3.60E-1	1.02E+2 1.41E+0 7.22E-4 5.60E-1	1.20E+3 1.42E+1 7.22E-3 5.60E-1	1.95E+3 1.41E+2 7.22E-2 8.60E+1
		(G)~0 (V)~0 (P)~0 (E)~0	3.05E+1 4.23E-1 2.17E-4 ~0	3.05E+1 4.23E-1 2.17E-4 2.00E-1	1.20E+3 1.42E+1 7.22E-3 2.00E-1	1.95E+3 1.41E+2 7.22E-2 8.60E+1
		$T_1$ (500)	$T_2$ (600)	$T_3$ (650)	$T_4$ (1050)	
		Thermal response (lead mid-thickness temperature, °F)				

(G)=Noble gases, curies  
(V)=Vapors, curies  
(P)=Particles, curies  
(E)=Exposure, curies

E+x=10<sup>x</sup>

Figure 8-7 Radiological hazards estimated for response regions for a representative truck cask.

Structural response (maximum strain on inner shell, %)	S <sub>3</sub> (30)	(G)4.10E+4 (V)2.96E+3 (P)1.51E+0 (E)1.11E+3	4.10E+4 2.96E+3 1.51E+0 1.11E+3	4.10E+4 2.96E+3 1.51E+0 1.11E+3	4.10E+4 2.96E+3 1.51E+0 1.11E+3	4.10E+4 2.96E+3 1.51E+0 1.11E+3
	S <sub>2</sub> (2)	(G)2.14E+4 (V)2.96E+2 (P)1.51E-1 (E)1.10E+2	2.14E+4 2.96E+2 1.51E-1 1.10E+2	2.14E+4 2.96E+2 1.51E-1 1.11E+2	2.52E+4 2.96E+2 1.51E-1 1.11E+2	4.10E+4 2.96E+3 1.51E+0 1.11E+3
	S <sub>1</sub> (0.2)	(G)2.14E+3 (V)2.96E+1 (P)1.51E-2 (E)2.75E+1	2.14E+3 2.96E+1 1.51E-2 2.75E+1	2.14E+3 2.96E+1 1.51E-2 2.85E+1	2.52E+4 2.96E+2 1.51E-1 2.85E+1	4.10E+4 2.96E+3 1.51E+0 1.11E+3
	S <sub>0</sub> (0.2)	(G)~0 (V)~0 (P)~0 (E)~0	6.40E+2 8.88E+0 4.56E-3 ~0	6.40E+2 8.88E+0 4.56E-3 1.00E+0	2.52E+4 2.96E+2 1.51E-1 1.00E+0	4.10E+4 2.96E+3 1.51E+0 1.11E+3
		T <sub>1</sub> (500)	T <sub>2</sub> (600)	T <sub>3</sub> (650)	T <sub>4</sub> (1050)	
		Thermal response (lead mid-thickness temperature, °F)				

(G)=Noble gases, curies  
(V)=Vapors, curies  
(P)=Particles, curies  
(E)=Exposure, curies  
E+x=10<sup>x</sup>

Figure 8-8 Radiological hazards estimated for response regions for a representative rail cask.

## 9.0 RESULTS AND CONCLUSIONS

### 9.1 Introduction

In previous sections, a detailed evaluation is made of how spent fuel casks designed to current regulations would respond in railway and highway accident environments. The loading conditions that could conceivably affect the response of a spent fuel cask are determined from surveys of accident records. The responses of the representative truck and rail casks to a wide variety of accident conditions are calculated and categorized into 20 cask response regions. These response regions define specific levels of damage that could be experienced by the cask during an accident. The boundaries of these regions are defined in terms of structural strain experienced by the cask containment shell and by material temperatures attained within the cask's lead shield. The potential for radioactive material releases or increased levels of external radiation are estimated for each of the 20 response regions for both the representative truck and rail casks.

The first response region is defined by structural and thermal response limits which would be within acceptable bounds implied by current regulations.<sup>1</sup> A major objective of this study is to determine the fraction of accidents causing responses within this region. This process is called the first-stage screening. For accidents which cause responses outside this region, a second-stage screening is conducted. This screening involves calculating cask responses to a wide variety of accident conditions and subsequently classifying the responses into the remaining 19 response regions. The expected fraction of transportation accidents resulting in responses in each region is then determined based on historical accident data using probabilistic analysis.

In Section 9.2 the results of both the first- and second-stage screenings are discussed. These results are compared with estimates made in the "Final Environmental Statement on the Transportation of Radioactive Material by Air or other Modes", NUREG-0170.<sup>2</sup> Several historical accidents are also categorized into response regions in order to provide a perspective on the

meaning of severe accidents as used in this study. Uncertainties in the study are discussed in Section 9.3. Conclusions and recommendations are provided in Section 9.4.

## 9.2 Results

### 9.2.1 First-Stage Screening

In the first-stage screening, accidents are characterized which will result in spent fuel cask responses that fall within the R(1,1) response region. Within the R(1,1) region, the cask structural response is elastic, and the strain on the inner shell of the cask does not exceed 0.2% ( $S_1$ ). The cask thermal response does not exceed 500°F ( $T_1$ ) at the middle of the lead shield thickness. Cask responses within the R(1,1) region are typically less than the response generated on real casks by the accident test conditions specified in 10 CFR 71.<sup>1</sup> Accidents which produce loading conditions that result in cask responses in the R(1,1) region do not result in significant damage to a spent fuel cask; therefore, no radiological significance is associated with these accident events.

Over 99.43% of all highway accidents result in a cask structural response falling within the 0.2% strain ( $S_1$ ) level. Making up the largest algebraic segment are the 94.7% of highway accidents which involve minor mechanical loads resulting from rollovers of the transporting vehicle or impacts with low-resistance objects. The remaining 5.3% of highway accidents have the potential for generating significant loads, e.g., impacts with bridge columns, abutments, or trains. The cask response to these potentially significant accidents is dynamically evaluated. The calculations consider variations in the impact velocity, the cask orientation, and the hardness of the object struck. When all the factors for mechanical loads are considered, an additional 4.7% of all highway accidents cause responses within the 0.2% strain ( $S_1$ ) level.

A similar evaluation is performed for railway accidents. The results indicate that over 99.67% of railway accidents cause structural responses not

exceeding 0.2% strain ( $S_1$ ) on the inner shell of the cask. As with truck accidents, a large percentage (96.1%) of railway accidents are minor and would not cause any significant cask damage.

The thermal loadings from accidents involving fires are analyzed to determine the response of the truck and rail casks. The evaluations consider the effects of fire duration, flame temperature, and cask location relative to the fire. Given a fire accident, 99.97% of the truck and 99.04% of the train accidents will generate heat loads on the casks less than those that can occur for a half-hour regulatory 1475°F engulfing fire. However, as calculated in Section 6.3, a half-hour regulatory 1475°F engulfing fire can only heat the massive truck and rail casks to lead mid-thickness temperatures of 280°F and 320°F, respectively, which are well below the 500°F temperature ( $T_1$ ) level where radiological hazards could be generated. Therefore, the fire must burn longer than one half-hour to reach the 500°F temperature ( $T_1$ ) level and consequently, a higher percentage of accidents is included. For the truck cask, 99.99% or more of the accidents involving fire result in a lead mid-thickness temperature not exceeding 500°F ( $T_1$ ). For the rail cask, 99.72% or more of the accidents involving fire result in temperature responses falling within similar bounds.

The number of all accidents that included either mechanical or thermal loads or both is estimated. These estimates are used to determine the percentage of all highway and railway accidents causing cask responses within the R(1,1) region. For the representative truck and rail casks, 99.43% and 99.40%, respectively, of the highway and railway accidents are estimated to cause cask responses within the R(1,1) region as shown in Figs. 7-10 and 7-11. In those areas when the thermal load is expected not to exceed the regulatory 1475°F engulfing fire, the percentage of accident conditions within the 10 CFR 71 mechanical and thermal loading conditions is 99.41% for the truck cask and 98.70% for the rail cask.

The structural and thermal responses within the R(1,1) response region are evaluated with standard engineering methods of analysis. The structural response limit for this region is selected such that the inner shell of the representative cask will behave elastically and will experience no permanent deformations. The thermal response limit is selected such that no thermal

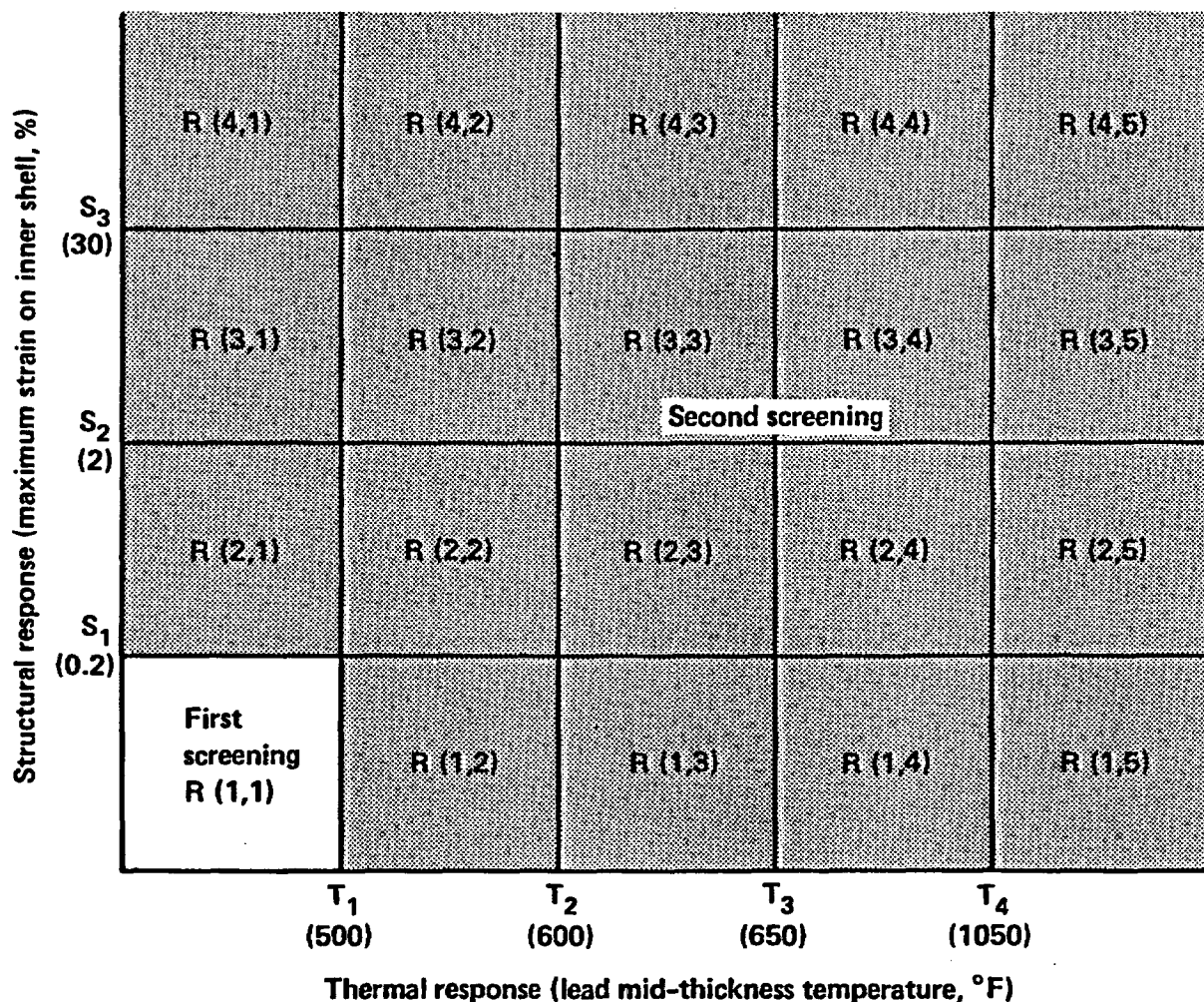
degradation will occur to the seals or other parts of the cask. Responses within these bounds will be within limits typically accepted when casks are subjected to the regulatory accident test conditions. At this level of cask damage, the radiological hazards are negligible and less than the 10 CFR 71 limits for radioactive material releases or for external radiation levels.

### 9.2.2 Second-Stage Screening

In the second-stage screening, accidents causing cask responses greater than the 0.2% strain ( $S_1$ ) and 500°F temperature ( $T_1$ ) levels are evaluated. At these higher levels of cask response, the potential exists for radioactive material releases and external radiation levels equal to or greater than the regulatory limits specified in 10 CFR 71. The highway and railway accident loading conditions not eliminated by the first-stage screening are included. A cask can be struck by a moving train or can fall off a bridge, plunge over an embankment, run into a slope, or strike a massive concrete structure. The thermal events include accidents involving high-temperature, long-duration, engulfing fires that can cause high ( $\geq 500^\circ\text{F}$ ) temperature responses.

The second-stage screening considers response outside the R(1,1) region as shown in Fig. 9-1. The fraction of accidents having cask responses within each of these individual regions is summarized in Figs. 7-10 and 7-11 for the truck and rail casks, respectively.

In most cases, the radiological hazard associated with accidents in the response regions immediately adjacent to R(1,1) is limited and can be negligible. The rationale for this judgment is that 2% strain ( $S_2$ ) will not cause extensive structural damage to the cask containment, and temperatures up to 600°F ( $T_2$ ) will not significantly degrade shield or seal materials currently in use. For accidents causing cask responses within regions R(1,2), R(2,2), and R(2,1), the occurrence of even a limited radiological hazard will be dependent on the actual cask design, the amount of fuel being shipped, and the specifics of the accident--especially with respect to how mechanical and thermal loads are applied to the cask. In this study, the radiological hazards estimated for these three regions are based on the performance of the



- Note:
- o First-stage screening radiological hazards are negligible and less than 10 CFR 71 limits.
  - o Second-stage screening radiological hazards can be equal to or greater than 10 CFR 71 limits.

Figure 9-1 Two-stage screening process in the 20 response regions.

representative truck and rail casks. The estimated radioactive material releases and radiation levels are then compared with the regulatory limits applicable to casks which have been subjected to the accident test conditions.

The result of this comparison indicates that the estimated radioactive material releases and radiation levels are generally lower than the regulatory limits as specified in 10 CFR 71. Compared with the representative truck and rail cask designs, most existing cask designs can withstand higher mechanical and thermal loads without significant damage. Approximately 0.39% of highway and railway accidents that could involve spent fuel casks could result in radiological hazards approaching or slightly exceeding those implied by regulatory limits. The stated percentages of accidents are those which produce cask responses less than the 2% strain ( $S_2$ ) and 600<sup>o</sup>F temperature ( $T_2$ ) levels and represent the sum of the percentages determined by regions R(1,1), R(2,1), R(1,2) and R(2,2).

Cask responses between the 2% ( $S_2$ ) and 30% ( $S_3$ ) strain levels and between the 600<sup>o</sup>F ( $T_2$ ) and 1050<sup>o</sup>F ( $T_4$ ) temperature levels indicate both the possibility of significant, permanent deformation to the cask structure and melting of the lead shield. The radiological hazard associated with this degree of cask damage, will likely exceed the hazard implied by the regulatory limits as specified in 10 CFR 71. Less than 0.001% of the truck shipment accidents and 0.012% of the rail shipment accidents are estimated to cause strains beyond 30% ( $S_3$ ) and temperatures beyond 1050<sup>o</sup>F ( $T_4$ ) in the casks.

### 9.2.3 Comparison with Previous Risk Assessments: NUREG-0170

In the second-stage screening, accidents are identified in which the mechanical and thermal loading conditions on a cask can result in radioactive releases beyond the regulatory limits. To assess the radiological risk of these potential releases, a comparison is made between the probabilities of specific radiological hazards calculated in this study and similar estimates made in NUREG-0170.

The NUREG-0170 assessment indicates that the risk involved in spent fuel shipments is small. This conclusion provided part of the technical

justification necessary for the Nuclear Regulatory Commission (NRC) to make the judgment that the existing 10 CFR 71 regulations are adequate and not in need of immediate change.

The comparison with NUREG-0170 begins by establishing the probability of occurrence for accidents that can result in spent fuel cask responses in each of the 20 regions; that is, the probabilities presented in Figs. 7-10 and 7-11. The probabilities are multiplied by the radiological hazards applicable to each region, which are presented in Figs. 8-7 and 8-8. This product is called a probability-hazard estimate. These probability-hazard estimates are calculated for each of the three types of radioactive material releases assessed in Section 8.0 (gas, vapor, and particle) and the cask external radiation levels.

Figure 9-2 shows the truck cask probability-hazard estimates for each of the 20 response regions. Estimates are given for the releases of radioactive gases ( $^{85}\text{Kr}$ ), radioactive vapors which include  $^{134,137}\text{Cs}$  and  $^{106}\text{Ru}$ , and radioactive solid particles which include  $^{238,239,240,241}\text{Pu}$ . The bottom estimate in each region applies to the external radiation level. This process provides numerical values which can be used for comparison. For instance, the maximum values calculated for these probability-hazard estimates occurs in region R(3,1). This region typically includes accidents involving high-velocity impacts which cause cask containment strain levels between 2% ( $S_2$ ) and 30% ( $S_3$ ) and a lead mid-thickness temperature of less than  $500^\circ\text{F}$  ( $T_1$ ).

Figure 9-3 presents similar probability-hazard estimates for spent fuel shipments made by rail. For rail shipments, region R(1,5) has the maximum estimates with the single exception of radioactive gas release. Region R(1,5) includes accidents involving hot, long-duration fires resulting in lead mid-thickness temperatures beyond  $1050^\circ\text{F}$  ( $T_4$ ). The region which has the highest radioactive gas release is R(1,4). The consequence of radioactive gas release, however, is extremely small in comparison to the significance implied by the other hazards.

The calculational methods and presentation of results in NUREG-0170 differ from those used in this study. In the NUREG-0170 evaluation, accident

Structural response (maximum strain on inner shell, %)	$S_3$ (30)	(G) 2.98E-4 (V) 2.16E-5 (P) 1.11E-8 (E) 1.29E-5	7.65E-11 5.54E-12 2.83E-15 3.31E-12	2.91E-11 2.11E-12 1.08E-15 1.26E-12	1.49E-12 1.08E-13 5.54E-17 6.46E-14	~0 ~0 ~0 ~0
	$S_2$ (2)	(G) 1.83E+0 (V) 2.54E-2 (P) 1.30E-5 (E) 1.51E-2	1.61E-4 2.22E-6 1.14E-9 1.32E-6	2.07E-4 2.87E-6 1.47E-9 1.71E-6	1.10E-4 1.52E-6 7.78E-10 9.07E-7	9.50E-4 6.87E-6 3.52E-9 4.10E-6
	$S_1$ (0.2)	(G) 3.90E-1 (V) 5.36E-3 (P) 2.76E-6 (E) 1.37E-3	2.38E-5 3.29E-7 1.68E-10 8.39E-8	3.06E-5 4.24E-7 2.17E-10 1.14E-7	1.90E-4 2.24E-6 1.15E-9 6.05E-8	1.40E-4 1.02E-5 5.20E-9 6.60E-6
	$S_1$ (0.2)	(G)~0 (V)~0 (P)~0 (E)~0	5.15E-4 7.14E-6 3.66E-9 ~0	7.20E-4 9.99E-6 5.13E-9 4.72E-7	1.83E-2 2.15E-4 1.10E-7 3.05E-7	1.87E-2 1.35E-3 6.90E-7 8.06E-4
		$T_1$ (500)	$T_2$ (600)	$T_3$ (650)	$T_4$ (1050)	
		Thermal response (lead mid-thickness temperature, °F)				

(G) = Noble gases, curies  
(V) = Vapors, curies  
(P) = Particles, curies  
(E) = Exposure, curies

E + x = 10<sup>x</sup>

Figure 9-2 Probability-hazard estimates in curies for the 20 truck cask response regions.

Structural response (maximum strain on inner shell, %)	$S_3$ (30)	(G) 7.32E-5 (V) 5.29E-6 (P) 2.70E-9 (E) 1.96E-6	1.35E-8 9.74E-10 4.97E-13 3.65E-10	8.76E-9 6.32E-10 3.23E-13 2.35E-10	6.82E-9 4.92E-10 2.51E-13 1.84E-10	1.41E-9 1.02E-10 5.22E-14 3.80E-11
	$S_2$ (2)	(G) 1.19E+1 (V) 1.64E-1 (P) 8.37E-5 (E) 6.09E-2	2.19E-3 3.02E-5 1.54E-8 1.12E-5	1.42E-3 1.96E-5 1.00E-8 7.36E-6	1.30E-3 1.53E-5 7.80E-9 5.73E-6	4.41E-4 3.18E-5 1.62E-8 1.18E-5
	$S_1$ (0.2)	(G) 5.82E+0 (V) 8.05E-2 (P) 4.11E-5 (E) 7.48E-2	1.07E-3 1.48E-5 7.57E-9 1.38E-5	6.97E-3 9.63E-6 4.91E-9 9.28E-6	6.38E-3 7.49E-5 3.82E-8 7.21E-6	2.17E-3 1.57E-4 8.00E-8 5.82E-5
		(G)~0 (V)~0 (P)~0 (E)~0	7.86E-1 1.09E-2 5.60E-6 ~0	5.09E-1 7.06E-3 3.62E-6 7.95E-4	1.55E+1 1.81E-2 9.27E-5 6.14E-4	5.12E+0 3.70E-1 1.89E-4 1.37E-1
		$T_1$ (500)	$T_2$ (600)	$T_3$ (650)	$T_4$ (1050)	
		Thermal response (lead mid-thickness temperature, °F)				

- (G) = Noble gases, curies
- (V) = Vapors, curies
- (P) = Particles, curies
- (E) = Exposure, curies (equivalent)

$E + x = 10^x$

Figure 9-3 Probability-hazard estimates in curies for the 20 rail cask response regions.

probability estimates, radioactive release fractions, and radiation levels were classified into eight categories of accident severity. The classification process was accomplished, in large part, through the use of conservative engineering judgments. The first two accident categories in NUREG-0170 were defined to include accidents with severities and radiological hazards less than the 10 CFR 71 hypothetical accident conditions and release limits. These two accident categories generally correspond to accidents causing responses within the R(1,1) region defined in this study. There is no direct correspondence between the other 6 NUREG-0170 categories and the remaining 19 response regions in this study. Therefore, only two direct comparisons can be made with NUREG-0170. The first involves a comparison of the fraction of transportation accidents which generate cask responses that cause no significant radiological hazards. The second point of comparison involves the average radiological risk calculated in this report and the average radiological risk estimate given in NUREG-0170.

In this study, the estimated percentage of accidents within region R(1,1) is 99.4% for both truck and rail shipments. The radiological significance of accidents involving R(1,1) cask responses is negligible. As a result, the estimated percentages of accidents that could create a radiological hazard to the public are 0.6% for both truck and rail shipments.

In contrast, the percentages of accidents estimated in NUREG-0170 to result in negligible radiological hazard is 91% for truck shipments and 80% for rail shipments. By subtraction, the estimated percentage of accidents that could result in radioactive releases is 9% for truck shipment and 20% for rail shipment. In comparing the estimated percentage of accidents that could have a radiological significance, the more detailed estimates in this study indicate that significantly fewer accidents are of radiological concern.

The second comparison between this study and NUREG-0170 essentially involves measures of radiological risk, given that an accident occurs. In this study, such a measure can be obtained by summing the probability-hazard values for all of the 20 response regions. The summation is performed for gas, vapor, and particle releases and for direct radiation level effects.

The components of the summation are shown for each type of release listed in Figs. 9-2 and 9-3. The same calculational method is used in summing the probability-hazard estimates for the eight accident categories in NUREG-0170. Since NUREG-0170 did not evaluate particle releases, a direct comparison is not possible. The comparative measures of radiological risk/accident from both studies are presented in Tables 9.1 and 9.2 for truck and rail shipments of spent fuel, respectively.

The expected gas, vapor, and direct radiation risks/accident in this study for truck shipment are at least 3 times lower than those documented in NUREG-0170. The estimated risk/accident for vapor releases (Cs) is at least 25 times lower in this study than in the NUREG-0170 evaluation. If radioactive particle releases are not considered, it is the vapor release that dominates the public health hazard.

In this study, the representative rail cask is designed to carry 21 fuel assemblies compared with 7 fuel assemblies for the rail cask assumed in NUREG-0170. When the differences in the carrying capacities are adjusted for comparison, the gas, vapor, and direct radiation risks/accident estimated in this study for rail shipment are at least 3 times lower than those documented in NUREG-0170. As with truck shipments, risk/accident from vapor releases (Cs) is at least 25 times lower in this study than that in NUREG-0170.

The release of aerosolized radioactive particles is considered in this study but not in NUREG-0170. The release of small quantities of aerosolized particles is important because the radiological hazard associated with particles containing transuranic isotopes such as  $^{238}\text{Pu}$  can be 3,330 times higher on a curie-for-curie basis than the hazard from  $^{134}\text{Cs}$  or  $^{137}\text{Cs}$ . As Figs. 8-7 and 8-8 indicate, the estimated curie release of particles is about a factor of 1,950 less than the release of cesium vapors.

Further perspective on the significance of the particle releases predicted in this study can be gained by recalling that the cesium releases/accident in this study are at least a factor of 25 less than those that were predicted in NUREG-0170. As a result, the predictions of particle release made in this study produce an overall public health hazard less than one-tenth of the cesium hazard estimated in NUREG-0170.

Table 9.1  
Comparative Measure of Risk/Accident for Spent Fuel  
Shipment by Truck

	<u>Twenty Response Regions</u> (Ci)	<u>NUREG-0170</u> (Ci)
Gas	2.26	10.7
Vapors	$3.24 \times 10^{-2}$	1.26
Particles	$1.65 \times 10^{-5}$	--
Direct radiation	$1.73 \times 10^{-2}$	$6.93 \times 10^{-2}$

Table 9.2  
 Comparison of Release Risk/Accident for Spent Fuel  
 Shipment by Rail

	<u>Twenty Response Regions</u> <u>(21 Fuel Assemblies)</u> (Ci)	<u>NUREG-0170</u> <u>(7 Fuel Assemblies)</u> (Ci)	<u>NUREG-0170</u> <u>(21 Fuel Assemblies)</u> (Ci)
Gas	39.6	61.0	183.
Vapors	0.651	7.17	21.9
Particles	$4.16 \times 10^{-4}$	--	--
Direct radiation	0.276	0.300	0.900

The radiological risk on a per accident basis can be expanded into risk/year estimates by considering highway and railway accident rates and by estimating the number of cask-miles traveled in a year. NUREG-0170 assumed that 3,000 metric tons of spent fuel would be transported annually in future shipments (1,530 truck, 652 rail). Spent fuel, when shipped by truck, was assumed to travel 1,525 miles/trip and, when shipped by rail, to travel 735 miles/trip. Based on current information, these assumptions on spent fuel shipments made in NUREG-0170 are reasonable and are used in this study, except that the rail mileage/trip is presumed to equal that for trucks, that is, 1,525 miles.

The estimated truck accident rate used in this study is  $6.4 \times 10^{-6}$  truck accidents/truck-mile compared to  $1.7 \times 10^{-6}$  truck accidents/truck-mile used in NUREG-0170. The truck accident risk/year associated with releases of radioactive material in gaseous, volatile, or particulate form or external radiation levels are estimated in this study as follows:

$$\text{Annual risk} = 6.4 \times 10^{-6} \frac{\text{truck accident}}{\text{truck-mile}} \times \frac{1525 \text{ truck-miles}}{\text{shipment}} \times 1530 \frac{\text{shipments}}{\text{year}} \times \frac{\text{release or external radiation level}}{\text{truck accident}}$$

Values for the last term (release or external radiation level/truck accident) appear in the first column (Twenty Response Regions) of Table 9.1.

The risk/year is calculated in a similar manner using values from NUREG-0170. Comparing the results of this study with NUREG-0170 values indicates that the estimated risks/year are smaller in this study, with the exception of particle releases which are not considered in NUREG-0170. If the risk/year for vapors and particles are combined after being weighted to account for their relative public health hazard, the total risk calculated in this study will be at least 3 times lower than the risk/year of vapor releases derived from the NUREG-0170 report. The risk/year from rail shipments can be compared in a manner similar to that used for truck transport.

The estimated train accident rate in this study is  $1.19 \times 10^{-5}$  train accidents/train-mile compared with the  $1.05 \times 10^{-5}$  train accidents/train-mile figure used in NUREG-0170. Assuming, as was done in NUREG-0170, that an average train length is 70 cars and an average of 10 cars are involved in each accident, the overall estimated accident rate in this study is  $1.7 \times 10^{-6}$  rail car accidents/rail car mile. Again, as with the truck shipments, the comparison indicates that the risks/year in this study are within those calculated for NUREG-0170, except for the particle release consideration. Combining the risk/year in this study for vapors and particles after appropriate weighting of the public health impacts results in a risk at least 4 times lower than the risk/year from vapor release calculated in NUREG-0170.

#### 9.2.4 Estimated Responses for Sample Severe Accidents

In the previous section, emphasis is placed on compiling and analyzing a broad range of accident loading data. This data is used to estimate the probability of representative cask responses to accident loading conditions. In this section, estimates are made regarding representative cask responses to certain historic severe accidents.

From an extensive literature survey of historical accidents, approximately 400 truck and train accidents are selected as having high loading conditions. The selected accidents are summarized in Appendix A. For each accident, the following information is provided: report source, date of accident, type of accident, number of vehicles involved, velocity prior to the accident, height of any fall involved, object struck, and duration of any fire involved.

The loading conditions associated with four severe accidents are evaluated to identify the response region into which each accident would be categorized.

##### 9.2.4.1 Caldecott Tunnel Fire<sup>3</sup>

A truck fire accident occurred in the Caldecott Tunnel near Oakland, California, on April 7, 1982. The fire was caused by collisions of a gasoline truck-trailer, a bus, and an automobile. The fire resulting from

approximately 8,800 gallons of gasoline had a peak flame temperature of 1900°F. Although it took 2 hours 42 minutes to completely extinguish the fire, the peak flame temperature and the burning of most of the gasoline occurred in less than 40 minutes, after which protected personnel entered the tunnel to search for survivors and to extinguish the fire.

The probable response of the representative truck cask to the mechanical and thermal loading conditions that occurred in the Caldecott Tunnel fire is estimated using the accident information and the cask response information in Section 6.0 and Appendix F.

The primary objects involved in the collisions were an automobile, a truck-trailer, and a bus. Accidents involving these relatively soft objects (i.e., when compared to a truck cask) are minor from a structural response standpoint. These objects cause low levels of force to be imposed on a truck cask regardless of the impact velocity and the cask orientation. Such impact forces cannot cause a strain at the inner cask shell to exceed 0.2% ( $S_1$ ).

If the representative truck cask were exposed to an engulfing 1900°F fire such as the one in the Caldecott Tunnel, the fire duration required to reach 500°F ( $T_1$ ) at the middle of the lead shield thickness is 45 minutes. The hot, engulfing fire lasted less than 40 minutes in the Caldecott Tunnel; therefore, a 500°F temperature ( $T_1$ ) at the middle of the lead shield thickness would not be reached during this accident.

From this evaluation, the response of the representative truck cask to a Caldecott Tunnel fire accident environment is in region R(1,1) near the border with region R(1,2). The containment inner shell of the cask, the closure shell, and the lead shield would provide their safety functions without any significant degradation during and following the accident. No radioactive release or increase in radiation level is expected under these accident conditions.

#### 9.2.4.2 I-80 Bridge Accident<sup>4</sup>

In March, 1981, a truck-tractor-trailer was struck by a pickup truck while on an overpass bridge on Interstate I-80 near San Francisco,

California. The truck-tractor-trailer veered into the bridge railing, broke through the railing and fell 64 feet to the soil surface below.

The probable response of the representative truck cask to the mechanical loading conditions that occurred with the drop onto the soil is estimated, assuming that the truck struck the ground at an orientation angle between  $20^{\circ}$ - $70^{\circ}$  and an impact angle of  $90^{\circ}$  for free fall onto a flat surface.

In this accident, the cask impact velocity would be approximately 44 mph as determined by the fall of 64 feet. An impact velocity of at least 44 mph is required to reach a 0.2% strain ( $S_1$ ) at the inner wall of the cask. Therefore, this accident is also just within the R(1,1) response region.

#### 9.2.4.3 Livingston Train Fire<sup>5</sup>

On September 28, 1982, 43 railroad cars derailed near Livingston, Louisiana. Following the derailment, a fire started to burn various materials which included plastic pellets, vinyl chloride, and petroleum products. The fire which covered a wide area was allowed to burn for several days because of the toxic chemicals and explosions involved. A railroad car carrying motor fuel anti-knock compound (tetra-ethyl lead) exploded about 19 hours after the derailment. A second thermally induced explosion occurred on October 1, 82 hours after the derailment, involving a car carrying vinyl chloride. The fire cooled down sufficiently on the fifth day to permit fire-fighting operations. Six cars carrying vinyl chloride materials were purposely detonated on October 11 to dispose of the remaining unvented materials within them.

The probable response of the representative rail cask to the thermal loading conditions in the Livingston train fire accident is estimated by using the accident information and the cask response information in Subsections 6.3.2, 7.3.2, and Appendix F.

The representative rail cask could have been located anywhere in the derailed train wreckage and fire. The worst place for the cask would have been in the environment of the seven cars burning vinyl chloride, where one of the cars exploded and rocketed over 400 feet to the north of the derailment.

A maximum thermal loading condition on the cask can be calculated, assuming that the cask was in the position of the rocketing car. First, it is conservatively assumed that sufficient heat was absorbed by the vinyl chloride in the car to vaporize all of the compressed gas, thus causing the explosion. This would take no more than  $3.5 \times 10^7$  Btu. It took approximately 82 hours to heat the vinyl chloride and cause the explosion. The cask area exposed to the fire is estimated to be no greater than 1370 ft.<sup>2</sup> The average heat transfer to the car during the entire period is then

$$\dot{Q} = \frac{3.5 \times 10^7}{(1.3 \times 10^3) (8.2 \times 10^1)} = 3.1 \times 10^2 \frac{\text{Btu}}{\text{hr-ft}^2} .$$

This is the average heat flux to which the neutron shield or thermal barrier on the cask would have been exposed. The average heat transfer to the cask lead shield would have been approximately a factor of 3 lower due to the thermal shield. Assuming an average heat transfer rate of 103 Btu/hr-ft<sup>2</sup>, the lead mid-thickness temperature would reach 500°F (T<sub>1</sub>) in 62 hours. At 82 hours, when the railroad car carrying the vinyl chloride exploded, the lead mid-thickness temperature would have reached just over 600°F (T<sub>2</sub>), with some lead melt occurring.

Assuming that the thermal conditions continued until the fifth day when cool down started, the lead mid-thickness temperature would have reached a temperature of 720°F, which is above 650°F (T<sub>3</sub>), but lower than 1050°F (T<sub>4</sub>). This assumption of thermal conditions is very conservative, particularly considering that the other six cars carrying vinyl chloride did not explode.

From this evaluation, the response of the representative rail cask to the environment of the Livingston derailment fire accident is in the R(1,1), R(1,2), R(1,3) or R(1,4) region depending on the location of the cask. Even using the worst assumptions, the lead mid-thickness temperature would not exceed 720°F. Any radioactive releases would be much less than those estimated in Section 8.0 for the R(1,4) region.

#### 9.2.4.4 Derailment into the Alabama River<sup>6</sup>

On January 19, 1979, a train derailed off a bridge into the Alabama River near Hunter, Alabama.<sup>6</sup> One of the rail cars was carrying a pipe which struck the bridge and caused the derailment. Five rail cars fell into the mud of the river 75 feet below.

The probable response of the representative rail cask to the mechanical loading condition caused by impact on the water was estimated by assuming that the cask would strike the water at an orientation angle between 20°-70°.

In the accident, the rail cask impact velocity would be approximately 47 mph as determined by the fall of 75 feet onto the water surface. An impact velocity of at least 90 mph is required to reach a 0.2% strain ( $S_1$ ) at the inner wall for the cask impact; therefore, this accident is placed well within the R(1,1) response region.

### 9.3 Uncertainties

This study evaluates the safety provided through current regulations for the transport of spent fuel. Structural and thermal responses of a representative shipping casks to a range of loading conditions which could occur in potential transportation accidents are evaluated. These evaluations are performed using realistic methods and assumptions. In many cases a range of values is possible for a specific parameter. However, when the realism of the assumption or method can be questioned or when an otherwise complex analysis can be simplified, elements of conservatism are introduced into the evaluations. These conservatisms, typically identified from sensitivity studies, are discussed individually in previous sections of this report. They are discussed collectively in this section, because an understanding of the collective uncertainties is crucial to any judgment made on the overall quality of study results.

Basically, the uncertainties can be classified under three headings: (1) cask response, (2) radiological significance of cask response, and (3) likelihood of accident events, cask response, and resulting radiological hazard.

### 9.3.1 Uncertainty in Cask Response

The calculated responses of a spent fuel cask subjected to mechanical and thermal loading conditions primarily depend on: (1) selection of the representative cask designs, (2) definition of accident loads, and (3) computer code applicabilities and modeling techniques used to estimate the cask response to accident loads.

#### 9.3.1.1 Selection of Representative Cask Designs

The accident resistance of the representative cask determined the percentage of accidents causing specific cask response levels. The representative truck and rail casks are purposely defined to meet existing regulations. That is, the casks, if subjected to the accident test conditions in the regulations will respond in an acceptable manner. The representative truck cask is selected to have a capacity of 1 pressurized water reactor (PWR) fuel assembly while the rail cask capacity is 21 PWR fuel assemblies. Both cask designs use lead as a gamma shield material, and the fuel assemblies in both cases are presumed to have experienced a 5-year decay period prior to shipment.

The representative lead-shielded cask designs are selected by considering currently licensed cask designs and the purported design capabilities of future casks. Future casks are primarily being designed to transport existing spent fuel to the planned geologic waste repositories. These repositories are being designed to accept fuel which has experienced a decay time of 5 years or more. Because of this lengthy decay time, the gamma radiation emanating from the spent fuel is far less than the current casks are designed to accommodate. As a result, shielding for casks can be accomplished by all-steel containment shells, particularly for rail casks. Also, uranium-shielded casks may be used to transport spent fuel to the repositories. Any all-steel or uranium shielded cask design will be intrinsically more resistant to accident forces than either of the study's two representative cask designs. Therefore, the results of this study underpredict the performance of the total population of current and future cask designs.

The single element capacity chosen for the truck cask is typical for casks whose shipment does not require highway overweight permits. If capacity should be increased to two or, at most, three PWR assemblies, the minimum cask resistance to accident forces, assumed in this study, will not change significantly. Since the amount of radioactive material would be increased by, at most, a factor of 3, the radiological hazard associated with a specific accident sequence could conceivably increase by a similar factor. On the other hand, a larger capacity cask would require fewer shipments, by a factor of 3, hence the annual radiological risk would be unchanged.

An increase or decrease in the capacity of the rail cask would have a similar effect in increasing or decreasing the potential radiological hazard for a specific accident, but would not change the annual radiological risk.

#### 9.3.1.2 Definition of Accident Loads

Real accidents can involve many different types of loading conditions such as impact, crush, torch fires, engulfing fires, and burial. In this study, the focus is on the response of representative casks to impact and large fire loadings. Three loading parameters are used to determine the impact loads: impact velocity, object hardness, and cask orientation. Three loading parameters are also used to determine the fire loads: fire duration, flame temperature, and fire location. Based on the reviews and sensitivity studies included in this study, the conclusion is that impact collisions and large fires impose loads which generally exceed those which can be achieved by other loading conditions. When the massiveness of the cask is considered, the loading magnitudes imposed by high-velocity impacts and large engulfing fires conservatively bound all values which can be achieved by other loading conditions.

#### 9.3.1.3 Computer Code Applications and Modeling

The response of the representative casks to mechanical and thermal loads are calculated with computer codes. Where possible the computer models and results are benchmarked against existing test data. An elastic-plastic

material model is selected for performing response calculations for cask impacts on soil, soft rocks, and hard rocks. Although an elastic-plastic model oversimplifies real soil and rock characteristics, the shortcomings in the model are accommodated by benchmarking against penetration test data (see Appendix E).

The cask model is developed using, where possible, standard finite element model techniques, bounding conditions, and material properties. The modeling areas with the most uncertainty are the lead properties and the lead interfaces with the stainless steel shell of the cask. In the absence of reliable test data, the lead properties and boundary conditions are conservatively selected to estimate lead slump and resulting strain on the inner shell of the cask.

Ideally, three-dimensional (3-D) soil and cask models could be developed and benchmarked against test data on representative casks impacting well-characterized soil and rock surfaces. This benchmarking approach could reduce the uncertainties in the modeling and would improve the accuracy of calculating the structural response of the cask. However, the benefits derived from the improvement of modeling accuracy and the reduction of modeling uncertainty cannot be fully realized unless the soil distributions and soil uncertainties are better defined.

The thermal modeling of the cask and the fire are idealized. The modeling depend strongly on the use of structural engineering material properties, bounding conditions, and finite element techniques. A one-dimensional (1-D) fire and cask model is used to predict the cask response. The fire is represented by a homogeneous constant temperature and constant location. In reality, fires are a 3-D phenomenon in which the temperature and location can vary significantly in any given accident. Several conservative assumptions are made to accommodate the simplifications in modeling the fire and cask. For example, the mid-plane of the cask, which would be the hottest portion, is selected for the 1-D model. The temperature response levels representing thermal degradation are selected to exist at the mid-plane of the cask and over-predict the realistic response of the cooler

portions. For non-engulfing fires, heat absorption effects are included in the modeling, but heat loss effects, such as thermal radiation to the environment, are conservatively excluded.

Ideally, 3-D fire and cask models could be developed and benchmarked against test data on representative casks involved in well-characterized fires. This approach could reduce the uncertainties in the modeling and would improve the accuracy in calculating the thermal response of the cask. However, the benefits derived from the improvement of the thermal model cannot be fully realized unless the fire duration and flame temperature at fire locations are better defined.

### 9.3.2 Uncertainty in Estimating an Accident's Potential Radiological Hazard

A damaged spent fuel cask could potentially cause a radiological hazard with a magnitude dependent on (1) release of radioactive material from failed fuel rods, (2) release of radioactive material from the cask, (3) reduction in radiation shielding, and (4) reduction in subcriticality control.

#### 9.3.2.1 Radioactive Releases from Fuel Rods

Endwise impact of the fuel rods is assumed to determine the fraction of rods which fail. This assumption is conservative in estimating the impact failure of fuel rods for all other cask orientations. The release of radioactive material from the fuel rods into the cask is estimated using Oak Ridge National Laboratory (ORNL) test data. The ORNL tests were performed by heating the rods to failure at high temperatures (greater than 1300°F). The radioactive release is through a single leakage path caused by high internal pressure bursting the rod. Under accident conditions, rod failure is more likely during high impacts where multiple fractures to the rods can occur. In contrast to test conditions, the fuel rods will likely be at relatively low pressures and temperatures when impact occurs. Thus, the ORNL test data may or may not overestimate the actual releases under high-impact conditions. The radiological hazards could be better estimated with pertinent tests performed at high-impact conditions for the spent fuel rods.

#### 9.3.2.2 Radioactive Releases from Casks

Radioactive releases from a cask depend on many factors which include failure of the fuel cladding, the temperature and pressure in the cask cavity, and a leakage path that could be through a closure seal. In this study, the assumption is made that all of the radioactive material released from failed fuel rods will be released from the cask. In reality, only a portion of the radioactive material from the failed fuel rods will be released from the cask cavity. Radioactive vaporous materials like cesium and its compounds will deposit on the cooler inner shell of the cask and the cooler flange areas. Radioactive particles will also be deposited on the walls and within the leakage paths. In some cases, the particles may plug the leakage path. Thus the estimates of the radioactive releases are higher than can be expected.

#### 9.3.2.3 Reduction in Radiation Shielding

The external radiation from the representative cask is estimated by using lead slump calculations. These lead slump calculations assume boundary conditions that maximize the lead slump, hence the amount of external radiation. In reality, the lead slump will be less. Also, the use of depleted uranium or steel shielding will not allow shield slump and will exhibit lower external radiation for the same accident loading conditions.

#### 9.3.2.4 Reduction in Subcriticality Control

For large casks containing more than three PWR bundles, the effectiveness of measures used to prevent a criticality event can be reduced under extreme loading conditions. Any reduction in criticality safety depends on both the cask and fuel basket design. However, since the margins used to prevent criticality are very high, and since careful evaluations of the criticality analysis and the design features are performed during cask licensing, the possibility of a criticality event is small even under extreme loading conditions. Using the probabilistic methods in Section 5.0, the probability of a rail cask's having a structural response greater than 2% strain ( $S_2$ ) and

becoming submerged in water is estimated to be 0.00000078%, given an accident. Using the accident and rail shipment rates in this study, this type of accident is estimated to occur approximately once every ten million years.

### 9.3.3 Uncertainty in Probability Models

There is uncertainty associated with the probability distributions used in this study. However, two points should be emphasized. First, although direct experience with events involving the transport of casks would be the best source of information, very little, if any, such information is available. Thus, it is necessary to use data derived from similar types of experiences--results which can be considered to be a sample of what potentially will be experienced in the transport of spent fuel casks. Second, similar types of probabilistic analyses have been done based on sparse data similar to that used in this study. The important point for those other studies, and for this study as well, is the need to recognize that the uncertainty exists and to consider this uncertainty in the use of the results.

The estimated probabilities and probability distributions used in the probabilistic analyses are based on (1) accident statistics, (2) surveys of physical structures/features, (3) past analyses and models, and (4) engineering judgment, when no data is available.

#### 9.3.3.1 Accident Statistics

The estimated accident rate for highway accidents is based on the number of accidents experienced by trucks transporting petroleum products during 1973-1981. The extent to which the past experience of trucks transporting petroleum products can be considered to be a random sample of the future experiences of trucks transporting fuel casks determines the quality of the estimate of the highway accident rate used in the analysis.

Similarly, the distributions of truck and train velocities in an accident are based on statistics compiled from actual accidents. The train velocities are derived from recorders in the locomotives, and are likely to represent a good sample. That velocity is directly attributed to the cask upon impact,

but does not include braking effects. Truck velocities are based on estimates by law enforcement officers in their investigation of accidents. The subset of accidents used in this study is based only on data accumulated in California. These accidents involved injury or fatality events that occur at higher velocities than non-injury accidents. It is assumed that the accident report data from 1973-1981 represent a sample of future incidents involving cask transports. Also, the experiences in North Carolina are used to empirically adjust for braking. Overall, the distributions of train and truck velocities used in this study are conservative.

#### 9.3.3.2 Surveys of Structures and Features

The hardness of earth surfaces adjacent to highways can vary over a wide range. This variability can have a significant effect on the loadings that could be imposed on a cask or any other impacting object. The water and land (hard rock, soft rock, and soil) distribution along proposed spent fuel shipment routes between the east coast and west coast is initially estimated using agricultural soil survey data and geological highway maps for the United States. The initial distribution indicates the types of surfaces which can be impacted along highways in the various regions of the United States. The initial distribution is adjusted to an expected highway distribution by performing highway surveys along representative portions of Federal Interstates 5 and 80 in California. Also, these highway surveys are used to estimate the distributions of bridge heights and column sizes along Federal Interstates.

Improved distribution estimates could be made if the highway surveys were actually performed along proposed spent fuel routes. However, for evaluating the risk for cross-country transportation of spent fuel, the representative distributions are reasonable.

#### 9.3.3.3 Past Analysis and Models

Information on the occurrence of fires is very limited. Thus the thermal evaluations rely on the models developed in a previous analysis of severe

accidents<sup>7</sup>. As mathematical models, the flame temperature and fire duration distributions are only approximations of reality. Little or no information has been compiled which directly models the fire accident environment. The fire parameters, duration, temperature, and location, jointly affect the thermal loading on the cask and hence its response.

#### 9.3.3.4 Engineering Judgment

Finally, engineering judgment is used to model the distributions of some accident parameters--impact angle and fire location. Distribution on these important parameters could not be found in actual data. For instance, a uniform distribution is assumed for impact angle and a linear model for fire location. In general, where judgment is used, conservative assumptions are made.

#### 9.3.4 Overall Statement of Uncertainty

As discussed, there are numerous uncertainties associated with the analysis of the risks from transport of spent nuclear fuel. Related highway and railway accident data is limited, and what is reported is often insufficient or not applicable to developing the appropriate distributions and models necessary to estimate risk. Similarly, mathematical models of the fire environment in an accident and the structural and thermal responses of a cask given the corresponding accident loadings are limited in their ability to approximate the actual physical processes that occur during an accident. Thus, the estimated probabilities and risks have uncertainty associated with them.

However, recognizing the limited data and information on past accidents, the limitations of using mathematical models to model complex physical phenomena, and the limitations on the resources and time to do this analysis, it is felt that a reasonably conservative estimate of risk is provided.

### 9.4 Conclusions

The focus of this report is on the integrity of casks used for U.S. shipments of commercially generated spent fuel, specifically on the level

of safety provided in the event of a transportation accident. Since all shipping casks are designed to meet an existing set of regulatory standards, the report evaluates the level of safety being provided by current regulations.

The response of representative spent fuel casks are assessed under a range of transportation accident conditions. The accident conditions are derived from historical accident data applicable to truck and rail shipments. The responses of the casks are categorized by a two-stage screening process and compared with two benchmarks: 10 CFR 71 regulations, and NUREG-0170.

The first benchmark is chosen to evaluate cask responses to accident loading conditions which fall within the 10 CFR 71 accident test conditions. As discussed in Subsection 9.2.1, approximately 99.4% of the truck accidents and 98.7% of the rail accidents have both mechanical and thermal loading conditions less than those implied by 10 CFR 71 regulations. The 10 CFR 71 benchmark is also chosen to represent a level of radiological hazard currently reflected in existing regulations. This benchmark specifies limits for both radioactive material releases and the magnitude of the radiation level external to a cask. The limits are chosen to provide high assurance that public radiation exposures would be less than permissible annual limits established for workers in occupations involving the use of radioactive materials. When considering real cask capabilities to withstand thermal loading conditions beyond the regulatory ones, approximately 99.4% of the truck and rail accidents would result in negligible radiological hazards which are less than those implied by 10 CFR 71 regulations. As discussed in Subsection 9.2.2, an additional 0.4% of both highway accidents and railway accidents could result in radiological hazards near the regulatory limits.

The second benchmark value is chosen to provide a risk perspective; that is, a benchmark which includes probabilistic consideration of all possible levels of public radiological hazard. The probabilistic consideration was originally presented in NUREG-0170, an environmental impact statement which considered radiological risk from all shipments of radioactive material in the

U.S., including spent fuel. The significance of this particular document is that based, in part, on the overall assessment of risk which it provided, the NRC made a judgment on the adequacy of its transportation regulations. The judgment was made that the regulations were adequate and not in need of immediate change.

The benchmark taken from NUREG-0170 is the risk calculated specifically for spent fuel shipments. The evaluations in Subsection 9.2.3 indicate that the risks from spent fuel shipments derived in this study, are less than those previously estimated in the NUREG-0170 document. The evaluations in NUREG-0170 indicate that the expected radiological consequences from the shipment of 3000 metric tons of spent fuel per year is less than 1 latent cancer fatality every 2300 years.

The results of this study depend primarily on the quality of the cask response models, the radiation release models, and the probability models and distributions used in the analysis. Models for cask responses, radioactive releases, and distributions for the accident parameters are new developments based on current computer codes, limited test data on radioactive releases, and limited historical accident data. The results of this study apply to spent fuel casks which can be licensed by the NRC and are designed, manufactured, operated, and maintained in accordance with national codes and standards (or equivalent) which have adequate margins of safety embedded in them.

If the objective of this study is to precisely define spent fuel transportation risks, many improvements need to be made to these models to calculate the probability and radioactive release estimates and to quantify the uncertainties in the estimates. For example, tests could be performed to benchmark the DYNA/NIKE computer codes for predicting lead slump for a variety of realistic boundary conditions which would provide nominal values with uncertainty bounds. Similarly, more sophisticated modeling of rock surfaces, which includes cracking, could be developed and benchmarked for improving the prediction of cask responses to a variety of rock properties and impact conditions. Finally, the probability distributions for all the accident parameters, e.g., velocity, fire duration, impact angle, could be improved

with further research, data analysis and sensitivity studies. Human factors which affect the cask design, manufacture, operation, and maintenance could also be considered because they affect the cask response and contribute to the overall risk in transporting spent fuel.

None of these improvements are being considered at this point for two reasons: (1) the objective of this study is to estimate the level of safety provided to the shipment of spent fuel using casks licensed to current regulatory standards (a conservatively estimated measure of safety), and (2) the radiological risk in current and future commercial spent fuel shipments is a small component of the total risks applicable for all radioactive material shipments.

The attempt is made in this study to use realistic, yet conservative when appropriate, models and probabilistic distributions. Thus, the estimates derived from the analysis are usable to achieve the study's objective.

## REFERENCES

All references are listed numerically by sections. Appendix references are at the end of each appendix.

### Section 1.0

1. Office of the Federal Register, Title 10, Code of Federal Regulations, Part 71, Office of the Federal Register, Washington, DC, January 1984.
2. U.S. Nuclear Regulatory Commission, Final Environmental Statement on the Transportation of Radioactive Material by Air and Other Modes, U.S. Nuclear Regulatory Commission, Washington, DC, NUREG-0170, December 1977.
3. P. Eggers, Severe Rail and Truck Accidents: Toward a Definition of Bounding Environments for Transportation Packages, U.S. Nuclear Regulatory Commission, Washington, DC, NUREG/CR-3499, 1983.

### Section 2.0

1. Accident Data on California State Highways, State of California Business, Transportation and Housing Agency, Department of Transportation, Division of Traffic Engineering, Sacramento, CA. Report prepared in cooperation with the U.S. Department of Transportation, Federal Highway Administration, 1983.
2. Office of the Federal Register, Title 49, Code of Federal Regulations, Part 177, Office of the Federal Register, Washington, DC, January 1983.
3. 1969 Accidents of Large Motor Carriers of Property, Bureau of Motor Carrier Safety, Federal Highway Administration, U.S. Department of Transportation, Washington, DC, December 1970.

4. 1970 Accidents of Large Motor Carriers of Property, Bureau of Motor Carrier Safety, Federal Highway Administration, U.S. Department of Transportation, Washington, DC, March 1972.
5. 1971-1972 Accidents of Large Motor Carriers of Property, Bureau of Motor Carrier Safety, Federal Highway Administration, U.S. Department of Transportation, Washington, DC, May 1974
6. Summary of Motor Vehicle Accidents in the Petroleum Industry for 1977, American Petroleum Institute, Washington, DC, May 1978.
7. Summary of Motor Vehicle Accidents in the Petroleum Industry for 1978, American Petroleum Institute, Washington, DC, August 1979.
8. Summary of Motor Vehicle Accidents in the Petroleum Industry for 1979, American Petroleum Institute, Washington, DC, June 1980.
9. Summary of Motor Vehicle Accidents in the Petroleum Industry for 1980, American Petroleum Institute, Washington, DC, September 1981.
10. Summary of Motor Vehicle Accidents in the Petroleum Industry for 1981, American Petroleum Institute, Washington, DC, August 1982.
11. Accident/Incident Bulletin No. 145, Calendar Year 1976, Office of Safety, Federal Railroad Administration, U.S. Department of Transportation, Washington, DC, December 1977.
12. Accident/Incident Bulletin No. 146, Calendar Year 1977, Office of Safety, Federal Railroad Administration, U.S. Department of Transportation, Washington, DC, August 1978.
13. Accident/Incident Bulletin No. 147, Calendar Year 1978, Office of Safety, Federal Railroad Administration, U.S. Department of Transportation, Washington, DC, October 1979.

14. Accident/Incident Bulletin No. 148, Calendar Year 1979, Office of Safety, Federal Railroad Administration, U.S. Department of Transportation, Washington, DC, July 1980.
15. Accident/Incident Bulletin No. 149, Calendar Year 1980, Office of Safety, Federal Railroad Administration, U.S. Department of Transportation, Washington, DC, June 1981.
16. Accident/Incident Bulletin No. 150, Calendar Year 1981, Office of Safety, Federal Railroad Administration, U.S. Department of Transportation, Washington, DC, June 1982.
17. Accident/Incident Bulletin No. 151, Calendar Year 1982, Office of Safety, Federal Railroad Administration, U.S. Department of Transportation, Washington, DC, June 1983.
18. 1973 Accidents of Motor Carriers of Property, Bureau of Motor Carrier Safety, Federal Highway Administration, U.S. Department of Transportation, Washington, DC, July 1975.
19. 1974 Accidents of Motor Carriers of Property, Bureau of Motor Carrier Safety, Federal Highway Administration, U.S. Department of Transportation, Washington, DC, 1975.
20. 1975 Accidents of Motor Carriers of Property, Bureau of Motor Carrier Safety, Federal Highway Administration, U.S. Department of Transportation, Washington, DC, 1976.
21. 1976 Accidents of Motor Carriers of Property, Bureau of Motor Carrier Safety, Federal Highway Administration, U.S. Department of Transportation, Washington, DC, October 1977.

22. 1977 Accidents of Motor Carriers of Property, Bureau of Motor Carrier Safety, Federal Highway Administration, U.S. Department of Transportation, Washington, DC, May 1980.
23. 1978 Accidents of Motor Carriers of Property, Bureau of Motor Carrier Safety, Federal Highway Administration, U.S. Department of Transportation, Washington, DC, May 1980.
24. 1979 Accidents of Motor Carriers of Property, Bureau of Motor Carrier Safety, Federal Highway Administration, U.S. Department of Transportation, Washington, DC, 1980.
25. 1980-1981 Accidents of Motor Carriers of Property, Bureau of Motor Carrier Safety, Federal Highway Administration, U.S. Department of Transportation, Washington, DC, August 1982.
26. 1982 Accidents of Motor Carriers of Property, Bureau of Motor Carrier Safety, Federal Highway Administration, U.S. Department of Transportation, Washington, DC, May 1983.
27. 1983 Accidents of Motor Carriers of Property, Bureau of Motor Carrier Safety, Federal Highway Administration, U.S. Department of Transportation, Washington, DC, October 1984.
28. TASAS Selective Record Retrieval Statewide Accident Summary for Year 1975, State of California Department of Transportation, Sacramento, CA, October 1979.
29. TASAS Selective Record Retrieval Statewide Accident Summary for Year 1976, State of California Department of Transportation, Sacramento, CA, October 1979.

30. TASAS Selective Record Retrieval Total Statewide Accidents for Year 1977, State of California Department of Transportation, Sacramento, CA, May 1978.
31. TASAS Selective Record Retrieval Statewide Accident Summary for Year 1978, State of California Department of Transportation, Sacramento, CA, April 1979.
32. TASAS Selective Record Retrieval, Summary Only, All Accidents for the Year 1978, State of California Department of Transportation, Sacramento, CA, August 1984.
33. TASAS Selective Record Retrieval, Summary Only, All Accidents for the Year 1979, State of California Department of Transportation, Sacramento, CA, August 1984
34. TASAS Selective Record Retrieval Statewide Accidents for Year 1981, State of California Department of Transportation, Sacramento, CA, April 1982.
35. TASAS Selective Record Retrieval Statewide Summary 1982, State of California Department of Transportation, Sacramento, CA, May 1983.
36. TASAS Selective Record Retrieval Statewide Summary 1983, State of California Department of Transportation, Sacramento, CA, April 1984.
37. Assessment of the Stiffness Characteristics of Bridge Substructure Components Encountered along a Section of Interstate 5, Engineering Computer Corporation, Sacramento, CA, February 1985. A contractor report to the Lawrence Livermore National Laboratory.
38. R. Imbsen, et al., Soil and Terrain Surveys, Engineering Computer Corporation, Sacramento, CA, January 1985. A contractor report to the Lawrence Livermore National Laboratory.

39. Soil Survey, United States Department of Agriculture, Bureau of Chemistry and Soils, Superintendent of Documents, Washington, DC.
40. Geological Highway Map, American Association of Petroleum Geologist, Tulsa, OK.
41. 1957 Annual Statistical Report, Department of California Highway Patrol, Sacramento, CA, May 1958.
42. 1958 Annual Statistical Report, Department of California Highway Patrol, Sacramento, CA, May 1959.
43. 1959 Annual Statistical Report, Department of California Highway Patrol, Sacramento, CA, May 1960.
44. 1960 Annual Statistical Report, Department of California Highway Patrol, Sacramento, CA, May 1961.
45. 1961 Annual Statistical Report, Department of California Highway Patrol, Sacramento, CA, May 1962.
46. 1962 Traffic Accident Statistics, Department of California Highway Patrol, Sacramento, CA, May 1963.
47. 1963 Traffic Accident Statistics, Department of California Highway Patrol, Sacramento, CA, May 1964.
48. 1964 Traffic Accident Statistics, Department of California Highway Patrol, Sacramento, CA, May 1965.
49. 1965 Traffic Accident Statistics, Department of California Highway Patrol, Sacramento, CA, April 1966.

50. 1966 Report of Fatal and Injury Motor Vehicle Traffic Accidents, Department of California Highway Patrol, Sacramento, CA, July 1967.
51. 1967 Report of Fatal and Injury Motor Vehicle Traffic Accidents, Department of California Highway Patrol, Sacramento, CA, July 1968.
52. E. G. Hamilton, Single, Variable Tabulations for 1979-1981 North Carolina Accidents, University of North Carolina Highway Safety Research Center, Chapel Hill, NC, September 1977.
53. R. K. Clarke, et al., Severities of Transportation Accidents, Sandia National Laboratories, Albuquerque, NM, SLA-74-0001, July 1976.
54. 1979 Virginia Traffic Crash Facts, Virginia Department of State Police, Richmond, VA, April 1980.
55. 1982 Virginia Traffic Crash Facts, Virginia Department of State Police, Richmond, VA, April 1983.
56. 1983 Virginia Traffic Crash Facts, Virginia Department of State Police, Richmond, VA, April 1984.
57. Rail-Highway Grade-Crossing Accidents/Incidents Bulletin for the Year Ended December 31, 1975, Office of Safety, Federal Railroad Administration, U.S. Department of Transportation, Washington, DC.
58. Rail-Highway Grade-Crossing Accidents/Incidents Bulletin for the Year Ended December 31, 1976, Office of Safety, Federal Railroad Administration, U.S. Department of Transportation, Washington, DC, December 1977.
59. Rail-Highway Grade Crossing Accident/Incident Bulletin No. 43, Calendar Year 1977, Office of Safety, Federal Railroad Administration, U.S. Department of Transportation, Washington, DC, July 1978.

60. Rail-Highway Crossing Accident/Incident and Inventory Bulletin No. 1, Calendar Year 1978, Office of Safety, Federal Railroad Administration, U.S. Department of Transportation, Washington, DC, October 1979.
61. Rail-Highway Crossing Accident/Incident and Inventory Bulletin No. 2, Calendar Year 1979, Office of Safety, Federal Railroad Administration, U.S. Department of Transportation, Washington, DC, September 1980.
62. Rail-Highway Crossing Accident/Incident and Inventory Bulletin No. 3, Calendar Year 1980, Office of Safety, Federal Railroad Administration, U.S. Department of Transportation, Washington, DC, June 1981.
63. Rail-Highway Crossing Accident/Incident and Inventory Bulletin No. 4, Calendar Year 1981, Office of Safety, Federal Railroad Administration, U.S. Department of Transportation, Washington, DC, June 1982.
64. Rail-Highway Crossing Accident/Incident and Inventory Bulletin No. 5, Calendar Year 1982, Office of Safety, Federal Railroad Administration, U.S. Department of Transportation, Washington, DC, June 1983.
65. 1969 Accidents of Large Motor Carriers of Property, Bureau of Motor Carrier Safety, Federal Highway Administration, U.S. Department of Transportation, Washington, DC, December 1970.
66. R. K. Clarke, et al., Severities of Transportation Accidents, Sandia National Laboratories, Albuquerque, NM, SLA-74-0001, July 1976.
67. P. Eggers, Severe Rail and Truck Accidents: Toward a Definition of Bounding Environments for Transportation Packages, U.S. Nuclear Regulatory Commission, Washington, DC, NUREG/CR-3499, 1983.

### Section 3.0

1. Safety Analysis Report for NLI 1/1 Truck Cask, Docket No. 71-9010, National Lead Industries, Inc., Wilmington, DE, November 1972.
2. Safety Analysis Report for TN-8/TN9 Shipping Casks, Docket No. 71-9015/16, Transnuclear, Inc., White Plains, NY, October 1976.
3. Design and Analysis Report IF-300 Shipping Cask, Docket No. 70-1220, General Electric Company, San Jose, CA, January 1971.
4. Safety Analysis Report for the NLI-10-24 Shipping Cask, Docket No. 70-9023, National Lead Industries, Inc., Wilmington, DE, February 1976.
5. Office of the Federal Register, Title 10, Code of Federal Regulations, Part 71, Office of the Federal Register, Washington, DC, January 1984.
6. U.S. Nuclear Regulatory Commission, Regulatory Guide 7.6: Design Criteria for the Structural Analysis of Shipping Cask Containment Vessels, U.S. Nuclear Regulatory Commission, Washington, DC, March 1978.
7. U.S. Nuclear Regulatory Commission, Regulatory Guide 7.4: Leakage Tests on Packages for Shipment of Radioactive Materials, U.S. Nuclear Regulatory Commission, Washington DC, June 1975.
8. U.S. Nuclear Regulatory Commission Regulatory Guide 7.8: Load Combinations for the Structural Analysis of Shipping Casks, U.S. Nuclear Regulatory Commission, Washington, DC, May 1977.
9. U.S. Nuclear Regulatory Commission, Regulatory Guide 7.9: Standard Format and Content of Part 71 Applications for Approval of Packaging of Type B, Large Quantity, and Fissile Radioactive Material, U.S. Nuclear Regulatory Commission, Office of Standards Development, Washington, DC, January 1980, Rev-1.

10. U.S. Nuclear Regulatory Commission, Regulatory Guide 7.10: Establishing Quality Assurance Programs for Packaging Used in the Transport of Radioactive Material, U.S. Nuclear Regulatory Commission, Washington, DC, January 1983.
11. American Society of Mechanical Engineers, ASME Boiler and Pressure Vessel Code, the American Society of Mechanical Engineers, United Engineering Center, 345 East 47th Street, New York, NY 10017, July 1983.
12. U.S. Nuclear Regulatory Commission, (Draft) Regulatory Guide, Fracture Toughness Criteria for Ferritic Steel Shipping Cask Containment Vessels with a Maximum Wall Thickness of Four Inches (0.1m), U.S. Nuclear Regulatory Commission, Office of Nuclear Regulatory Research, Washington, DC, June 1986.
13. W. R. Holman, and R. T. Langland, Recommendations for Protecting Against Failure by Brittle Fracture in Ferritic Steel Shipping Containers Up to Four Inches Thick, Lawrence Livermore National Laboratory, Livermore, CA, UCRL-53013, NUREG/CR-1815, June 1981.
14. M. W. Schwartz, Recommendations for Protecting Against Brittle Fractures in Ferritic Steel Shipping Containers Greater Than Four Inches Thick, Lawrence Livermore National Laboratory, Livermore, CA, UCRL-53538, NUREG/CR-3826, April 1984.
15. L. E. Fischer, and W. Lai, Fabrication for Shipping Containers, Lawrence Livermore National Laboratory, Livermore, CA, UCRL-53544, NUREG/CR-3854, March 1985.
16. R. E. Monroe, H. H. Woo, and R. G. Sears, Recommended Welding Criteria for use in the Fabrication of Shipping Containers for Radioactive Materials, Lawrence Livermore National Laboratory, Livermore, CA, UCRL-53044, NUREG/CR-3019, March 1984.

#### Section 4.0

1. American Society of Mechanical Engineers, ASME Boiler and Pressure Vessel Code, Section III, Division 1, The American Society of Mechanical Engineers, United Engineering Center, 345 East 47th Street, New York, NY 10017, July 1983.
2. Manual of Steel Construction, 7th ed., American Institute of Steel Construction, Inc., 101 Park Avenue, New York, NY 10017, 1970.
3. M. G. Fontana and N. D. Greene, Corrosion Engineering, 2nd ed., McGraw-Hill Book Company, New York, NY, 1978.
4. A. J. Romano, et al., The Investigation of Container Materials for Bi and Pb Alloys, Part 1., Thermal Convection Loops, Brookhaven National Laboratory, Upton, NY, BNL 811(T313), July 1963.
5. G. M Tolson and A. Taboada, A Study of Lead and Lead-Salt Corrosion in Thermal Convection Loops, Oak Ridge National Laboratory, Oak Ridge, TN, 1966.

#### Section 5.0

1. E. G. Hamilton, Single, Variable Tabulations for 1979-1981 North Carolina Accidents, University of North Carolina Highway Safety Research Center, Chapel Hill, NC, September 1977.
2. R. K. Clarke, et al., Severities of Transportation Accidents, Sandia National Laboratories, Albuquerque, NM, SLA-74-0001, July 1976.

#### Section 6.0

1. Office of the Federal Register, Title 10, Code of Federal Regulation, Part 71, Office of the Federal Register, Washington, DC, January 1984.

2. J. O. Hallquist, NIKE-2D: An Implicit, Finite-Deformation, Finite Element Code for Analyzing the Static and Dynamic Response of Two-Dimensional Solids, Lawrence Livermore National Laboratory, Livermore, CA, UCRL-52678, 1979, and Revision 1, NIKE-2D: An Implicit, Finite-Deformation, Finite Element Code for Analyzing the Static and Dynamic Response of Two-Dimensional Solids, Lawrence Livermore National Laboratory, Livermore, CA, UCID-18822, 1981.
3. T. A. Nelson, et al., SCANS - Shipping Cask Analysis System, Vol. 1, Impact Analysis Code User's Manual, Lawrence Livermore National Laboratory, Livermore, CA, UCID-20674/Vol. 1, Draft Report to be published, U.S. Nuclear Regulatory Commission, Washington, DC, NUREG/CR-4554, 1986.
4. J. O. Hallquist, User's Manual for Dyna-2D--An Explicit Two-Dimensional Hydrodynamic Finite Element Code with Interactive Rezoning, Lawrence Livermore National Laboratory, Livermore, CA, UCID-18756, Rev. 2, 1984.
5. C. W. Young, "Depth Prediction for Earth-Penetrating Projectiles", Journal of the Soil Mechanics and Foundations Division, Proceedings of the American Society of Civil Engineers, Vol. 95, No. SM3, Proceedings Paper 6558, American Society of Civil Engineers, New York, NY, May 1969.
6. Institute of Mechanical Engineers, "The Resistance to Impact of Spent Magnox Fuel Transport Flasks", Power Industries Division of the Institute of Mechanical Engineers and the British Nuclear Energy Society, Seminar Paper, Mechanical Engineering Publications Ltd., London, England, April 30 and May 1, 1985.
7. International Atomic Energy Agency, Regulations for the Safe Transport of Radioactive Materials, Safety Series No. 6, International Atomic Energy Agency, Vienna, Austria, 1985.

8. P. J. Burns, TACO-2D-A Finite Element Heat Transfer Code, Lawrence Livermore National Laboratory, Livermore, CA, UCID-17980, Rev. 2, January 1982.

### Section 7.0

1. Office of the Federal Register, Title 10, Code of Federal Regulations, Part 71, Office of the Federal Register, Washington, DC, January 1984.
2. J. O. Hallquist, User's Manual for Dyna-2D--An Explicit Two-Dimensional Hydrodynamic Finite Element Code with Interactive Rezoning, Lawrence Livermore National Laboratory, Livermore, CA, UCID-18756, Rev. 2, 1984.
3. J. O. Hallquist, NIKE-2D: An Implicit, Finite-Deformation, Finite Element Code for Analyzing the Static and Dynamic Response of Two-Dimensional Solids, Lawrence Livermore National Laboratory, Livermore, CA, UCRL-52678, 1979, and Revision 1, NIKE-2D: An Implicit, Finite-Deformation, Finite Element Code for Analyzing the Static and Dynamic Response of Two-Dimensional Solids, Lawrence Livermore National Laboratory, Livermore, CA, UCID-18822, 1981.
4. A. J. Neilson, A Dyna-3D Calculation for Impact on a Pipe Target, Safety and Engineering Science Division, Winfrith, AEEW-M2058, United Kingdom Atomic Energy Authority, Winfrith, England, 1981/82, November 1983.
5. Institute of Mechanical Engineers, "The Resistance to Impact of Spent Magnox Fuel Transport Flasks", Power Industries Division of the Institute of Mechanical Engineers and the British Nuclear Energy Society, Seminar Paper, Mechanical Engineering Publications Ltd., London, England, April 30 and May 1, 1985.
6. M. Huerta and H. R. Yoshimura, A Study and Full-Scale Test of a High-Velocity Grade-Crossing Simulated Accident of a Locomotive and a

Nuclear-Spent-Fuel Shipping Cask, Sandia National Laboratories, Albuquerque, NM, SAND79-2291, TTC308, February 1983.

7. M. Huerta, Analysis, Scale Modeling, and Full-Scale Tests of a Truck Spent-Nuclear -Fuel Shipping System in High Velocity Impacts Against a Rigid Barrier, Sandia National Laboratories, Albuquerque, NM, SAND77-0270, 1978.
8. P. J. Burns, TACO-2D-A Finite Element Heat Transfer Code, Lawrence Livermore National Laboratory, Livermore, CA, UCID-17980, Rev. 2, January 1982.
9. H. J. Rack and H. R. Yoshimura, Postmortem Metallurgical Examination of a Fire-Exposed Spent Fuel Shipping Cask, Sandia National Laboratories, Albuquerque, NM, SAND-79-1424, UC-71, TTC-0018, April 1980.
10. R. B. Pope, et al., "An Assessment of Accident Thermal Testing and Analysis Procedures for Radioactive Materials Shipping Package," Paper Contributed by the American Society of Mechanical Engineers Heat Transfer Division to the Joint ASME/AICHE National Transfer Conference at Orlando, FL, April 8, 1980, American Society of Mechanical Engineers, New York, NY, April 1981.
11. U.S. Nuclear Regulatory Commission, Final Environmental Statement on the Transportation of Radioactive Material by Air and Other Modes, U.S. Nuclear Regulatory Commission, Washington, DC, NUREG-0170, December 1977.

### Section 8.0

1. Office of the Federal Register, Title 10, Code of Federal Regulations, Part 71, Office of the Federal Register, Washington, DC, January 1984.

2. U.S. Nuclear Regulatory Commission, Final Environmental Statement on the Transportation of Radioactive Material by Air and Other Modes, U.S. Nuclear Regulatory Commission, Washington, DC, NUREG-0170, December 1977.
3. Generic Environmental Impact Statement on Handling and Storage of Spent Light Water Power Reactor Fuel, U.S. Nuclear Regulatory Commission, Washington, DC, NUREG-0575, August 1979.
4. N. C. Finley, et. al., Transportation of Radionuclides in Urban Environs, Draft Environmental Assessment, U.S. Nuclear Regulatory Commission, Washington, DC, NUREG/CR-0743, July 1970.
5. L. B. Shappert, et al., A Guide for the Design, Fabrication and Operation of Shipping Casks for Nuclear Applications, Oak Ridge National Laboratory, Oak Ridge, TN, ORNL-NSIC-68, February 1970.
6. U.S. Department of Energy, Mission Plan for the Civilian Radioactive Waste Program (Draft), U.S. Department of Energy, Washington, DC, DOE/RW-0005, April 1984.
7. L. Wilmot, Transportation Accident Scenarios for Commercial Spent Fuels, Sandia National Laboratory, Albuquerque, NM, SAND80-2124, February 1981.
8. H. K. Elder, et al., An Assessment of the Risk of Transporting Spent Nuclear Fuel by Truck, Pacific Northwest Laboratory, Richland, WA, PNL-2588, November 1978.
9. H. K. Elder, An Analysis of the Risk of Transporting Spent Nuclear Fuel by Train, Pacific Northwest Laboratory, Richland, WA, DE82-001048, September 1981.

10. W. H. Rhyne, et al., A Scoping Study of Spent Fuel Cask Transportation Accidents, U.S. Nuclear Regulatory Commission, Washington, DC, NUREG/CR-0811, SAI-OR-79-140-04, June 1979.
11. R. A. Lorenz, et al., Fission Product Release from Highly Irradiated LWR Fuel, U.S. Nuclear Regulatory Commission, Washington, DC, NUREG/CR-0722, February 1980.

### Section 9.0

1. Office of the Federal Register, Title 10, Code of Federal Regulations, Part 71, Office of the Federal Register, Washington, DC, January 1984.
2. U.S. Nuclear Regulatory Commission, Final Environmental Statement on the Transportation of Radioactive Material by Air and Other Modes, U.S. Nuclear Regulatory Commission, Washington, DC, NUREG-0170, December 1977.
3. Highway Accident Report, Multiple Vehicle Collisions and Fire, Caldecott Tunnel, Near Oakland, CA, April 7, 1982, National Transportation Safety Board, Bureau of Accident Investigation, Washington, DC, PB83-916201, May 1983.
4. Newspaper Clipping, San Jose Mercury News, San Jose, CA, March 1981.
5. Railroad Accident Report, Derailment of Illinois Central Gulf Railroad Freight Train Extra 9629 East (GS-2-28) and Release of Hazardous Materials at Livingston, LA, September 28, 1982, National Transportation Safety Board, Bureau of Accident Investigation, Washington, DC, PB83-916305, NTSB/RAR-83/05, May 1983.
6. Railway Accident Report, National Transportation Safety Board, Bureau of Accident Investigation, Washington, DC, ATL 78 FR018.

7. P. Eggers, Severe Rail and Truck Accidents: Toward a Definition of Bounding Environments for Transportation Packages, U.S. Nuclear Regulatory Commission, NUREG/CR-3499, 1983.



NRC FORM 335 (2-84) NRCM 1102, 3201, 3202		U.S. NUCLEAR REGULATORY COMMISSION	
<b>BIBLIOGRAPHIC DATA SHEET</b>		1. REPORT NUMBER (Assigned by TIDC, add Vol. No., if any) NUREG/CR-4829, Vol. 1 UCID-20733	
SEE INSTRUCTIONS ON THE REVERSE.		3. LEAVE BLANK	
2. TITLE AND SUBTITLE Shipping Container Response to Severe Highway and Railway Accident Conditions  Main Report		4. DATE REPORT COMPLETED MONTH   YEAR April   1986	
5. AUTHOR(S) L.E. Fischer, C.K. Chou, M.A. Gerhard, C.Y. Kimura, R.W. Martin, R.W. Mensing, M.E. Mount, M.C. Witte		6. DATE REPORT ISSUED MONTH   YEAR February   1987	
7. PERFORMING ORGANIZATION NAME AND MAILING ADDRESS (Include Zip Code) Lawrence Livermore National Laboratory P. O. Box 808, L-197 Livermore, California 94550		8. PROJECT/TASK/WORK UNIT NUMBER	
10. SPONSORING ORGANIZATION NAME AND MAILING ADDRESS (Include Zip Code) Division of Reactor System Safety Office of Nuclear Regulatory Research U.S. Nuclear Regulatory Commission Washington, D.C. 20555		9. FIN OR GRANT NUMBER  A0397	
12. SUPPLEMENTARY NOTES		11a. TYPE OF REPORT  Technical	
13. ABSTRACT (200 words or less) This report describes a study performed by the Lawrence Livermore National Laboratory to evaluate the level of safety provided under severe accident conditions during the shipment of spent fuel from nuclear power reactors. The evaluation is performed using data from real accident histories and using representative truck and rail cask models that likely meet 10 CFR 71 regulations. The responses of the representative casks are calculated for structural and thermal loads generated by severe highway and railway accident conditions. The cask responses are compared with those responses calculated for the 10 CFR 71 hypothetical accident conditions. By comparing the responses it is determined that most highway and railway accident conditions fall within the 10 CFR 71 hypothetical accident conditions. For those accidents that have higher responses, the probabilities and potential radiation exposures of the accidents are compared with those identified by the assessments made in the "Final Environmental Statement on the Transportation of Radioactive Material by Air and other Modes," NUREG-0170. Based on this comparison, it is concluded that the radiological risks from spent fuel under severe highway and railway accident conditions as derived in this study are less than risks previously estimated in the NUREG-0170 document.		b. PERIOD COVERED (Inclusive dates)	
14. DOCUMENT ANALYSIS - a. KEYWORDS/DESCRIPTORS  spent fuel casks severe highway and railway accident conditions		15. AVAILABILITY STATEMENT  Unlimited	
b. IDENTIFIERS/OPEN-ENDED TERMS		16. SECURITY CLASSIFICATION (This page) Unclassified (This report) Unclassified	
		17. NUMBER OF PAGES	
		18. PRICE	

